Sustainable Tram Track Structure

Design of a more durable and sustainable tram track structure on soft soil

Master thesis

Rick van Noort

Delft University of Technology

TU Delft

Sustainable Tram Track Structure

Design of a more durable and sustainable tram track structure on soft soil

by

Rick van Noort

to obtain the degree of Master of Science

at the Delft University of Technology,

to be defended publicly on **July 15, 2025** at **09:00**

Student number:	5227534	
Project duration:	February 3, 2025 - June 27, 2025	
Chairman:	Dr. V. L. Markine,	TU Delft, Railway Engineering
Thesis committee:	Dr. ir. R. B. J. Brinkgreve,	TU Delft, Geo-engineering
	Dr. Z. Yang,	TU Delft, Railway Engineering
Supervisor company:	ing. L. P. van der Tang,	RET N.V.

Cover: R. van Noort, *1e Middellandstraat*.

An electronic version of this thesis is available at http://repository.tudelft.nl/.

TU Delft

RET

Preface

Before you lies the master thesis "*Sustainable Tram Track Structure - Design of a more durable and sustainable tram track structure on soft soil*". This thesis is my final assignment to obtain the Master of Science degree in Civil Engineering at Delft University of Technology. This study addresses the challenges of constructing civil engineering infrastructures in areas with soft soil conditions, such as the Netherlands, and aims to optimise the sustainability performance of a tram track structure at these locations. The research was conducted in collaboration with RET, which is the public transport operator in the city of Rotterdam. Furthermore, the RET is as asset manager responsible for the construction and maintenance of the fleet, (railway) infrastructure and stations in and around Rotterdam.

I am grateful to Dr. V.L. Markine, Dr. ir. R.B.J. Brinkgreve and Dr. Z. Yang for their guidance and feedback throughout the duration of the project. Their criticism and especially Mr. Brinkgreve's support to get me acquinted with the PLAXIS Finite Element software program really helped me during my research.

Furthermore, I am profoundly grateful to my RET supervisor, Pieter van der Tang. Not only did he provide his support during the project, but he also shared his great passion and drive for the RET and the light-rail sector. He introduced me to the company and the working group *Meerstedenoverleg - Duurzaamheid en klimaat*, which really helped me to see the bigger contextual framework of my research in practise.

I want to thank the members of the RET engineering department, who really made me feel welcome during the months I was conducting my research. Furthermore, I want to thank the members of the municipality of Rotterdam for sharing their (geotechnical) information from the case study location in the borough of IJsselmonde.

Rick van Noort
Delft, July 2025

Summary

In the borough of IJsselmonde on the south bank of the Meuse river in the city of Rotterdam, there are significant problems with the tram track geometry. The subsoil consists of soft soil types, such as peat and clay, which are characterised by consolidation and creep. At certain locations, these settlements result in severe irregularities of the vertical alignment. At the roundabout at the Groeninx van Zoelenlaan, the track deflections are so severe that the protective shield underneath the front end of the tram touches the surface level and the emergency brakes are activated, which is very uncomfortable for the passengers. The tram track structure is only 18 years old, which is significantly lower than the intended life span of 30 years. Moreover, restoring the vertical alignment requires frequent maintenance activities and high costs. Hence, the RET wants a structure that is more durable. In addition to that, the RET wants to have a structure that is more sustainable. Not only a structure that has a low carbon footprint, but also provides resilience against extreme heat and precipitation. This research aims to balance and optimise the sustainability and durability performance and therefore, the following research question is defined: "*To what extent can the durability and sustainability performance of a tram track structure on soft soil conditions be improved while preserving the vertical track geometry?*".

For this research, a case study is performed for a tram track section parallel to the Groeninx van Zoelenlaan between the roundabout and tram stop Akkeroord. PLAXIS 2D simulations, which results are validated with InSAR satellite data and field measurements, and a sensitivity analysis are performed to identify the main causes for the settlements. These calculations show that the composition of thick layers of soft soils, the high ground water table and the self-weight of the structure are driving causes for the vertical settlements. However, the extreme track deflection of the track at the location where the emergency brakes are applied cannot be clarified. This specific connection was built 6 years later than the track at the roundabout to connect with the newly built preloaded track towards shopping center Keizerswaard. Hence, this connection is characterised with differential settlements and a differential vertical stiffness of track support and is therefore a transition zone. As a result, this point becomes the lowest point in the area where waterlogging occurs. The sand fill foundation layer underneath the track structure gets fully saturated and flows out from underneath the structure under dynamic loading of the trams. This results in the extreme deflections of the tram track structure and application of the emergency brakes.

To mitigate these settlements, a light-weight filler material should be used which does not flow out under saturated and dynamic loading conditions. Rockwool elements, foam concrete and EPS are all suitable state-of-the art engineering solutions which fulfil these criteria. A PLAXIS 3D model was developed to calculate the occurring bending moments and rail deflections for the existing situation and the situation for which the three state-of-the-art engineering solutions are applied. These calculations show that all solutions are suitable. However, for foam concrete, the rail deflections reduce with 36.1% and the track is therefore significantly stiffer, which might result in transition zone problems with the subsequent track on a normal foundation. For Rockwool and EPS, this problem does not occur.

Now that is clear that a foundation consisting of Rockwool, foam concrete or EPS increases the life span of the structure from 18 to 30 years, the link with sustainability can be made. When using EPS or Rockwool after having electrified the factory, the total carbon footprint over 30 years for the structure reduces with 3.4% and 1.5% respectively. Further CO_2-reduction can be obtained when embedding the track in olivine ballast and producing rails from recycled steel in Electric arc Furnaces. This leads for a track built on Rockwool to a carbon footprint reduction of 72.3% compared to the existing structure. This is even 74.4% when EPS is used as foundation. When taking into consideration that Rockwool can be used as water buffer and therefore contributes to a more climate-resilient neighbourhood, this is considered to be the most sustainable alternative.

So overall, when Rockwool and EPS are used, the sustainability and durability performance of the tram track structure on soft soil improves while preserving the vertical track geometry.

Contents

1 Introduction

The company RET is responsible for the operations and infrastructure management of the public transport system in the city of Rotterdam. The company has an extensive bus, tram and metro network and possesses a wide variety of infrastructure assets, such as railway tracks and stations. The RET tram network in Rotterdam is therefore of vital importance for the urban mobility.

1.1. Problem statement

In the boroughs on the south bank of the Meuse river in the city of Rotterdam, there are significant problems with the tram track geometry. The tram tracks are subjected to local settlements, resulting in long-wave track irregularities. These settlements can for example be observed around the shopping center Keizerswaard in the borough of IJsselmonde. Photographs of these track irregularities are shown in figure 1.1 and 1.2. The extreme deflections of a tram driving over the pit from figure 1.2 is clearly captured in figure 1.3.

Figure 1.1: Long wave track irregularity nearby Keizerswaard - Groeninx van Zoelenlaan

Figure 1.2: Pit next to a roundabout nearby Keizerswaard

Figure 1.3: Tram driving over the pit next to a roundabout nearby Keizerswaard [1]

Another example of the settlement of the tram track can be observed in figure 1.4. In this picture, the differential settlement between the road, surrounding vegetation and the tram track is clearly visible. These settlements cause cracking of the pavement next to the rails. Furthermore, the grass layer is damaged by the front end of the tram. This also indicates that the track deflects too much under loading from the trams.

Figure 1.4: Settlements of the tram track in Beverwaard [2]

The RET tram tracks are usually made of a concrete slab, which is placed on a layer of sand fill above the subgrade. The rails are installed on top of these slabs and eventually, these are embedded in either the pavement, a ballast layer or soil with grass (see Appendix A).

The borough of IJsselmonde is built on soft soil types, such as clay and peat [3]. These types of soil are characterised by settlements under loading due to consolidation and creep. InSAR-satellite data clearly shows a significant settlement of 6.7 [mm/year] around the pit of figure 1.2, whereas the surrounding buildings built on pile foundations do not settle [4].

The settlements of the tram track are sometimes higher than the settlements of the surrounding roads, which causes water logging. Moreover, when an inadequate drainage system is installed, the sand layer between the impermeable clay layer and the concrete slab could get fully saturated. Under loading, when there is a tendency for volume decrease, the pore pressure will increase. This causes a reduction in effective stresses, which leads to a lower bearing capacity of the soil and inadequate support of the tram track structure, resulting in more extreme deflections of the track under dynamic loading [5].

The track irregularities are uncomfortable for the passengers. In addition to that, these track irregularities cause dynamic amplification of the static wheel loads of the tram on the railway tracks, which leads to further track degradation and damages [6]. In addition to that, severe deformations of the structure under loading are unsafe, which result in temporary speed restrictions. Therefore, the RET would like to have a tram track structure design which is less susceptible to settlements on weak soils such as peat and clay. In addition to that, the RET preferably wants a tram track that is sustainable, one that not only has a low carbon footprint, but also provides resilience in the urban environment with respect to extreme precipitation and heat. So, this research study aims to propose a design for a tram track structure which is more durable and preferably more sustainable on the weak subgrade in the borough of IJsselmonde. This balance between durability of railway track structures on soft soils and sustainability is the **research gap** which will be evaluated. The improved design of the structure will be based on state-of-the-art technologies.

1.2. Research questions

To develop this improved tram track structure design, the following main research question is defined:

To what extent can the durability and sustainability performance of a tram track structure on soft soil conditions be improved while preserving the vertical track geometry?

In order to answer this main research question, the following sub-questions are developed:

- ***What are the main driving mechanisms for the vertical deformation of the tram tracks?***
  This sub-question aims to analyse the driving mechanisms for the vertical settlement of the tram tracks. The influence of the dynamic loading of the trams, the concrete slab track and the geotechnical data of the soil will be elaborated.
- ***Which state-of-the-art engineering solutions could mitigate the vertical settlement of the tram track on the soft soil?***
  Once the main driving factors for the vertical settlement are investigated, a range of potentially effective state-of-the-art engineering mitigation measures are elaborated. By using FEM-software, the effectiveness of the proposed mitigation measures on the vertical settlement of the tram track on weak soil will be assessed based on design criteria.
- ***How sustainable are the existing and proposed tram track structures and which engineering solutions can be applied to improve the sustainability performance of this structure?***
  A sustainable tram track structure can be characterised by a climate resilient, climate mitigating and if possible a circular design [7]. A climate resilient track structure provides resilience in the urban environment with respect to extreme precipitation, drought and heat. A climate mitigating tram track design is related to a low-carbon footprint design.

- ***To what extent are the state-of-the-art engineering solutions affecting the sustainability performance of the tram track structure and how does this relate to the lifetime equivalent CO_2 emissions?***
  Although the state-of-the-art engineering solutions might improve the sustainability performance of the track structure, the vertical track geometry, and therefore the durability of the structure, should meet the design requirements. However, implementing state-of-the-art engineering solutions could lead to a higher CO_2-equivalent emissions over the lifetime of the structure, even though the lifespan of the structure increases. This balance between sustainability and durability should be investigated.

1.3. Research method

In order to properly perform this assessment, a 'case study' is executed for a specific section in the city of Rotterdam with a standard track structure on weak soil conditions. The location of this case study is nearby the shopping center *Keizerswaard*. The exact section is parallel to the *Groeninx van Zoelenlaan* between the tram stop *Akkeroord* and the junction with the street *Reyendijk* and the street *Groene Tuin*. The photographs from figures 1.1 and 1.2 were taken on this section as well. This section is of vital importance for the entire tram network, since it is the access to the RET tram depot *Beverwaard*, where more than 100 trams are maintained [8]. Further details on the case study location are discussed in chapter 2.

To assess the vertical settlements of the tram track, the vertical loads from the structure and the tram are taken into consideration. Furthermore, the horizontal loads in curves (centrifugal force) and the Klingel-motion are taken into consideration, especially when the soil layers underneath the track are asymmetrical and uneven settlements are expected.

By using the FEM software program PLAXIS 2D, the long term settlements of the tram slab track due to consolidation and the creep of the soil can be calculated. The FEM program PLAXIS 3D can be used to determine the rail deflection and the track stiffness.

The qualitative sustainability assessment regarding a climate resilient city and tram track structure are based on literature research and climate data from the Dutch government. Clear maps are published on the website *Atlas Leefomgeving*, which is developed by order of the Ministry of Infrastructure and Water Management and the 12 provinces. The quantitative assessment of the carbon footprint of the materials is based on publicly available Environmental Product Declarations (EPDs).

Eventually, the durability and sustainability performance of the tram track structure on soft soils can be balanced to answer the main research question.

Research structure

The four proposed sub-questions are used to answer the main research question. The research structure and the relationship between all the four sub-questions is displayed on the next page. In grey, the external input data and necessary knowledge from literature is indicated for the applicable research steps.

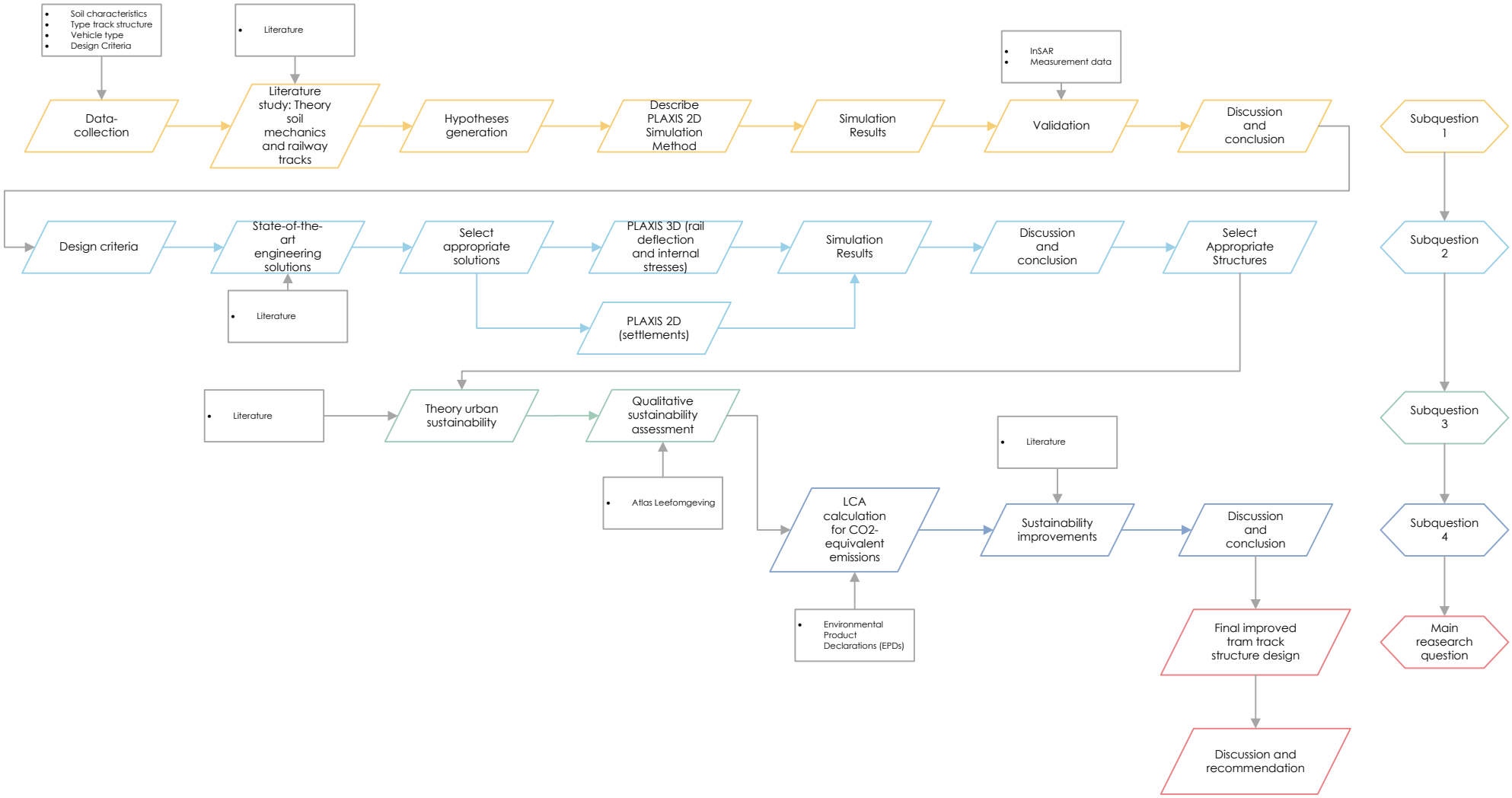
Soil characteristics
Type track structure
Vehicle type
Design Criteria
Literature
Data-collection
Literature study: Theory soil mechanics and railway tracks
Hypotheses generation
Describe PLAXIS 2D Simulation Method
Simulation Results
InSAR
Measurement data
Validation
Discussion and conclusion
Subquestion 1
Design criteria
State-of-the-art engineering solutions
Literature
Select appropriate solutions
PLAXIS 3D (rail deflection and internal stresses)
PLAXIS 2D (settlements)
Simulation Results
Discussion and conclusion
Select Appropriate Structures
Subquestion 2
Literature
Theory urban sustainability
Qualitative sustainability assessment
Atlas Leefomgeving
LCA calculation for CO2-equivalent emissions
Environmental Product Declarations (EPDs)
Literature
Sustainability improvements
Discussion and conclusion
Subquestion 3
Subquestion 4
Final improved tram track structure design
Discussion and recommendation
Main reasearch question

The overall workflow is thus as follows:

- **Sub-question 1 primarily focuses on the understanding and assessment of the existing structure on the local weak soil conditions in the borough of IJsselmonde**. As a first step, data from the case study location should be collected. Subsequently, a literature review about soil mechanics, railway tracks, vertical settlement of the railway tracks and the relationship between these topics is examined. Hypotheses can be generated about the main driving mechanisms for the vertical deformations of the tram tracks. For the assessment of the existing tram track structure, the FEM program PLAXIS 2D is used to calculate the vertical settlement of the existing track structure. InSAR sattelite data and measurement data are used to validate the obtained results from the PLAXIS 2D FEM calculations. The deformation results are compared to the design criteria.
  The results from the literature study on slab tracks on weak soil and the assessment of the existing structure are necessary input data to select feasible state-of-the-art engineering solutions, which is the starting point for sub-question 2.

- **For sub-question 2, the settlements for a selection of state-of-the-art engineering solutions are calculated.** The state-of-the-art engineering solutions, which should mitigate the vertical settlements on the weak subgrade, are proposed based on literature research. Note that there might be a wide variety of possible solutions, but only the most economically feasible solutions will be assessed. For example, a slab track on a pile foundation is over-dimensioned and too expensive for a tram track and will therefore not be considered. The vertical settlements for the proposed state-of-the-art engineering solutions are calculated with PLAXIS 2D as well. Furthermore, the PLAXIS 3D software is used to calculate the rail deflection and bending moments in the slab track under dynamic loading conditions. Eventually, the state-of-the-art engineering solutions which have less vertical settlements than the original tram track structure will be selected for the sustainability optimisation step.

- **Sub-question 3 focuses on the theory of urban sustainability and on how measures could be taken to improve the sustainability of the selected state-of-the-art engineering solutions.** In addition, the term sustainability and the investigated sustainability performance factors are defined. The risk of urban heat stress and water run-off is assessed qualitatively.

- **Sub-question 4 assesses whether the improvements from sub-question 2 do not affect the sustainability performance of the structure.** The vertical track geometry, and therefore the durability of the structure, should meet the design requirements. However, when state-of-the-art engineering solutions are applied, the carbon footprint of the structure probably increases. This sub-question aims to discuss and balance sustainability and durability performance of the structure.

As a last step, the final improved tram track structure design to preserve the vertical track geometry is proposed based on the durability and sustainability optimisation from sub-question 2, 3 and 4. This is the answer on the main research question. Eventually, the outcomes of the master thesis will be discussed and recommendations will be given for improvements and further research projects.

2

Case Study Introduction

In order to properly perform the assessment of the tram track structure, a case study will be executed for a specific section in the city of Rotterdam with weak soil conditions. In this chapter, the following sections are elaborated:

- RET Tram Network (section 2.1)
- RET Tram Rollins Stock - Alstom Citadis (section 2.2)
- Location - Groeninx van Zoeenlaan (section 2.3)
- Track structure (section 2.4)
- Soil conditions (section 2.5)
- Stakeholders (section 2.6)

2.1. RET Tram Network

The RET Tram network consists of 9 tram lines, which connect the neighbourhoods in the agglomeration of Rotterdam with the city center. The map of the network from January 2025 is displayed in the following figure 2.1.

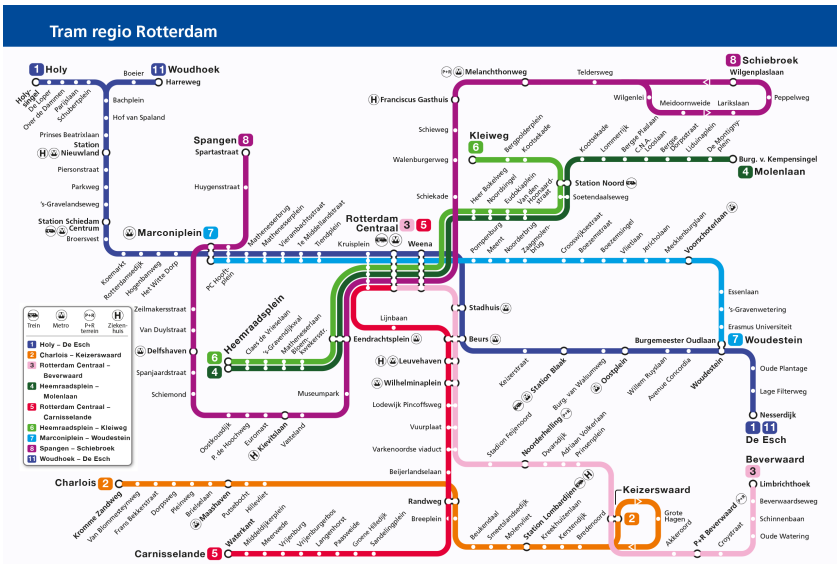

Figure 2.1: RET Tram Network [9]

2.2. RET Tram Rolling Stock - Alstom Citadis

The RET has 112 trams [10] of the type '*Citadis*', which are constructed by the French manufacturer Alstom in La Rochelle. The first generation, Citadis I, was built in 2003 and 2004 and has a length of 31.30 meters. The second generation, Citadis II, was built between 2009 and 2012 and is slightly shorter. The length of the Citadis II is 30.85 meters. Both the Citadis I and II have an empty mass of 37.7 tons [11]. The nominal load is 49,870 [kg] and the load of a fully loaded Citadis is 54,420 [kg]. More than 100 of these trams are maintained in the tram depot Beverwaard, which is located on the south bank of the Meuse river [8]. A picture of an Alstom Citadis I RET tram on the old line 25 (now part of line 5) is depicted in figure 2.2.

Figure 2.2: RET tram Alstom Citadis I on line 25 at tram stop Wilhelminaplein

The Alstom Citadis is a low-floor tram. Low-floor trams are advantageous for tram operations. Not only are these vehicles better accessible for elderly and people with a handicap, but also the passenger change at the stops is quicker, which increases the average speed on the line and lowers total travel times. Opting for this low-floor configuration forces manufacturers to install the electrical equipment on the roof of the tram. Moreover, there is significantly less space available for the bogies compared to older tram-types and conventional railway vehicles [12]. The bogie of a low-floor Citadis tram is shown in figure 2.3a. The bogie of an older, high-floor tram type in Milan (ATM 4900 series) is depicted in figure 2.3b.

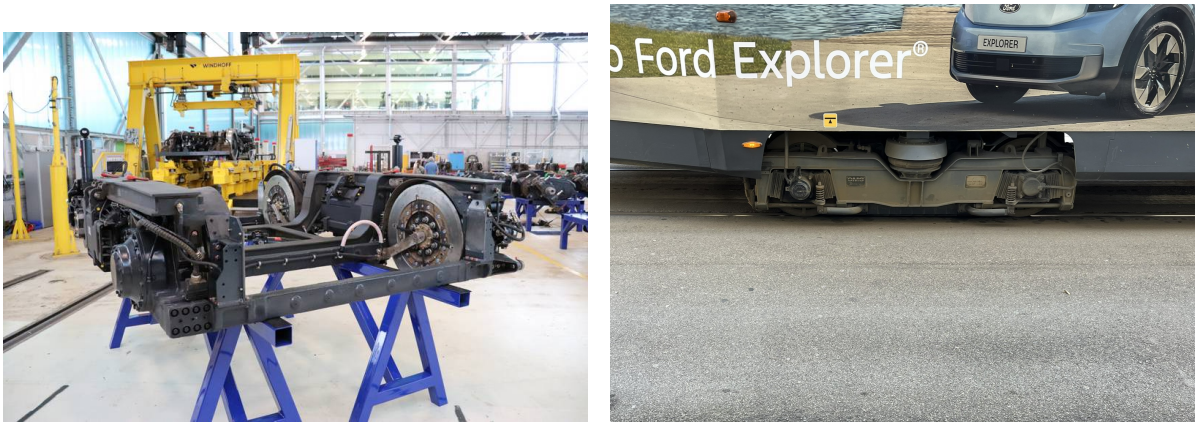

(a) Bogie low-floor tram Alstom Citadis (RET) [13]

(b) Conventional bogie tram (ATM 4900 series - Milan)

Figure 2.3: Bogie comparison: high-floor and low-floor trams

Another peculiarity of the low-floor tram bogie is that the right and left wheels are not connected by a wheel shaft, which can be observed in figure 2.3a [12]. For the Citadis, the brake disks, gearbox and traction motors are assembled on the outside of the bogie frame. Only the bogies on the first and last (fifth) car are motorised. The bogie in the middle (third) car is trailed.

Railway tracks are uneven, both in the horizontal and vertical directions. These track irregularities can be deliberately part of the design, such as turnovers and curves, but also occur as the result of track degradation. To mitigate the effect of horizontal and vertical vibrations caused by these track irregularities, bogies are equipped with a sophisticated suspension system in horizontal and vertical direction, which consists of springs and dampers [12].

The conical profile of the tram wheels and the rails are guiding the vehicle. Due to the small clearance between the wheel flange and the rail, the bogie can follow a zigzag-shaped motion when driving at higher speeds. This horizontal displacement was first described by Klingel. The Klingel-motion can be described as a sinusoidal movement, with a certain wavelength and amplitude, which can be related to the velocity, conicity, gauge width and radius of the wheel [14].

$$y = y_0 \sin\left(2\pi \frac{vt}{\lambda}\right) \tag{2.1}$$

Where:

$$\lambda = 2\pi \sqrt{\frac{rs}{2\gamma}} \tag{2.2}$$

With:

- y_0 = amplitude of the klingel-motion (horizontal displacement)
- v = velocity
- λ = wavelength
- r = radius of the wheel
- s = gauge width
- γ = conicity of the wheel profile

The lateral forces can be found by Newton's Second Law ($F = ma$), where a = $\frac{\partial^2 y}{\partial t^2}$ = $\ddot{y}$. So, by taking the second time derivative of equation 2.1, the relationship between force, velocity and wavelength can be found. The second time derivative of equation 2.1 is:

$$\ddot{y} = y_0 \frac{4\pi^2 v^2}{\lambda^2} \sin\left(2\pi \frac{vt}{\lambda}\right) \tag{2.3}$$

Note that the lateral forces of the railway can be significantly higher, especially in narrow curves where flange contact occurs. This results in excessive wear of the track. Damping is provided in the bogies to minimise the yaw motion caused by the Klingel-motion [12]. However, the maximum amplitude y of the Klingel-motion is already low due to the low velocity v. Therefore, there are no yaw-dampers installed on the Citadis trams or the RET metro trains (5300, 5400, 5500, 5600 and 5700 series).

2.3. Location - Groeninx van Zoelenlaan

In the boroughs on the south bank of the Meuse river in the city of Rotterdam, there are significant problems with the tram track geometry. The tram tracks are subjected to local settlements, resulting in long-wave track irregularities. These settlements can for example be observed nearby the shopping center Keizerswaard in the borough of IJsselmonde. Photographs of these track irregularities and the deflections of the tram are shown in figure 1.1, 1.2 and figure 1.3 in the introduction (Chapter 1).

The borough of IJsselmonde is built on weak soil types, such as clay and peat [3]. These types of soil are characterised by settlements under loading due to consolidation and creep. InSAR-sattalite data clearly shows a significant settlement of 6.7 [mm/year] around the pit of figure 1.2, whereas the road on the roundabout only settles with 2.7 to 4.0 [mm/year] [4]. The InSAR data is displayed in figure 2.4.

Figure 2.4: InSAR settlement data from the location of figure 1.2 [4]

Furthermore, the InSAR data displays the difference in settlements of the houses built on pile foundation, which do not settle, compared to the road and tram tracks, which settle about 4 [mm/year].

In conclusion, this section seems well suited for the case study. The location of this case study is nearby the shopping center *Keizerswaard*. The exact section is parallel to the *Groeninx van Zoelenlaan* between the tram stop *Akkeroord* and the junction with the street *Reyendijk* and the street *Groene Tuin*. The exact location of this section is indicated on the map in figure 2.5.

Figure 2.5: Location case-study nearby tram stop and shopping center *Keizerswaard* (based on [15])

The InSAR data from the settlement of tram track parallel to the Groeninx van Zoelenlaan is displayed in figure 2.6. Settlements occur with a rate of 4 [mm/year].

Figure 2.6: InSAR settlement data of the Groeninx van Zoelenlaan [4]

Th section of this case study is of vital importance for the entire tram network. Not only is this line used by tram line 3 (Centraal station - Beverwaard), but it is also the access to the RET tram depot *Beverwaard*, where more than 100 trams are maintained [8]. Therefore, when state-of-the-art engineering solutions are proposed, the track availability during the construction phase must be guaranteed to ensure tram network operations. A photograph from the *Beverwaard* tram depot is shown in figure 2.7.

Figure 2.7: RET tram in Beverwaard [16]

2.4. Track structure

As can clearly be seen in figure 1.1, there are two type of track structures visible. Both these track structures are considered as a basic type of track structure, which are installed throughout the entire RET tram network. These are:

- **Tram slab track embedded in grass**
  Over the junction, the track structure is embedded in grass. This type of track structure mainly consists of the following elements:
  - **Duo-block sleepers** are directly placed on the sand subgrade with a spacing of 1 meter.
  - A **concrete foundation plate** is casted around the sleepers.
  - **Ri60 rails** are connected to the concrete sleepers by **fasteners**. The track width is 1435 [mm]
  - The **soil** and **grass layer** are placed on the concrete foundation plate.
  - Every 2 meters, **PVC drainage tubes** are installed. These are filled with coarse aggregates.

  The technical drawing of this structure is shown in Appendix A.1.
- **Tram slab track embedded in ballast**
  Parralel to the *Groeninx van Zoelenlaan*, the straight track is embedded in ballast. Apart from this ballast layer, the main elements of this type of track structure are identical to those used for the track embedded in grass. The following elements are mainly used for the tram track embedded in ballast:
  - **Duo-block sleepers** are directly placed on the sand subgrade with a spacing of 1 meter.
  - A **concrete foundation plate** is casted around the sleepers.
  - **Ri60 rails** are connected to the concrete sleepers by **fasteners**. The track width is 1435 [mm]
  - The **ballast** is placed on the concrete foundation plate.
  - Every 2 meters, **PVC drainage tubes** are installed. These are filled with coarse aggregates.

  The technical drawing of this structure is shown in Appendix A.3.

The installation of the duo-block sleepers with the rails on the sand fill is depicted in figure 2.8. The track structure after casting the concrete foundation plate is shown in figure 2.9.

Figure 2.8: Placement of the duo-block sleepers and rails on the sand subgrade on the RET network [17]

Figure 2.9: RET tram track structure after casting the concrete foundation plate [18]

2.5. Soil conditions

Data on the soil conditions are publicly available via the website DinoLoket, which was developed by TNO commissioned by the Ministry of Housing and Spatial Planning [3]. Around the section for this case study, data of many Cone Penetration Tests (CPT) are available. Furthermore, the City of Rotterdam has an even bigger database of CPTs in the city. During a CPT test, a cone is driven into the ground at a constant rate. The following measurements are performed:

- Resistance at the tip of the conus
- Friction around the sleeve of the conus
- Pore water pressure

Based on these characteristics, the soil types on the location can be determined based on the Robertson Chart. Furthermore, the bearing capacity of the soil (for pile foundations) can be estimated [5].

In the following figure, the available CPTs in the database of the City of Rotterdam nearby the are displayed in figure 2.10.

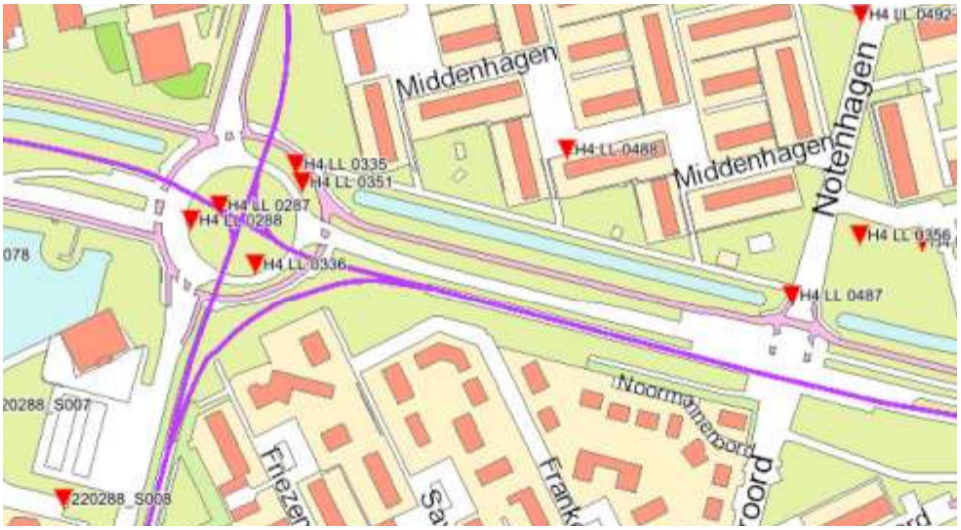

Figure 2.10: Locations used CPT data

The CPTs H4 LL0287, H4 LL0288, H4 LL0555, H4 LL0366, H4 LL0351 and H4 LL0487 are used for this research and displayed in appendix B.

The City of Rotterdam has a dense ground water table monitoring network throughout the city. These data are updated on the website GisWeb 2.2 [19]. The data from Peilbuis 134562-1 and Peilbuis 134562-93 show that the ground water table was 2.28 meters below NAP on the 15th of November 2024. The surface level are 1.49 and 1.41 meters below NAP for Peilbuis 134562-1 and Peilbuis 134562-93 respectively. This implies that the ground water table is roughly 0.8 meters below surface level. This high ground water table was also expected based on the high water level of the surrounding canals during the site inspection on the 13th of November 2024. The high water level compared to the tram structure is shown in figure 2.11.

Figure 2.11: High water levels in the canals (13th of November 2024 - nearby Keizerswaard)

Note that the ground water table can fluctuate throughout the year, based on weather conditions (e.g. long and dry summers compared to autumn with higher amount of precipitation). In this area, the ground water table fluctuates roughly between 2.95 and 1.75 meters below NAP [19].

2.6. Stakeholders

There are multiple stakeholders involved in this system. These are:

- RET
- City of Rotterdam
- Metropoolregio Rotterdam Den Haag (MRDH)
- Utility companies
- Neighbouring residents
- Tram passengers

2.6.1. RET

The company RET is the public transport operator in the city of Rotterdam. The RET is not only responsible for the operation of the buses, trams and metros, but also for the construction and maintenance of the required (railway) infrastructure and stations. The RET has the following wishes and needs regarding this case study:

- The tram track structure should have a long lifetime and should not require many maintenance activities. Maintenance activities might cause disruptions in the tram operations, which is inconvenient for the passengers. In addition to that, the maintenance costs should be minimised.
- Speed restrictions due to track irregularities should be avoided to prevent deviations in the timetable.
- The tram depot Beverwaard should remain accessible in order to guarantee tram network operations.

- Sustainability measures and ambitions from the City of Rotterdam should not interfere with the durability performance of the tram track structure.
- The RET should meet the concession requirements from the Metropoolregio Rotterdam Den HAAG (MRDH). These requirements are for instance the frequency on the lines [20] and the punctuality.

2.6.2. City of Rotterdam

The City of Rotterdam is responsible for the safety and the management of the public space. This consists of a wide variety of assets ranging in size, from small benches in parks and vegetation (e.g. grass, trees) to big civil infrastructures and constructions, such as roads and bridges. The City of Rotterdam has the following influence on this case study:

- The tram structure is placed on a sand layer which is used to elevate the tram track and the surrounding roads.
- Construction works on the tram track should have minimum impact on the traffic on the surrounding roads.
- The City of Rotterdam is responsible for the regulation of the ground water table and the the rainwater run-off via the sewage system [21].
- The City wants a climate-resilient city, which is able to cope with the prospected extreme weather conditions, such as extreme precipitation and drought. To achieve this, the city should have more vegetation and [22] and water storages to avoid waterlogging and overflow of the sewage system.

2.6.3. Utility companies

In the ground, there might be cables and pipelines from utility companies. These utilities must remain intact and should be diverted if necessary for construction works. In addition to that, the corrosion of pipelines (especially gas pipelines) due to stray current from the trams must be avoided.

2.6.4. MRDH

The MRDH is the transportation authority for 21 municipalities in the province of South Holland. The MRDH grants concessions to the public transport operators and imposes requirements for for example the minimum connections and frequency. Furthermore, the MRDH pays the RET a fee for the exploitation and maintenance of the tram network [20]. This contribution is necessary, since the ticket price paid by the passengers is insufficient to cover the exploitation and maintenance costs. In short, the MRDH has the following requirements for the RET regarding this case:

- The pubic transport connection with the borough of Beverwaard should remain.
- The tram network must remain operational and therefore, the tram depot Beverwaard must remain accessible.
- Maintenance costs should be minimised.
- The RET must meet the requirements regarding punctuality and minimum frequency as described in the concession contract.

2.6.5. Neighbouring residents

The interests of the neighbouring residents should also be taken into consideration. On one hand, these residents expect punctual and frequent tramway operations from the RET, but one the other hand, nuisance from construction and maintenance activities and noise and vibrations from the trams must be minimised.

Furthermore, the shop owners of the nearby shopping center *Keizerswaard* want that their businesses are good accessible by car and public transport. Hence, disruptions in tramway operations are unwanted.

2.6.6. Passengers

The passengers of the RET tram line 3 want to have smooth journey. With respect to the case study, the passengers have the following interest:

- Track irregularities should be minimised. First off all, these are uncomfortable for the passengers. Secondly, possibly imposed speed restrictions cause delays and have a negative influence on the time-table.
- The tramway line should have a maximum track availability. Therefore maintenance activities which affect the tram line operations should be minimised.

3

Assessment of the Existing Track Structure

Before effective mitigation measures can be taken against the vertical deformation of the tram track structure, the main driving mechanisms for these deformations should be investigated. Therefore, the first sub-question, *"What are the main driving mechanisms for the vertical deformation of the tram tracks?"*, has to be answered.

The following sections are elaborated in this chapter:

- 3.1 Literature Study
- 3.2 Hypotheses generation
- 3.3 Design criteria
- 3.4 Simulation method
- 3.5 PLAXIS 2D Simulation
- 3.6 Results and validation
- 3.7 Problem Location - Pit next to roundabout Groeninx van Zoelenlaan
- 3.8 Overview problem sections
- 3.9 Conclusion
- 3.10 Discussion and recommendations

3.1. Literature Study

The city of Rotterdam is built on weak soil types, such as peat and clay [3], [23]. These soil types are sensitive to settlements under loading conditions, which are mainly caused by the construction of structures, such as buildings and roads [23]. These settlements can take a long time to develop, especially for soil layers with a low permeability, such as clay. The settlements require the void volume to reduce and therefore, the ground water has to be expulsed out of the soil layer. This process is called consolidation. Furthermore, these soft soil layers can have additional settlements due to creep [5]. The vertical settlements of the soil are sometimes enhanced by drainage activities from the water board. Differential vertical settlements cause many problems in the built environment, such settlements of buildings on poor foundations, the need for regular elevation of the roads, waterlogging and breakage of utility pipelines. To mitigate these effects, more maintenance activities have to be performed, which clarifies that municipalities of cities which are built on soft soil conditions have higher costs due to these differential settlements when compared to cities built on a strong sand layer [23].

The RET also encounters problems with differential settlements of the tram track structure, especially on the south bank of the Meuse river. The differential settlements result in long-wave track irregularities. These irregularities cause dynamic amplification of the static wheel loads of the tram on the railway tracks, which leads to further track degradation and damages [6].

The effect of this problem is amplified when the tram track has settled more compared to the surrounding infrastructures. Waterlogging occurs around the track structure. When the fill sand layer above the low permeable clay subgrade is saturated, the effective stresses and therefore the bearing capacity of the structure reduce significantly [5], [24]. This inadequate support further enhances deflection of the track structure under dynamic loading. Severe deformations of the tram track structure is unsafe. Underneath the front end of a tram, a protective shield is installed, which activates the emergency brakes when it touches an object. If the track deflection is too extreme, the protective shield could touch the track and activate the emergency brake. This is unsafe for the passengers in the tram. The protective shield can be observed in figure 3.1 below. The protective shield is the bar underneath the front skirt of the vehicle.

Figure 3.1: RET Alstom Citadis - Protective Shield (based on [25])

To reduce the safety risks and the dynamic amplification of the railway vehicle, a temporary speed limit is applied on these sections. Then, an appropriate repair and maintenance stratagy is proposed by the maintenance engineers. In conclusion, the differential settlements create the following problems for the RET:

- Shorter life-time of the track structure
- Higher maintenance costs
- Speed restrictions, which are uncomfortable for passengers and unfavourable for the time-table.

The problems of the differential settlements of ballastless tracks on weak soils are observed and studied around the world. In the city of Antwerp, the tram track structure on the left bank of the Scheldt river was completely replaced. The original track structure, which was built on a peat soil layer, was unstable and susceptible to vertical settlements. The new tram track was built on an embankment with pile foundations. These piles have a length varying from 8 to 11 meters [26], [27]. The application of piled embankments with a geogrid over thick clay soil layers has extensively been studied and been proven as a successful method to mitigate the vertical settlement of roads and railways [28]. Moreover, the RET has two sections which are built on embankments with pile foundations as well, which are indeed less susceptible to settlements [29]. However, these structures require more construction materials and a longer construction time compared to a conventional tram track structure.

In China, innovative tram track designs are installed to mitigate the differential settlements on soft soil. In Shanghai, a pile-plank-supported ballastless tram track is installed on a clay layer. During operation, the pressure on the soil has decreased and only uniform settlement was observed. Due to the consolidation of the soil, the slab is only supported by the piles, which causes bending moments and stresses in the structure, which requires reinforcement. However, the internal normal stresses in the slab were more related to temperature variations than to the difference in support condition [30]. On the same track network, the critical transverse differential settlement between the track structure and the surrounding pavement subgrade. Similar distresses were observed as in figure 1.4, but in Shanghai the road had settled more compared to the tram track structure than vice versa. This result is expected, since the Chinese structure was built on a more sophisticated foundation. To not exceed the maximum tensile strength of the pavement, the maximum transversal differential settlement is stated to be 3‰ [31].

Track irregularities and degradation due to local soil conditions are not only limited to ballastless tram tracks, but can be observed in conventional ballast railway tracks and even on High Speed Lines with slab tracks on pile foundations. The Dutch railroad infrastructure manager ProRail has launched a research program on the stability of railroad embankments. This research was incited for the following reasons [32]:

- Longer and faster trains will run more frequently on the Dutch railway network
- The composition of soil types in the subgrade has not always been identified for the entire network
- Due to climate change, more extreme precipitation and longer periods of drought might effect the stability of the embankments.

Embankments can be prone to several types of distresses. The most common types are:

- (Non-)uniform settlement of the embankment
- Settlement of the foundation
- Slope failure (Stability)

Changes in strength and stability of the embankment can be related to a wide variety of causes, such as a change in loading conditions or moisture content of the subsoil [33]. Embankment and earthwork failures can have risks on the track availability and potentially lead to closure of the line. The British railroad infrastructure manager, Network Rail, faces the same technical challenges regarding earthwork asset management across the network, especially on soft soils in the south-east of England. Where necessary, earthwork strengthening measures are being taken to ensure track availability and the safety [34].

Furthermore, in conventional railway tracks, soft soil conditions cause extreme track degradation around *transition zones*. These transition zones are characterised by a difference in vertical stiffness of rail support and are usually observed around civil structures, such as bridges, tunnels and railway level crossings. The main causes for the problems in transition zones are as follows [35], [36]:

- **Differential settlements**
  The railway track on a railway embankment is more susceptible to settlements compared to the civil structures built on a (pile) foundation, such as bridges and tunnels. Moreover, culverts built on a foundation underneath a railway embankment can have a significant impact on the track geometry, especially when the embankment is built on soft soils.
- **Change in vertical track stiffness**
  Abrupt changes in vertical rail stiffness influences the deflection of the rail and therefore the acceleration of the vehicle. Open tracks on soft soils are less stiff compared to tracks on bridges or embedded track structures, such as (Harmelen-type) level crossings.

Both the differential settlements and the change in vertical track stiffness support cause dynamic amplification of the wheel loads, increase in ballast stresses and lead eventually to track degradation. Ballast degradation can eventually lead to unsupported (‘hanging’) sleepers. The dynamic amplification of the wheel loads can increase up to 85.6% and 91.2% on main lines with a track speed of 140 [km/h] [36].

Although the wheel-loads of NS heavy rail rolling stock compared to a RET Alstom Citadis light-rail tram vehicle and the type of track structures are not one-to-one comparable, certain elements of transition zones and transition zone problems can be observed in the case study location. The roundabout and the tram track around the pit from figure 1.2 are characterised by differential stiffness in track support. Furthermore, differential settlement between the tram track and the roundabout was observed in the InSAR settlement data in figure 2.4. The roundabout only settles with 2.7 to 4.0 [mm/year], whereas the observed settlement of pit in the tram track is 6.7 [mm/year] [4]. Moreover, mitigation measures against differential stiffness and settlements is investigated more extensively in chapter 4.

The subsoil layer characteristics have a significant influence on the deformations and stability of train track structures. Van Wessem [37] investigated the horizontal deformations and track instability of the Dutch High Speed Line track nearby Rijpwetering. Due to the strict track alignment margins for safe operations on high speed lines, the structure was built on pile foundations and deformations should be minimised. However, the subgrade underneath the structure at this section was asymmetrical. Only one side of the structure was built on the sand fill of the adjacent motorway A4, whereas the other side of the structure was built on the soft soils, such as peat and clay. These asymmetrical sublayers caused horizontal deformation of the structure. These deformations take a long time to develop due to creep of the soft soils. By installing sheetpiles on the side of the open field or reducing weight of the embankment on the side of the motorway by installing Expanded Polystyrene (EPS), these deformations can be reduced. The horizontal deformations were calculated by using the software program PLAXIS 2D and the results were validated with GNSS data.

Summarised, these are the main findings for the literature study on railways on soft soils:

- Soft soils, such as peat and clay, are susceptible to settlements under loading conditions, such as the construction of buildings and civil (infra)structures. These settlements can take a long time to develop due to consolidation (primary compression) and creep (secondary compression).
- Differential settlements in the built environment cause several problems, such as settlements of buildings, roads, waterlogging and breakage of utility pipelines. The maintenance activities to mitigate those effects are extra costs for the municipality and other asset managers.
- Track irregularities cause dynamic amplification of the wheel loads, which lead to further track degradation and damages.
- A saturated sandfill due to waterlogging reduces the bearing capacity of the tram structure, leading to excessive deformations. These deformations are unsafe and necessitate a temporary speed restriction.
- Embankments on pile foundations are effective structural measures to reduce the vertical settlements on soft soils. However, these structures require more construction materials and a longer construction time. Therefore, for existing tram lines, this option is not always preferred.
- In Shanghai, a pile-plank-supported ballastless tram track is installed on a clay layer. Due to consolidation of the soil underneath slab, the track is only supported by the piles, which requires reinforcement in the slab. However, the deformations of the track structure itself were significantly reduced. A drawback is that the surrounding roads settles more than the tram track structure, which leads to pavement distresses. Moreover, this is a very unsustainable and expensive solution.
- Transition zones in railway tracks are caused by differential settlements and changes in vertical stiffness of rail support. As discussed earlier, the differential settlements are more significant for tracks on soft soils, especially when the civil structure is built on a more sophisticated (pile) foundation. Effective measures to mitigate the track settlements can be taken into consideration for this research.
- Asymmetrical subgrade layers, for example due to the sandfill foundation of an adjacent road on one side compared to soft soils on the other side, can cause horizontal deformations and instability of a railway track.

3.2. Hypotheses Generation

Based on the visual inspection on site and the literature review, the following hypotheses are generated about the driving mechanisms for the vertical settlement:

- The thick layers of Holocene deposits, such as peat and clay, are very susceptible to consolidation and creep under loading. These deformations take a long time to develop. Especially the presence of high-compressible layers of peat has a significant influence on the settlements.
- The high Ground Water Table compared to the surface level reduces the effective stresses and therefore leads to settlements.
- The weight of the concrete tram slab track causes more settlements compared to the surrounding infrastructures.
- The high axle loads of the trams cause severe settlements of the tram track structure.
- The transition zone between the tram track and the road of the roundabout is characterised by differential vertical stiffness in rail support. This causes dynamic amplification of the wheel loads, which leads to higher stresses on the sandfill foundation. When this sandfill layer is fully saturated with water, the deflections are higher and lead eventually to track degradation. This might clarify the pit and high deflections as shown in figure 1.2 and figure 1.3 respectively.

3.3. Design criteria

The tram track structure should comply with the RET design criteria. The settlements are related to the horizontal and vertical alignment, cross-section geometry and drainage criteria. The relevant RET design criteria are listed below [38]:

- **Vertical curves**
  The minimum vertical curve radius $R_{v,min} = 1200$ [m].
- **Cant in curves**
  The cant in an open track is calculated as follows:

$$H_{theoretical} = \frac{11.8 * V^2}{R} \tag{3.1}$$

  Where:

  - $H_{theoretical}$ = theoretical cant in [mm]
  - V = velocity [m/s]
  - R = curve radius [m]

  The maximum cant allowed is 150 [mm]. The cant used in the tram track structure is calculated as follows:

$$H_t = H_{theoretical} - a \tag{3.2}$$

  Where:

  - H_t = cant in the design [mm]
  - a = cant deficit [mm]

  The maximum value of a is as follows:

  - Concrete slab track : a = 90 [mm]
  - Ballast track : a = 60 [mm]
- **Foundation**
  The tram track structure should be constructed on a foundation layer of 0.5 [m] compacted sand.
- **Ground Water Table**
  The average ground water table should not be higher than 1.0 [m] below the top of the rail. If this criterion cannot be met, a drainage system must be installed.

3.4. Simulation Method

To assess the settlement of the existing track structure and test the generated hypotheses from Section 3.2, an appropriate geotechnical model and simulation method must be developed. First of all, based on the field observations and the available CPT tests, a choice must be made between an evaluation of the longitudinal profile or (several) cross-sections. Then, the input parameters of the CPTs and loads are elaborated. At last, the assessment method will be discussed. This workflow is schematised in figure 3.2 below. Eventually, once the appropriate simulation method is selected, the structure can be modelled and simulated in PLAXIS. The PLAXIS simulation results are validated by the ZETDYK and InSAR-data. If necessary, the input data or simulation procedure are updated to get more accurate results. After having validated the PLAXIS simulation results, a sensitivity analysis is performed to evaluate the influence of input parameters of the model. The output of the sensitivity analysis can be used to answer the main research question.

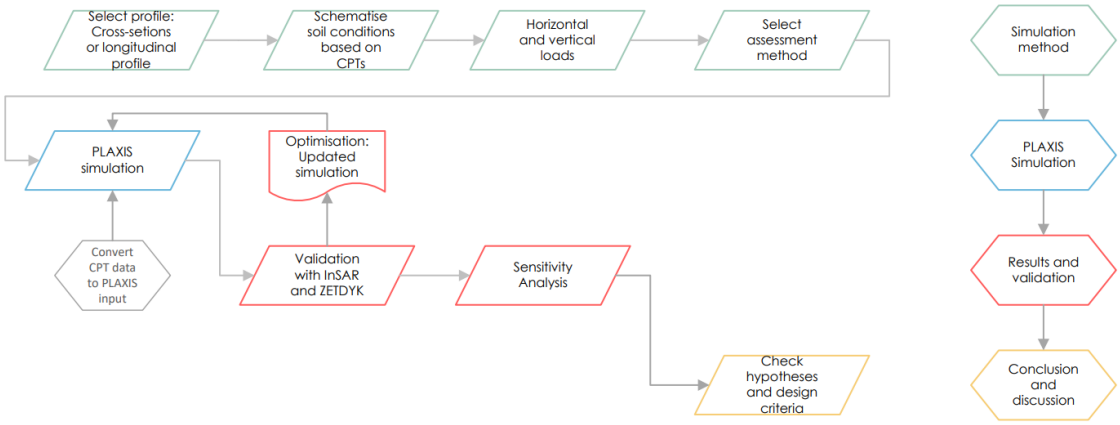

Figure 3.2: Workflow - Model Development, Simulation, Results and Validation

3.4.1. Cross-sections

To get insight in the settlements of the slab track, this effect will be investigated for two cross-sections. The location of these cross-sections is indicated in figure 3.3.

Figure 3.3: Case study location and cross-sections (based on [15])

Cross-sections are evaluated instead of the longitudinal profile for the following reasons:

- The soil layers may have unequal thickness over the width underneath the slab track, resulting in unequal settlements under the same self-weight of the structure.
- By using cross-sections, the settlements of the tram track can be compared to the surrounding area and infrastructures. If the settlements are larger compared to the surrounding area, there is more waterlogging on and underneath the structure, resulting in an inadequately supported track structure. Moreover, when engineering solutions are proposed in Chapter 4, elevation of the structure might have influence on the surrounding infrastructures as well. This is an important aspect for the City of Rotterdam, which is a powerful stakeholder as was mentioned in Chapter 2. In contradiction to a longitudinal profile, a cross-section gives insight in these effects.
- The effect of horizontal forces in curves and the Klingel-motion can be taken into consideration.
- There are too little CPTs available within the case study area to perform a usefull analysis of the longitudinal profile. There are only CPTs available next to the roundabout and the tram stop Akkeroord, which implies that only a linear interpolation between those two points can be made. This analysis can also be performed when comparing the cross-sectional calculations. In conclusion, a cross-sectional analysis at point 1 and 2 provides more (accurate) information compared to an analysis of the longitudinal profile.

A schematisation of the soil layers at the locations of the cross-sections has been determined based on the CPT-data. The CPT-data is evaluated in Appendix B. The schematisation for cross-section 1 and 2 are displayed in figure 3.4 and 3.5 respectively.

Cross-section 1 (Roundabout Groeninx van Zoelenlaan)
Cross-section 1 is located at the pit of figure 1.2. CPTs H4 LL02877 and H4 LL0288 are used to determine the soil types, whereas CPT H40366 is used to determine the unit weight and permeability. There is no numerical data available of CPTs H4 LL02877 and H4 LL0288. Therefore, CPT H40366 is necessary to calculate the unit weight and permeability. Cross-section 1 is characterised by an asymmetrical peat and clay layers between 2.20 and 5.00 meters below NAP, which can be observed in figure 3.4. Moreover, the track is located in a curve with a radius R of 130 [m]. This provides an extra horizontal force component on the track. In combination with the asymmetrical sublayers, this could cause instability of the track structure.

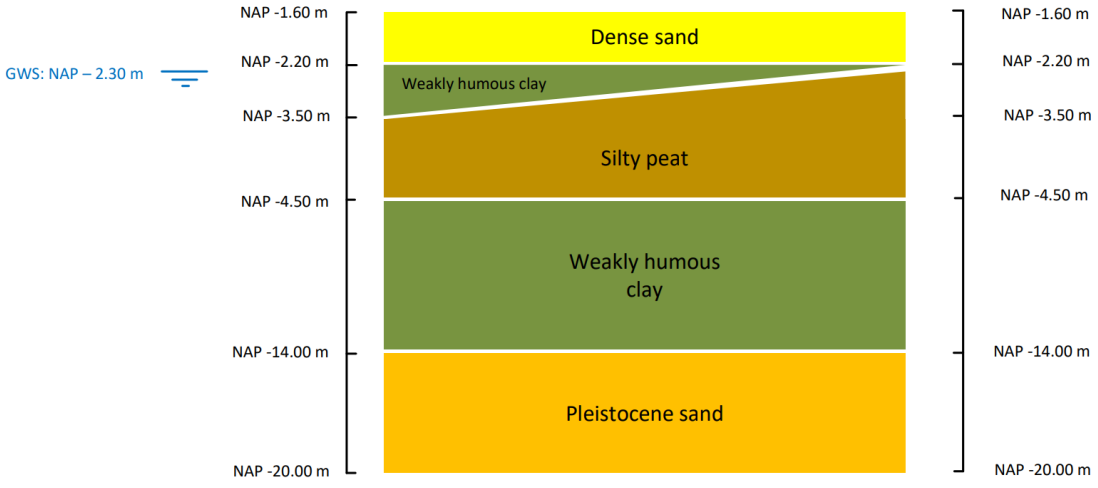

Figure 3.4: Cross-section Roundabout Groeninx van Zoelenlaan

Cross-section 2 (Tram stop Akkeroord)
Cross-section 2 is located at the tram stop Akkeroord. At this location, the tram track is straight. There is only one CPT test available at this location (CPT LL0847). Therefore, the layers underneath the track structure are assumed to be symmetrical. A sketch of the cross-section is displayed in figure 3.5

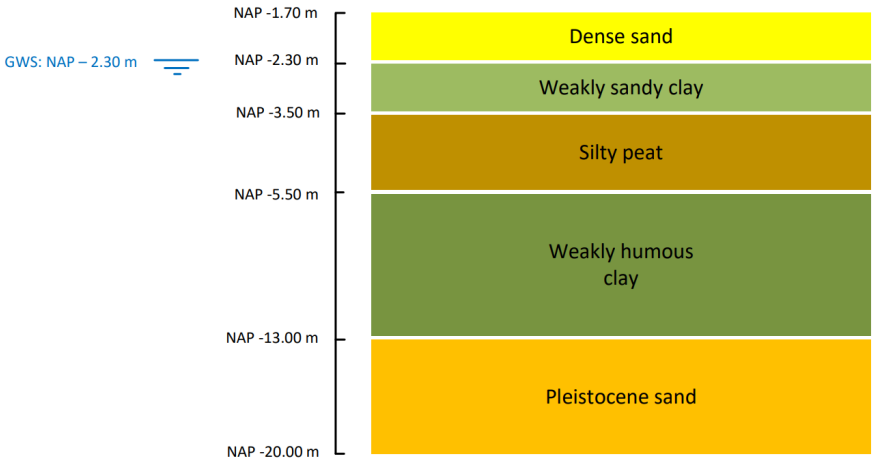

Figure 3.5: Cross-section Tram stop Akkeroord

3.4.2. Vertical loads
The following vertical loads can be distinguished:

- Self-weight of the slab track structure
- Vertical wheel-loads of the tram (including the Dynamic Amplification Factor)

The load based on self-weight of the slab structure is permanent, whereas the load of the trams is not permanent. The weight of the tram is dependent on the amount of passengers. Moreover, the line frequency is not constant for every time of the day. The influence of the wheel-loads of the tram load is modelled as a semi-permanent load.

Self-weight of the Structure
The self-weight of the structure can be derived from the standard RET cross-sections displayed in Appendix A. The density of concrete is 2400 [kg/m^3]. The concrete base-plate has a thickness of 0.17 [m] (or 169 [mm]). The following densities are assumed for the grass and ballast top layer:

- Grass (based on clay) = 1500 [kg/m^3]
- Ballast = 1120 [kg/m^3] [39]

Wheel-loads of the tram
The force of the wheel-loads of the trams can be modelled as a point load on the structure. The magnitude of this force component is dependent on the following factors:

- The static load on the wheels, which is related to the weight of the vehicle and the passenger load.
- A dynamic amplification of the loads due to track irregularities.

Static load
The static wheel load is dependent on the weight of the vehicle. This is related to the load of the passengers. The RET characterises the following three categories and weights for the Citadis I series:

- Empty weight : 37,200 [kg]
- Nominal load (4.5 [passengers/m^2]) = 49,870 [kg]
- Maximum load (7 [passengers/m^2]) = 54,420 [kg]

To determine the wheel load for the PLAXIS model, the maximum load is used. This load is eventually divided over the length of the vehicle and divided by two to get the wheel load. This gives the following static wheel load:

$$F_{wheel,static} = \frac{544.2}{30 \cdot 2} = 9.07 \quad [kN] \tag{3.3}$$

Dynamic loads
As was mentioned in the Literature Study section (section 3.1), track irregularities cause dynamic amplification of the static wheel loads. To get a first impression of this factor, the Eisenmann Dynamic Amplification Factor (*DAF*) is used. This factor takes the track quality, train velocity and exceeding probability into consideration. The equation to calculate the DAF is as follows [40]:

$$DAF = 1 + t \cdot n \cdot \varphi \tag{3.4}$$

Where:

- V = velocity [km/h]
- t = multiplication factor for confidence interval
- n = factor related to track quality
- φ is given by:

$$\varphi = \begin{cases} 1, & \text{if } V \leq 60 \text{ km/h} \\ 1 + \frac{V-60}{140}, & \text{if } 60 < V < 200 \text{ km/h} \end{cases}$$

For the worst track quality and smallest exceeding probability, t = 3 and n = 0.3. Substituting these values in equation 3.4 gives a DAF of 1.9. An increase in wheel loads up to 85.6% and 91.2% was also observed in transition zones on main lines of the national railway network. However, at that specific location, the track speed was 140 [km/h] [36]. According to the equation 3.4, the DAF should then be 2.41, which is an increase of 141%. So, the Eisenmann DAF overestimates the actual dynamic amplification of the wheel loads.

Another way to get a rough indication of the dynamic amplification of the wheel loads is by performing acceleration measurements, for example by using a smartphone [41]. Note that this does not give a direct representation of the actual dynamic loads since the vibrations inside the vehicle are different due to damping from the suspension system. However, extreme accelerations, such as in transition zones, can still be observed from the data [41]. For this experiment, a smartphone was placed on the window frame above the bogie in the last wagon. The vertical acceleration measurements in the direction of Beverwaard and Central Station are displayed in figures 3.6 and 3.7 respectively.

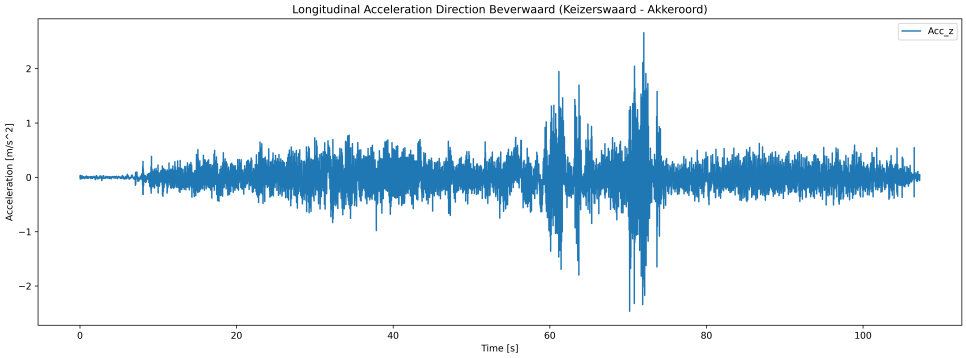

Figure 3.6: Vertical acceleration measurement between Keizerswaard and Akkeroord

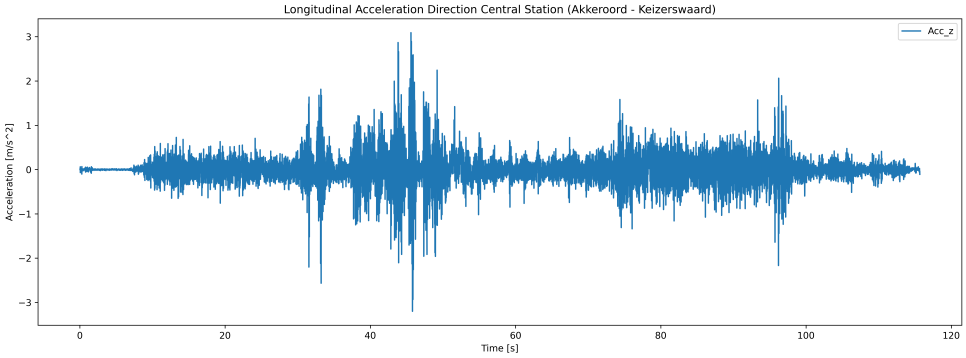

Figure 3.7: Vertical acceleration measurement between Akkeroord and Keizerswaard

In both figures, significant peaks can be observed. However, those were measured at the location of the turnouts. For the rest of the case study location, the measured acceleration in the vehicle did not exceed 0.5 $[m/s^2]$. Based on this observation and the overestimated wheel loads in the transition zone research from Wang and Markine [36], the calculated DAF of 1.9 from equation 3.4 seems rather conservative. Taking a track quality factor n of 0.2 lowers the DAF value to 1.6, which seems more reasonable. The dynamic wheel load used is computed by using equation 3.5.

$$F_{wheel,dynamic} = F_{wheel,static} \cdot DAF \tag{3.5}$$

Substituting the calculated wheel load from equation 3.3 and a DAF value of 1.6 into equation 3.5 gives a dynamic wheel load of 14.51 [kN].

Semi-permanent loading

As was mentioned before, the loading of the vehicle is not permanent on the structure. The frequency on line 3 is 6 trams per hour in both directions. However, there are extra trams from/towards the RET tram depot Beverwaard. During the night, there are no trams in service. So, 6 trams per hour is assumed to be the average frequency over the day. For a velocity of 6 [m/s] at the location of the cross-section, the loading time (t_{tram}) is 5 [s] for a tram with a length of 30 [m]. The total loading duration over 30 years (or 10,000 days) is then as follows:

$$t_{loading;30years} = N_{trams/hour} \cdot t_{tram} \cdot 24 \cdot 365 \cdot 30 \tag{3.6}$$

For 6 trams per hour and 5 [s] per tram, the total loading time is 90.7 days in 30 years. For the simulation, these loads are applied at t = 3000 days, in line with Van Wessem [37]. However, changing the starting time, for example to the first day of exploitation, does not have significant influence on the final settlements over 30 years.

3.4.3. Horizontal loads

For the horizontal loads, the following two factors may be influential:

- Curves
- Klingel-motion

To investigate the magnitude of these forces, the lateral acceleration was measured as well by using a smartphone. The measurement results in the direction of Beverwaard and Central Station are displayed in figures 3.8 and 3.9 respectively.

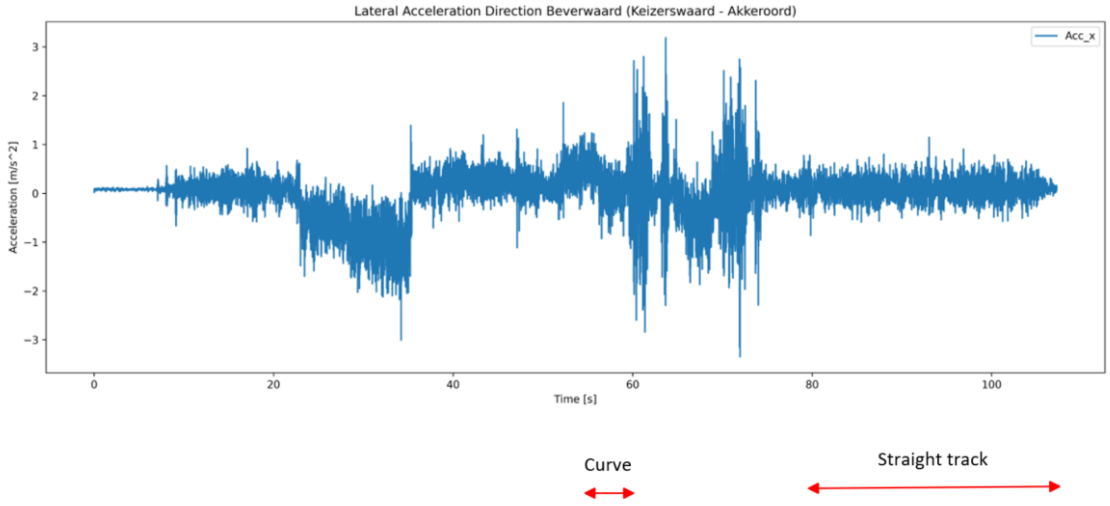

Figure 3.8: Lateral acceleration measurement between Keizerswaard and Akkeroord

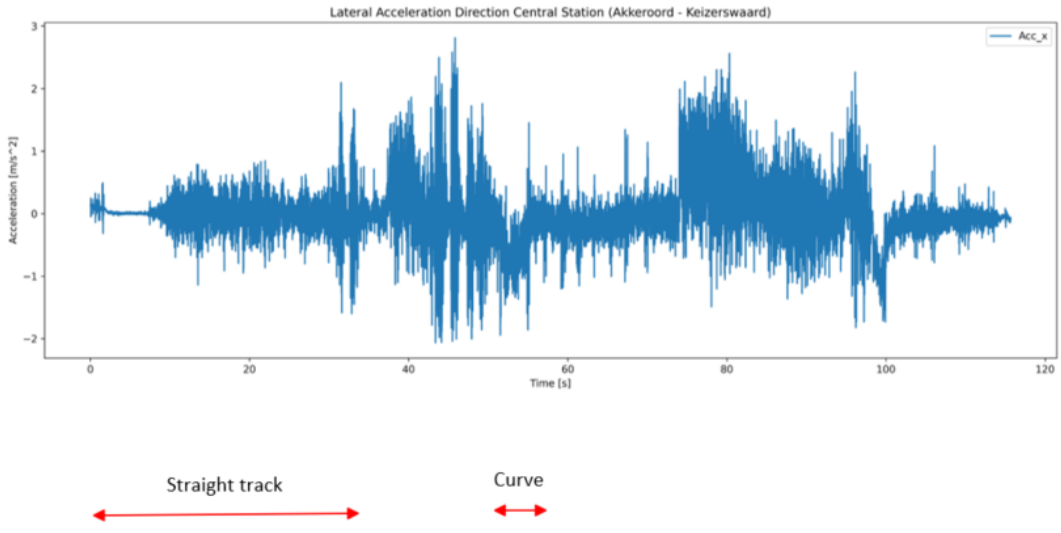

Figure 3.9: Lateral acceleration measurement between Akkeroord and Keizerswaard

The Klingel-motion is of interest on straight sections where the line-speed is higher, which is from 80 [s] in figure 3.8 and the first 30 seconds in figure 3.9. Apart from the measured noise, there is no significant lateral acceleration. However, a clear horizontal acceleration can clearly be observed by the curve before the roundabout. Moreover, a significant horizontal acceleration is observed between 20 and 35 seconds in figure 3.8 and between 75 and 90 seconds in figure 3.9, but these are related to the curve nearby the tram stop Keizerswaard, which is outside the case study section.

The horizontal acceleration can be calculated by using the following equation:

$$a = \frac{v^2}{R} \tag{3.7}$$

Where:

- v = velocity [m/s]
- R = curve radius [m]

At the curve before the roundabout, the tram has a velocity of 6 [m/s] and the curve radius is 130 [m]. Entering these velocity and curve radius in equation 3.7 gives a horizontal acceleration a of 0.28 [m/s^2].

Substituting equation 3.7 in Newton's second law ($F = ma$) gives the horizontal centrifugal force (see equation 3.8).

$$F_{hor} = \frac{mv^2}{R} \tag{3.8}$$

Where:

- m = total mass of the vehicle [kg]
- v = velocity [m/s]
- R = curve Radius [m]

For the nominal load of 49,870 [kg], the horizontal force in the curve is 30.075 [N] (= 0.030 [kN]), which is distributed equally over the three bogies. For the 2D PLAXIS model, there is only 1 meter of depth considered. For simplicity and taking into consideration the influence zone of the horizontal force is larger than 1 meter, the horizontal load of 1 bogie is modelled in PLAXIS. This is 10.025 [N] or 0.010 [kN].

3.4.4. Assessment Method

Now that the soil composition, ground water table and loads on the structure are known for both cross-section 1 and 2, the settlements of the existing structure can be calculated by using the PLAXIS 2D software. The PLAXIS Soft Soil Creep model computes the deformations of the soil and takes consolidation and creep into consideration. Therefore, these autonomous settlements of the soil without loading should be validated with available research data and InSAR data of surrounding infrastructures without significant self-weight, such as sidewalks. Then, the settlements for the tram track structure can be compared with InSAR satellite data and the ZETDYK model (developed by the Engineering department of the City of Rotterdam) to validate the PLAXIS model under loading conditions.

Once the model has been validated, the influence of the thickness of the structure, height of the ground water table, and the loads on the settlements can be determined by performing a sensitivity analysis.

3.5. PLAXIS 2D Simulation

Now that the soil parameters, structure, loads and assessment method are known, the PLAXIS 2D model can be made. The derivation of the parameters is discussed in Appendix B and C

PLAXIS 2D is a geotechnical finite element program, which was developed at Delft University of Technology in the second half of 1980s in collaboration with with the Dutch Ministry of Infrastructure and Water Management (Rijkswaterstaat). The numerical methods, based on non-linear constitutive stress-strain models, used by the finite element program should give more accurate insight in the behaviour of soil structures compared to analytical or empirical methods, resulting in better and more economical geotechnical designs. Nowadays, PLAXIS is known as a well-established geo-engineering tool [42].

Finite element programs are widely used in various engineering fields to compute the physical behaviour of large systems or objects with a complex geometry. For a Finite Element Model, these objects or systems are partitioned into smaller elements. This step is called 'meshing'. The size of these elements ('mesh size') can differ from coarse to fine. By using algebraic equations, the results are calculated for the nodes of the elements. This implies that for a coarser mesh the computation time is shorter, whereas for a finer mesh, the results are more accurate. To get the right results, appropriate initial and boundary conditions must be inserted into the model.

For PLAXIS 2D, the Cartesian coordinate system is used. This coordinate system and the positive stress directions are displayed in figure 3.10.

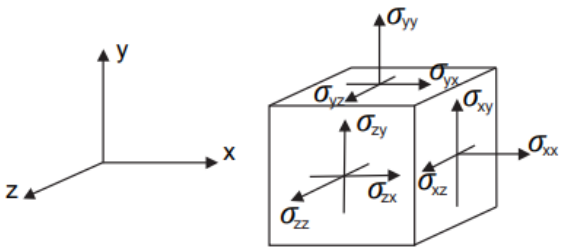

Figure 3.10: Cartesian coordinate system used in PLAXIS 2D [43]

The material models for soil and rock are generally expressed as a relationship between infinitesimal increments of effective stress ('effective stress rates') and infinitesimal increments of strain ('strain rates'). This relationship is defined in equation 3.9 [44].

$$\dot{\underline{\sigma'}} = \mathbf{M}\dot{\underline{\varepsilon}} \tag{3.9}$$

Where:

- $\dot{\underline{\sigma'}}$ = effective stress increment vector in Cartesian coordinates
- $\mathbf{M}$ = stiffness-matrix
- $\dot{\underline{\varepsilon}}$ = strain increment vector in Cartesian coordinates

PLAXIS has a wide variety of material models which can be used for the simulation. These models have their advantages and disadvantages. Some of these models have a shorter calculation time, but only give a first impression of the soil behaviour, such as the Mohr-Coulomb model. Other models are specifically tailored for the behaviour of soft soils, such as the Soft Soil Creep model, which take secondary compression of the soft soil layer into consideration So, for different type of soil layers, a different material model should be selected. In Appendix B of the PLAXIS 2D Material Models Manual, the most appropriate methods are indicated for each soil type [44].

3.5.1. Soils - Material Models

As stated in section 3.4 and in Appendix C, the main soil types for the case study location are sand, normally consolidated clay and peat (OCR = 1.0). The following material models are recommended to be used according to Appendix B of the PLAXIS 2D Material Models Manual [44]:

- **Sand** : *Hardening Soil Model*
- **Normally Consolidated clay** : *Soft Soil Creep Model*
- **Peat** : *Soft Soil Creep Model*

Hardening Soil Model

The Hardening Soil model can be used for both stiff and soft soils. This model is a hardening plasticity model instead of an elastic perfectly-plastic model. For the Hardening Soil model, the soil stiffness is stress dependent. Shear hardening and compression hardening are implemented in the model. Some basic characteristics of the model are [44]:

- Stress dependent stiffness according to a power law: Input parameter m
- Plastic straining due to primary deviatoric loading: Input parameter E_{50}^{ref}
- Plastic straining due to primary compression: Input parameter E_{oed}^{ref}
- Elastic unloading/reloading: Input parameters E_{ur}^{ref}
- Failure according to the Mohr-Coulomb failure criterion: Parameters c, φ and ψ

In table 3.1, the input parameters for the Hardening Soil Model are listed.

Table 3.1: Input parameters Hardening Soil Model [44]

Symbol	Parameter	Unit
c	(Effective) cohesion	$[kN/m^2]$
φ	(Effective) angle of internal friction	[°]
ψ	Angle of dilatancy	[°]
E_{50}^{ref}	Secant stiffness in standard drained triaxial test	$[kN/m^2]$
E_{oed}^{ref}	Tangent stiffness for primary oedometer loading	$[kN/m^2]$
E_{ur}^{ref}	Unloading / reloading stiffness (default $E_{ur}^{ref} = 3 \cdot E_{50}^{ref}$)	$[kN/m^2]$
m	Power for stress-level dependency of stiffness	[-]
ν_{ur}	Poisson's ratio for unloading-reloading (default $\nu_{ur} = 0.2$)	[-]
p_{ref}	Reference stress for stiffness (default $p^{ref} = 100[kN/m^2]$)	$[kN/m^2]$
K_0^{nc}	K_0-value for normal consolidation (default $K_0 = 1 - sin(\varphi)$)	[-]
R_f	Failure ratio $\frac{q_f}{q_a}$ (default $R_f = 0.9$)	[-]
$\sigma_{tension}$	Tensile strength (default $\sigma_{tension} = 0$)	$[kN/m^2]$
c_{inc}	As in Mohr-Coulomb model (default $c_{inc} = 0$)	$[kN/m^3]$

The following rules of thumb can be used to determine the parameters, which cannot be determined based on the CPT-test and the volumetric weight γ_w. These parameters are stated in the CUR 166 and are also used by Stikvoort [45]:

- To calculate the angle of dilatancy (ψ) of sand, the following equation is used:

$$\psi = \varphi' - 30° \tag{3.10}$$

- For clay and peat, the dilatancy angle is equal to zero.

- For the Poisson's ratio for unloading and reloading (ν_{ur}), a value of 0.15 is assumed for sand and a value of 0.20 is assumed for peat and clay.
- The standard value for the triaxial unloading / reloading stiffness is $E_{ur}^{ref} = 3 \cdot E_{50}^{ref}$. However, for soft soils with an OCR of 1.0 (which is the case in Rotterdam), $E_{ur}^{ref} = 4 - 8 \cdot E_{50}^{ref}$. Furthermore, for sand or gravel, $E_{ur}^{ref} = 4 - 5 \cdot E_{50}^{ref}$. For this research, $E_{ur}^{ref} = 5 \cdot E_{50}^{ref}$ will be used.
- For clay with an OCR of 1.0, $E_{50}^{ref} = 2 \cdot E_{oed}^{ref}$. For sand, the values for $E_{50}^{ref} = E_{oed}^{ref}$.
- The power for stress-level dependency of stiffness m is 1.0 for clay and peat and 0.5 for non-cohesive soils such as sand and gravel.

Soft Soil Creep Model

The soft Soil Creep model takes the secondary compression of soft soils into consideration. A significant percentage of the total settlements result from creep and should therefore be implemented in the PLAXIS model.

The characteristics of the Soft Soil Creep are as follows [44]:

- Stress-dependent stiffness (logarithmic compression behaviour)
- Distinction between primary loading and unloading-reloading
- Secondary (time-dependent) compression
- Ageing of pre-consolidation stress
- Failure behaviour according to the Mohr-Coulomb criterion

The input variables for the Soft Soil Creep Model are as follows:

Table 3.2: Input parameters Soft Soil Creep Model [44]

Symbol	Parameter	Unit
c'_{ref}	(Effective) cohesion	[kN/m^2]
φ'	(Effective) angle of internal friction	[°]
ψ	Angle of dilatancy	[°]
κ^*	Modified Swelling Index	[-]
λ^*	Modified compression index	[-]
μ^*	Modified creep index	[-]
ν_{ur}	Poisson's ratio for unloading-reloading (default $\nu_{ur} = 0.15$)	[-]
K_0^{nc}	$\frac{\sigma'_{xx}}{\sigma'_{yy}}$ stress ratio in a state of normal consolidation	[-]
M	K_0^{nc}-related parameter	[-]

The soft soil creep parameters are related to the parameters C_c (Compression index), C_s (Swelling index) and C_α (Creep index for secondary compression), and therefore as well to the Bjerrum and a,b,c-parameters as discussed in Appendix C.

The soft soil creep model accounts for elastic, plastic and creep strains in the 3D model. The elastic strain rate and the creep rate are calculated by using equation 3.11 and 3.12 respectively [44].

$$-\dot{\varepsilon}_v^e = \kappa^* \frac{\dot{p}'}{p'} \approx \frac{1+\nu_{ur}}{1-\nu_{ur}} \frac{1}{1+2K_0} \frac{\dot{\sigma}'}{\sigma'} \tag{3.11}$$

$$-\dot{\varepsilon}_v^c = \frac{\mu^*}{\tau} \left(\frac{1}{OCR}\right)^{\frac{\lambda^* - \kappa^*}{\mu^*}} \tag{3.12}$$

The soil parameter M represents the critical state line of the model and is related to the coefficient of lateral earth pressure K_0^{nc}. When the Mohr-Coulomb failure line is reached, plastic strains can develop [44].

From the City of Rotterdam, the primary and secondary consolidation coefficients (C_p' and C_s') are known for each of the soil types. These coefficients are converted to κ^*, λ^* and μ^*. However, the C_p value, which is the primary consolidation coefficient below the preconsolidation stress, is unknown. If this parameter is known, the following equations are used [46]:

$$\lambda^* = \frac{1}{C_p'} \tag{3.13}$$

$$\kappa^* \approx \frac{1-\nu_{unloading}}{1+\nu_{unloading}} \cdot \frac{1+2K_0}{C_p} \tag{3.14}$$

$$\mu^* = \frac{1}{C_s' \ln(10)} \tag{3.15}$$

Automated Parameter Determination (APD)
Geotechnical laboratory tests are expensive to execute. In early design stages or for certain projects, these tests are not carried out (yet) and therefore, there is limited soil data available. An alternative way to determine these parameters is by using Automated Parameter Determination (APD) software, which is based on relatively inexpensive or available data from CPT tests. The software uses correlations to determine soil and PLAXIS material model parameters based on data from CPT tests. Hence, this software can be used to determine the Soft Soil Creep parameters λ^*, κ^* and μ^*. These parameters are calculated based on equations to determine C_c and C_s [47]. For this research, where only existing CPTs are available, the APD is a suitable method to obtain the necessary parameters for the PLAXIS FEM simulation.

3.5.2. Geometry and Boundary Conditions

When based on the CPT test a clear insight is given on the local soil conditions, the geometry of the cross-section of interest can be modelled in PLAXIS. The model was constructed until NAP - 20 [m] to properly model the behaviour of the thick Holocene deposits onto the pleistocene sand layer. The lower boundary in PLAXIS, $u_{y,min}$, is characterised by 0 displacement in y-direction. Placing this layer too close to the structure would influence the calculated strains and displacements. The boundaries on the sides are fixed in the x-direction but can freely move vertically. Therefore, the sides must be modelled with sufficient distance from the structure such that the boundaries do not distort the calculations.

Furthermore, the groundwater flow at the boundary conditions must be set up. These groundwater flow boundary conditions have a significant influence on the consolidation calculations and the rate of dissipation of the excess pore pressures. The pleistocene sand layer is a water-bearing package. Hence, the ground water flow at $u_{y,min}$ is set to open. Furthermore, the ground water flow at surface level $u_{y,max}$ is set to open as well. In contrast, due to the high ground water table, in combination with the low permeability of the saturated holocene deposits, allow only little ground water flow. Therefore, the ground water flow at the edges is set to closed.

3.5.3. Structures

Once the soil geometry and the appropriate material models have been selected, the structures can be built. PLAXIS provides a variety of structural elements, such as plates, beams, drains and tunnels. Moreover, point loads or displacements can be applied on the structural elements. In general, there is no perfect bond between structure and the soil and shearing can occur. Interfaces can be added to properly model the soil-structure interaction. In the soil material input, the interface factor R_{inter} can be defined, which is dependent on the material of the structure and the soil [48].

3.5.4. Meshing

After having created the soil geometry, structures and applied the loads, the elements of the Finite Element Model can be generated automatically. PLAXIS generates meshes from very coarse to very fine. A very coarse mesh is charaterised by short computation time, whereas the very fine mesh gives the most accurate results. Since the model is rather simple, a fine mesh still has a short computation time. To combine this with the accurate results, the fine mesh is used for the simulation.

3.5.5. Staged Construction

At last, the staged construction phase is defined. During this phase, the effect of different stages of the construction process on the soil is elaborated. The first phase is the K_0-procedure, which determines the stresses in the soil due to the self weight. Subsequently, the soil can be loaded for different construction phases with a prescribed duration. For this research, where there are many undrained soft soil layers, excess pore pressures can develop under loading. Therefore, a consolidation analysis is used for all construction phases. PLAXIS calculates the dissipation of these pore water pressures based on the permeabilities k_x and k_y as defined in the groundwater tab for each defined soil material [48].

3.5.6. Modelling of the cross-sections

The PLAXIS model used for simulation is set up for cross-section 1 and 2 based on the local soil and loading conditions.

Cross-section 1 (Roundabout Groeninx van Zoelenlaan)

Cross-section 1 has a width of 42 meters and is viewed in easterly direction. The slab track has a width of 6 [m] and is place in the middle of the cross-section. The grass layer with a thickness of 205 [mm] is added as a line-load on top of this concrete layer. Multiplying this thickness with the density of the grass-layer of 1500 $[kg/m^3]$ (15 $[kN/m^3]$) gives a distributed line load of 3.075 $[kN/m^2]$. The semi-permanent load of the wheels of the trams are added as point loads on top of the concrete plate. The PLAXIS model of this cross-section is displayed in figure 3.11.

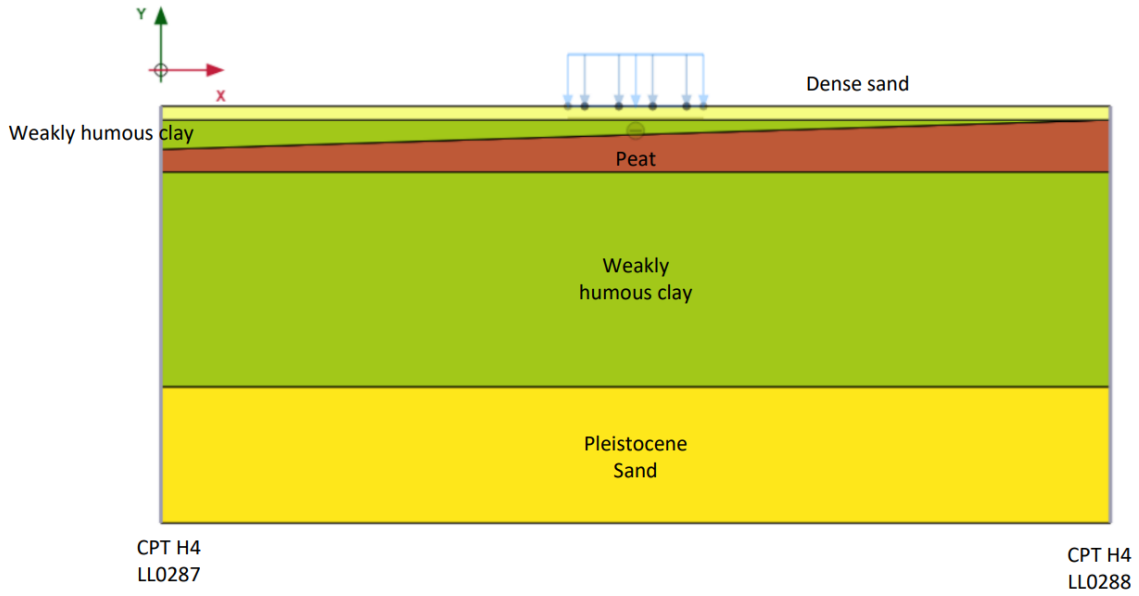

Figure 3.11: PLAXIS model of cross-section 1 (Groeninx van Zoelenlaan)

The corresponding parameters for the PLAXIS simulation per soil layer are stated in table 3.3 below.

Table 3.3: Soil Parameters PLAXIS input - Cross-section 1 (Roundabout Groeninx van Zoelenlaan)

	Dense sand (dr)	**Weakly humous clay**	**Silty peat**	**Weakly humous clay**	**Pleistocene sand**	**Unit**
Material Model	Hardening soil	Soft Soil Creep	Soft Soil Creep	Soft Soil Creep	Hardening Soil	
γ_w	19.00	15.00	12.00	15.00	19.00	$[kN/m^3]$
φ'	28.00	20.10	16.90	20.10	28.00	[°]
c'	0.00	2	2	2	0.00	$[kN/m^2]$
ν	0.15	0.20	0.20	0.20	0.15	[-]
λ^*		0.06263	0.09812	0.08655		[-]
μ^*		0.002619	0.005456	0.0044		[-]
κ^*		0.01253	0.1962	0.01731		[-]
E_{oed}	1722				31610	$[kN/m^2]$
E_{50}	2910				31050	$[kN/m^2]$
E_{ur}	11640				94830	$[kN/m^2]$
ψ	0.00	0.00	0.00	0.00	0.00	[°]
K_0^{nc}	0.6514	0.6073	0.6709	0.6465	0.4531	[-]
K_0^{init}	0.7329	0.7310	0.9359	0.8110	0.4531	[-]
OCR	1.00	1.30	1.30	1.30	1.00	[-]
k_x/k_y	11.08	0.01	0.03	0.02	3.27	[m/day]

The corresponding parameters for the structural element (concrete base plate) are listed in table 3.4. The width of the structure is 1 [m] depth in-plane. The slab track is constructed with C25/30 concrete. The coefficient of reduction at the interface R_{inter} between concrete and dense sand is assumed to be 0.8 based on a study from Ahmad [49].

Table 3.4: Structural Parameters PLAXIS input - Concrete slab

Parameter	**Value**	**Unit**
w	4.080	$[kN/m/m]$
E	31000	$[MPa]$
$A = h \cdot 1$	0.17	$[m^2]$
$I = \frac{1}{12} \cdot 1 \cdot h^3$	$4.09 \cdot 10^{-4}$	$[m^4]$
R_{inter}	0.8	[-]

There is a high ground water table in the area. Therefore, the groundwater flow boundaries of the model are assumed to be closed at all sides, apart from the side of the sand layer above the ground water table close to the ditch parallel to the model. The used settings for staged construction phases are listed in table 3.5.

Table 3.5: Staged Construction Phases

Phase	Calculation time	Duration	Unit
Initial phase	K0-procedure	-	[-]
Tram track construction	Consolidation	28	[days]
Tram loading	Consolidation	90.70	[days]
Consolidation and creep	Consolidation	10,000	[days]

Cross-section 2 (Tram stop Akkeroord)
Cross-section 2 has a width of 60 meters and is viewed in a easterly direction. The left end of the cross-section is the location of the ditch parallel to the Groeninx van Zoelenlaan. 31.9 meters from the left end of the cross-section, the concrete slab of the tram track structure is modelled as a plate with a width of 6.1 meters. The weight of the ballast on top of the concrete plate is calculated and added as a line load on top of the structure. Multiplying the height of the ballast layer (0.17 [m]) with the self-weight of ballast (1120 [kg/m^3] or 11.20 [kN/m^3]) gives a distributed line load of 1.904 [kN/m^2]. The semi-permanent load of the wheels of the trams are added as point loads on top of the concrete plate. The PLAXIS model of this cross-section is displayed in figure 3.12.

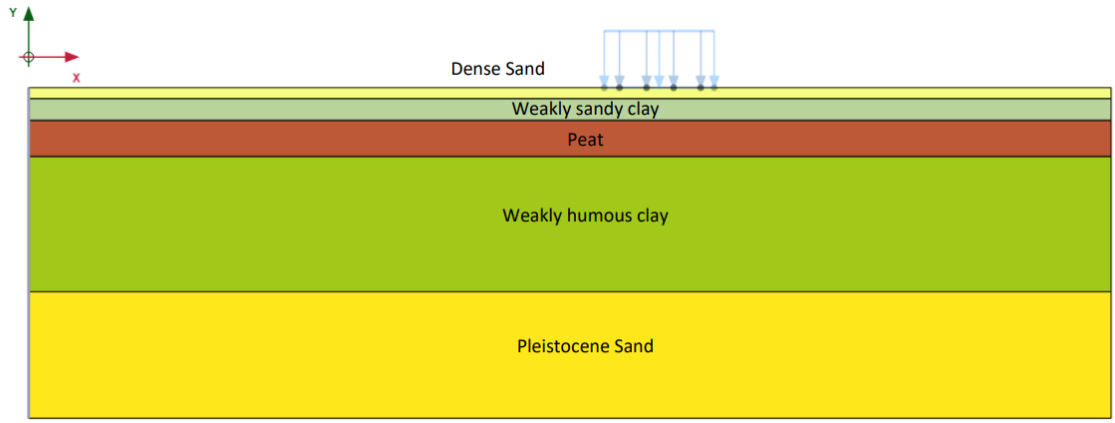

Figure 3.12: PLAXIS model of cross-section 2 (Akkeroord)

The corresponding parameters for the PLAXIS simulation per soil layer are stated in table 3.6 below. The parameters of the concrete slab track, which are listed in table 3.4, remain unchanged.

Table 3.6: Parameters PLAXIS input -Cross-section 2 (Tram stop Akkeroord)

	Dense sand (dr)	**Weakly sandy clay**	**Silty peat**	**Weakly humous clay**	**Pleistocene sand**	**Unit**
Material Model	Hardening soil	Soft Soil Creep	Soft Soil Creep	Soft Soil Creep	Hardening Soil	
γ_w	19.00	17.00	12.00	15.00	19.00	$[kN/m^3]$
φ'	28.00	24.10	16.90	20.10	28.00	[°]
c'	0.00	2	2	2	0.00	$[kN/m^2]$
ν	0.15	0.20	0.20	0.20	0.15	[-]
λ^*		0.087	0.102	0.08993		[-]
μ^*		0.004489	0.005816	0.004731		[-]
κ^*		0.01742	0.02041	0.01799		[-]
E_{oed}	50350				37320	$[kN/m^2]$
E_{50}	59690				37830	$[kN/m^2]$
E_{ur}	179100				113500	$[kN/m^2]$
ψ	0.00	0.00	0.00	0.00	0.00	[°]
K_0^{nc}	0.4749	0.5638	0.6494	0.6701	0.4527	[-]
K_0^{init}	1.561	0.8695	1.045	0.8226	0.5256	[-]
OCR	1.00	1.50	1.30	1.30	1.00	[-]
k_x/k_y	11.08	0.04	0.10	0.06	5.33	[m/day]

3.6. Results and validation

Now that the PLAXIS model has been developed, the settlements of the structure can be simulated. These settlements are calculated until the secondary settlements have finished, which is assumed to be after 10,000 days or 30 years [50]. These simulation results are validated for the following scenarios:

- The autonomous settlement of the soil due to consolidation and creep is calculated with the PLAXIS model without loading of the tram track structure. These results are compared with available research data and InSAR data for data points which do not correspond with buildings built on pile foundations or heavy loaded infrastructures, such as roads and tramways. Suitable datapoints are for example sidewalks.
- The settlements for only the self-weight of the structure is compared to the ZETDYK model of the City of Rotterdam. The ZETDYK-model computes the settlements by using the Koppejan formulae and takes load distribution into consideration according to the Jurgenson model. Furthermore, the total settlements of the roundabout are known based on measurements.
- At last, the settlements are computed, taking the tram load into consideration. These settelements are compared to the settlement rate of the InSAR-data points at the tram track structure.

3.6.1. Cross-section 1 (Roundabout Groeninx van Zoelenlaan)

The deformations of the structure for the three scenarios are calculated separately.

Autonomous settlements

The autonomous settlements due to consolidation and creep of the soft soils over time are displayed in figure 3.13. The InSAR data is collected from 2017 to 2022 [4]. Therefore, the settlement rate in 2020, which is the tangent line 12 years after construction (t = 4,380 [days]) is most relevant for further analysis.

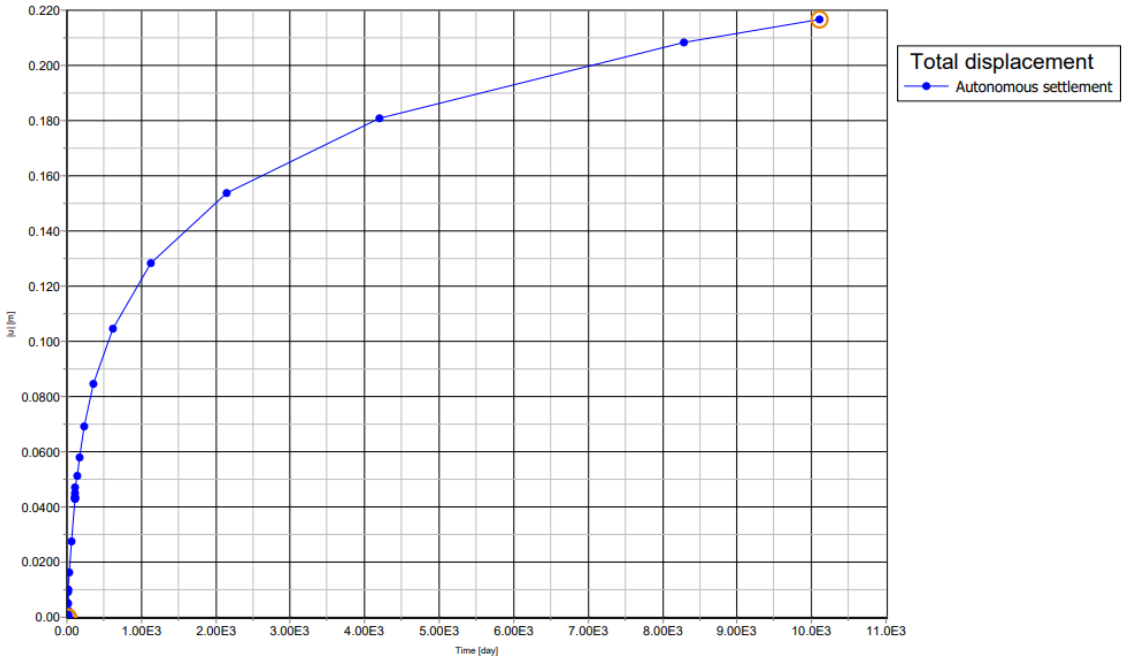

Figure 3.13: Autonomous settlements existing structure cross-section 1

A contour plot of the autonomous settlements at the location of cross-section 1 is displayed in figure 3.14 below.

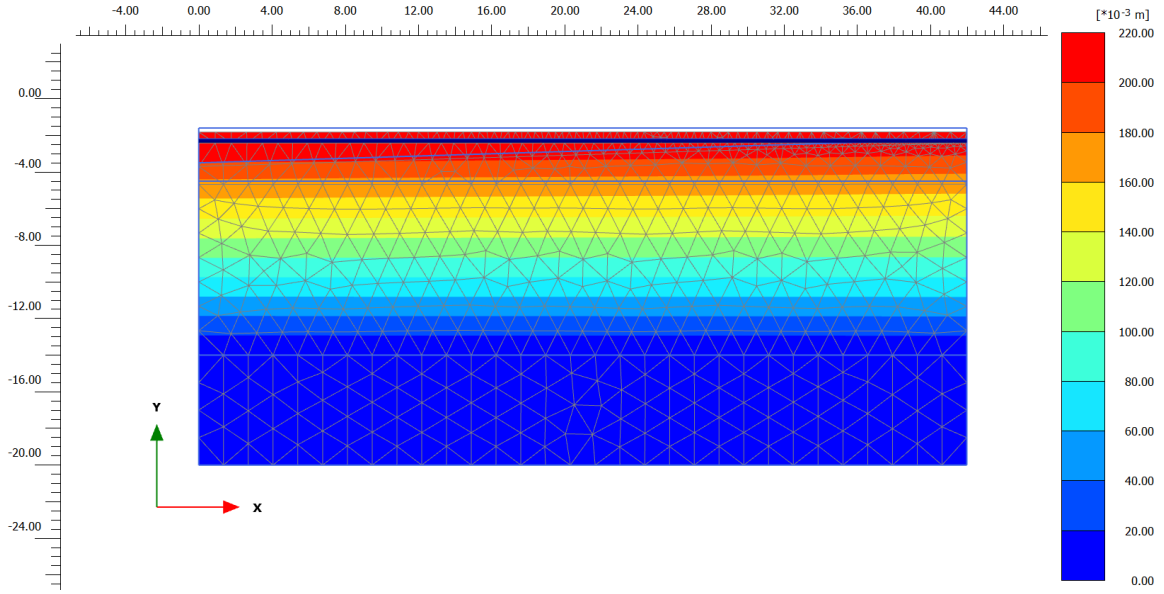

Figure 3.14: Contour plot autonomous settlements existing structure cross-section 1

The calculated settlement rate at t = 4,380 [days] is 2.50 [mm/year]. Furthermore, high initial settlements are observed in the first 1,000 days of the simulation.

Deformations due to self-weight of the structure

A graph of the total deformations ($|u|$) in time due to the self-weight of the tram track structure is displayed in figure 3.15. Since the subsoil layer is asymmetrical, there are three points of interests chosen for the calculation, which are the left corner, middle of the plate and the right corner. In addition, the autonomous settlement is plotted.

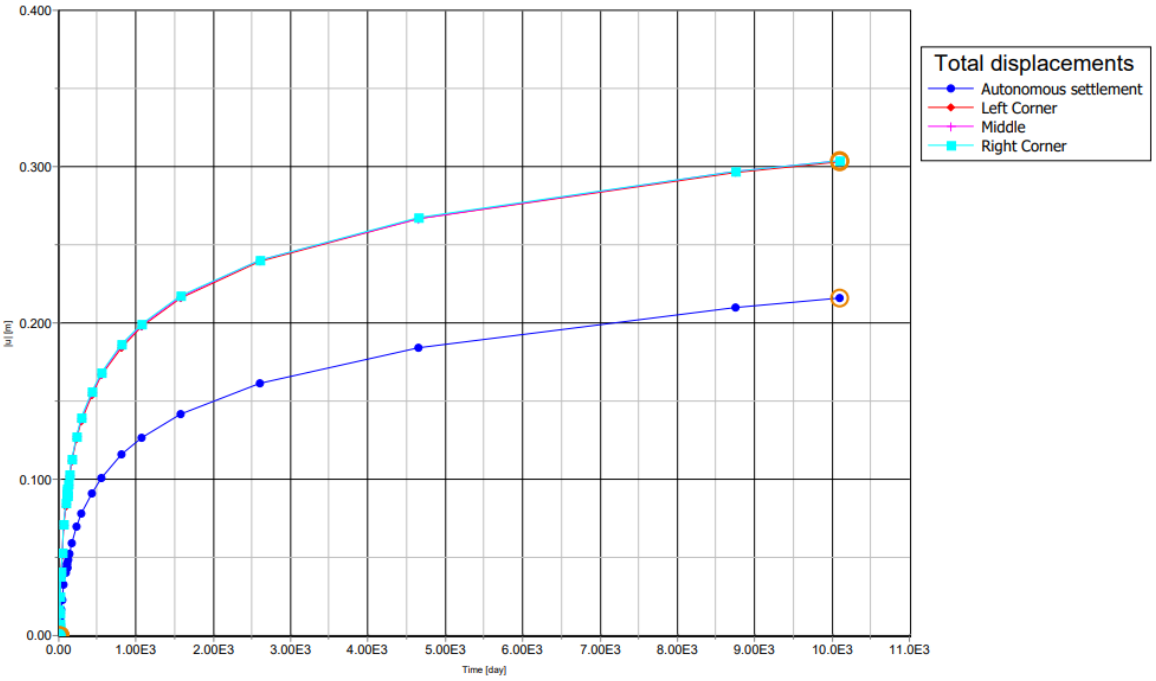

Figure 3.15: Total displacements existing structure cross-section 1 (self-weight only)

In figure 3.15, there is almost zero differential settlement observed between the three points of interest. This means that there is no rotation of the track structure and that the structure can be considered as stable.

A contour plot which shows the total displacement ($|u|$) at 10000 days after construction is shown in figure 3.16.

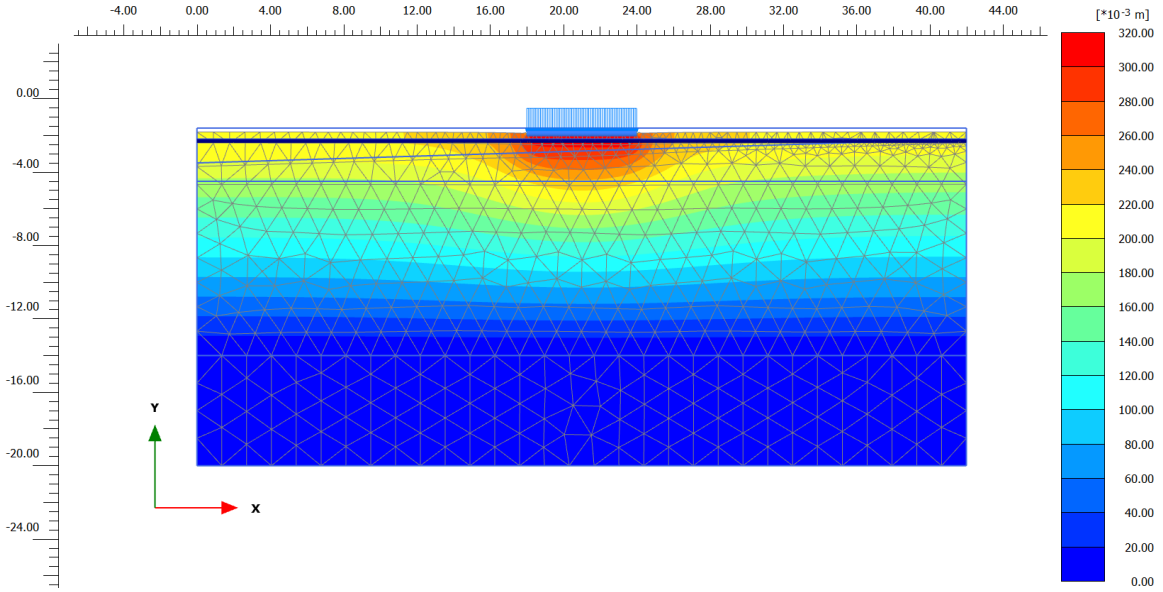

Figure 3.16: Contour plot of the total displacements existing structure cross-section 1 at t = 10000 [days] (self-weight only)

Deformations including weight of the tram

A graph of the total deformations ($|u|$) of the tram track structure including the weight of the tram is displayed in figure 3.17.

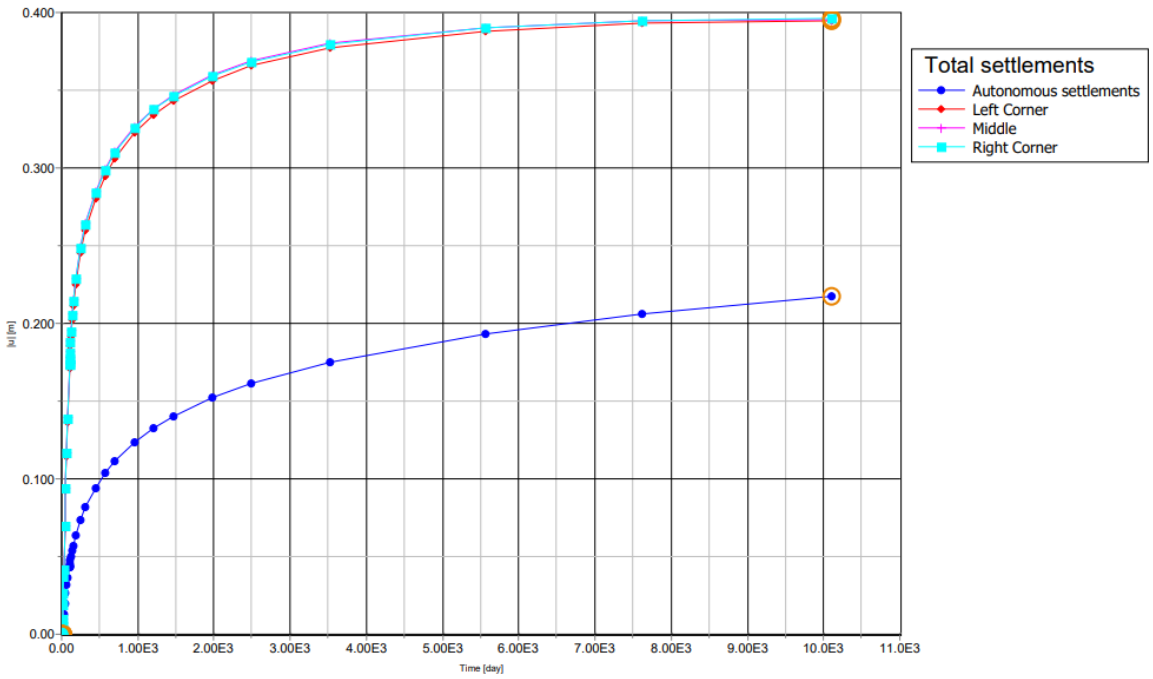

Figure 3.17: Total displacements existing structure cross-section 1 (weight tram included)

A contour plot which shows the total displacement ($|u|$) at 10000 days after construction is shown in figure 3.18.

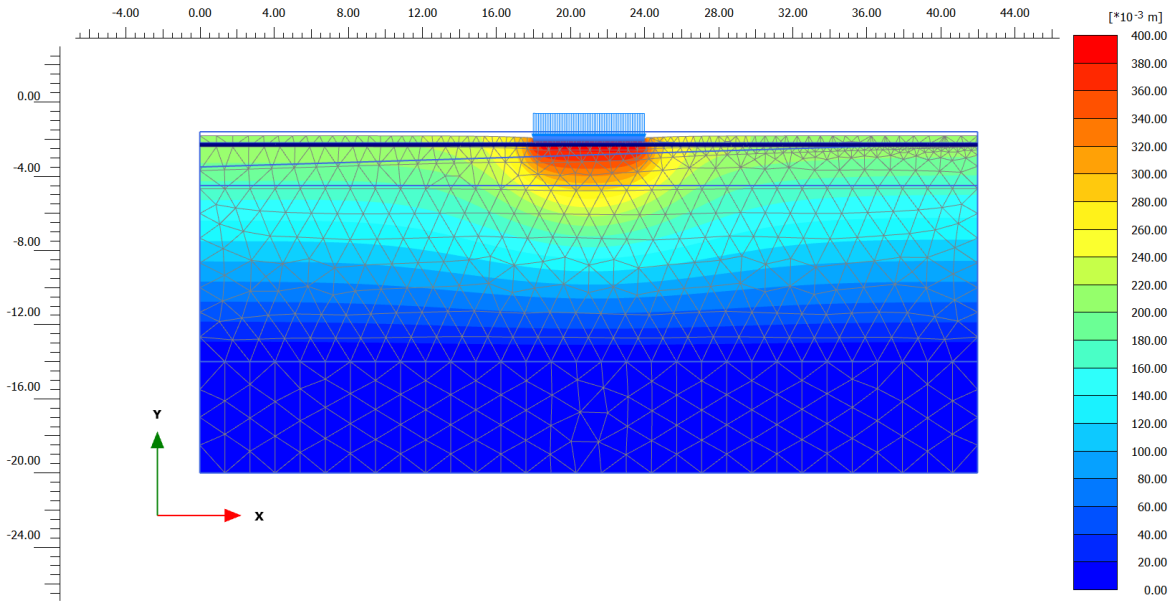

Figure 3.18: Contour plot of the total displacements existing structure cross-section 1 at t = 10000 [days] (weight tram included)

3.6.2. Cross-section 2 (Tram stop Akkeroord)

Just as for cross-section 1, the autonomous settlements and the deformations of the structure with and without the load of the trams are calculated separately.

Autonomous settlements

The autonomous settlements due to consolidation and creep of the soft soils over time are displayed in figure 3.19. As discussed before, for the settlement rate, the tangent line 12 years after construction (t = 4,380 [days]) is most relevant for further analysis. This is 2.31 [mm/year]. Once again, high initial settlements are observed in the first 1,000 days of the simulation.

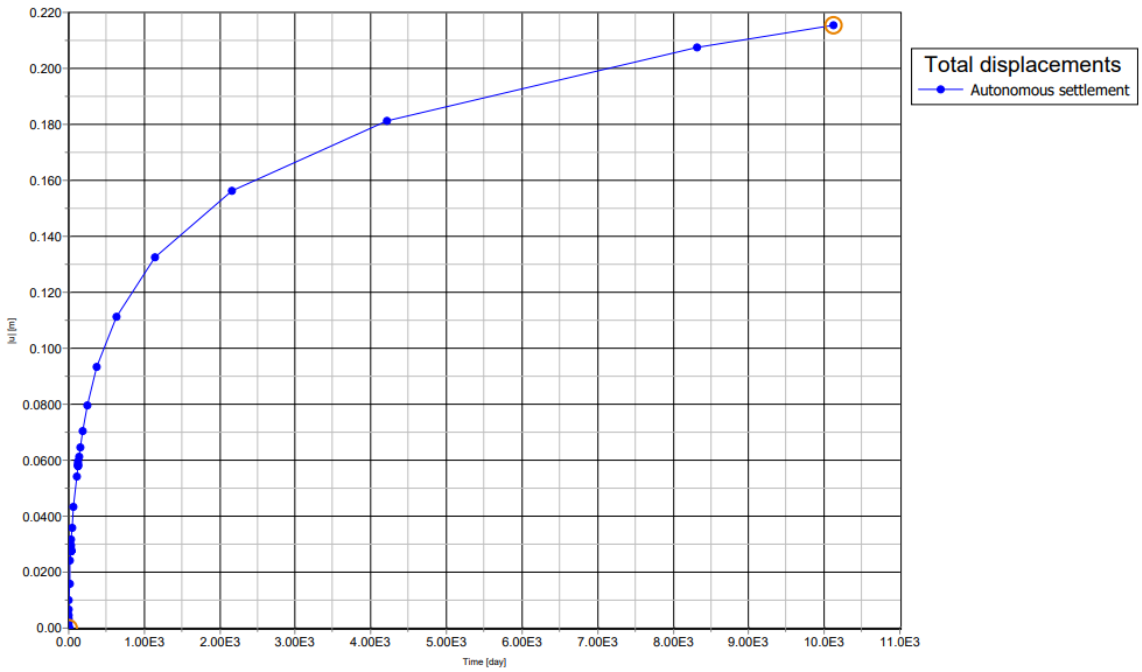

Figure 3.19: Autonomous settlements existing structure cross-section 2

A contour plot of the autonomous settlements at the location of cross-section 1 at t = 10,000 days is displayed in figure 3.20 below.

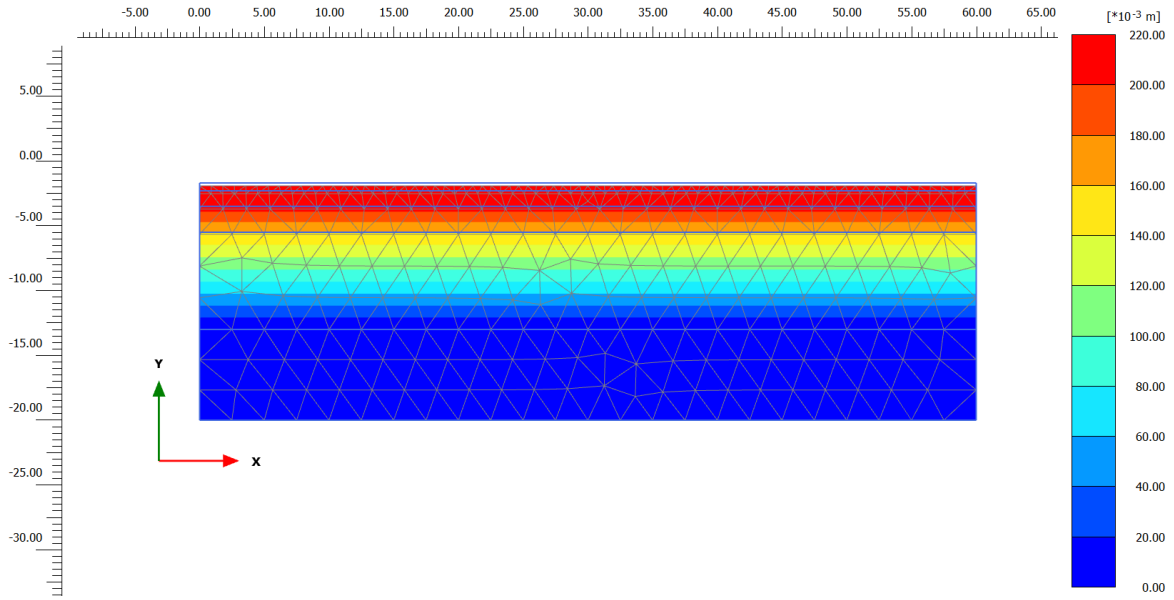

Figure 3.20: Contour plot autonomous settlements existing structure cross-section 2

Deformations due to self-weight of the structure

A graph of the total deformations ($|u|$) in time due to the self-weight of the tram track structure is displayed in figure 3.21.

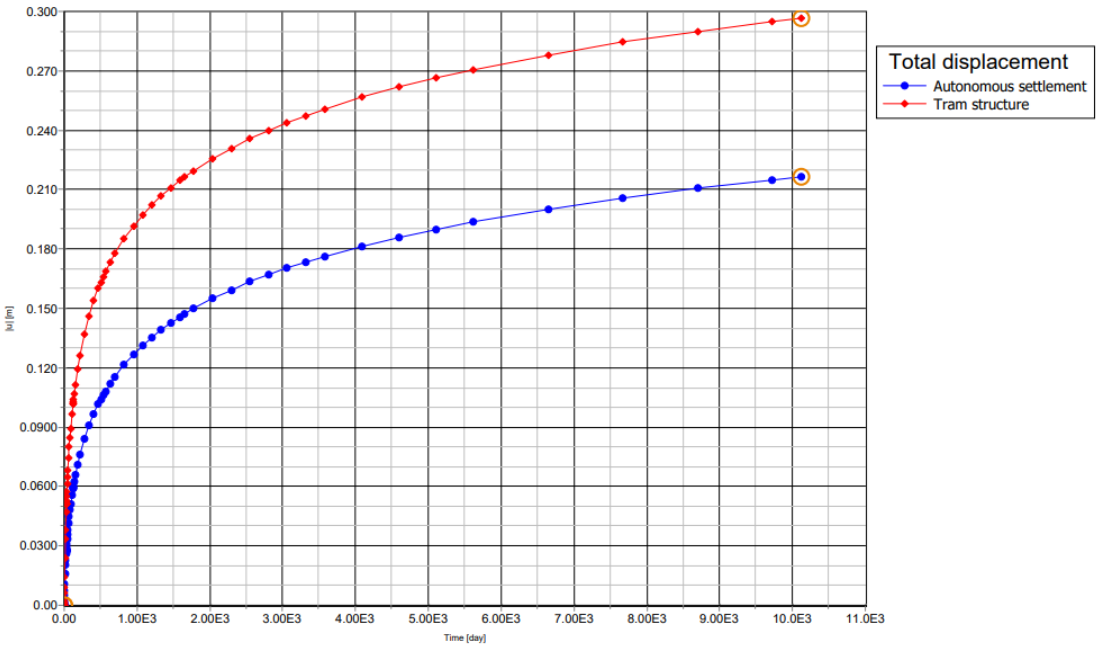

Figure 3.21: Total displacements existing structure cross-section 2 (self-weight only)

A contour plot which shows the total displacement ($|u|$) at 10000 days after construction is shown in figure 3.22.

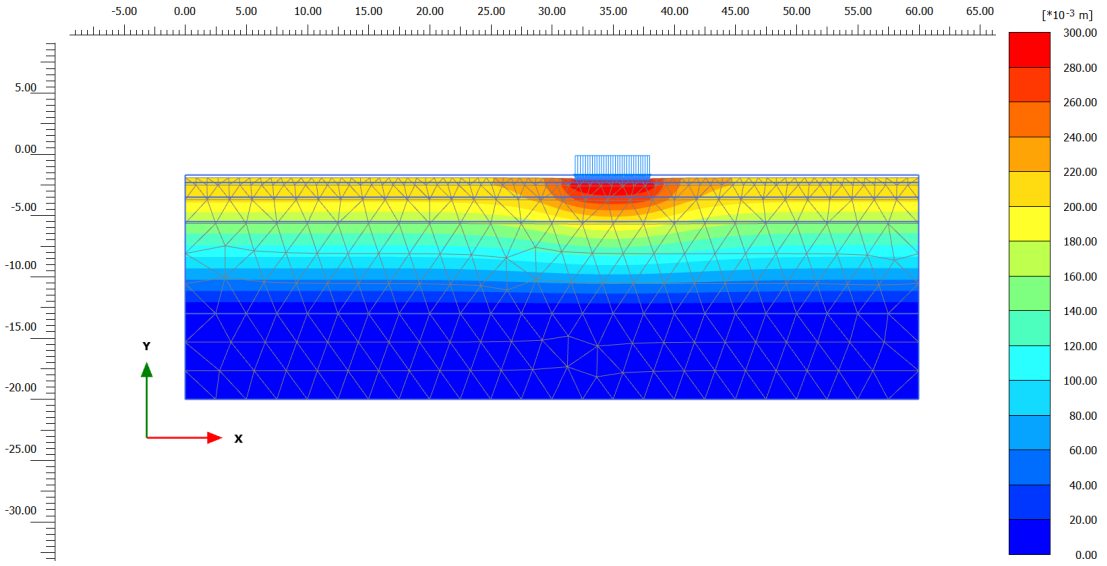

Figure 3.22: Contour plot of the total displacements existing structure cross-section 2 at t = 10000 [days] (self-weight only)

Deformations including weight of the tram

A graph of the total deformations ($|u|$) of the tram track structure including the weight of the tram is displayed in figure 3.23.

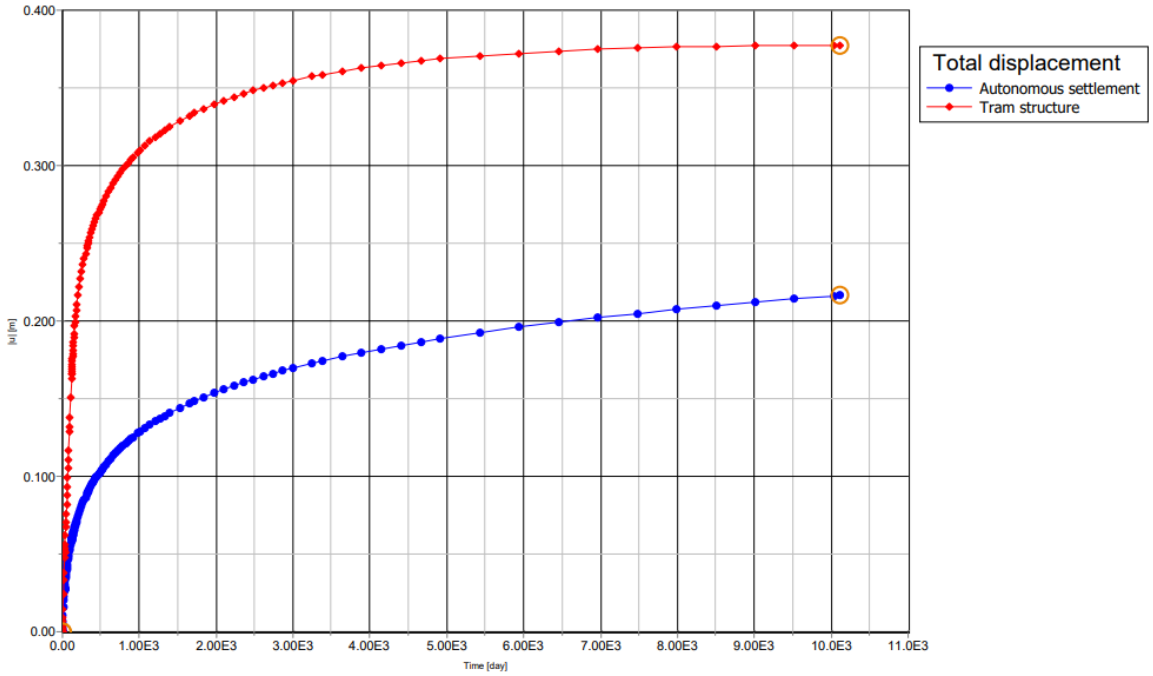

Figure 3.23: Total displacements existing structure cross-section 2 (weight tram included)

A contour plot which shows the total displacement ($|u|$) at 10000 days after construction is shown in figure 3.24.

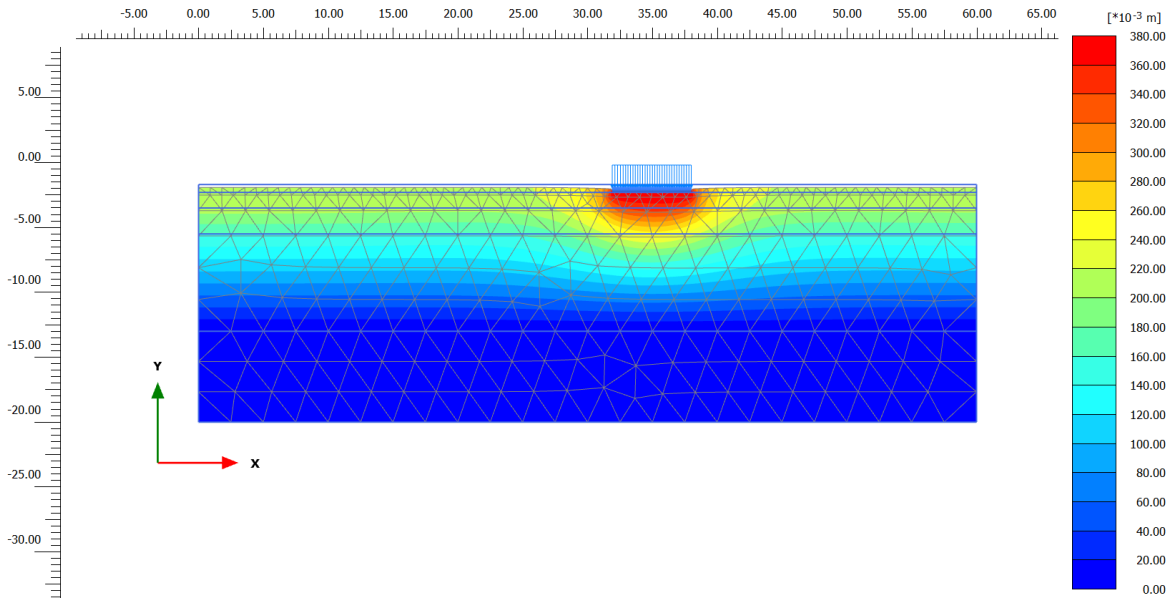

Figure 3.24: Contour plot of the total displacements existing structure cross-section 2 at t = 10000 [days] (weight tram included)

3.6.3. Validation

Subsequently, the PLAXIS model is validated. The results for cross-section 1 and cross-section 2 are validated separately. To get a good impression of the results, the following geotechnical processes and loading cases are differentiated and validated separately:

- **Autonomous settlements**
  The soft soil is subjected to consolidation and creep, which is enhanced by drainage activities from the waterboards and loading of the soil. In the city of Rotterdam, these settlements are significant and are also measured by InSAR-data [51]. Moreover, in certain parts of the Netherlands, peat can settle due to oxidation when these peat layers are above the ground water table. Deltares, TNO and Wageningen Environmental Research have developed maps which predict the settlements of the soil until 2050 and 2100. For the project location, an autonomous settlement of 3 - 10 [cm] is predicted for a mild and severe climate change scenario until 2050 [52]. In addition, these settlements are checked based on certain InSAR-satellite data points at the case study location. Appropriate points are for example sidewalks, which are not subjected to heavy loading, but are also not built on (piled) foundations [51]. These points are therefore only subjected to these autonomous settlements. The InSAR-data report a settlement of 2.4 [mm/year], which results in a total settlement of 72 [mm] in 30 years [4]. This is in line with the range predicted by Deltares, TNO, and Wageningen Environmental Research (WENR) [52]. However, this value is significantly higher than the total calculated settlements from the PLAXIS simulations, which are 22 [cm] and 21.5 [cm] for cross-section 1 and cross-section 2 respectively. This is related to the high initial settlements in the first 1,000 days of the simulation.
- **Settlement of the structure: Self-weight only**
  The settlements for the self-weight of the structure can be compared with the ZETDYK-model, which was developed by the city of Rotterdam. The ZETDYK model only uses the Koppejan consolidation parameters C'_p and C'_s, which are listed for every soil type in table 3.3 and 3.6 for cross-section 1 and 2 respectively. The ZETDYK programme can only calculate settlements due to a surface load added on the existing soil and can therefore only be compared to the self-weight-only results. The total PLAXIS autonomous settlements should be deducted from the total predicted settlements.

- **Settlement of the structure: tram-weight included**
  Furthermore, the results for the total settlements including the tram-weight of the tram should be compared to the InSAR-satellite data. The InSAR data is measured between 2017 and 2022, on which a constant settlement rate is computed. The tram line was constructed in 2008. Therefore tangent of the total settlement at 2020 ($t = 4380$ [days]) will be compared to the settlement rate. Note that the measured results in InSAR should be interpreted with care. Around the roundabout, the settlement rate of nearby data points can be significantly lower/higher. Moreover, PLAXIS only calculates the settlement under perfect theoretical conditions, whereas in practise, problems could occur. For example, when saturated sand fill foundation layer is pumped out under the tram tracks, this is observed in InSAR, but not visible in PLAXIS.
  Furthermore, for the Groeninx van Zoelenlaan, the original height of the tram track structure is known and the current height is recently measured. This measurement data can be used to validate PLAXIS results for cross-section 1. The PLAXIS results 17 years after construction (at $t = 6205$ [days]) should be compared to the to the measurement results, which show a settlement of 15 [cm].

The calculated results and the difference compared to the ZETDYK and InSAR-data are reported for cross-section 1 and cross-section 2 in table 3.7 and 3.8 respectively.

Table 3.7: Validation PLAXIS Deformation Results Existing Structure - Cross-section 1

Autonomous settlements			
Model/Source	**Consolidation and creep**	**Unit**	**Reference**
PLAXIS	0.22	[m]	
Autonomous settlement prediction	1 - 3.33	[mm/year]	[52]
PLAXIS (tangent)	2.50	[mm/year]	[52]
InSAR	2.4	[mm/year]	[4], [52]
Difference tangent and InSAR	4% and within range from [52]	[-]	
Self-weight structure			
Model/Source	**Settlement**	**Unit**	**Reference**
PLAXIS	0.098	[m]	
ZETDYK	0.18	[m]	
Difference	-45.6%	[-]	
Tram-weight included			
PLAXIS ($t = 6,205$ [days])	0.175	[m]	
Measurement data	0.150	[m]	[4]
Difference	+16.7%	[-]	
Model/Source	**Settlement rate**	**Unit**	**Reference**
PLAXIS (tangent)	1.78	[mm/year]	
InSAR	4.0	[mm/year]	[4]
Difference	-55.5%	[-]	

Based on table 3.7, the following conclusions can be drawn:

- The model accurately estimates the autonomous settlement rate of the soil.
- The total autonomous settlements predicted by the PLAXIS model are too high.
- The model underestimates the settlements for the self-weight-only loading condition of the structure.
- The model overestimates the settlement for the tram-weight included loading condition in 2025.
- The model does not predict an accurate settlement rate when the weight of the tram is included.

Table 3.8: Validation PLAXIS Deformation Results Existing Structure - Cross-section 2

Autonomous settlements			
Model/Source	**Consolidation and creep**	**Unit**	**Reference**
PLAXIS	0.215	[m]	
Autonomous settlement prediction	1 - 3.33	[mm/year]	[52]
PLAXIS (tangent)	2.31	[mm/year]	[52]
InSAR	2.4	[mm/year]	[4], [52]
Difference tangent and InSAR	-4% and within range from [52]	[-]	
Self-weight structure			
Model/Source	**Settlement**	**Unit**	**Reference**
PLAXIS	0.081	[m]	
ZETDYK	0.15	[m]	
Difference	-46%	[-]	
Tram-weight included			
Model/Source	**Settlement rate**	**Unit**	**Reference**
PLAXIS (tangent)	2.85	[mm/year]	
InSAR	4.3	[mm/year]	[4]
Difference	-49%	[-]	

Based on table 3.8, the following conclusions can be drawn:

- The model accurately estimates the autonomous settlement rate of the soil.
- The model overpredicts the total autonomous settlements.
- The model underestimates the settlements when only the self-weight of the structure is taken into consideration.
- The calculated settlement rate when the tram-weight is included is significantly lower compared the the InSAR-data.

The high difference between the ZETDYK and PLAXIS settlement for the self-weight only loading condition can be based on the high initial settlements for the autonomous settlement, which is already almost 13 centimetres in the first 1000 days (see figure 3.13 and 3.19). This is an unrealistic settlement rate for a soil that is not subjected to loading applied from structures or vehicles. Furthermore, the high difference in calculated settlement rate at the time of construction is related to the simplified loading condition, which is already at t = 28 days. This leads to a very strong increase in settlement in the first 1000 days of construction compared to the remaining 9000 days, which can be observed in figure 3.17 and 3.23.

3.6.4. Updated simulation

To get a more accurate approximation of the settlement rate in 2020, the construction stages are altered. The semi-permanent loading has a strong influence on the settlement rate and therefore gives unrealistic results over the lifetime of the structure. To minimise this effect, the loading time of the vehicle, which is 90.7 days, is spread over 10,000 days. Therefore, the point load is reduced with a factor $\frac{90.7}{10,000}$. Multiplying the original wheel load from equation 3.5 wich this factor, gives the following dynamic wheel load:

$$F_{wheel,dynamic} = 14.51 \cdot \frac{90.07}{10000} = 0.13 \quad [kN] \tag{3.16}$$

When multiplying the horizontal wheel load with this factor, the load is approximately zero and is therefore neglected.

The updated staged construction phases are listed in table 3.9. During the *Tram track construction* and *Consolidation and creep* phases, the structure and loads are activated in the PLAXIS-model.

Table 3.9: Updated Staged Construction Phases

Phase	Calculation type	Duration	Unit
Initial phase	K0-procedure	-	[-]
Tram track construction	Consolidation	5	[days]
Consolidation and creep	Consolidation	10,000	[days]

Furthermore, the soil input parameters for both cross-sections are updated. The high initial autonomous settlements due to the self-weight of the soil have to be reduced. Therefore, the following parameters are changed:

- The effective cohesion c' is lowered from 2 to 1 [kPa] for the peat layer.
- The overconsolidation ratio (OCR) is increased to 1.5 for the peat layer and to 1.4 for the weakly humous clay layer.
- For the peat layer, the vertical groundwater flow k_y is assumed to be 5 times lower compared to the horizontal groundwater flow k_x.
- The K_0^{nc} value is changed to 0.75 for cross-section 1 and 0.80 for cross-section 2.

The updated input data for cross-section 1 and cross-section 2 listed in table 3.10 and table 3.11 respectively.

Table 3.10: Updated Soil Parameters PLAXIS input - Cross-section 1 (Roundabout Groeninx van Zoelenlaan)

	Dense sand (dr)	**Weakly humous clay**	**Silty peat**	**Weakly humous clay**	**Pleistocene sand**	**Unit**
Material Model	Hardening soil	Soft Soil Creep	Soft Soil Creep	Soft Soil Creep	Hardening Soil	
γ_w	19.00	15.00	12.00	15.00	19.00	[kN/m^3]
φ'	28.00	20.10	16.90	20.10	28.00	[°]
c'	0.00	2	1	2	0.00	[kN/m^2]
ν	0.15	0.20	0.20	0.20	0.15	[-]
λ^*		0.06263	0.09812	0.08655		[-]
μ^*		0.002619	0.005456	0.0044		[-]
κ^*		0.01253	0.1962	0.01731		[-]
E_{oed}	1722				31610	[kN/m^2]
E_{50}	2910				31050	[kN/m^2]
E_{ur}	11640				94830	[kN/m^2]
ψ	0.00	0.00	0.00	0.00	0.00	[°]
K_0^{nc}	0.6514	0.6073	0.75	0.6465	0.4531	[-]
K_0^{init}	0.7329	0.7310	0.9359	0.8110	0.4531	[-]
OCR	1.00	1.40	1.50	1.40	1.00	[-]
k_x	11.08	0.01	0.03	0.02	3.27	[m/day]
k_y	11.08	0.01	0.006	0.02	3.27	[m/day]

Table 3.11: Parameters PLAXIS input -Cross-section 2 (Tram stop Akkeroord)

	Dense sand (dr)	**Weakly sandy clay**	**Silty peat**	**Weakly humous clay**	**Pleistocene sand**	**Unit**
Material Model	Hardening soil	Soft Soil Creep	Soft Soil Creep	Soft Soil Creep	Hardening Soil	
γ_w	19.00	17.00	12.00	15.00	19.00	$[kN/m^3]$
φ'	28.00	24.10	16.90	20.10	28.00	[°]
c'	0.00	2	1	2	0.00	$[kN/m^2]$
ν	0.15	0.20	0.20	0.20	0.15	[-]
λ^*		0.087	0.102	0.08993		[-]
μ^*		0.004489	0.005816	0.004731		[-]
κ^*		0.01742	0.02041	0.01799		[-]
E_{oed}	50350				37320	$[kN/m^2]$
E_{50}	59690				37830	$[kN/m^2]$
E_{ur}	179100				113500	$[kN/m^2]$
ψ	0.00	0.00	0.00	0.00	0.00	[°]
K_0^{nc}	0.4749	0.5638	0.80	0.6701	0.4527	[-]
K_0^{init}	1.561	0.8695	1.045	0.8226	0.5256	[-]
OCR	1.00	1.50	1.50	1.40	1.00	[-]
k_x	11.08	0.04	0.10	0.06	5.33	[m/day]
k_y	11.08	0.04	0.02	0.06	5.33	[m/day]

A graph of the total settlements for cross-section 1 is displayed in figure 3.25. The results for the *self-weight only* and *tram-weight-included* loading conditions are almost identical. Furthermore, although less extreme than for the original simulation method, there are still high initial autonomous settlements.

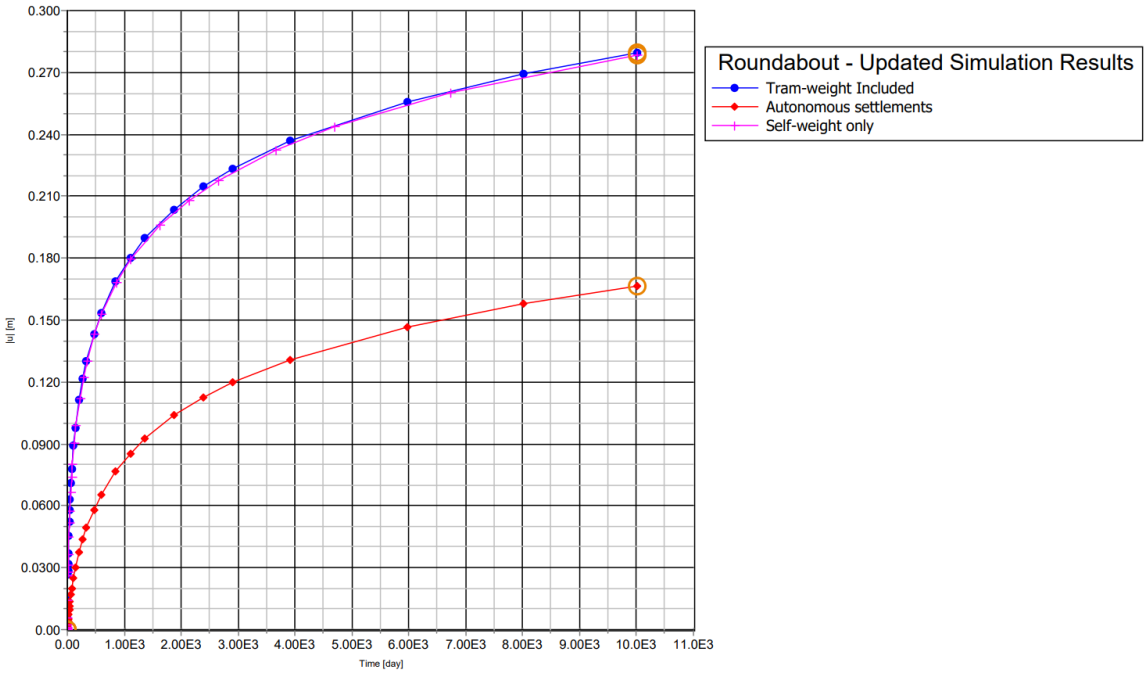

Figure 3.25: Roundabout Groeninx van Zoelenlaan - Updated Simulation Results

This updated simulation results and the differences compared to InSAR and the ZETDYK data for cross-section 1 are reported in table 3.12. The PLAXIS settlement is calculated differently for the self-weight of the structure. The autonomous settlement of 7.2 [cm] in 30 years is deducted from the total calculated autonomous settlements. The result of this computation equals the unrealistic high initial settlements of the simulation. Subsequently, these high initial settlements are deducted from the total calculated settlements in PLAXIS. This approach should give more representative results.

Table 3.12: Validation updated PLAXIS Deformation Results Existing Structure - Cross-section 1

Autonomous settlements			
Model/Source	**Consolidation and creep**	**Unit**	**Reference**
PLAXIS	0.165	[m]	
Autonomous settlement prediction	1 - 3.33	[mm/year]	[52]
PLAXIS (tangent)	2.5	[mm/year]	
InSAR	2.4	[mm/year]	[4], [52]
Difference tangent and InSAR	+4.1% and within range from [52]	[-]	
Self-weight structure			
Model/Source	**Settlement**	**Unit**	**Reference**
PLAXIS	0.185	[m]	
ZETDYK	0.18	[m]	
Difference	+3.8 %	[-]	
Tram-weight included			
PLAXIS ($t = 6,205$ [days])	0.161	[m]	
Measurement data	0.150	[m]	
Difference	+7.3 %	[-]	
PLAXIS (tangent)	4.3	[mm/year]	
InSAR	4.0	[mm/year]	[4]
Difference	+7.5 %	[-]	

Compared to the original validation results from table 3.7, the following differences are observed:

- The creep rate is 2.5 [mm/years]. Hence, the model gives a good approximation of the autonomous settlements. This is in line with the original model.
- The computed settlement of the self-weight only loading condition is only 3.8% above the ZETDYK prediction. This is a significant improvement compared to the original simulation.
- In 2025, the calculated settlement is only 7.3 % above the actual measurement data, which is a very good approximation.
- When the tram weight is included, the tangent line of the updated model is only 7.5% percent above the InSAR observation during this period. This is a very good approximation. Therefore, the current tram-load modelling gives a more accurate representation of the actual settlement rate of the tram track structure.

A graph of the total settlements for the updated simulation for cross-section 2 is displayed in figure 3.26. Just as for cross-section 1, the results for the *self-weight only* and *tram-weight-included* loading conditions are almost identical. In addition, there are high initial autonomous settlements.

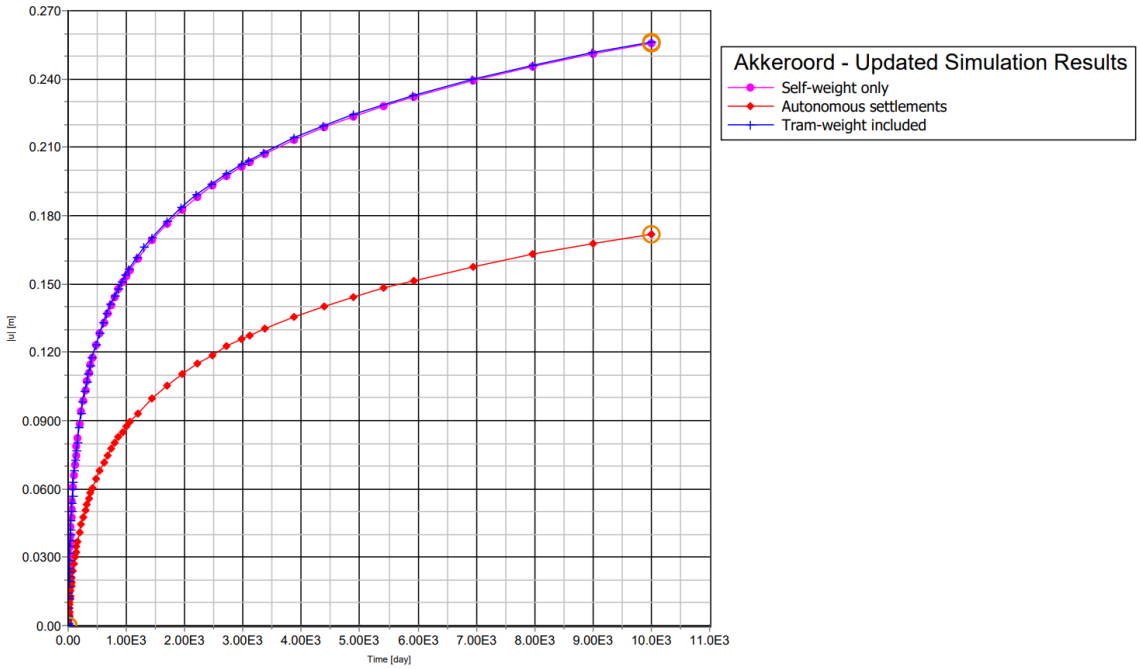

Figure 3.26: Akkeroord - Updated Simulation Results

The updated simulation results and the differences compared to InSAR and the ZETDYK data for cross-section 2 are stated in table 3.13.

Table 3.13: Validation updated PLAXIS Deformation Results Existing Structure - Cross-section 2

Autonomous settlements			
Model/Source	**Consolidation and creep**	**Unit**	**Reference**
PLAXIS	0.172	[m]	
Autonomous settlement prediction	1 - 3.33	[mm/year]	[52]
PLAXIS (tangent)	2.8	[mm/year]	
InSAR	2.4	[mm/year]	[4], [52]
Difference tangent and InSAR	16.7% and within range from [52]	[-]	
Self-weight structure			
Model/Source	**Settlement**	**Unit**	**Reference**
PLAXIS	0.156	[m]	
ZETDYK	0.15	[m]	
Difference	+4%	[-]	
Tram-weight included			
PLAXIS (tangent)	4.3	[mm/year]	
InSAR	4.3	[mm/year]	[4]
Difference	0	[-]	

When compared to the original validation results in table 3.8, the following differences are observed:

- The creep rate is slightly overestimated compared to the InSAR data and the rate calculated for cross-section 1.
- The PLAXIS model slightly overestimates the total settlements due to the self-weight of the structure with 4% compared to the ZETDYK model. So, this is a very accurate approximation.
- When the tram weight is included, the tangent line of the updated model is identical to the InSAR observation during this period. The nearby InSAR points report a settlement rate of 4.1 and 4.0 [mm/year] during this reference period. Therefore, the PLAXIS model is a very accurate approximation. Therefore, the current tram-load modelling gives a more accurate representation of the actual settlement rate of the tram track structure.

In conclusion, the current predicted settlement rate is significantly more accurate for both cross-sections compared to the original simulation method.

3.6.5. Sensitivity Analysis

To test the generated hypotheses and be able to answer the sub-question *"What are the main driving mechanisms for the vertical deformation of the tram tracks?"*, a sensitivity analysis is performed. To get a clear view of the influence of the parameters, only one cross-section will be elaborated. For simplicity, only cross-section 2 will be tested, because the soil layers are symmetrical.

The following range of parameters is used for the sensitivity analysis:

- **Weight of the structure**
  For the weight of the structure, the displacements due to the weight of ballast, grass and pavement are compared.
- **Holocene deposits**
  The effect of replacing the *Silty peat*-layer with a *Weakly sandy clay*-layer on the total settlements is evaluated. The influence factor is based on the increase in E_{oed}-value. This is gives a theoretical indication of the influence of the difference of the parameters used for these soft Holocene deposits on the displacements of the structure.
- **Ground water table**
  The effect the Ground Water Table variation from NAP -1.75 [m] and NAP -2.95 [m] is investigated. The reference situation is NAP -2.30 [m].
- **Dynamic loading**
  The effect of the loading of the vehicles on the settlements is investigated by lowering the DAF from 1.6 to 1.5, 1.4 and 1.3.
- **Height of the concrete plate**
  The effect of increasing the height of the concrete plate on the displacements will be evaluated with and without loading of the trams.
- **Strength class of concrete**
  The effect of increasing the strength class of the concrete plate on the displacements will be investigated. This parameter is mainly of interest under loading conditions, since has minimum influence on the self-weight and the deflections of the structure. The current strength class is C25/30 with E = 31 [GPa]. Increasing the strength class to C30/37 or C35/45 result in an increase of the E-modulus to respectively 33 and 34 [GPa].

In figure 3.27, the results of the sensitivity analysis are displayed in a graph.

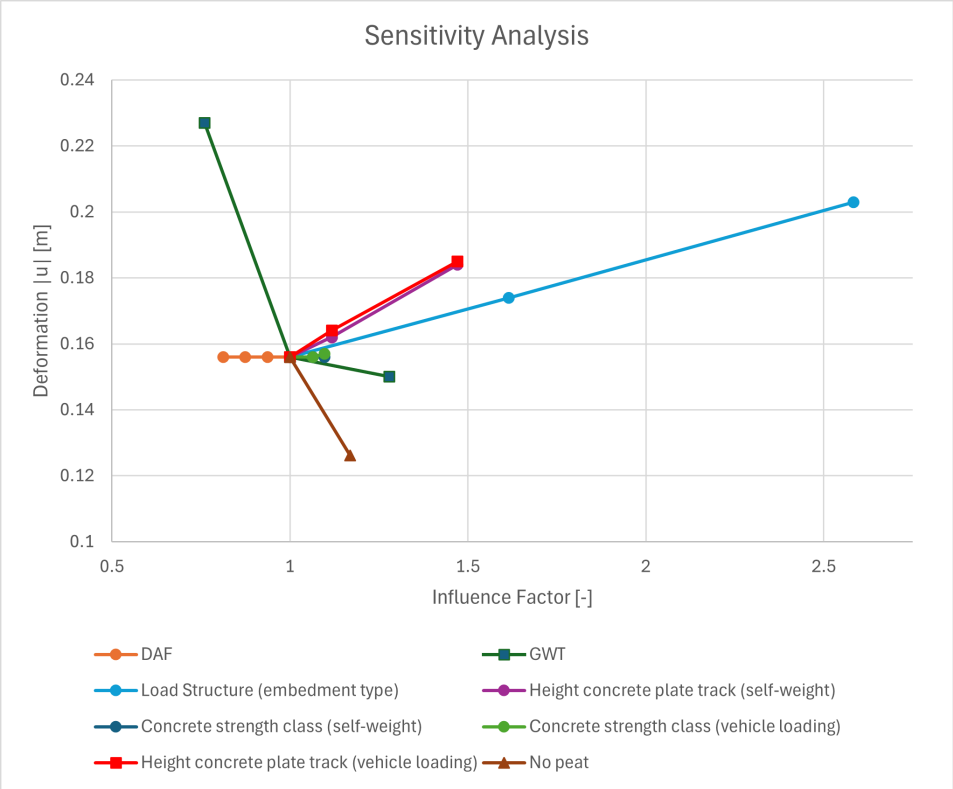

Figure 3.27: Sensitivity Analysis Existing Structure

The main findings from this sensitivity analysis are as follows:

- There is no difference in final settlements when the wheel-load of the tram is taken into consideration.
- Reducing the DAF from 1.6 to 1.3 has no influence on the total settlements. The wheel load is only 0.13 [kN], which is significantly smaller compared to the self weight of the structure. This 0.13 [kN] already has no effect on the final settlements of the structure over 30 years. Therefore, changing the DAF has little influence on the magnitude of the wheel load and therefore on the total settlements of the tram track structure.
- Increasing the Ground Water Table to the highest measured level, which is NAP -1.75 [m], gives a significant increase in track deformation. The sand layer is almost fully saturated, which results in a decrease of the effective stresses. The total settlements are 0.227 [m], which is 45.5 % higher compared to the settlements for a Ground Water Table of NAP - 2.30 [m]. Lowering the Ground Water Table to 2.95 has a little effect on the total settlements, which reduces from 0.156 [m] to 0.150 [m].
- Increasing the stiffness of the soil layers reduces the settlements with 19.1%.
- Embedding the track in grass or asphalt increases the self-weight and therefore the total settlements of the structure. Compared to a track covered with ballast, the settlements increase with 11.5% for a track embedded in grass and 30.1% for a track embedded in asphalt.
- Increasing the height of the concrete slab to 19 [cm] or 25 [cm] increases the settlements with 3.8 % and 17.9 % respectively. The increase of the self weight of the structure is more significant compared to the spread of the weight of the vehicle.
- Increasing the strength class of concrete from C25/30 to C30/37 or C35/45 has no effect on the settlements for both loading conditions. This makes sense since the weight of the structure remains unchanged.

3.7. Problem Location - Pit next to roundabout Groeninx van Zoelenlaan

Based on the PLAXIS calculations, the differential settlement of the tram track structure at the roundabout compared to the surrounding roads can be clarified. However, the extreme settlement rate and observed damages and distresses at the pit from figure 1.2 cannot be clarified based on the regular settlement behaviour of the plate. The settlement rate at the location of the pit is 6.7 [mm/year]. However, the settlement rate of the tram track structure at the roundabout is 4.0 [mm/year] and PLAXIS predicts a settlement rate of 4.3 [mm/year]. Therefore, there is a different cause for these excessive settlements.

One or a combination of the following points clarify the excessive settlements at this location:

1. **Different construction stage**
   The tram line towards shopping center Keizerswaard (on the left) was constructed in 2014, which is later than the roundabout. To reduce the settlements for the new tram line, the soil was preloaded. A curve in the vertical alignment was foreseen in the original design to connect the newly built track and the (settled) roundabout. This connection has **not** been preloaded. Since the connection is built more recently, the settlement rate is higher compared to the existing track structure, for which consolidation has already largely taken place. Based on the PLAXIS simulation for the roundabout, the settlement rate 6 years after construction is 5.7 [mm/year]. So, this differential settlement eventually leads to a pit in the vertical alignment. Then, water flows to the pit and the sand fill layer underneath gets saturated. The dynamic loading of the tramway causes this saturated sand fill to flow out from under the structure, hence leading to more severe track deflections under dynamic loading conditions.
2. **Transition zone**
   Due to the differential settlements between the roundabout, preloaded track structure and the pit, a transition zone occurs. Moreover, the preloaded track structure and the roundabout are characterised by a different vertical track stiffness support compared to the problem location. As was mentioned during the literature study, this difference causes dynamic amplification of the wheel loads, hence resulting in further track degradation.

3.8. Overview Problem Sections

So, based on the observed distresses in the introduction of this research, the InSAR-satellite data and the geotechnical calculations, three different sections with different problems can be distinguished. These three sections are indicated 3.28.

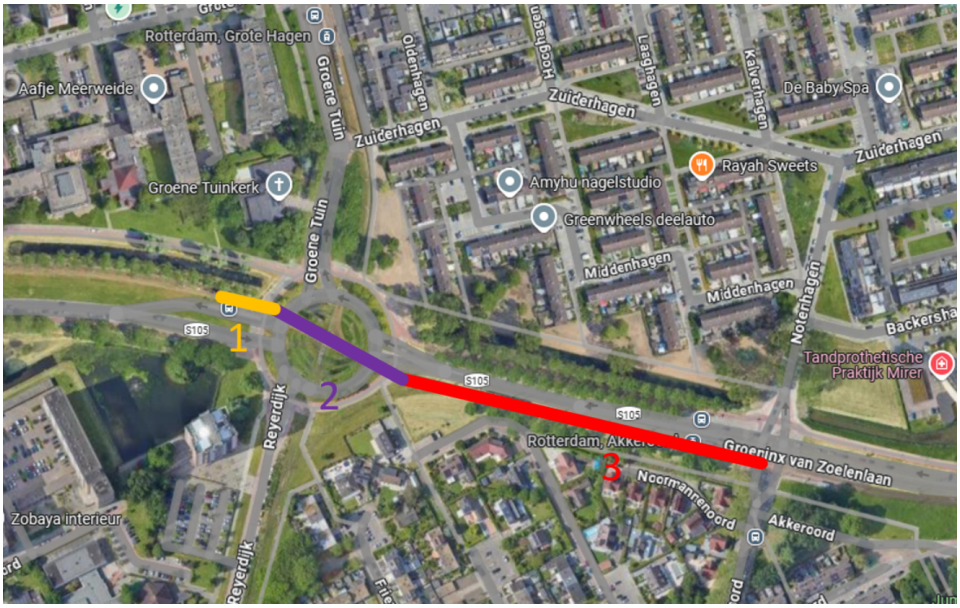

Figure 3.28: Case study location - Problem sections (based on [15])

- **Section 1**
  Section 1 has the most severe problems compared to section 2 and 3. This location is built in 2014 to make a connection between the new track towards shopping center Keizerswaard and the roundabout, which was built in 2008. This location has a higher settlement rate (6.7 [mm/year], [4]) than the preloaded track (west from section 1) and the roundabout (section 2, 4.3 [mm/year]). Therefore, this zone is characterised as a transition zone.
  Moreover, due to the higher settlements and the curve from the design in the vertical alignment, section 1 is the lowest point in the area, which results in waterlogging. The sand fill foundation layer above the low-permeable clay layer underneath the track gets fully saturated. Under dynamic loading conditions, such as a passage of a tram, the sand fill layer is flushed out from underneath the slab track.
  In this area, waterlogging occurs. Furthermore, the track deflects under loading. Application of the emergency brakes was reported when the protective shield touched the surface level. Moreover, serious pavement distresses are observed in the cycle lane and the sidewalks directly next to the track structure.
  The following problems should be tackled to mitigate these problems:
  - Minimize the differential settlement between the track structure and the surrounding infrastructures
  - Avoid abrupt changes in vertical stiffness of track support
  - Install an appropriate drainage system to allow water outflow from the sand fill layer.
- **Section 2**
  Section 2 is at the center of the roundabout. This section settles more (4.3 [mm/year]) compared to the surrounding roads (3.1 [mm/year] [4]). Waterlogging occurs. This is unwanted for the sanding system of the vehicles. However, no extreme deflections under dynamic loading conditions are reported. For this location, the following two points should be tackled:
  - Minimize the differential settlement between the track structure and the surrounding infrastructures
  - Install an appropriate drainage system to allow water outflow from the sand fill layer.
- **Section 3**
  Section 3 settles with 4.3 [mm/year]. No differential settlement rate between the roads and the track structure are observed [4]. Furthermore, no waterlogging or distresses are observed. Therefore, no measures or construction works have to be undertaken at section 3.

3.9. Conclusion

Based on the PLAXIS Simulation and sensitivity analysis results, the following conclusions can be drawn:

- The autonomous settlements at the case study location are 2.4 [mm/year].
- The most significant driving mechanism is a too high ground water table. This results in a decrease in effective stresses and higher total settlements. Providing a proper drainage system is necessary to avoid excessive deformations.
- The weight of the structure is the second most driving mechanism for the total settlements. When the track is fully embedded in asphalt instead of ballast, the total settlements over 30 years increase with 25.8%.
- The thick layer of Holocene deposits, especially layers of peat, worsen the vertical settlements over 30 years.
- The wheel-load of the vehicle has no influence on the final settlements over 30 years. The wheel-load is only 0.13 [kN] when a DAF of 1.6 is used, which is a significantly smaller order of magnitude compared to the self-weight of the structure. Therefore, measurements which should help spreading the weight of the structure, such as a concrete class with a higher stiffness or structural height, do not have this result. Moreover, increasing the structural height increases the self-weight of the track, which results in higher settlements over 30 years. However, the deflections of the structure of the structure can be reduced with a higher structural height, but that is not the goal of this research.
- The extreme settlement rate at the pit from figure 1.2 is higher due to the fact that this location was improperly designed. This point is located at the connection between a newly built track structure and the settled roundabout. The newly built track structure is preloaded and has limited settlements. Furthermore, the roundabout has a lower settlement rate compared to the pit, since the most part of consolidation has already taken place. These differential settlements lead to a pit in the vertical alignment, resulting in waterlogging, a saturated sand fill foundation and outflow of this material. Moreover, this zone is a transition zone, which is characterised by dynamic amplification of the wheel loads. This leads to more excessive settlements and track degradation.

In short, the main driving mechanisms are as follows:

- Subsoil consists of thick layers of Holocene deposits, which are soft soils
- High Ground Water Table
- Self-weight of the structure
- The transition zone between the preloaded track, roundabout and the connection in between these two

So, this answers the first sub-question, *"What are the main driving mechanisms for the vertical deformation of the tram tracks?"*

In conclusion, in order to reduce the settlements of the structure, the structure should be lifted to its original level. However, light-weight filler material should be used to minimise the effect of primary and secondary consolidation. In addition, a proper drainage system should be installed to avoid a saturated layer of sand fill.

3.10. Discussion and recommendations

The following points should be taken into consideration when interpreting the results:

- The permanent loading of the trams is an appropriate method to speed up modelling and computation time for the total settlements of the structure over 30 years. However, this is not the actual loading condition, where trams are loading the structure 6 times per hour for 5 seconds.
- The data in table 3.3 and 3.6 are calculated based on Automated Parameter Determination Software, which is based on the interpretation of CPTs. However, to determine the PLAXIS input parameter more accurately, geotechnical laboratory tests (such as triaxial tests) should be performed on the project location. However, for this research, the APD data is considered sufficiently accurate to get an estimation of the settlement behaviour over 30 years.
- The InSAR data is measured on a trend from 2017 to 2022 and shows a linear plot. However, primary and secondary consolidation have a logarithmic correlation with the loading over time. To get more accurate insight in these measured settlements over time, a longer reference period is preferred. This would improve the accuracy of the validation method.
- The InSAR satellite measurements are performed with different satellites and sensors, which are characterised by different measurement frequencies and accuracies [51].
- The influence of the self weight of road structure parallel to the tram track and the passing vehicles on the Groeninx van Zoelenlaan was not taken into consideration.
- The hydraulic conductivity of the soil layers and the seepage at the boundary conditions is considered constant. However, the effect of vibrations of the passing trams on the microstructure and therefore the hydraulic properties of the subsoil have not been taken into consideration. In general, a higher vibration frequency leads to the development of soil pores, which increases the permeability k of the soil. Moreover, the pore water pressure increases, which results in a lower effective stress σ' [53]. In extreme cases, these vibrations can lead to liquefaction of the soil. However, for this location, the line frequency of 10 minutes and the relatively low track speed, the influence of vibrations on the microstructure of the subsoil is assumed to be negligible.
  To further investigate and study this effect in detail, pore pressure sensors should be installed. The layer of interest is then the low-permeable first clay layer to check the increase and dissipation of the pore water pressure after the passage of a tram.

4

Track Settlement Mitigation Measures

Now that the main driving mechanisms for the vertical settlements are known, effective state-of-the-art settlement mitigation measures can be selected. To assess the effectiveness of these settlement mitigation measures, these improved structures will be modelled in the validated PLAXIS 2D model from Chapter 3. So, this chapter is focussed on answering the following research question: "*Which state-of-the-art engineering solutions could mitigate the vertical settlement of the tram track on the soft soil?*"

In this chapter, the following sections are elaborated:

- 4.1 Design criteria
- 4.2 State-of-the-art engineering solutions
- 4.3 Assessment and simulation method
- 4.4 Select innovations: Multi-Criteria Decision Analysis
- 4.5 PLAXIS 3D Model
- 4.6 Dimensioning and structural calculations
- 4.7 PLAXIS 2D Simulation - Results
- 4.8 Conclusion
- 4.9 Discussion and recommendations

4.1. Design Criteria

First of all, design criteria have to be set up in order to select and assess the potential performance of the proposed mitigation measures. Moreover, these criteria can also be used to compare the performance of the different mitigation measures.

- **Design lifetime**
  The main goal is to increase the lifetime of the structure without significant maintenance works. Therefore, the settlements of the tracks should not be higher than the surrounding infrastructures. According to InSAR-data, the settlement of the surrounding roads between 2017 and 2022 differs between 2.4 and 4 [mm/year]. Not all these data points have the same accuracy. The data point with the highest accuracy at the roundabout nearby the pit towards Keizerswaard has a settlement rate of 3.1 [mm/year] [4]. The roads are raised to the original level once every 30 years. For the RET, it is therefore preferred to increase the lifetime of the track structure to **30 years** in order to carry out maintenance works at the same time with the municipality, which reduces maintenance costs and inconvenience for the passengers and neighbouring residents. This implies that the settlement rate of the structure should be reduced about to 3.1 [mm/year] 12 years after construction.

- **Bearing resistance**
  The main function of the structure is to bear the wheel load of the trams and distribute the load to the subgrade. When light-weight mitigation measures are proposed, one must check if the material can withstand the dynamic loads of the vehicle and not only if the settlement of the track is reduced due to the self-weight and the distributed load over 30 years. Furthermore, the change in stiffness of track support has its effect on the occurring bending moments in the concrete slab and ensure that these do not exceed f_{ctm}.
- **Performance in saturated or undrained condition**
  As was mentioned in the previous chapter, the high ground water table has a significant influence on the settlements of the structure, especially when there is a risk that the structure settles below the ground water table. Moreover, there is a risk that when mitigation measures are installed in the sand fill layer underneath the structure, certain parts of the structure settle below the ground water table. This risk and the performance of the (partly) immersed and saturated elements should be evaluated.
- **Material failure**
  The possible failure modes and their probability should be evaluated.
- **Structural durability and maintainability**
  Furthermore, if the unlikely occasion of failure occurs, the effect on the remaining bearing capacity performance of the structure should be evaluated. For example, does failure only lead to a slight reduction of the design lifetime, or are a track speed restriction and maintenance activities directly necessary? Moreover, the transition zone between the roundabout and the track towards Keizerswaard requires extra attention in the track design.

The sustainability requirements and improvements are separately discussed in chapter 5. However, taking the sustainability optimisation already in consideration, concrete slab tracks built on a pile foundation are completely excluded based on the high amount of required construction materials.

4.2. State-of-the-art engineering solutions

Road and railway engineers all over the world encounter geo-engineering difficulties regarding settlements and embankment stability. This sections contains a literature review of state-of-the-art engineering solutions that could mitigate the settlements of a concrete tram track structure on soft soils.

4.2.1. Rockwool: Rockflow

Rockflow is originally developed by Rockwool Rainwater Systems as an extra water infiltration system. In the urban environment, there are many paved surfaces. The precipitation is directly diverted to the sewage system. In older sewage systems, the rainwater and precipitation is combined and directly transported to the wastewater treatment plant. In case of extreme precipitation, the sewage can overflow and discharge water directly in nearby ponds/canals. Note that this water was not cleaned in a water treatment plant, which therefore has a negative influence on the water quality of the ponds or canals onto which the water was discharged [54]. The Rockflow infiltration system consists of stone wool block elements, which can be installed underneath paved surfaces, such as roads and concrete slab tracks. In Amsterdam, the Rockflow infiltration has already successfully been installed underneath the tram track structure and provides sufficient bearing capacity for the trams. The rockwool elements have a void ratio of 95%, which can provide in this case a water buffer capacity of 565 [m^3] and is designed for a downpour of 60 [mm/hour] [55]. An illustration of this solution is displayed in figure 4.1.

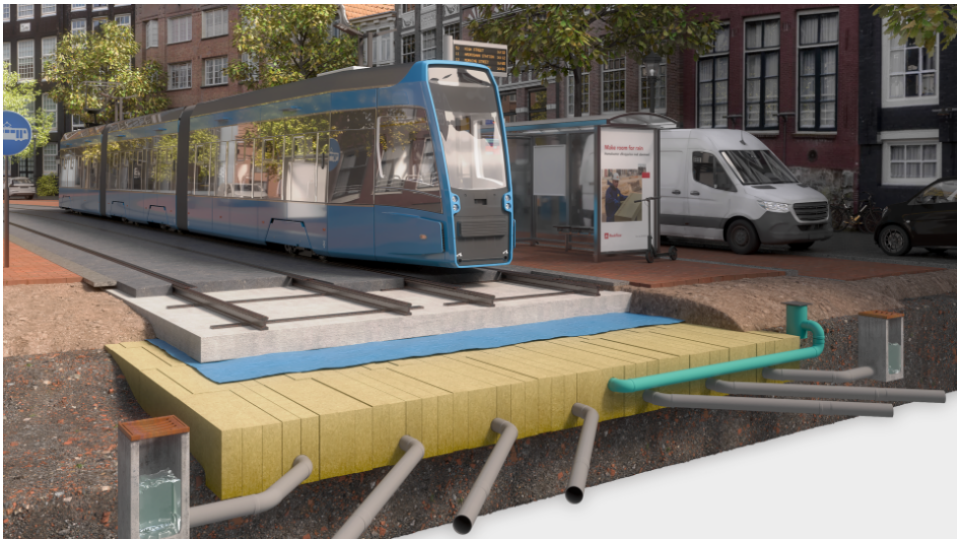

Figure 4.1: Illustration of the Rockwool elements underneath a concrete slab track structure [56]

Drainage gullies are installed parallel to the slab track structure. Water flows through the gullies and pipes to the bottom of the stonewool elements. The voids in the stonewool are filled with water. Air vent pipes are installed into the system to release air from the stonewool elements when being filled with water. This pipe is displayed in blue in figure 4.1. When the water is stored in the stonewool elements, it can either subsequently slowly infiltrate into the ground water or be diverted into the sewage system. Sometimes, the water can be used to irrigate nearby vegetation [57]. In areas with a high ground water table, the infiltration possibilities are minimised [58]. In this situation, the slow run-off to the sewage still has a positive effect, because the risks of overflow are minimised. Furthermore, although rainwater is considered to be relatively clean, pollutants can be filtered out in the stonewool elements. Moreover, stonewool elements are already used in Scandinavia underneath heavy rail tracks to provide damping and reduce vibrations [59], [60]. Gatzwiller reported in 2008 that fatigue tests have shown that the dynamic stiffness of stone-wool anti-vibration solutions remains constant over 100 million fatigue load cycles [60]. However, the effect of vibrations on the surrounding area are beyond the scope of this research.

Apart from the sustainability advantages, another main advantage of the stonewool elements is the low-self weight, which is only 163 $[kg/m^3]$ for the Rockflow WM2007. When the stonewool elements are fully saturated, this weight increases to 10.8 $[kN/m^3]$ [61]. Moreover, the outflow of sandfill underneath the track structure is already minimised.

The general material parameters for the Rockflow WM2007 are listed in table 4.1. If a linear elastic material model is used for computer simulations, an E-modulus of 21 [MPa] can be used [62].

Table 4.1: General material parameters for Rockflow WM2007 [61], [63]

	Value	Unit
Porosity	94%	[-]
Void ratio	15.7	[-]
Unit weight (effective)	1.63	$[kN/m^3]$
Unit weight (total)	10.8	$[kN/m^3]$
$\sigma_{max,static}$	110	[kPa]
$E_{50,10\%sat}$ - 10% saturation	7	[MPa]
$E_{50,100\%sat}$ - 100% saturation	$0.66 \cdot E_{50,10\%sat}$	[MPa]
$E_{resilient}$	45	[MPa]
φ	53.4	[°]
c	17.8	[kPa]
ν	0	[-]
k_x/k_y	80	[m/day]

4.2.2. Geosynthetics

Geosynthetics, such as geocells, geogrids and geotextiles are widely used in road and railway applications. These geosynthetics are a cost-effective measure to reduce the layer-thickness of the unbound foundation layers whilst maintaining or increasing the durability of the structure. These systems provide a lateral constraint, especially when subjected to a vertical wheel load. This increases the stiffness of the foundation layer, which improves the load distribution to the subgrade and reduces the stresses on the subgrade [64]. Moreover, this stress-reduction should reduce the settlements of the structure.

The application of geogrids and geocells are common practise in the construction of conventional ballast tracks. Both systems are displayed in figure 4.2 below.

(a) Application of Tensar Geogrids in Romania [65]

(b) Installation of geocells to stabilise the sub-ballast [66]

Figure 4.2: Application of geosynthetics in conventional ballast track construction

A schematic representation of ballast interlocking and a possible location of geogrids in the subballast

layer are displayed in figure 4.3a and 4.3b respectively.

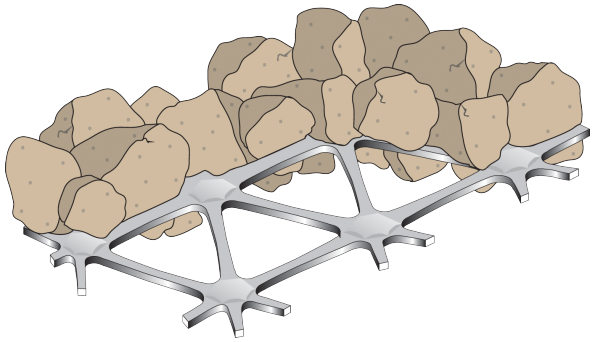

(a) Ballast interlocking by a geogrid [67]

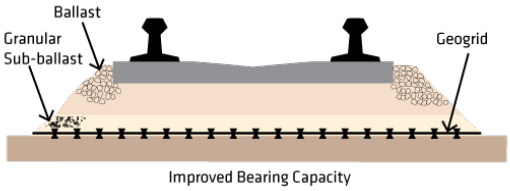

(b) Sub-ballast stabilisation by a geogrid [68]

Figure 4.3: Schematic impression - geogrids in conventional ballast track

Geocells have successfully been applied in the UK national railway network at several locations. The sub-ballast height can significantly be reduced whilst preserving the vertical alignment of the railway line. For example, the Willesden North crossing case study has shown that on soft soil conditions, the track settlement reduced with 55%. The sub-ballast height reduced from 550 to 200 [mm] [69].

Yaba reported that Network Rail has performed a comparable study for the application of geogrids. The settlement rate was reduced from 40% up to 72% for certain cross-sections [70].

In conclusion, geosynthetics are a well-proven technology to reduce settlements of a conventional ballast track. Moreover, reducing the height of the sub-ballast layer reduces required material used to construct the railway line and hence reduces the total carbon footprint of the project.

4.2.3. Light-weight filler material

Moreover, to reduce the settlements of the infrastructures, light-weight filler material should be used instead of sand. For sand, a dry self weight ($\rho_{sand,dry}$) of 1800 [kg/m^3] is assumed. A wide variety of these materials are available, such as [71]:

- Foam Glass (ρ = 400 [kg/m^3])
- Bims (800 < ρ < 1200 [kg/m^3])
- Light-Expended Clay Aggregate (LECA, 700 < ρ < 900 [kg/m^3])
- Foam Concrete (400 < ρ 1600 [kg/m^3])
- EPS (15 < ρ < 100 [kg/m^3])

These materials have a great potential to reduce the settlement of the tram track structure. In combination with the geosynthetics from the previous subsection 4.2.2, sufficient stiffness can be provided. However, attention must be paid to the following points:

- Some of the materials have a lower density than water ($\rho_{water} = 1000[kg/m^3]$). The risk of buoyancy or outflow of the material must be avoided, for example by wrapping the layer in geotextile.
- The crushing resistance must not be exceeded. For some materials, this resistance is rather low. For example, for glass foam from Glasopor AS, the crushing resistance is 770 [kPa] [72]. Note that the stresses under dynamic loading conditions can be significantly higher compared to the self-weight of the structure. The stresses underneath the concrete slab must not exceed the crushing resistance of the material. If there is a risk of exceeding this threshold, a layer of sand fill between the concrete plate of the track structure and the light-weight filler material is necessary. For a conventional ballast track with a track speed of 146 [km/h] and trains with an axle load of 225 [kN], a vertical stress of 460 [kPa] has been reported by Chen, Indraratna, McDowell, *et al.* [73]. However, this load is the applied stress on the ballast bed. The unbounded aggregate particles have a smaller contact contact area, which are therefore characterised by higher contact stresses.

For the tram track structure, the applied stresses are expected to be lower due to the lower axle loads, track speeds and a more efficient load distribution compared to sleepers. However, this does not give any information about the contact stresses between the particles.

- Under dynamic loading conditions, the ballast bed is characterised by settlements due to compaction of the unbounded ballast aggregates. These settlements can add up to 1 [cm] in the first 1,000 loading cycles, even when a geogrid is applied [73]. This value is significant compared to the predicted settlements of 15 [cm] at the cross-section nearby tram-stop Akkeroord (cross-section 2).

Foam glass

Foam glass is a light-weight filler material that is made from 100% recycled glass with good drainage capabilities. As a first step in the manufacturing process, the wet glass is dried. Subsequently, the glass is milled to powder. Then, this powder is mixed with a foaming agent (usually silicone carbide). At last, this mixture is heated in a rotary kiln to a temperature between 800 - 900 °C. The glass particles melt together. The foaming agent reacts with the ambient air, which releases gases that result in the pore structure of the aggregates [74].
The particles visually resemble to ballast particles and have a grain size distribution between 10 - 60 [mm]. For several Scandinavian infrastructure projects, such as the Bergen Light Rail and highways in Norway, foam glass from the company Glasopor AS has been used as a light-weight and sustainable filler material. The material has a dry density of 180 [kg/m^3] and a saturated density of 380 [kg/m^3]. This lower than the density of water. The maximum static load is 80-120 [kPa]. The crushing resistance is only 770 [kPa], which might be exceeded under dynamic loading conditions [72]. The unaxial dynamic behaviour of glass aggregates under different compaction ratio's was studied by Mustafa and Szendefy for a deviatoric stresses up to 200 [kPa]. For a deviatoric stress of 200 [kPa], a compaction ratio of 40% is required to provide a stable foundation under the track [75]. In the Netherlands, glass foam has been mixed with cement, in situ clay and the Geosta® additive and used as a road foundation. However, additional research is required to find the correlation between the mixing circumstances, the final strength and stiffness properties and how this leads to a reduction in height of the foundation and asphalt layers [76].

Bims

Bims is low-weight, volcanic type of rock that is widely used as a light-weight filler material in road construction. A well-known type of Bims is YALI®-bims, which is mined at the Greek island Gyali and has extensively been used in the Dutch construction sector [77]. Furthermore, there are other type of volcanic bims, which are mined for example in the Eiffel-region in Germany or in Turkey [78].

Light-Expanded Clay Aggregate (LECA)

LECA granulates are created by sintering clay at a high temperature. These aggregates have a strong shell and weak porous centre. Due to the voids, this porous material has a low density [79]. However, these porous aggregates can absorb significant amount of water, hence resulting in a higher particle density [80]. Expanded Clay and Shale materials were used in the construction of a highway embankment on soft soils in Arlington, Texas. A PLAXIS FEM Analysis validated with field measurements has shown that the total settlements of the embankments were reduced with $\frac{2}{3}$ due to the use of this low-weight filler material [81]. The crushing resistance is correlated to the diameter of the aggregate [79]. For aggregates from Argex NV with a 4/10 [mm] grading, a crushing resistance of 1.20 [N/mm^2] is reported. The particle density is 1090 [kg/m^3], but the lower bound for the loose bulk density is 366 [kg/m^3] [82].

Foam Concrete

Replacing the sand fill foundation layer of road and railway structures with a layer of foam concrete reduces the weight on the soft soil layers and therefore minimises the settlements [83]. Foam concrete is a mix of cement, water, filler, admixtures and foam. Foam concrete is available in a wide range of densities (from 400 to 1600 [kg/m^3]). In general, a higher density results in a higher cubic compression strength [84]. Attention must be paid to floating of the structure due to the high ground water table. Moreover, if necessary, local and temporary drains should be installed to lower the ground water table during construction of the foam concrete foundation slab [83].

EPS

Expanded Polystyrene (EPS) is the filler material with the lowest density. Originally, EPS geofoam was developed and used in Norway as a light-weight filling material to protect the subsoil against freezing, which is common for the extreme Scandinavian climate conditions [80], [85]. EPS is made of Styrene monomers, a liquid hydrocarbon made from petroleum. During a polymerisation process, these monomers are converted to solidified beads, which are eventually used for the EPS production. A blowing agent is added to the beads. When these agents evaporate due to heat or when being exposed to steam, the material expands and the cellular structure of the material is formed. At last, the hot EPS is moulded in blocks and cools down [80], [86]. The Young's modulus of EPS is related to the density. This dependence is described by the following equation, with ρ_{EPS} in [kg/m^3] and E_{EPS} in [MPa] [80]:

$$E_{EPS} = 0.1284\rho_{EPS}^{1.368} \tag{4.1}$$

EPS has limited water absorption capacity. Furthermore, the low temperatures, water absorption and freeze-thaw cycles do not have a negative effect on the mechanical properties of EPS. Moreover, the thickness of the EPS-layer has little influence on the stresses and strains in the pavement layer [80].

The potential of an EPS subbase layer underneath a ballastless railway track structure has already been studied by Esveld, Markine, and Duškov in 2001 [87]. The weight of the removed soil should balance with the weight of the newly-built track structure plus the light-weight filler material. Due to the low weight and stiffness of EPS, it cannot be placed underneath a conventional ballast track structure. However, this research does not include the performance of a test track with an EPS sub-base under operating conditions. Furthermore, the authors recommended to formulate uniform design criteria [87].

The Norwegian Public Road Administration (Statens Vegvesen) has monitored and studied the durability performance of the road structures where EPS was used as light-weight filler material. No degradation of the material (strength) properties were observed. The only failure of the structures that were reported occurred due to excessive buoyancy forces caused by more extreme fluctuating water levels than originally accounted for, such as floodings [85].

4.2.4. Overview engineering solutions

In table 4.2, an overview is given of the material performance based on the defined design criteria.

Table 4.2: Overview of state-of-the-art engineering solutions

	Rockwool	Foam glass	Bims	LECA	Foam concrete	EPS
Density	Due to the limited infiltration capacity, the elements are considered to be fully saturated. The density is 1080 [kg/m^3] [61].	The saturated particle density is 380 [kg/m^3] [72]	The density of Bims varies between 800 and 1200 [kg/m^3] [71]. For certain manufacturers and mining locations, densities of 750 [kg/m^3] (Eiffel) or 900 [kg/m^3] are reported [78].	Values are reported between 700 and 900 [kg/m^3] [71].	There is a wide variety available, which is related to the required mechanical strength properties. Densities are reported between 400 and 1200 [kg/m^3] [88].	Densities are reported between 15 and 100 [kg/m^3].
Bearing resistance	For linear-elastic calculations, the E-modulus is 21 [MPa] [62]. The E_{50}-modulus for a fully saturated element is 4.62 [MPa] [61]. The maximum static pressure is 110 [kPa] [61].	The crushing resistance is 770 [kPa]. The maximum static load pressure is 80 - 120 [kPa] [72]. A compaction ratio of 40% is necessary to obtain a stable foundation under 200 [kPa] cyclic loading [75].		The crushing resistance for aggregates from Argex NV with a 4/10 [mm] grading is 1.20 [MPa].	At 28 days, the E-modulus ranges between 300 and 5800 [MPa]. The cubic compressive strength varies between 0.5 to 6.0 [MPa].	The E-modulus is related and can be calculated by using equation 4.1 [80].

Continues next page..

	Rockwool	Foam glass	Bims	LECA	Foam concrete	EPS
Performance saturated/undrained conditions	Elements can get fully saturated and remain their strength under static and dynamic loading conditions. There is no risk of buoyancy or outflow of the material.	There is risk of buoyancy and outflow of the material. The bulk layer of foam glass should be wrapped in geotextiles to avoid outflow of the elements.	The risk of buoyancy is related to the density of the used Bims. The bulk layer should be wrapped in geotextiles.	There is risk of buoyancy and outflow of the material. The bulk layer of foam glass should be wrapped in geotextiles to avoid outflow of the elements.	There is minimum influence of water absorption on the material characteristics. The buoyancy of the material should be checked.	There is a high risk of buoyancy. Accidents reported during floodings in Norway [85]. There is no risk of outflow of the material. Water absorption, low temperatures and freeze-thaw cycles do not have a negative effect on the mechanical properties of EPS [80].
Material failure	There is no risk of brittle failure under compression. Moreover, there is no risk of outflow or buoyancy of the material.	The occurring stresses under dynamic loadings conditions must be checked if these do not exceed the crushing resistance of the aggregates. Moreover, there is a risk of outflow of the material. In addition, buoyancy should be checked.		The occurring stresses under dynamic loadings conditions must be checked if these do not exceed the crushing resistance of the aggregates. Moreover, there is a risk of outflow of the material. In addition, buoyancy should be checked.	There is no risk of outflow of the material. The risk of buoyancy should be checked for the highest possible ground water table level. Moreover, the maximum cubic stress should not be lower than the maximum stresses under dynamic loading conditions.	There is a severe risk of buoyancy due to the low density of the material, the high water table and poor drainage conditions. There is no risk of brittle failure or outflow of the material.

Continues next page..

	Rockwool	Foam glass	Bims	LECA	Foam concrete	EPS
Structural durability and maintainability	The stonewool elements creep with only 2% over a period of 50 years. There is no risk of damage due to damage by tree roots [89]. All other mechanical properties, such as the density and dynamic stiffness, remain constant over the lifetime of the structure [60]. It is recommended to inspect and clean the infiltration channels to remove sediments [89]. Note that when not being designed properly, differential settlement between the elements could occur, resulting in a locally unsupported track structure. Repairs cannot be made without removing the track structure.	Excessive deformations could occur when not compacted properly. Furthermore, crushing of the aggregates could lead to excessive deformations. Repairs cannot be made without removing the track structure and unwrapping the geotextile.	Excessive deformations could occur when not compacted properly. Repairs cannot be made without removing the track structure and unwrapping the geotextile.	Excessive deformations could occur when not compacted properly. Repairs cannot be made without removing the track structure and unwrapping the geotextile.	When differential settlements still occur underneath the foam concrete slab, the effect is assumed to be small due to the beam action from the foam concrete and the slab track. If necessary, expanding material can be injected between the concrete slab track and the foam concrete, comparable to the Uretek floorlift method [90]. When using this method, the concrete slab track structure does not have to be removed.	When not being designed properly, differential settlement between the elements could occur, resulting in a locally unsupported track structure. Repairs cannot be made without removing the track structure. However, a study of the Norwegian Public Road Administration has shown that the material (strength) properties of EPS remain constant over the life span of the road structures. Therefore, EPS is a durable light-weight filler material [85].

Continues next page..

	Rockwool	Foam glass	Bims	LECA	Foam concrete	EPS
Sustainability	There is a reference service lifetime of 40 years. However, in practice, the life-time will be well beyond 40 years. At the end-of-Life-stage, 50% of the material will be reused in new Rockwool products, whereas the other 50% is brought to a landfill as a basic scenario [91]. Furthermore, the material reduces the runoff the the sewage system, provides irrigation possibilities for vegetation and filtrates the water [57], [91].	The Glasopor AS glass foam aggregates are fully made of recycled glass from households in Norway. According to the manufacturer, all the aggregates can directly be reused without treatment at the end-of-life-stage [74].		The majority of clay aggregates can be reused. The EPDs of multiple producers report different percentages of reused aggregates in the end-of-life stage in the LCA (25% landfill for [92], 5% landfill for the Dutch market [93]).	Foam concrete is fully recyclable [88].	EPS production is based on a petrochemical process [80], [86]. For the recovery of EPS used as insulation material, a conservative scenario based on incineration and energy recovery is assumed [94]. However, EPS can be used in the production of new EPS, which reduces the need for raw materials [95].

4.3. Assessment and Simulation Method

Based on the design criteria and findings from the literature study, the most suitable innovations for the project location are selected. Subsequently, the thickness of the layers of the installed materials is determined and sketches of the cross-sections are provided. The improved structure is checked for buoyancy (if necessary). Furthermore, the effect of changing the foundation on the structural strength parameters of the track structures are evaluated. If necessary, the thickness of the material layers are altered if the buoyancy or strength criteria are not met.

For the tram track structure, the following structural strength parameters are evaluated:

- **Deflection of the rail**
  To properly calculate the deflection of the rails on soft soil, the PLAXIS 2D model is converted to a 3D model in PLAXIS 3D. In PLAXIS 3D, the rail deflection due to a point load can be calculated. Considering the transition zone problem, a difference in vertical stiffness of track support must be avoided. Therefore, the rail deflection of the improved structures must be comparable to the existing structure to avoid dynamic amplification of the wheel loads and excessive track degradation.
- **Internal stresses and cracking of the concrete slab**
  The stresses and bending moments in the concrete slab can be calculated from the PLAXIS 3D output as well. These stresses must not exceed the mean concrete tensile strength f_{ctm}. When this maximum tensile strength is exceeded, cracks could form.

Then, the engineering solutions are modelled in the validated PLAXIS 2D model to determine the long-term settlement behaviour of the plate. Two distinctive scenarios are evaluated:

- **Scenario 1 : Application in the original design**
  In order to make a good comparison with the existing structure, the exact same simulation is performed for the improved designs as for the existing structure from Chapter 3.
- **Scenario 2 : Replacement of the existing structure in 2026**
  The second scenario is based on the replacement of the structure in 2026. The tram line was originally constructed in 2008. This means that when the structure is rebuilt in 2026, the soil has already been preconsolidated. A conventional elevation with a sand layer of 20 [cm] is already foreseen for cross-section 1. This is slightly higher than the PLAXIS calculation of 18 [cm]. This can be explained by the fact that the actual settlements were higher due to the outflow of the sand from the saturated sand layer under dynamic loading conditions.

After the simulation, the results are discussed and conclusions about the most appropriate engineering solutions a drawn. One or multiple solutions are then proposed for the final improved structure. A flowchart of this approach is displayed in figure 4.4.

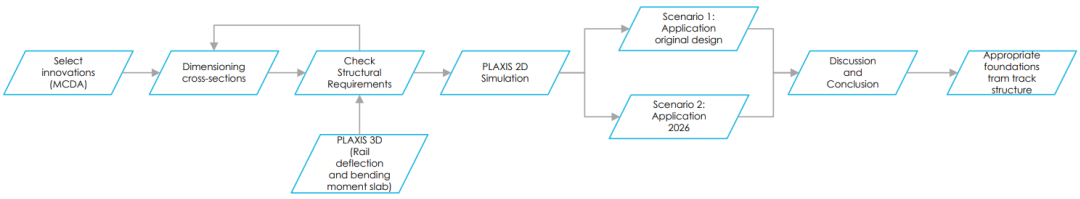

Figure 4.4: Flowchart assessment state-of-the-art engineering solutions

4.4. Select innovations: Multi-Criteria Decision Analysis

To select the most promising innovations underneath the track structure, a Multi-Criteria Decision Analysis (MCDA) is performed. The selected criteria are the design criteria as listed in section 4.1. The potential performance is rated '- -' (very negative), '-' (negative), '0' (neutral), '+' (positive) or '++' (very positive based on the findings listed in table 4.2. Furthermore, a score is also given to the scenario where a regular sand fill elevation is considered.

The MCDA results are listed in table 4.3 below.

Table 4.3: MCDA - Selection State-of-the-art engineering solutions

	Rockwool	Foam glass	Bims	LECA	Foam concrete	EPS	Sand fill
Density	0	++	0	0	+	++	- -
Bearing resistance	++	- -	-	-	+	+	++
Performance saturated / undrained conditions	++	–	0	-	0	- -	- -
Material failure	+	- -	- -	- -	++	-	0
Structural durability and maintainability	+	-	-	-	++	+	- -
Total	+6	-4	-4	-5	+6	+1	-4

Remarkable is the worst score for a conventional elevation with sand-fill, which distresses the need for a different material to increase the durability of the tram track structure on soft soils. Furthermore, the application of foam glass, Bims and LECA requires measures against outflow of the material (geotextiles), because there is a risk of buoyancy when the Ground Water Table increases. Furthermore, the crushing strength might be exceeded. Although EPS scores '- -' due to the extreme risk of buoyancy, this effect can easily be checked and if necessary, elements with a lower height are used in the design. The potential of using EPS to mitigate settlements in the field of road and railway engineering due to the very low density has already been studied [80], [87]. In conclusion, only the following materials will be evaluated:

- Rockflow
- Foam concrete
- EPS

4.5. PLAXIS 3D Model

To calculate the rail deflection under a point load, the PLAXIS 3D software is used. The validated soil input parameters from cross-section 2 (table 3.11) can directly be used for the 3D model. In order to get an accurate representation of the rail deflection, the 3D model should be more detailed compared to the 2D model. The following changes are implemented in the 3D model:

- The rail pads placed on with a spacing of 1 [m] to accurately model the support of the rails.
- Between the rails and the concrete slab, a layer of XPS is applied. XPS provides support and damping of the rail between the sleepers and avoids high impact loading on the concrete due to deflection of the rails.

In a first attempt, the sleepers and the concrete slab were modelled as a linear elastic soil volumes instead of a plate. However, this resulted in excessive deflection due to a low shear resistance. Therefore, the model has been changed. Now, the slab is modelled as a plate element.

Another major advantage of using PLAXIS 3D for these calculations is that the point load can actually modelled as a moving point load in the Cartesian coordinate system. PLAXIS 2D, however, is a plane-strain model, which implies that the point load located in the x, y coordinate system has a depth of 1 [m], which results in inaccurately high deflections. Moreover, the 3D model allows the analysis of 2D bending of the plate and calculates the corresponding bending moments in the plate.

4.5.1. Geometry and boundary conditions

The PLAXIS 2D model for cross-section 2 is given a depth of 100 meters. This length is necessary to simulate a dynamic analysis. An overview of the model is displayed in figure 4.5.

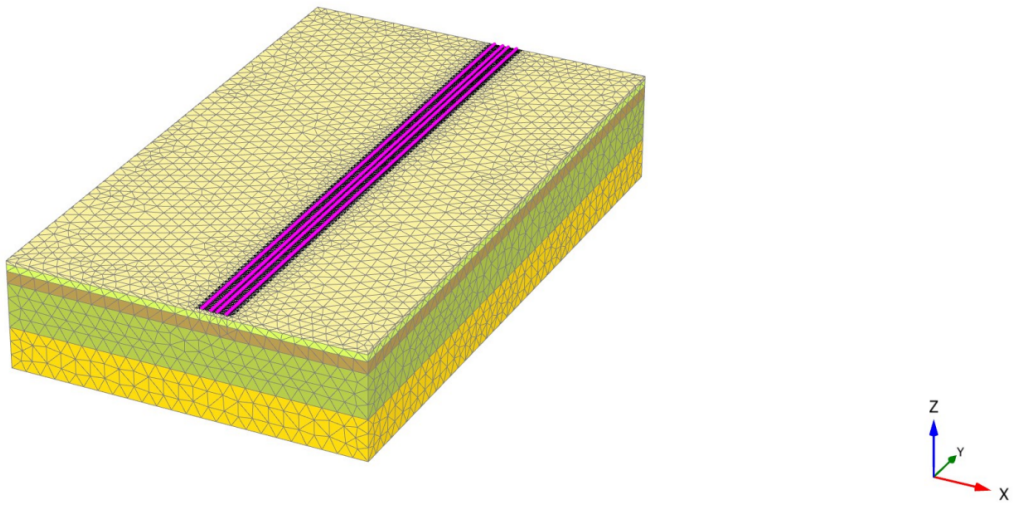

Figure 4.5: PLAXIS 3D model - Akkeroord

For the 3D model, the same boundary conditions are used as for the 2D model. For the 3D Cartesian coordinate system, the boundary conditions are the following:

- $u_{z,min} = 0$ in z-direction
- $u_{x,min} = u_{x,max} = u_{y,min} = u_{y,max}$: normally fixed (fixed in horizontal direction, free to move in vertical direction)
- $u_{z,max}$: free

Moreover, the groundwater flow at the boundary conditions is open at the top and the bottom of the model and closed at the edges of the model.

Furthermore, there are specific boundary conditions applicable for a dynamic analysis. To avoid reflection of propagated waves at the boundaries, all boundaries (apart from z_{max}) are set to viscous.

4.5.2. Soil

As mentioned in the introduction of this section, the validated soil parameters of the 2D model are used. These are listed in table 3.11.

4.5.3. Structures

In the PLAXIS 3D model, the following elements elements are modelled:

- The rails are modelled as beam elements and are supported by the rail pads.
- The slab track is modelled as a plate element.
- The rail pads are modelled as soil volumes and placed on top of the sleeper.
- The volume between the rail foot and the concrete plate is filled with XPS, which is modelled as a soil volume as well.

If the rail pads are modelled as plates, there is a continuous fixation between the rails and the plate. However, in practice, the rail is locally supported by the rail pads on the sleepers to allow rotation of the rails. The same observation and approach was done by Kunicka [96]. Therefore, the rail pads are modelled as soil volumes.

Rails

The Ri60 rails are modelled as 3-node beam elements. Beams have six degrees of freedom in the global coordinate system, which are the 3 translational degrees of freedom (u_x, u_y and u_z) and 3 rotational degrees of freedom (φ_x, φ_y and φ_z) [97]. The material properties are listed in table 4.4.

Table 4.4: Structural Parameters PLAXIS input - Ri60 Rails (based on [98])

Parameter	Value	Unit
γ	78.00	$[kN/m^3]$
E	$210 \cdot 10^6$	$[kN/m^2]$
A	$7.719 \cdot 10^{-3}$	$[m^2]$
$I_2 = I_z$	$9.280 \cdot 10^{-6}$	$[m^4]$
$I_3 = I_y$	$0.03353 \cdot 10^{-3}$	$[m^4]$

Concrete slab

The concrete slab is modelled as a plate element with a height of 170 [mm] over the entire length of the model. In PLAXIS 3D, the plate element has a triangular shape and consists of 6 nodes. Since these plates cannot sustain torsional moments, only 5 degrees of freedom per node in the rotated coordinate system are defined, which are three translational degrees of freedom (u_x^*, u_y^* and u_z^*) and two rotational degrees of freedom (φ_y^* and φ_z^*).

The 6-noded triangular plate element with the 3 integration points is displayed in figure 4.6 below.

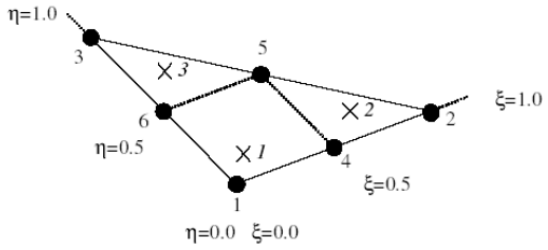

Figure 4.6: PLAXIS 3D Plate element (• -node ; x -integration point) [97]

The material properties for the PLAXIS 3D model are stated in table 4.5.

Table 4.5: Structural Parameters PLAXIS 3D input - Concrete slab (soil volume)

Parameter	Value	Unit
Material	Elastic	[-]
Drainage type	Non-porous	[-]
γ	24.00	$[kN/m^3]$
E	$31 \cdot 10^6$	$[kN/m^2]$
d	0.17	[m]
ν	0.2	[-]

Rail pads

The rail pads used by RET have a dimension of 175 mm x 200 mm x 6 mm. However, in order to properly mesh the model and allow rotation of the rail, the rail pads are modelled 10 times larger. So, the modelled pads have a size of 175 mm x 200 mm x 60 mm. To not add extra weight to the structure, the self weight of the pads is divided by a factor 10 as well.

Moreover, in practice, the stiffness of the rail support is not only dependent on the rail pads, but also on the applied fastener system. In the Netherlands, average values for this stiffness k are reported to be equal to 1300 [MN/m] [96]. However, for the PLAXIS 3D model, stiffness k is not an input parameter and should therefore be converted to a modulus of elasticity E. For this conversion, equation 4.2 is used.

$$E = \frac{kL}{A} \tag{4.2}$$

Where:

- E = Young's Modulus
- k = stiffness
- L = height of the railpad
- A = area of the railpad

Inserting a height L of 0.06 [m] and an area A of $0.170 \cdot 0.200$ $[m^2]$ in equation 4.2 gives a Young's modulus of $2.3 \cdot 10^6$ $[kN/m^2]$.

An overview of all the used input parameters for the modelled railpads are listed in table 4.6.

Table 4.6: Structural Parameters PLAXIS 3D input - Rail pads

Parameter	Value	Unit
Soil model	Linear Elastic	[-]
Drainage type	Non-porous	[-]
γ_{unsat}	1.116	$[kN/m^3]$
E_{ref}	$2.30 \cdot 10^6$	$[kN/m^2]$
ν	0.2	[-]

XPS

Between the rail foot and the concrete slab, 30 [mm] of extruded polysterene foam (XPS, type Floormate 200-A) is installed, which provides support and damping of the rail between the sleepers and avoids high impact loading on the concrete due to deflection of the rails.

The elements are modelled as soil volumes in PLAXIS 3D. In order to have a continous rail support, the XPS elements have the same height as the rail pads (6 [cm]). This is twice the actual height.

An overview of all the used input parameters for the XPS are listed in table 4.7.

Table 4.7: Structural Parameters PLAXIS 3D input - XPS

Parameter	Value	Unit	Reference
Soil model	Linear Elastic	[-]	
Drainage type	Non-porous	[-]	
γ_{unsat}	0.45	$[kN/m^3]$	
E_{ref}	$10 \cdot 10^3$	$[kN/m^2]$	[99]
ν	0	[-]	

Close-up 3D Model

A close-up of the PLAXIS 3D model is shown in figure 4.7 below. The following elements are visible:

- Rails: Pink beams
- Concrete slab: Grey
- Rail pads: Light green
- XPS: Dark green

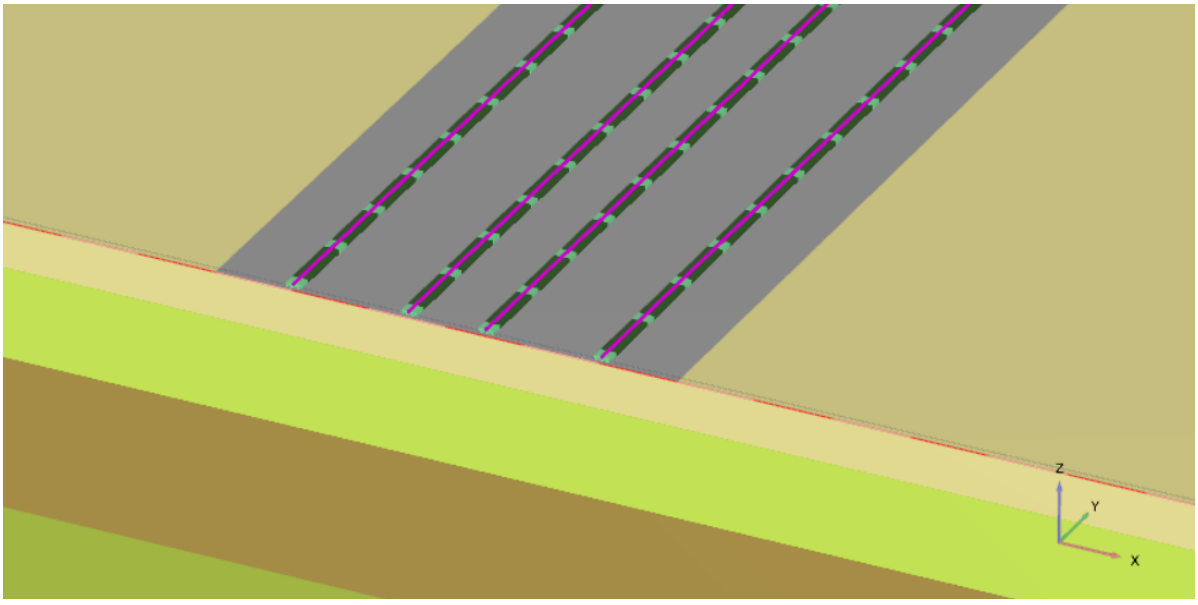

Figure 4.7: PLAXIS 3D model - Close-up

4.5.4. Loads

As mentioned in section 3.4, the maximum load of the tram equals 54,420 [kg], which is equal to 544.2 [kN]. This weight is distributed equally over the three bogies and the four wheels per bogie. Furthermore, the wheel load is multiplied with the Eisenmann DAF of 1.3. Since the trams are not on a busy route, it is very uncommon that the maximum load of 544.2 [kN] is reached. Therefore, a DAF of 1.3 is assumed to be more realistic than 1.6. So, the wheel load is as follows:

$$F_{wheel\ max,dynamic,3D} = DAF \cdot F_{wheel\ max,static,3D} = 1.3 \cdot \frac{544.2}{3 \cdot 4} = 59.085 \quad [kN] \tag{4.3}$$

In PLAXIS 3D, a moving point load can be simulated. This should represent the actual loading time of the vehicle on the structure and the underlying soil.

Two point loads which equal the calculated wheel load from equation 4.3 are placed on top of the rails at $y = 30$ [m]. The line speed is 50 [km/h], which equals 14 [m/s]. So, the defined movement function has a constant velocity of 14 [m/s].

Furthermore, a static surface load σ_z of 1.904 [kN] is placed on top of the concrete slab to model the weight of the ballast.

4.5.5. Mesh size and time step

Passing railway vehicles cause vibration of the soil body. This dynamic loading condition causes waves which propagate through the soil. Railway induced ground vibrations are widely studied for light-rail [100], heavy rail and high-speed lines [101], [102], since these vibrations might cause nuisance for neighbouring residents and damage to nearby buildings. The characteristics of these vibrations are related to the dynamic interaction between the railway vehicle, the track structure and the local soil properties.

To properly model the propagation of waves caused by the dynamic load, the most dominant frequency and wavelengths are determined. In practise, the free field vibration of the soil can be measured with seismic accelerometers. Based on these measurements, the frequency response of the soil can be derived with a Discrete Fourier Transform (DFT). A study for low-floor trams on concrete slab tracks in the Spanish city of Allicante was performed by Real, Martínez, Montalbán, *et al.* in 2011. Field measurements showed that the most significant field accelerations were measured for each axle passage [100]. So, based on the acceleration measurements, the most dominant frequency is assumed to be the frequency between an axle passage. However, no DFT was performed to confirm this assumption.

Nevertheless, actual field measures nearby the roundabout confirm this assumption. At the location, the measured dominant frequency was 4 [Hz] and the average speed of the trams at that location was 27 [km/h], which is 7.5 [m/s] [103]. If this is related to the axle distance, dividing the velocity over the frequency should give the distance between the axles in a bogie. For the RET Citadis trams, the spacing between two axles per bogie is 1.87 [m]. This indeed turned out to be the case, as is computed in equation 4.4 below.

$$s = \frac{v}{f} = \frac{7.5}{4} = 1.875 \quad [m] \tag{4.4}$$

For the PLAXIS 3D model, the wheel loads are modelled as single point loads with a spacing of 1.87 [m]. As mentioned before, the movement function has a velocity of 14 [m/s]. This gives the following dominant frequency:

$$f = \frac{v}{s} = \frac{14}{1.87} = 7.48 \quad [Hz] \tag{4.5}$$

Subsequently, the shear wave speed propagation V_s in the dense sand layer should be calculated. V_s can be calculated with equation 4.6.

$$V_s = \sqrt{\frac{G}{\rho}} \tag{4.6}$$

Where:

- G = shear modulus
- ρ = density

The shear modulus can be derived from the Young's Modulus E with equation 4.7. This value is derived from E_{oed} and the Poisson's ratio ν with equation 4.8. Note that the actual value ofE_{oed} is stress dependent and that the values are reported for a reference stiffness p_{ref} of 100 [kPa]. The actual oedometer stiffness in the top sand layer is calculated with equation 4.9.

$$G = \frac{E}{2(1+\nu)} \tag{4.7}$$

$$E = E_{oed} \cdot \frac{(1+\nu)(1-2\nu)}{(1-\nu)} \tag{4.8}$$

$$E_{oed} = E_{oed}^{ref} \cdot \left(\frac{\sigma_v}{p_{ref}}\right)^m \tag{4.9}$$

Where:

- E = Young's Modulus
- E_{oed}^{ref} = Reference oedometer modulus at 100 [kPa]
- E_{oed} = oedometer modulus
- σ_v = vertical stress
- m = power for stress-level dependency of stiffness (0.5 for sand)
- ν = Poisson's ratio [-]

Inserting the E_{oed}^{ref} of 50350 [kN/m^2], vertical stress σ_v of 9.5 [kPa] and a ν of 0.15 in equation 4.7, 4.8 and 4.9 and a density of 1900 [kg/m^3] in equation 4.6 yields a wave speed V_s of 58 [m/s].

Then, the wave length λ can be determined with equation 4.10.

$$\lambda = \frac{V_s}{f} = \frac{58}{7.48} = 7.75 \quad [m] \tag{4.10}$$

The soil volume consists of 10-noded tetrahedral elements with 3 nodes on each side. In figure 4.8, the tetrahedral soil volume element with the position of the nodes and the integration points is displayed.

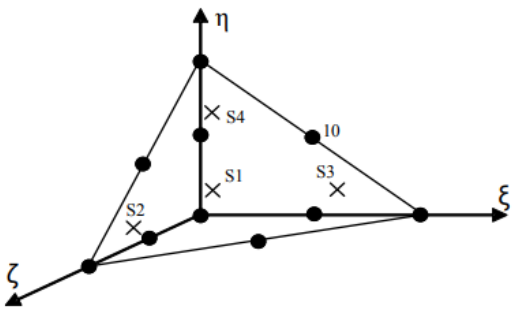

Figure 4.8: PLAXIS 3D tetrahedral soil volume element (• -node ; x -integration point) [97]

To properly model the sinusoidal shape of a wave, at least 9-10 nodes are necessary. So, 4 elements are needed. Based on these characteristics, the maximum size of one tetrahedral element can be determined.

$$size_{element} = \frac{7.75}{4} = 1.9 \quad [m] \tag{4.11}$$

Moreover, to properly simulate the wave propagation in the model, the time steps should be appropriate. Once again, 9-10 time points are necessary. The maximum time step is determined with equation 4.12.

$$\Delta t = \frac{1}{10 \cdot f} = \frac{1}{74.8} = 0.013 \quad [s] \tag{4.12}$$

4.5.6. Staged Construction

The staged construction phases corresponding to this simulation are listed in table 4.8. To make a clear distinction in rail deflection and settlement of the plate, a track construction phase is implemented before performing the dynamic analysis.

Table 4.8: Tram loading 3D analysis - PLAXIS Staged Construction Phases

Phase	Calculation type	Duration	Unit
Initial phase	K0-procedure	-	[-]
Track construction	Plastic	5	[days]
Tram movement	Dynamic	3.00	[s]

4.5.7. Validation PLAXIS 3D Model

The soil parameters have already been validated with the ZETDYK model, measurement data and InSAR-satellite data in section 3.6. However, to ensure that the simulations in PLAXIS 3D give the correct results as well, the 3D model of the tram track structure should be validated as well. The most ideal method to validate the rail deflection is by performing field measurements, where the wheel load of the passing tram is measured and the deflection is captured with a high speed camera. Koziak, Melnik, and Firlik used this method to determine the track stiffness k for different types of trams across the tram network in the Polish city of Poznan [104].

In 2024, RET engineers have measured the track deflection under loading conditions at the case study location. This was reported to be 0.5 [cm] (or 5 [mm]) [105]. Based on this observation, the track stiffness k can be determined with equation 4.13. The found value for k should be compared with the results from PLAXIS.

$$k = \frac{F_{wheel}}{w_{rail}} \tag{4.13}$$

For the reported measurement on rail deflection, the weight of the vehicle, and therefore F_{wheel}, was unknown, in contradiction to the research from Koziak, Melnik, and Firlik [104]. However, since the case study location is located at the final branch of line 3 and nearby tram depot Beverwaard, it is assumed that the weight of the tram is not excessively higher than the empty load of 37,200 [kg]. Equal distribution over the 3 bogies and four wheels per bogie results in a wheel load of 31 [kN]. Inserting this in equation 4.13 yields a foundation stiffness of 6.2 [MN/m].

A rail can be modelled as an Euler-Bernouilli Beam on elastic foundation. The corresponding fourth order ordinary differential equation to describe this model is equation 4.14 [106].

$$EI\frac{\partial^4 w}{\partial x^4} + kw = 0 \tag{4.14}$$

Where:

- E = Young's Modulus
- I = Moment of Inertia
- w = displacement of the beam (in this case track deflection)
- k = track stiffness

The following boundary conditions are applied to get the rail deflection under a wheel load applied at $x = 0$:

- $w(\infty) = 0$
- $\varphi(0) = \frac{\partial w}{\partial x}|_{x=0} = 0$
- $V(0) = \frac{\partial^3 w}{\partial x^3}|_{x=0} = 0$

Solving the differential equation for these boundary conditions gives the rail deflection as a function of position x. The solution is given in equation 4.15.

$$w(x) = \frac{Q}{2kL}\eta(x) \tag{4.15}$$

Where:

- Q = Wheel load
- k = track stiffness
- $L = \sqrt[4]{\frac{4EI}{k}}$ = characteristic length
- $\eta(x) = e^{-\frac{|x|}{L}}[\cos\frac{x}{L} + \sin\frac{|x|}{L}]$
- EI = bending stiffness of the rails

In appendix E, a Python code is shown which is used to calculate the rail deflection under two wheel loads. The rail deflection is calculated. A plot of the rail displacement is shown in figure 4.9. The calculated rail deflection is 4.6 [mm].

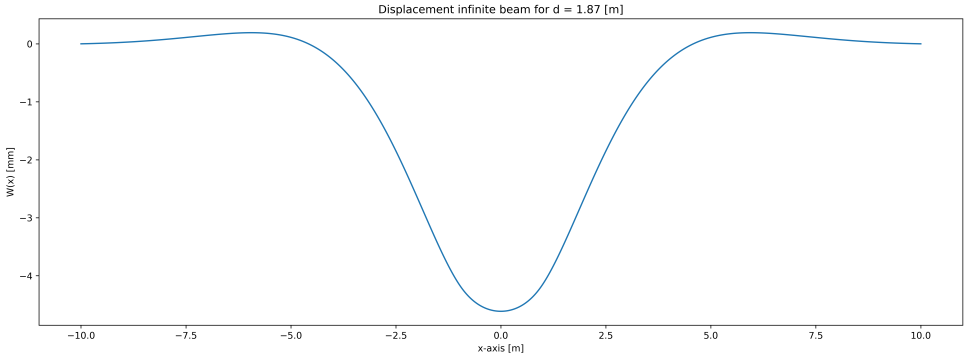

Figure 4.9: Rail deflection for k = 6.2 [MN/m] - analytical solution

The PLAXIS 3D simulations for the existing structure are evaluated in section 4.6.1. For these simulations, a track stiffness k of 6.1 [MN/m] is derived. This is only 1.6% below the reported value of 6.2 [MN/m] derived from the measurment data from the RET engineers [105]. Hence, the model is validated.

4.6. Dimensioning and structural calculations

Under the tram track structure, there is 600 [mm] of sand fill. In this layer, the innovations will be installed. As mentioned in the Case Study Introduction (Chapter 2), the Ground Water Table fluctuates between NAP -2.90 [m] and NAP -1.75 [m]. In this section, the following topics are adressed:

- Structural calculations existing structure
- Dimensioning and structural calculations improved structure

4.6.1. Existing structure

For the existing structure, a structural calculation is performed as well based on the PLAXIS 3D dynamic simulation. The following data are reported:

- Rail deflection [mm]
- Bending moments

A close-up of the meshed 3D model is shown in figure 4.10, where the concrete plate is directly placed on the dense sand layer.

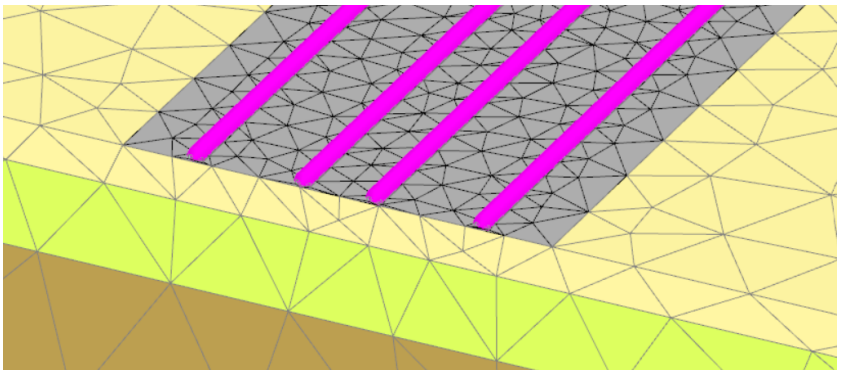

Figure 4.10: Close-up PLAXIS 3D model - Akkeroord - Existing Structure

Structural calculation

The rail deflection itself is not directly related to a design criterion for this research. However, the current rail deflection is a benchmark to make a comparison with the rail deflection when the engineering solutions are applied in the foundation.

Furthermore, the stresses in the slab track should not exceed the maximum tensile strength of the concrete f_{ctm}, which is 2.9 [MPa] for concrete with strength class C30/37.

Rail deflection

First of all, the deflection of the rail is calculated. In figure 4.11, the total displacements of the rail are shown. To compensate for the settlement of the plate itself, the maximum value is deducted from the minimum value, which results in a rail deflection of 9.7 [mm].

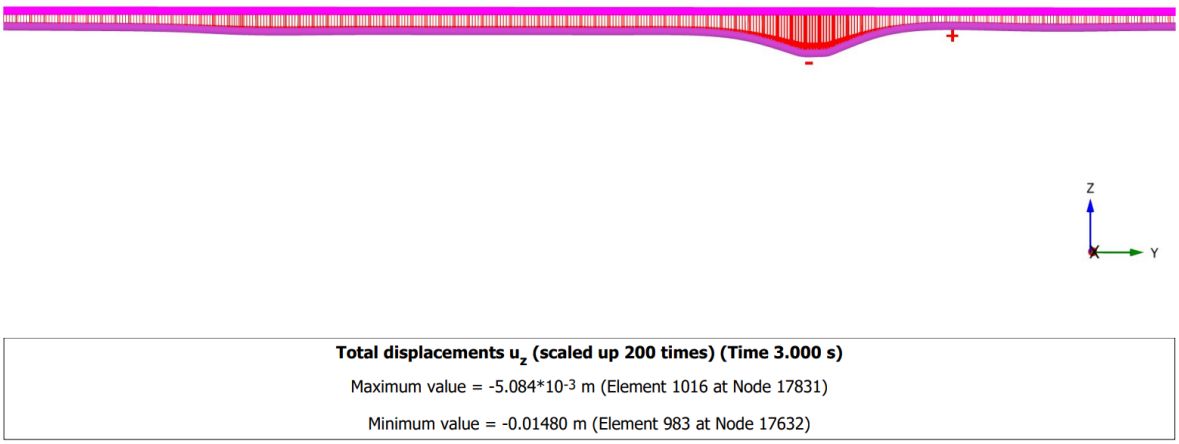

Figure 4.11: Rail deflection - Akkeroord Existing structure

Based on the wheel load of 59.085 [kN] and the deflection of 9.7 [mm], the track stiffness k can be calculated, which is 6.10 [MN/m]. This is only 1.6% below the measured stiffness of 6.2 [MN/m], hence the model is accepted, as was mentioned in the validation section for the PLAXIS 3D model (section 4.6.1).

Stresses concrete plate

Furthermore, PLAXIS calculates the bending moments in the plate. The calculated bending moments are reported in [kNm/m]. The normal stresses due to bending in the slab can be calculated with equation 4.16. Note that for this equation, the bending moment M is constant over the width of the cross-section, and therefore, the PLAXIS output should not directly be used.

$$\sigma = \frac{M}{W} \tag{4.16}$$

Where:

- σ = normal stress [MPa]
- M = bending moment [Nmm]
- $W = \frac{1}{6}bh^2$ = section modulus [mm^3]

Note that for this equation the bending moment is constant over the width of the cross-section. Therefore, the bending moments from PLAXIS should be converted to [kNm]. To do so, the reported values perpendicular to the plane should be integrated over the length between the nodes. In short, the following equation should be used:

$$M_{total} = \int M(x) \cdot \partial x \tag{4.17}$$

In figure 4.12, the calculated bending moments for the existing slab structure are shown.

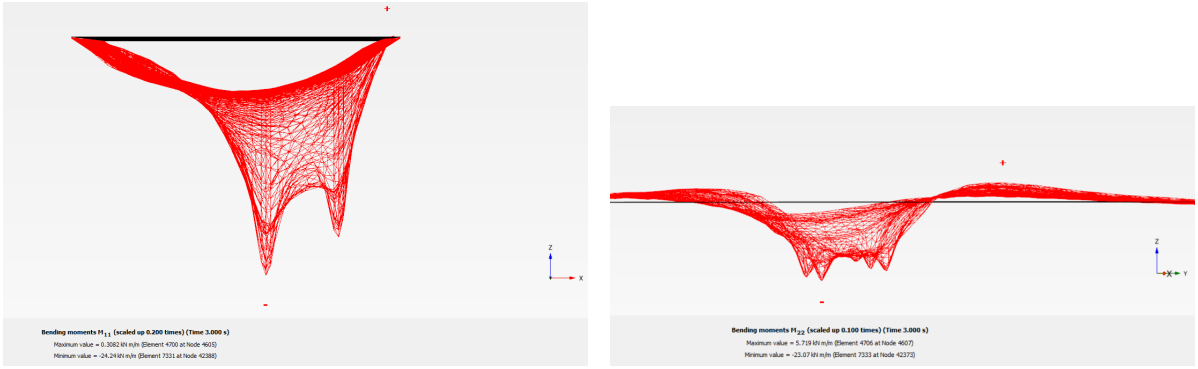

(a) Bending moments M_1 **(b)** Bending moment M_2

Figure 4.12: PLAXIS Results - Bending moments slab existing structure

In figure 4.12a is clearly visible that the highest bending moments occur on the side which is loaded. Therefore, the bending moment and the section modulus are only tailored to halve the width of the foundation plate. Therefore, a width b of 3 [m] is used to calculate the section modulus W.

The PLAXIS results are numerically integrated in Excel. For the existing structure, a bending moment of 47.44 [kNm] is computed. This results in a tensile stress of 3.3 [MPa], which is slightly above the threshold f_{ctm} of 2.9 [MPa]. However, note that a very high load is assumed (maximum tram load with a DAF of 1.3), which is a very conservative approach. In practise, no cracks are observed.

4.6.2. Rockwool: Rockflow

Rockflow elements are available in multiple heights. For the case study project location, elements of 33 or 50 [cm] can be used. To minimise the weight on the soft holocene deposits, the elements of 50 [cm] are selected.

In figure 4.13, a sketch of the RET ballast tram track structure is displayed. Underneath, the Rockflow elements, and the top of the clay layer is displayed. To avoid that the water of the concrete base plate mixture infiltrates in the Rockflow elements during casting, a foil should be placed above the rockwool elements. Note that this is not a complete technical drawing, which should contain the drainage gullies, pipes and air vent pipes are not displayed. Furthermore, for installation, a Rheda City sleeper is preferred in the design instead of the existing duo-block sleepers.

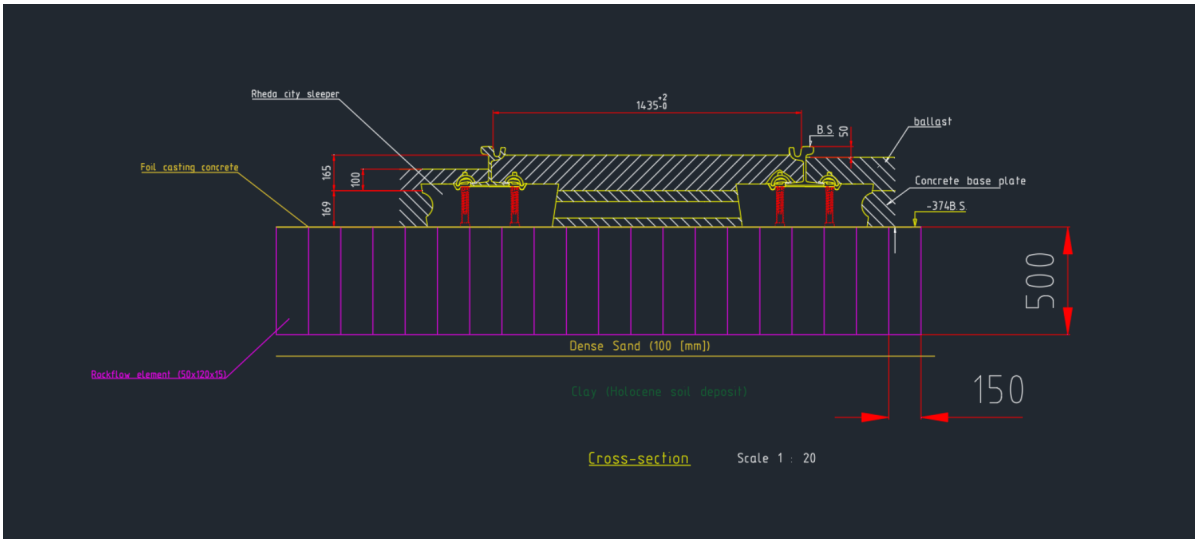

Figure 4.13: Sketch implementation Rockflow-elements

Buoyancy
Since the Rockflow elements absorb water, there is no risk of buoyancy of the material.

Structural calculation
Subsequently, the rail deflection and the stresses in the concrete plate are calculated in PLAXIS 3D when the Rockwool foundation is applied in the track design. The material properties are already listed in table 4.9.

Table 4.9: Structural Parameters PLAXIS 3D input - Rockflow Elements [61], [63]

Parameter	Value	Unit
Material Model	Linear elastic	
γ_{unsat}	10.80	$[kN/m^3]$
γ_{sat}	10.80	$[kN/m^3]$
E'_{ref}	21,000	$[kN/m^2]$
ν	0	[-]
k_x, k_y	80	[m/day]

A close-up of the meshed 3D model is shown in figure 4.14. The concrete plate is casted onto the layer of rockwool elements, which are displayed in red.

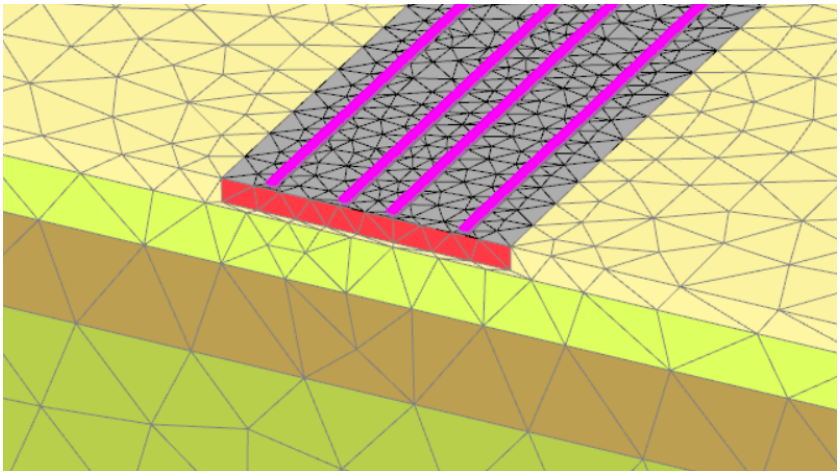

Figure 4.14: Close-up PLAXIS 3D model - Akkeroord - Rockwool

Rail deflection
In figure 4.15, the rail deflection is displayed when Rockflow-elements are installed underneath the slab track. The nominal track deflection is 8.31 [mm]. Compared to the existing structure, this is a reduction of 14.3%.

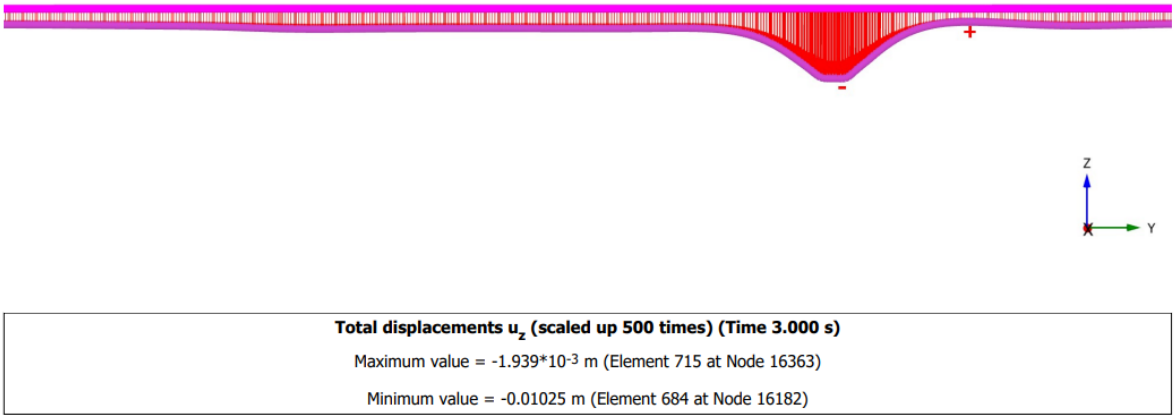

Figure 4.15: Rail deflection - Akkeroord - Rockwool

Based on equation 4.13 can be assumed that the track stiffness increases with 14.3%. However, this difference is not significant to expect excessive dynamic amplification of the wheel load and track degradation in the transition zone.

Stresses concrete plate
In figure 4.16, the calculated bending moments for the slab structure are shown when Rockwool is used as foundation.

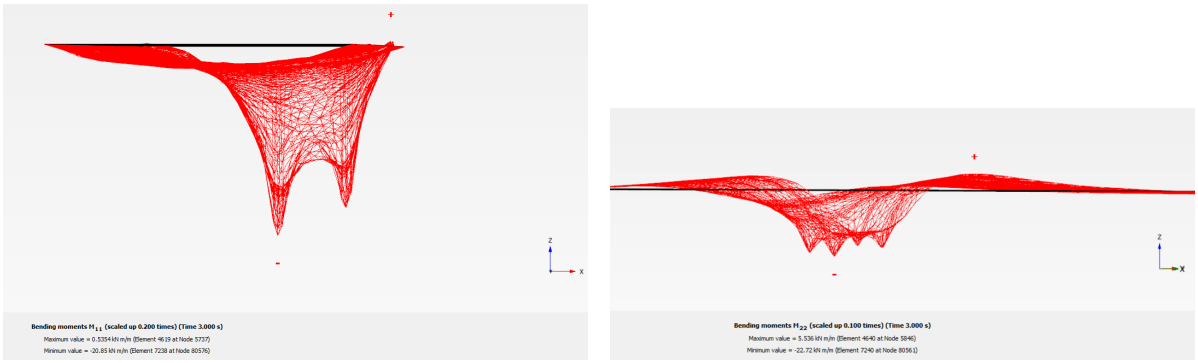

(a) Bending moments M_1 **(b)** Bending moment M_2

Figure 4.16: PLAXIS Results - Bending moments slab - Rockwool

When integrating the results in Excel, a total bending moment of 48.9 [kNm] is calculated. This results in a tensile stress of 3.4 [MPa], which is slightly higher compared to the existing structure.

4.6.3. Foam concrete

A foam concrete layer with a density of 600 [kg/m^3] is used for the design underneath the tram track structure. The maximum cubic compressive strength is 2 [MPa] [88].

The height of the structure is related to the weight of the removed sand layer. The weight of the tram track structure added to the weight of the foam concrete should balance the weight of the removed soil. This equation is given below:

$$5.98 + \gamma_{foam\ concrete} \cdot d_{foam\ concrete} = \gamma_{dense\ sand} \cdot d_{foam\ concrete} \tag{4.18}$$

Solving equation 4.18 gives $d_{foam\ concrete} = 0.46 \quad [m]$. Therefore, a structural height of 0.45 [m] was chosen to minimise the carbon footprint.

A sketch of the cross-section in which the foam concrete layer is applied is displayed in figure 4.17 below. Once again, the technical drawing is an adjustment of the existing cross-section. The duo-block sleepers are not the preferred Rheda City Sleepers.

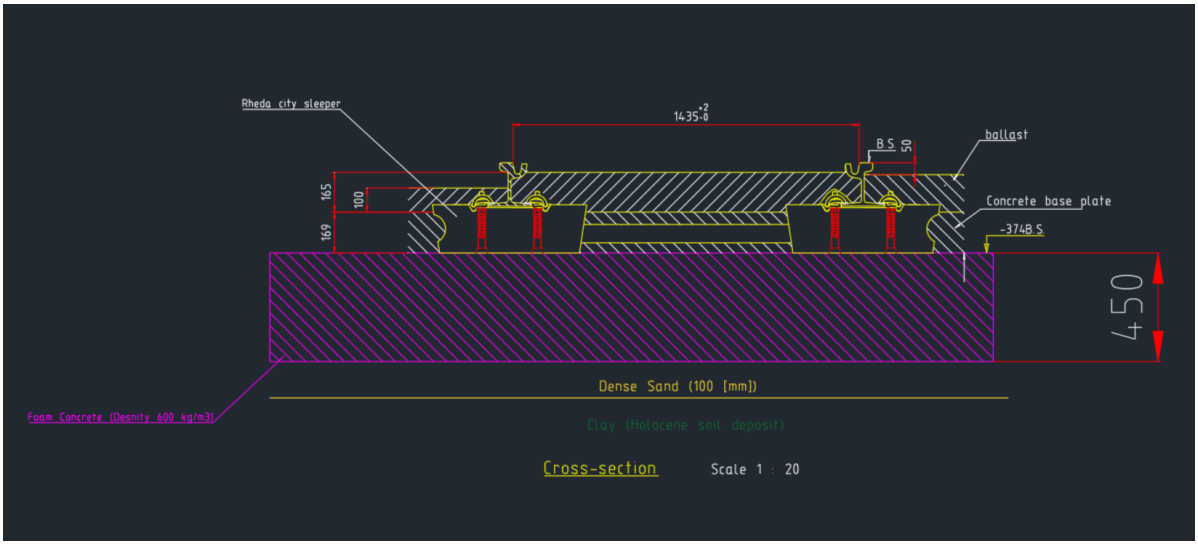

Figure 4.17: Sketch implementation foam concrete

Buoyancy

For the buoyancy calculation, the most unfavourable situation is assumed, which implies that the GWT is at NAP - 1.75 [m]. This gives the following water pressure at the bottom of the foam concrete:

$$\sigma_{w,bottom} = \gamma_w \cdot d = 10 \cdot 0.40 = 4.0 \quad [kPa] \tag{4.19}$$

This is lower then the weight of the tram track structure, which is already 5.98 [kPa]. The total weight at the bottom of the track structure is calculated in equation 4.20.

$$\sigma_{structure} = \sigma_{tram\ track} + \gamma_{foam\ concrete} \cdot d = 5.98 + 6 \cdot 0.45 = 8.68 \quad [kPa] \tag{4.20}$$

In conclusion, there is no risk of buoyancy of the tram track structure. However, during construction, a well drainage system must be installed to ensure a dry construction site and buoyancy of the foam concrete layer before the track structure is installed [83].

Structural calculation

Furthermore, the rail deflection and the bending moments in the concrete tram track structure are computed in PLAXIS 3D. The PLAXIS input parameters are listed in table 4.10 below. The voids can slightly absorb water, hence the small difference between γ_{unsat} and γ_{sat}. However, since the foam concrete is above the phreatic surface, the permeability k is set to zero. Moreover, the material can also be modelled as a non-porous material with $\gamma = 6.00 \quad [kN/m^3]$.

Table 4.10: Structural Parameters PLAXIS input - Foam Concrete [88]

Parameter	Value	Unit
Material Model	Linear elastic	
γ_{unsat}	6.00	$[kN/m^3]$
γ_{sat}	6.33	$[kN/m^3]$
E'_{ref}	1,200,000	$[kN/m^2]$
ν	0.2	[-]

A close-up of the meshed 3D model is shown in figure 4.18. The concrete plate is casted onto the foam concrete layer, which is displayed in dark grey.

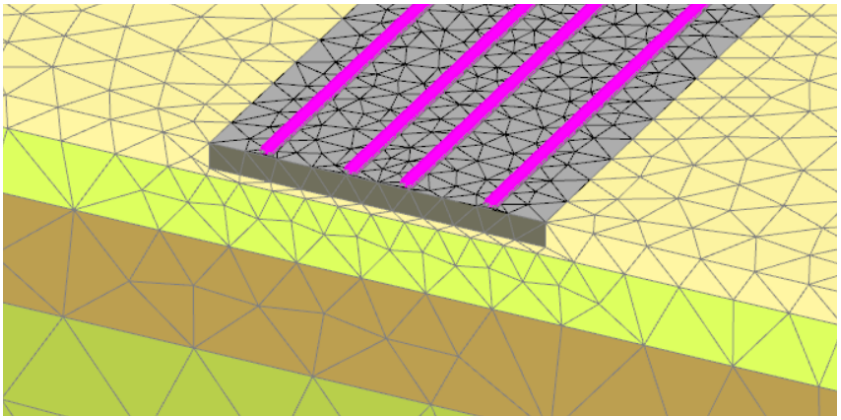

Figure 4.18: Close-up PLAXIS 3D model - Akkeroord - Foam concrete

Rail deflection

In figure 4.19, the rail deflection is displayed when a layer of foam concrete is used as foundation underneath the slab track. The nominal track deflection is 6.2 [mm]. This is a decrease of 36.1% compared to the rail deflection for the existing structure at this location. Based on equation 4.13, this implies a 36.1% stiffer track structure, which might be inappropriate considering the transition zone problem in problem section 1.

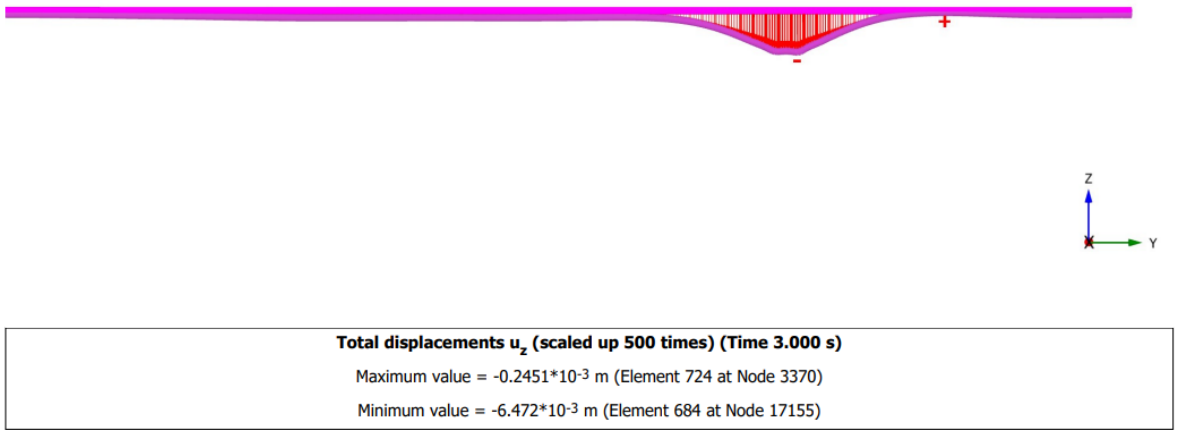

Figure 4.19: Rail deflection - Akkeroord - Foam concrete

Stresses concrete plate

In figure 4.20, the calculated bending moments for the slab structure are shown when foam concrete is used as foundation.

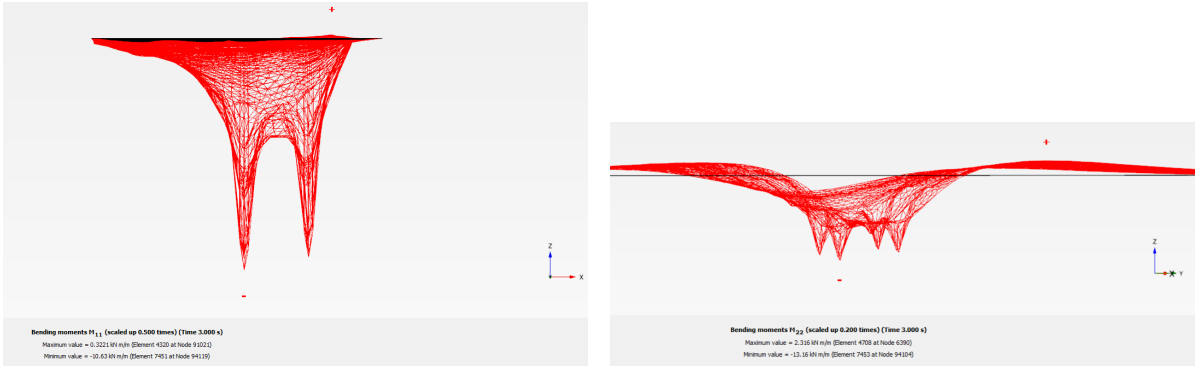

(a) Bending moments M_1 **(b)** Bending moment M_2

Figure 4.20: PLAXIS Results - Bending moments slab - Foam concrete

When integrating the results in Excel, a total bending moment of 23.5 [kNm] is calculated. This results in a tensile stress of 1.6 [MPa], which is a significant reduction compared to the existing structure.

4.6.4. EPS

The density of the used EPS-blocks (ρ_{EPS}) is assumed to be 20 [kg/m^3]. The weight of the tram track structure at cross-section 1 is 7.16 [kPa] and 5.98 [kPa] at the location of cross-section 2. To determine the height of the EPS layer, the thickness of sand fill that has to be removed should be equal to the static weight of the structure. The minimum required thickness of EPS for cross-section 1 and 2 is calculated in equation 4.21 and 4.22 respectively.

$$d_{EPS,1} = \frac{\sigma_{static}}{\gamma_{dense\ sand} - \gamma_{EPS}} = \frac{7.16}{19 - 0.2} = 0.38 \quad [m] \tag{4.21}$$

$$d_{EPS,2} = \frac{\sigma_{static}}{\gamma_{dense\ sand} - \gamma_{EPS}} = \frac{5.98}{19 - 0.2} = 0.32 \quad [m] \tag{4.22}$$

To minimise the carbon footprint, a structural height of 0.30 [m] is assumed for the EPS elements.

A sketch of the cross-section in which the EPS block elements are applied is displayed in figure 4.17 below. Once again, the technical drawing is an adjustment of the existing cross-section where the current duo-block sleepers are still used.

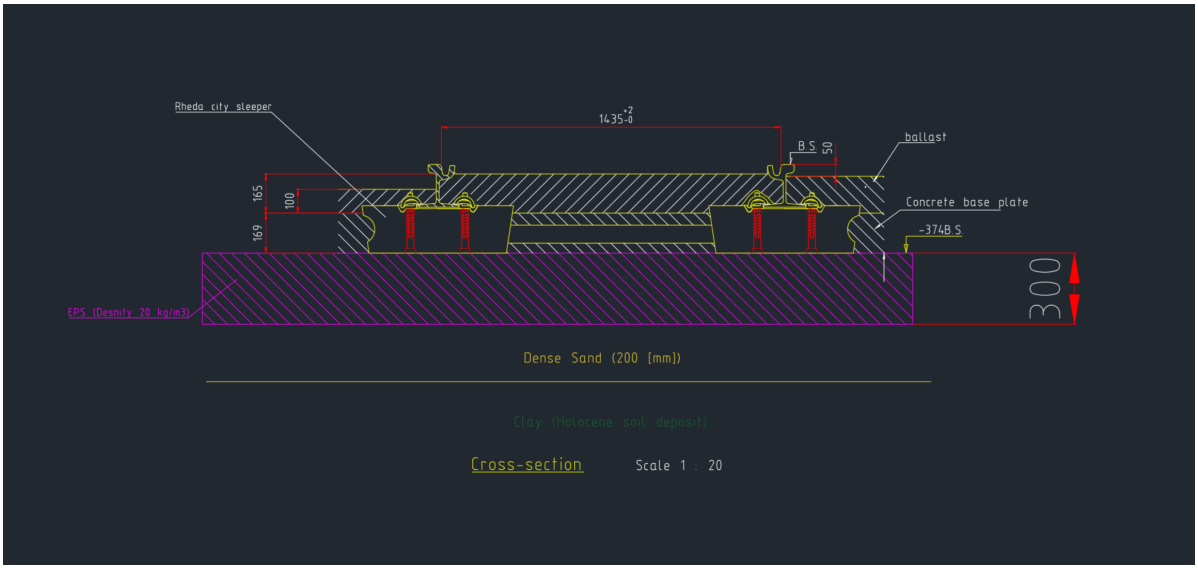

Figure 4.21: Sketch implementation EPS-elements

Buoyancy

Due to the extreme low self weight of the EPS elements, there is a severe risk of buoyancy. The most unfavourable situation, where the GWT is at NAP - 1.75 [m], the water pressure at the bottom of the EPS elements is as follows:

$$\sigma_{w,bottom} = \gamma \cdot d = 10 \cdot 0.25 = 2.5 \quad [kPa] \tag{4.23}$$

This is lower than the self-weight of the structure at cross-section 2, which is 5.98 [kPa]. The total weight of at the bottom of the track structure is computed in equation 4.24.

$$\sigma_{structure} = \sigma_{tram\ track} + \gamma_{EPS20} \cdot d = 5.98 + 0.2 \cdot 0.4 = 6.06 \quad [kPa] \tag{4.24}$$

Structural calculation

Now that the buoyancy of the material has been checked, further structural calculations in PLAXIS 3D are performed. The material properties for the PLAXIS model are listed in table 4.11 below. The material is modelled as non-porous.

Table 4.11: Structural Parameters PLAXIS input - EPS [80]

Parameter	Value	Unit
Material Model	Linear elastic	
γ	0.2	$[kN/m^3]$
E'_{ref}	7733	$[kN/m^2]$
ν	0.1	[-]

A close-up of the meshed 3D model is shown in figure 4.22. The concrete plate is casted onto the layer of EPS blocks, which are displayed in light green.

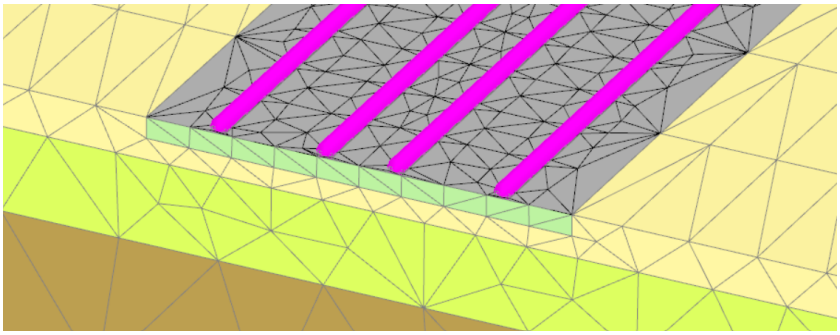

Figure 4.22: Close-up PLAXIS 3D model - Akkeroord - EPS

Rail deflection

In figure 4.23, the rail deflection is displayed when EPS elements are used as foundation underneath the slab track. The nominal track deflection is 8.38 [mm]. This is lower than the original track deflection of 9.7 [mm] and comparable with the deflection when Rockwool is used (8.31 [mm]). Hence, the rail deflection reduces with 13.6% compared to the existing situation. Furthermore, the track stiffness k increases with 13.6%. Just as for Rockwool, this difference is not significant to expect excessive dynamic amplification of the wheel load and track degradation in the transition zone.

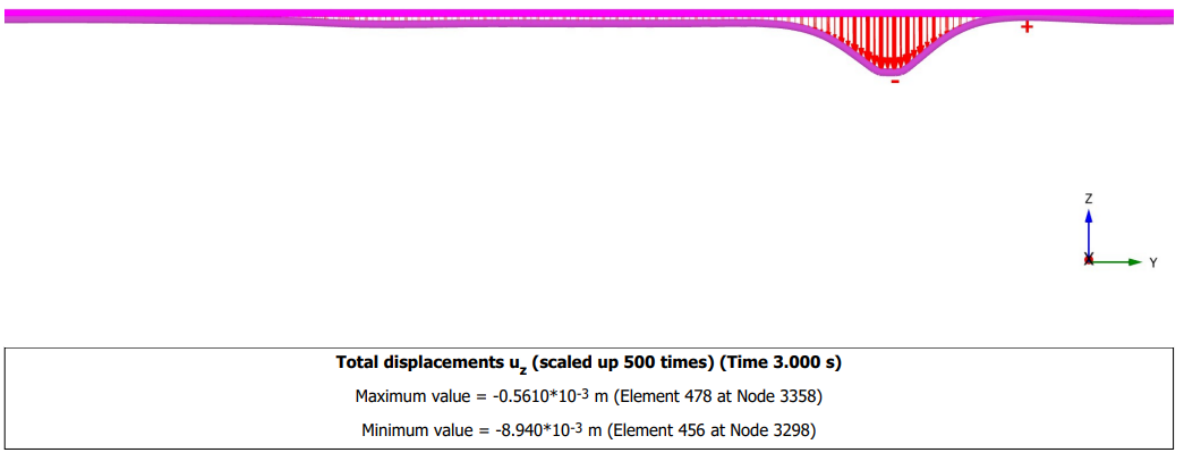

Figure 4.23: Rail deflection - Akkeroord - EPS

Stresses concrete plate
In figure 4.24, the calculated bending moments for the slab structure are shown when EPS blocks are used as foundation.

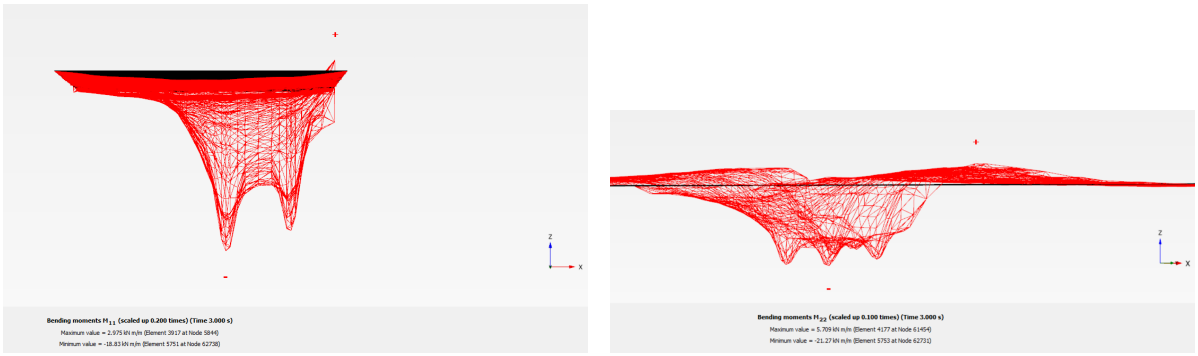

(a) Bending moments M_1 **(b)** Bending moment M_2

Figure 4.24: PLAXIS Results - Bending moments slab - EPS

When integrating the results in Excel, a total bending moment of 50.90 [kNm] is calculated. This results in a tensile stress of 3.5 [MPa], which is slightly higher than the existing structure and Rockwool.

4.6.5. Summary
To conclude, the following points are observed when performing the structural calculations:

- When applying Rockwool and EPS in the track design, a similar reduction in rail deflection is observed compared to the existing structure, which are 14.3% and 13.6% respectively. However, for foam concrete, a higher reduction of 36.1% is observed. Hence, there is a significant difference in track stiffness when the foam concrete foundation is used, which might result in a transition zone when applied in the track structure design. For Rockwool and EPS, this differential stiffness with the existing structure is considered to be reasonable. Excessive track degradation is not expected.
- For the modelled loading condition, the mean tensile strength of concrete (f_{ctm}) is slightly exceeded for the existing structure. Note that this extreme loading condition most likely does not occur in practise.
- When applying Rockwool and EPS in the track design, the occurring tensile stresses slightly increases compared to the existing structure. Note that this might not directly lead to problems since the most unfavourable loading conditions with a DAF of 1.3 is assumed.
- The following two solutions are possible to avoid exceeding f_{ctm}:
  - Increase the concrete strength class to C35/45 ($f_{ctm} = 3.2$ [MPa]) or C40/50 (f_{ctm} = 3.5 [MPa])
  - Slightly increasing the height of the concrete slab, for example from 170 to 200 [mm]. This increases the section modulus W with 38%. Note that further increasing is not preferred because of the increase of the self weight of the structure, which further enhances the settlements.
- For foam concrete, a significant reduction in bending moments is observed.

4.7. PLAXIS 2D Simulation - Results
Now that the dimensions of the materials are known and the structural requirements of the slab track have been checked, the long-term settlements can be computed in PLAXIS 2D.

As discussed previously, two distinctive scenarios are elaborated. For the first scenario is assumed that the tram track structure was constructed immediately with the proposed innovations. However, for the second scenario, the engineering solution is installed during track renewal works in 2026. For

scenario 1, the staged construction phases remain unchanged compared to the procedure followed in table 3.9. The Staged Construction Phases for scenario 2 are listed in table 4.12 below.

Table 4.12: Scenario 2 : Track renewal 2026 - PLAXIS Staged Construction Phases

Phase	Calculation type	Duration	Unit
Initial phase	K0-procedure	-	[-]
Track construction	Consolidation	5	[days]
First 18 years of service (2008 - 2026)	Consolidation	6,570	[days]
Install new foundation 2026	Consolidation	10	[days]
Rebuild track structure 2026	Consolidation	5	[days]
Extra 30 years of consolidation and creep	Consolidation	10,000	[days]

In this section, the results for the symmetrical cross-section 2 are elaborated and discussed in detail. However, the simulations are performed for both cross-section 1 and cross-section 2. The numerical results for cross-section 1 are listed in section 4.7.5. Furthermore, the plots are displayed in Appendix D.

4.7.1. Conventional method - Sand fill elevation

As a reference situation, the settlements are calculated when the conventional elevation method (sand fill) is used. A sand fill layer of 20 [cm] is assumed with a dry weight γ of 19 [kN/m^2]. Hence, at $t = 6,570$, the line-load is increased with $0.2 \cdot 19 = 3.8 \quad [kN/m^2]$.

In figure 4.25, the total settlements of the tram track structure is displayed when at t = 6570 [days], a sand fill layer with a height of 20 [cm] is applied. In pink, the trajectory for the settlements of the existing structure is displayed if the structure is not elevated.

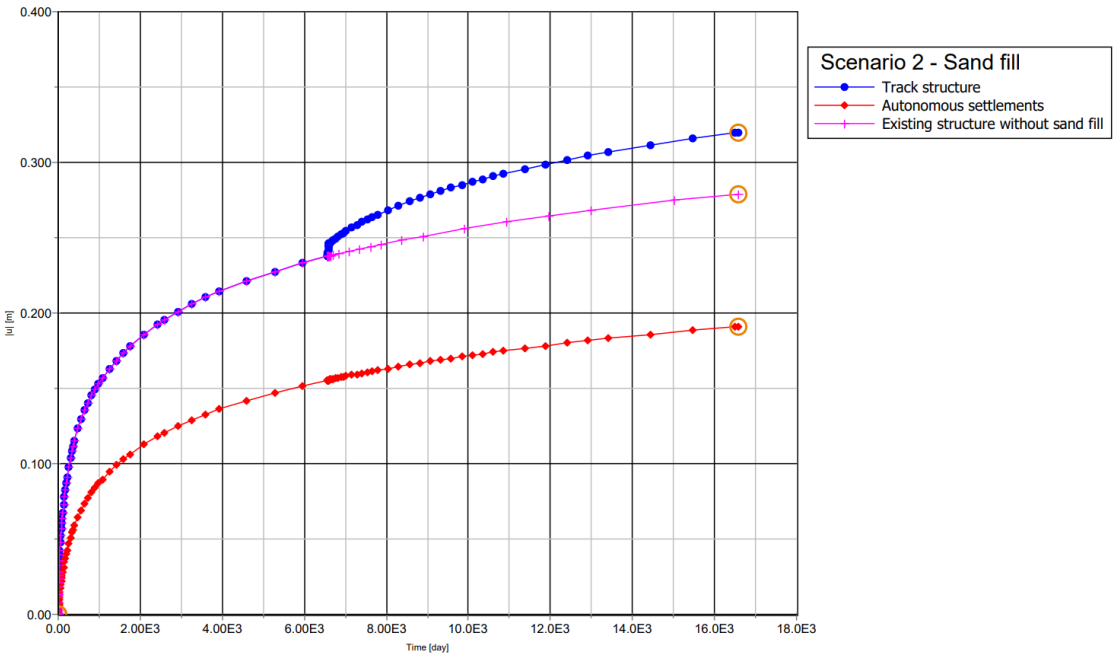

Figure 4.25: Settlements of the tram track structure - 20 cm sand fill elevation

These are the main findings from the obtained results:

- From 2026, the tram track settles 0.082 [m] over 30 years. This is in line with the ZETDYK model, which predicts settlements of 0.09 [m] when a preconsolidation stress of 5.98 [kPa] is used. This results in a settlement reduction of 45.3%.
- The settlement rate after 12 years is 2.8 [mm/year]. This is a reduction of 34.9%.

4.7.2. Rockwool: Rockflow

The Rockflow elements are modelled in PLAXIS as a soil polygon. The linear elastic Material Model is used. The elements are assumed to be fully saturated, even though these are located above the ground water table. Therefore, the values for γ_{unsat} and γ_{sat} are the same. The PLAXIS input is stated in table 4.13. A cross-section of the PLAXIS 2D model is displayed in figure 4.26. The Rockwool elements have a light-blue color.

Table 4.13: Structural Parameters PLAXIS input - Rockflow Elements [61], [63]

Parameter	Value	Unit
Material Model	Linear elastic	
γ_{unsat}	10.80	$[kN/m^3]$
γ_{sat}	10.80	$[kN/m^3]$
E'_{ref}	21,000	$[kN/m^2]$
ν	0	[-]
k_x, k_y	80	[m/day]
R_{inter}	0.66	[-]

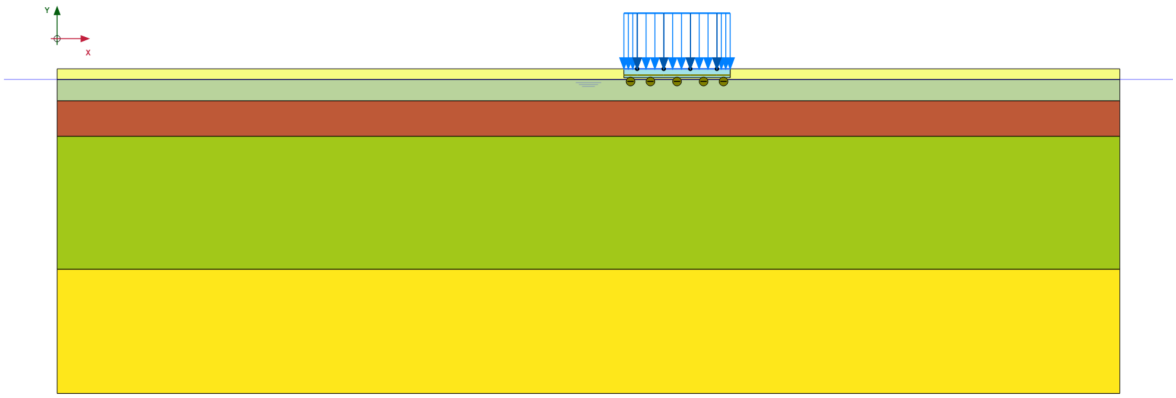

Figure 4.26: PLAXIS 2D Model - Rockwool

The computed settlement graphs for scenario 1 and scenario 2 are displayed in figure 4.27a and figure 4.27b respectively.

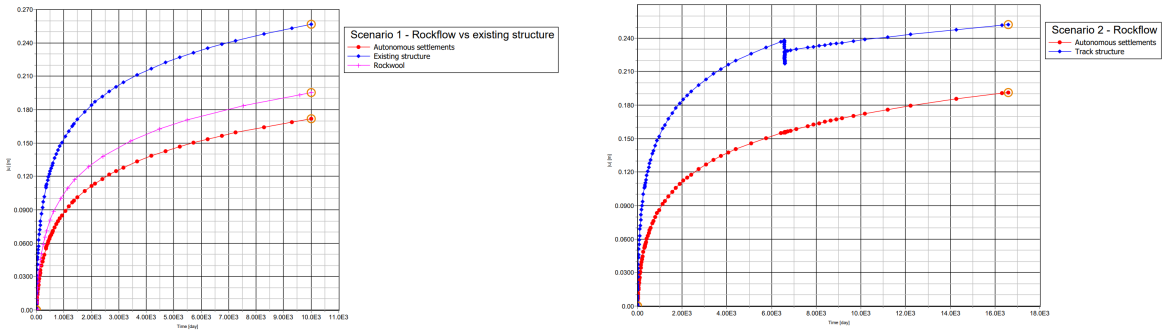

(a) Rockflow - Scenario 1

(b) Rockflow - Scenario 2

Figure 4.27: Rockflow - Settlement graphs of the tram track structure

The key results for scenario 1 are as follows:

- When correcting for the high initial settlement, as discussed in Chapter 3, the total settlements for scenario 1 have reduced significantly reduced with 39.2% from 0.156 [m] to 0.095 [m] over 30 years.
- The settlement rate in 2020 has decreased from 4.3 [mm/year] to 3.2 [mm/year], which is a reduction of 25.6%. This is close to the set target of 3.1 [mm/year].

The main results for scenario 2 are the following:

- Temporary unloading structure at t = 6,570 [days] reduces the settlement of the soil with 21 [mm].
- Installing the Rockwool elements and rebuilding the track structure gives an initial settlement of 11 [mm].
- From 2026 is the settlement rate 1.4 [mm/year]. This gives a total settlement of 0.042 [m] over 30 years. This is even lower than the current rate of autonomous settlements, which are 2.4 [mm/year]. The PLAXIS SSC model also foresees a reduction of this autonomous settlement rate. The track settlement and autonomous settlement rate are almost parallel after 2026, which implies a similar settlement rate.

So overall, when the Rockflow elements are installed directly underneath the track structure, the settlement rate and total settlements over 30 years reduce significantly. Furthermore, when Rockwool is installed in 2026, the total settlements and settlement rate of the structure are significantly lower over the upcoming 30 years due to preconsolidation of the soil. When changing the preconsolidation stress in ZETDYK to 5.98 [kPa], this model predicts 0.04 [m] of settlements over 30 years as well.

4.7.3. Foam concrete

Just as the Rockflow elements, the foam concrete layer with a height of 45 [cm] is modelled as a soil polygon. The linear elastic material model is used. The material input parameters are already listed in table 4.10. The cross-section of the PLAXIS model is displayed in figure 4.28. The foam concrete is modelled in gray.

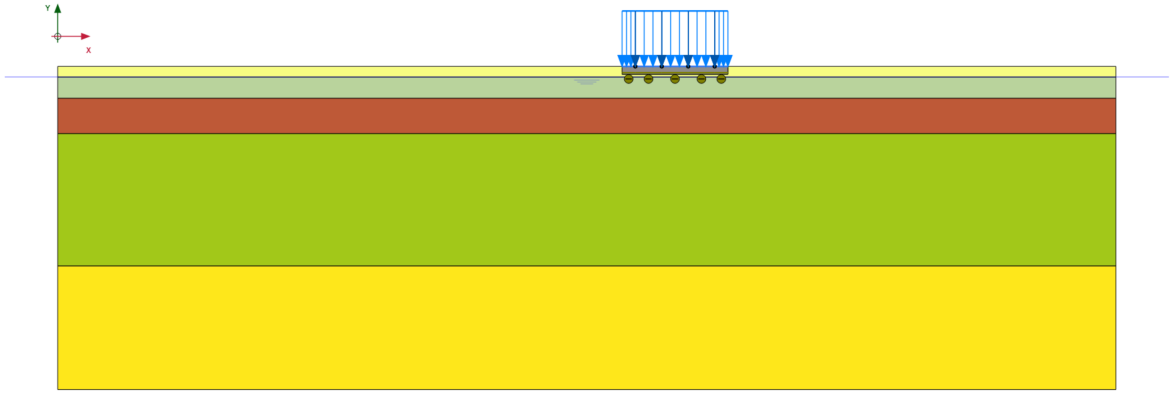

Figure 4.28: PLAXIS 2D Model - Foam concrete

The computed settlement graphs for scenario 1 and scenario 2 are displayed in figure 4.29a and figure 4.29b respectively.

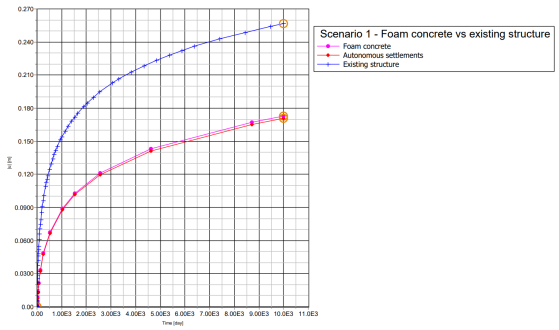

(a) Foam concrete - Scenario 1

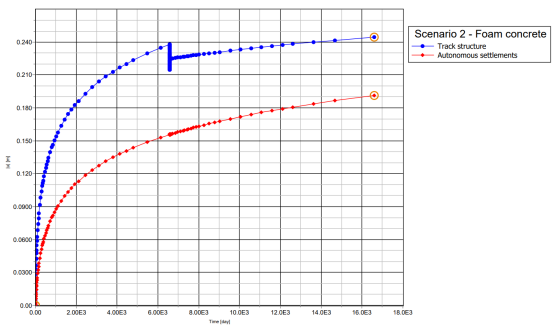

(b) Foam concrete - Scenario 2

Figure 4.29: Foam concrete - Settlement graphs of the tram track structure

For scenario 1, these are the following main results:

- When correcting for the high initial settlements, the total settlements over 30 years reduce with 52.6% from 0.156 [m] to 0.074 [m].
- The settlement rate has reduced from 4.3 [mm/year] to 2.4 [mm/year], which is a significant reduction of 44.2%. This is in line with the settlements of the surrounding sidewalks and even lower than the surrounding roads, which settle 4.0 [mm/year]. This settlement rate is equal to the autonomous settlements. This makes sense, since the weight of this new structure equals the self weight of the soil before construction.

Furthermore, these are the key results for scenario 2:

- When installing the new tram track structure in 2026, the total settlements of the soil reduce with 23 [mm].
- Casting the foam concrete and reinstalling the track structure leads to 10 [mm] of settlements.
- From 2026, the settlement rate is only 1.0 [mm/year]. Over the following 30 years, the settlements are 0.030 [m]. Just as for the Rockwool elements, this is lower than the autonomous settlements. However, the PLAXIS SSC model foresees a reduction in these autonomous settlements. In the creep branch of the graph displayed in figure 4.29b, the settlements of the track structure and the autonomous settlements are parallel, hence implying an equal settlement rate.

4.7.4. EPS

Furthermore, the EPS blocks with a height of 30 [cm] are modelled as linear elastic elements. The EPS blocks are modelled as a soil polygon underneath the track structure. The input parameters for the PLAXIS model are already stated in table 4.11 below. Furthermore, the cross-section of the PLAXIS 2D model with EPS is shown in figure 4.30. The EPS elements are shown in gray.

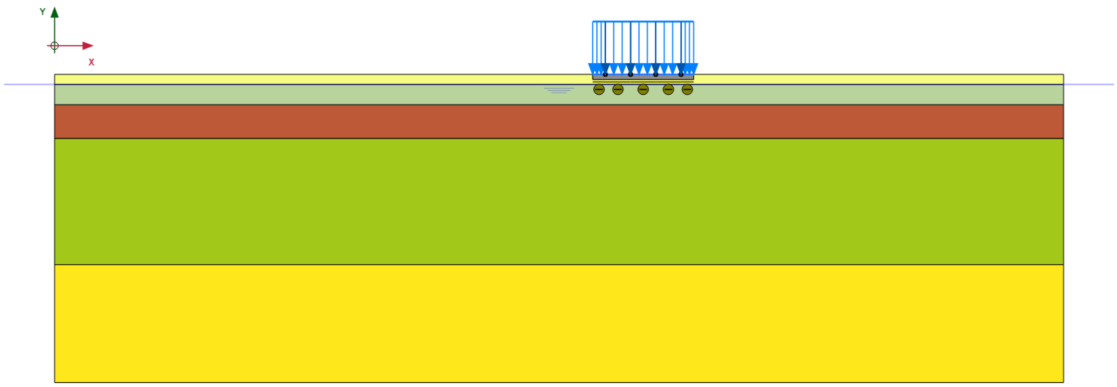

Figure 4.30: PLAXIS 2D Model - EPS

The computed settlement graphs for scenario 1 and scenario 2 are displayed in figure 4.31a and figure 4.31b respectively.

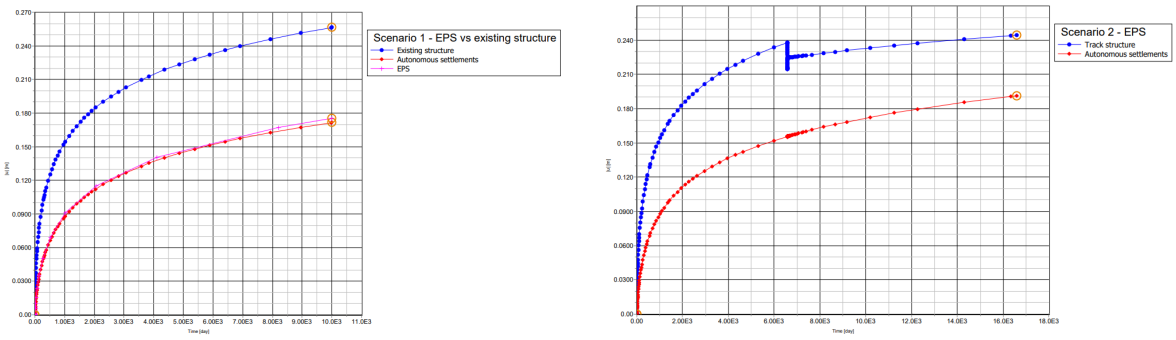

(a) EPS - Scenario 1

(b) EPS - Scenario 2

Figure 4.31: EPS - Settlement graphs of the tram track structure

The main results for scenario 1 are the following:

- The corrected settlements over 30 years reduce with 50% from 0.156 [m] to 0.075 [m], which is a reduction of 51.9%.
- The settlement rate has reduced from 4.3 to 2.4 [mm/year] in 2020. This is a significant reduction of 44.2%. This settlement rate is equal to the autonomous settlements. This makes sense, since the weight of this new structure equals the self weight of the soil before construction. Moreover, this settlement rate is lower than the surrounding roads, which settle with about 4.0 [mm/year].

The main results for scenario 2 are the following:

- When the track structure is removed and the EPS elements are installed, the total settlements of the soil reduce with 23 [mm].
- When installing the EPS elements, the soil settles with 10 [mm].
- From 2026 forward, the settlement rate of the tram track structure is only 1.1 [mm/year]. This gives a total settlement of 0.033 [m] over 30 years. This is lower than the autonomous settlement rate of 2.4 [mm/year]. However, the SSC Model predicts a decrease of this settlement rate. In the graph displayed in figure 4.31b, the creep branch of the settlements of the track structure and the autonomous settlements is parallel, which implies an equal settlement rate.

4.7.5. Overview Results

In table 4.14, the PLAXIS 2D simulation results for scenario 1 for cross-section 2 are reported. Furthermore, the difference between the reference situation (existing structure) is calculated for the settlement rate and the final settlement. All three selected innovations, which are Rockwool, foam concrete and EPS, reduce the settlement rate significantly. Foam concrete and EPS easily meet the set target of 3.1 [mm/year]. However, the Rockflow elements have an expected settlement rate of 3.2 [mm/year], which is just above the target. This difference in result between Rockwool and the other two light-weight filler materials is expected, since the self weight of saturated Rockwool elements is higher than the self-weight of the foam concrete foundation layer and the EPS elements.

Table 4.14: Overview PLAXIS Simulation results - Scenario 1 - Cross-section 2

	Initial	**Target** [4]	**Rockwool**	**Foam concrete**	**EPS**
Settlement rate [mm/y]	4.3	3.1	3.2	2.4	2.4
Difference	0%	-27.9%	-25.6%	-44.2%	-44.2%
Final settlement [m]	0.156		0.095	0.074	0.074
Difference	0%		-39.2%	-52.6%	-52.6%

Slightly higher settlement rates are observed for cross-section 1, which are listed in table 4.15. Rockwool and foam concrete slightly exceed the set target. For foam concrete, the thickness can be slightly increased to 50 [cm] to meet the target.

Table 4.15: Overview PLAXIS Simulation results - Scenario 1 - Cross-section 1

	Initial	**Target** [4]	**Rockwool**	**Foam concrete**	**EPS**
Settlement rate [mm/y]	4.3	3.1	3.5	3.2	2.8
Difference	0%	-27.9%	-18.6%	-25.6%	-34.9%
Final settlement [m]	0.185		0.116	0.098	0.092
Difference	0%		-37.3%	-49.7%	-50.2%

Furthermore, the same computation is performed for scenario 2. For both cross-sections, the settlement rate for the sand elevation scenario just meets the target. However, the surrounding roads are expected to have a lower settlement rate in the future as well. Therefore, the reported settlement rate of 2.8 [mm/year] for cross-section 1 and 2 are therefore considered to be too high and does not guarantee that the design life time of 30 years will be reached. Moreover, the risk of outflow of the material under saturated conditions still exists.

Furthermore, all light-weight solutions show a very low settlement rate and therefore only little total settlements over 30 years from 2026. This result is expected, since the soil has been preconsolidated between 2008 and 2026 due to the weight of the tram track structure.

The results for cross-section 2 and cross-section 1 for scenario 2 are reported in table 4.16 and table 4.17 respectively.

Table 4.16: Overview PLAXIS Simulation results - Scenario 2 - Cross-section 2

	Initial	**Target** [4]	**Sand fill**	**Rockwool**	**Foam concrete**	**EPS**
Settlement rate [mm/y]	4.3	3.1	2.8	1.4	1.0	1.1
Difference	0%	-27.9%	-34.9%	-67.4%	-76.7%	-74.4%
Final settlement [m]	0.15		0.082	0.042	0.030	0.033
Difference	0%		-45.3%	-72%	-73%	-78%

Table 4.17: Overview PLAXIS Simulation results - Scenario 2 - Cross-section 1

	Initial	**Target** [4]	**Sand fill**	**Rockwool**	**Foam concrete**	**EPS**
Settlement rate [mm/y]	4.3	3.1	2.8	1.1	1.0	1.0
Difference	0%	-27.9%	-38%	-77%	-80%	-80%
Final settlement [m]	0.185		0.092	0.033	0.030	0.030
Difference	0%		-50%	-82%	-83.7%	-83.7%

Based on scenario 2, all three light-weight materials meet the design lifetime criterium of 30 years.

4.8. Conclusion

Based on the MCDA in section 4.4 and the PLAXIS simulation results in section 4.7, the following conclusions can be drawn:

- A conservative approach to restore the vertical alignment of the tram track structure is to raise the track structure back to the original level by using sand fill. This would locally imply an elevation of 20 [cm]. This elevation increases the effective stresses and would therefore remain subjected to settlements due to consolidation and creep of the soil. Moreover, there is still a risk of outflow of the material under dynamic loading conditions when the sand layer is saturated. In short, this is an inappropriate solution, which will result in increased maintenance activities, maintenance costs and early track renewal.
- Glass foam, LECA and Bims are not preferred due to the risk of outflow of the material. This would require the application of geotextiles. Moreover, the density of Bims is relatively high compared to the glass foam and LECA.
- For the most unfavourable loading condition (maximum tram load and DAF of 1.3), the tensile stresses due to bending slightly exceed the mean concrete tensile strength f_{ctm} of 2.9 [kPa] for concrete strength class C30/37. However, this loading condition is rarely reached at this location. Changing the foundation to EPS and Rockwool slightly further increases the occurring bending moments and stresses. However, considering this is not significantly worse than the existing structure, EPS and Rockwool are still considered to be appropriate materials that can be used as foundation for the concrete slab track. However, when the stiff foundation of foam concrete is applied underneath the tram track structure, significantly lower bending moments and tensile stresses are computed.
- When Rockwool and EPS are installed in the track design, the rail deflection reduces with 14.3% and 13.6% respectively compared to the existing structure. When the much stiffer foam concrete layer is casted underneath, a reduction of 36.1% is observed. For the latter solution, this is a significant increase and might result in transition zone problems with the track structures without improved foundation further down the line.
- Installing Rockflow WM2007 elements with a height of 50 [cm] is an effective measure to reduce the total settlements of the tram track structure. If these were installed in the original track structure in 2008, the settlement rate would be 3.2 [mm/year]. This is only slightly above the settlement rate of the surrounding roads, which settle with a rate of 3.1 [mm/year]. When being installed in 2026 on overconsolidated soil, the remaining settlements are only 42 [mm] over 30 years for cross section 2 and 33 [mm] for cross-section 1.

- When 45 [cm] of sand is excavated and the space is then filled with foam concrete, the weight on the subgrade is significantly reduced. This results in even lower settlements compared to the Rockwool elements. For cross-section 2, the stress reduction equals the weight of the track structure, hence resulting in the same settlements as the autonomous settlements in the PLAXIS SSC model. Moreover, the settlement rate of the track structure has reduced to 2.4 [mm/year] for cross-section 1, which is significantly lower than the surrounding infrastructures. This settlement rate is 3.2 [mm/year] for cross-section 1. When the track structure is renovated in 2026, the remaining settlements over 30 years are only 30 [mm] for cross-section 1 and 2.
- The same weight reduction is reached when using EPS elements with a structural height of 30 [cm]. This results in a settlement rate of 2.4 [mm/year] for cross-section 2 and 2.8 [mm/year] for cross-section 1. Furthermore, when installing the elements in 2026 on preconsolidated soil, the remaining settlements are only 30 [mm] for cross-section 1 and 33 [mm] for cross-section 2.
- All three solutions meet the settlement target of 3.1 [mm/year] for scenario 2, which has the following advantages:
  - No excessive maintenance activities/costs
  - Structural design life time of 30 years will be reached, hence reducing the costs for big renovation works and elevating the structure before the city of Rotterdam performs the same activity for the surrounding roads.
  - Eliminating the differential settlement in the transition zone reduces the dynamic amplification of the wheel loads of the trams, hence resulting in less track degradation, maintenance activities and maintenance costs.

With this information, the second sub-question, "*Which state-of-the-art engineering solutions could mitigate the vertical settlement of the tram track on the soft soil?*", can be answered. The state-of-the-art engineering solution are as follows:

- Rockwool: Rockflow (Type WM2007)
- Foam concrete (attention should be paid to transition zones)
- EPS

4.9. Discussion and recommendations

The following points from this study should be taken into consideration when interpreting the results:

- This research is based on a static analysis, where the static wheel load is multiplied with the Dynamic Amplification Factor. For further research, the dynamic behaviour of the current and improved tram track structures should be investigated. This research should focus on the effect of changing the foundation on the occurring natural frequencies, resonance and excessive degradation of certain components and nuisance from noise and vibrations.
- In the PLAXIS 3D model, the slab track is modelled as a plate element, which resembles a shell. This model gives a good impression about the total deflection and bending moments under a moving load. However, in-depth information on the exact force distribution and internal stress-paths cannot be determined with this approach. Moreover, the slab is assumed to be continuous, whereas in practise, duo-bloc sleepers are embedded in the concrete slab track. To get accurate insight in these stress-paths, other finite element software programs should be used, such as DIANA or ANSYS. However, information about the support (stiffness from the soil) can still be obtained from the PLAXIS 3D model.
- Ideally, to get even more accurate results for the PLAXIS 3D model, the point load should be placed exactly on a node. This avoids inaccuracy of the results due to interpolation. The distance between the nodes is $\frac{1.9}{2} = 0.95$ [m]. For a velocity $v = 14$ [m/s], this results in a time step of 0.068 [s] to ensure that the point load is exactly placed on the subsequent node. This is above the threshold Δt of 0.013, as calculated in equation 4.12.

To avoid rounding errors, the element size should be changed to 1.75 [m]. This gives the following characteristics:

- $distance_{nodes} = \frac{1.75}{2} = 0.875$ [m]
- $\Delta t = \frac{distance_{nodes}}{v} = \frac{0.875}{14} = 0.0625$ [s]

To ensure that the criterion from equation 4.12 is met, the proposed Δt is divided by 5, which is 0.0125 [s]. This means that for every 5 steps, the load is exactly placed on a node.

- For the PLAXIS 3D model and the validation of this model, the wheel load was assumed based on the maximum tram load and a Dynamic Amplification Factor of 1.3. This might be a too conservative approach. Installing Weighing in Motion sensors to measure the axle and wheel loads of the tram should give greater certainty about the accuracy of the wheel loads used in the calculations at the case study location [107]. Using this data for the PLAXIS 3D simulation should eventually lead to a more accurate prediction and validation of the occurring rail deflection and bending moments in the slab.
- To get an accurate impression of the stresses underneath the concrete slab track, earth pressure cells should be installed underneath the tram track structure. The most representative locations are underneath the switches due to the high dynamic amplification of the wheel loads and at the straight section with the highest track speed. If these stresses are below 200 [kPa], glass foam aggregates can still be a suitable light-weight filler material. A compaction ratio of 40% is necessary, as was studied by Mustafa and Szendefy [75]. Therefore, the following researches should be performed:
  - The uniaxial cyclic loading test as executed by Mustafa and Szendefy should be performed for the observed stresses. The accumulated plastic strain should be measured for different compaction ratios. Moreover, the modulus of elasticity (M_r) and potential crushing of the material should be checked. Crushing of the aggregates implies exceeding the 770 [kPa] contact stress between the particles.
  - The contact force chains between the foam glass aggregates under dynamic loading conditions can be modelled in a Discrete Element Model (DEM). The settlement results of the uniaxial cyclic loading test can be used to validate the DEM. Moreover, if necessary, the effect of geogrids reinforcement on the contact force chains can be modelled in the Discrete Element Model [73].
- The PLAXIS 2D simulation results can only be validated by field measurements after having implemented the new type of foundation. However, the predicted results make sense for the following reasons:
  - For scenario 1, the predicted settlements for foam concrete and EPS are the same as the autonomous settlements. This can be explained by the fact that the weight of the engineering solution and the structure are equal to the weight of the removed sand layer, hence resulting in zero extra weight applied on the soil ($\Delta\sigma_z = 0$). When inserting this in the analytical equations from NEN Bjerrum (equation C.4 and equation C.5), the value for $S_1 = 0$. This implies that only settlements due to creep (the autonomous settlements) occur.
  - For scenario 2, the improved foundation with significantly lower weight is applied on preconsolidated soil. The settlement rate of the structure is equal to the autonomous settlement rate.
- The PLAXIS SSC model foresees a reduction in the autonomous settlement rate. This settlement rate is in line with the predicted settlements for scenario 2 for the Rockflow elements, foam concrete foundation layer and the EPS elements. The settlement rate of 1.1 to 1.3 [mm/year] is still within the range predicted by Deltares, TNO, and Wageningen Environmental Research (WENR) [52]. However, due to for example drainage activities from the water board, the creep rate might not decrease. On the other hand, the assumption that when light-weight solutions are applied on preconsolidated soil, the settlement rate of the structure is equal to the autonomous settlements is still plausible. To conclude, the structure will be durable and reach the design life time of 30 years, especially taking into consideration the promising results for scenario 1.

- The effect of the load and potential elevation of the surrounding roads on the settlements was not taken into consideration. Moreover, to minimise disruptions for all stakeholders, an integral renewal of the entire roundabout in 2026 is preferred. Furthermore, this reduces the risk of differential settlements between the tram structure, roads and cycle lanes. When these light-weight solutions are installed and the roads are reconstructed/re-elevated by using conventional sand fill methodologies, the roads could settle more than the tram track structure. These differential settlements can result in pavement distresses, such as cracks. Furthermore, the differential settlements can exacerbate the transition zone between the roundabout and the free tram track structure, once again resulting in excessive degradation of the tram track structure.
- For scenario 2, the structure has already settled for 6570 days. When installing the state-of-the-art engineering solution, the sand layer is excavated with the corresponding structural height of the engineering solution. However, in practice, when the vertical alignment has to be restored to the original position, less sand can be excavated. This will result in a higher overall settlements over the remaining 30 years. However, taking into consideration the good performance for scenario 1 and the very low results for scenario 2, the conclusion that these state-of-the-art engineering solutions are suitable light-weight fillers for this case study location still holds.

5

Sustainability Assessment of the Improved Track Structure

The last decennia have seen an increase in more extreme weather conditions, such as higher temperatures, heatwaves and more severe downpours. An increase of CO_2-emissions causes a temperature-rise, which results in more extreme climate and weather conditions. The Royal Dutch Meteorological Institute (KNMI) foresees a further increase in temperature. The magnitude of this temperature increase is related to the emitted green house gases. It is yet unclear how this influences the location of common high pressure and low pressure areas, and therefore the effect on precipitation. Therefore, the KNMI has developed 4 climate scenarios [108]:

- High CO_2-emissions, wet climate
- High CO_2-emissions, dry climate
- Low CO_2-emissions, wet climate
- Low CO_2-emissions, dry climate

In an urban environment, the effect of climate change is more present. Due to the high amount of impervious surfaces and low percentage of vegetation, there is in increase in air temperature in the cities compared to the surrounding rural areas characterised by well-wetted grasslands. This effect is known as the Urban Heat Island effect. This effect is most severe during the daytime [54], [108]. Furthermore, due to extreme precipitation, there is a risk of waterlogging and overflow of the combined sewage system [54].

A sustainable living quarter should comply with the following criteria [7]:

- **Climate Resilience**
  The neighbourhood should withstand the climate-related problems, such as extreme heat and precipitation
- **Climate Mitigation**
  The services in the neighbourhood should mitigate the effect of global warming by reducing the emission of greenhouse gases.
- **Circular**
  The amount of virgin materials should be minimised. Moreover, the amount of waste should be minimised and recycled as much as possible.
- **Provide wellbeing**
  The residents should live in a pleasant environment.

The RET tram tracks are constructed in the urban environment and therefore, these structures are directly related to the sustainability in the urban environment. In this chapter, the following research question will be answered: "*How sustainable are the existing and proposed tram track structures and which engineering solutions can be applied to improve the sustainability performance of these structures?*" Note that not all sustainability parameters are related to the tram track structure. For this project, only the most relevant factors are taken into consideration, which are:

- Climate resilience against heat stress and flooding
- Climate mitigation measures due to the use of low carbon-footprint materials
- Circularity of building materials

Another important aspect on the well-being of the residents are related to noise and vibrations caused by the trams. However, these complex phenomena are related to many factors and parameters, which is therefore outside the scope of this project.

The second point about low carbon-footprint materials raises another question regarding the durability of the structure. In the previous chapter (Chapter 4), state-of-the art engineering solutions are proposed to mitigate the settlement of the tram track structure. However, applying these construction materials in the track structure design increases the carbon footprint of the material. Therefore, the following research question is discussed in this chapter as well: "*To what extent are the state-of-the-art engineering solutions affecting the sustainability performance of the tram track structure and how does this relate to the lifetime equivalent CO_2 emissions?*".

5.1. Urban sustainability

As was mentioned in the introduction of this chapter, there are many factors related to a sustainable living quarter. First, it is important to define the characteristics of an urban environment. This is not always as easy as it seems. For example, some city centres may have tall skyscrapers, which is a contradiction to a suburban area with terraced houses. These types of neighbourhoods are characterised by different types of terrain, percentages of impervious surfaces and SkyViewFactor (ψ_{sky} , SVF). The SVF depends on the position and orientation of a surface relative the sky obstruction overhead and is therefore roughly related to the with of the street, the height of the buildings and the shadow provided by other obstacles, such as trees [54]. Stewart and Oke developed the Local Climate Zone (LCZ) concept to classify the urban environment [109]. These Local Climate Zones are displayed in figure 5.1.

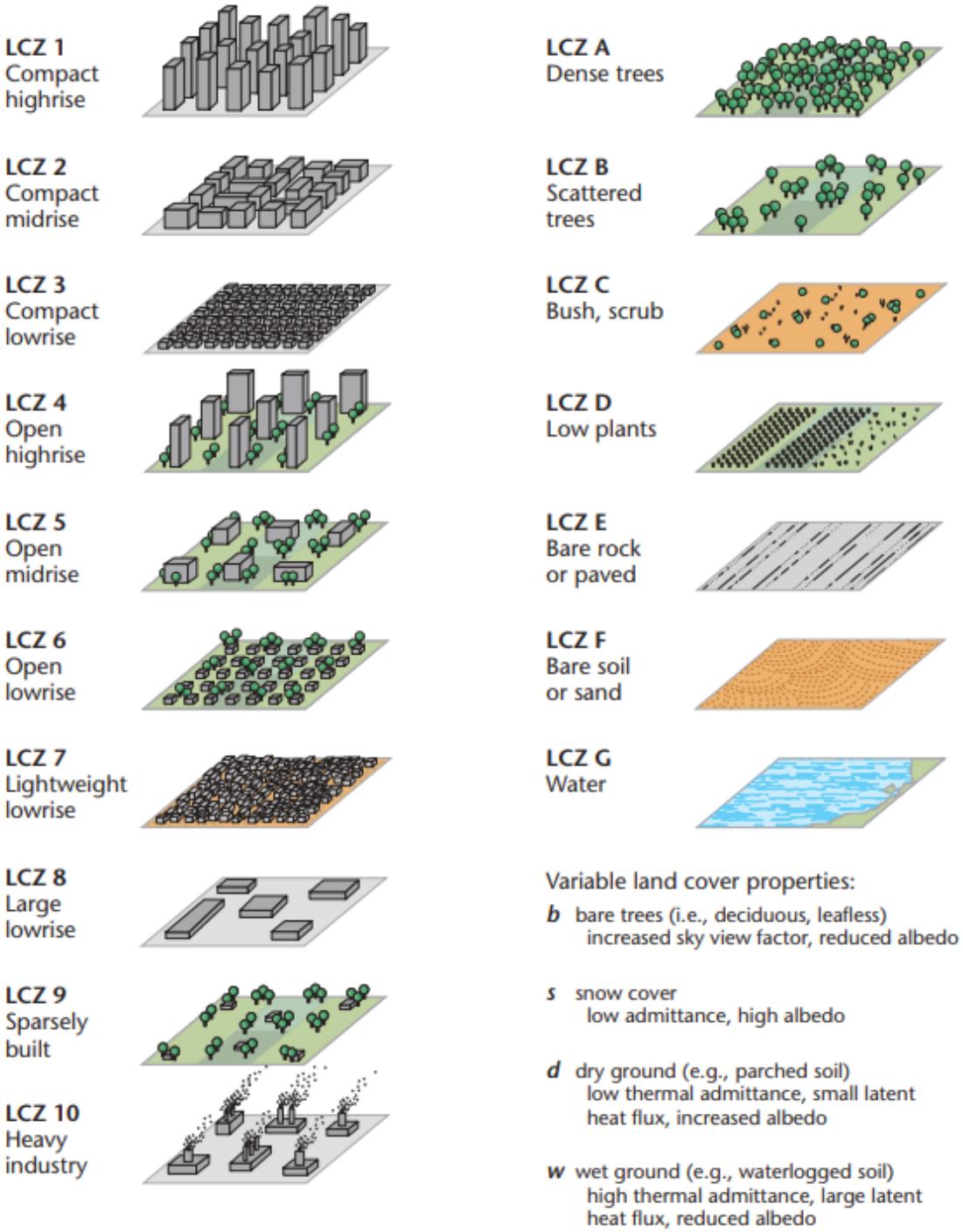

Figure 5.1: Local Climate Zones [109]

These differences can be observed along the RET tram network as well, as displayed in figure 5.2. The built environment around the Coolsingel can be considered as a Compact High Rise LCZ, whereas the neighbourhood around the shopping centre Keizerswaard is considered as an Open Mid Rise LCZ.

(a) Tram Track Coolsingel

(b) Tram Track Keizerswaard

Figure 5.2: Comparison in LCZs around the RET tram network

The difference in vegetation and SkyViewFactor has a significant influence on the climate-resilience parameters "*risk of heat stress*" and "*flooding*".

5.1.1. Climate Resilience - Risk of heat stress

The risk of heat stress is one of the key-factors when considering sustainability in the urban environment, especially taking into consideration the further temperature rise foreseen by the KNMI [108]. The contributing factors can be evaluated based on the Surface Energy Balance, which is stated in equation 5.1 [54].

$$Q^* + Q_F = Q_H + Q_E + \Delta Q_S + \Delta Q_A \tag{5.1}$$

Where:

- Q^* = net allwave radiation [Wm^{-2}]
- Q_F = anthropogenic heat flux density [Wm^{-2}]
- Q_H = sensible heat flux density [Wm^{-2}]
- Q_E = latent heat flux density [Wm^{-2}]
- ΔQ_S = heat storage [Wm^{-2}]
- ΔQ_A = advection [Wm^{-2}]

A schematic of the fluxes of the Surface Energy Balance (SEB) is depicted in figure 5.3.

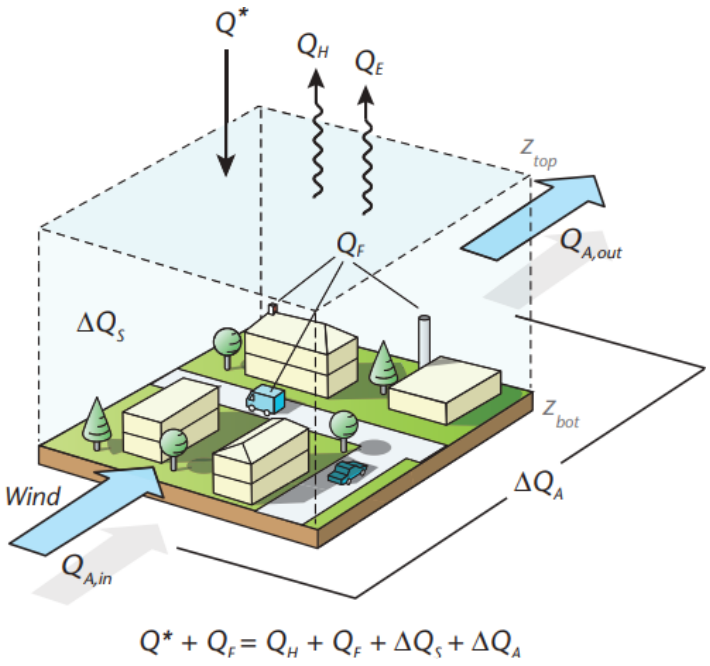

Figure 5.3: Schematic SEB in an urban building-soil-air volume [110]

The high amount of impervious area leads to less vegetation. Therefore, the latent heat flux Q_E reduces compared to the sensible heat flux Q_H, which implies that due to less evaporation of vegetation, the air temperature increases [54]. So, by increasing the amount of vegetation in the public area, the risk of heat stress reduces. Furthermore, the presence of trees provides shading. This reduces the SkyViewFactor, which therefore lowers the risk of heat stress as well.

5.1.2. Climate Resilience - Risk of flooding

In addition to the risk of heat stress, there is also an increased risk of flooding in the urban environment, since more extreme downpours are foreseen in the future [108]. In the urban environment, there is more paved surface, which ensures that water is diverted to the sewage system. Older sewage systems are combined sewage systems, which also diverts sanitary wastewater to the wastewater treatment plant. If the maximum discharge of the combined sewer is exceeded during extreme precipitation, sewage water can overflow on nearby surface waters such as ponds, rivers and canals [54], [111]. These overflows of untreated sewage water have a negative influence on the water quality and should therefore be avoided. In a modern sewage system, the sewage system for the rainwater and the sanitary wastewater are therefore split. If the rainwater sewer overflows, it does not affect the water quality, since it is not mixed with the sanitary wastewater [111].

Another key strategy to avoid flooding is to provide water buffers in the public space, where water can slowly infiltrate into the ground water. A first step is to reduce the amount of paved surface and ensure that water can slowly infiltrate in the ground. Sometimes, when there is enough space available, A wadi can be installed to provide an extra water buffer and allow slow water infiltration. However, in the boroughs on the South bank of the Meuse river, the water infiltration opportunities are minimised due to the impermeable clay layers and a high ground water table [58].

5.1.3. Climate Mitigation and Circularity - Low carbon footprint

According to the United Nations, the building sector is responsible for 37% of the global greenhouse gas emissions. These greenhouse gases are emitted by the production of construction materials such as concrete, steel and aluminium.

There are various ways to reduce these emissions [112]:

- Improve the production process of materials to reduce the CO_2-emissions
- Use electric equipment for transportation and construction
- Enhance the recyclability of construction materials and minimise the use of raw/virgin materials

At the moment, the buildings industry is a linear economy, which means that for construction, raw materials are used and at the end-of-life stage, all the materials are disposed to a landfill. To reduce the overall carbon footprint of the structure and reduce the amount of raw materials used, the loop of construction materials should be closed and the industry should strive for a circular economy.

In figure 5.4, the Life Cycle Stages in the construction process and the circularity loops are displayed.

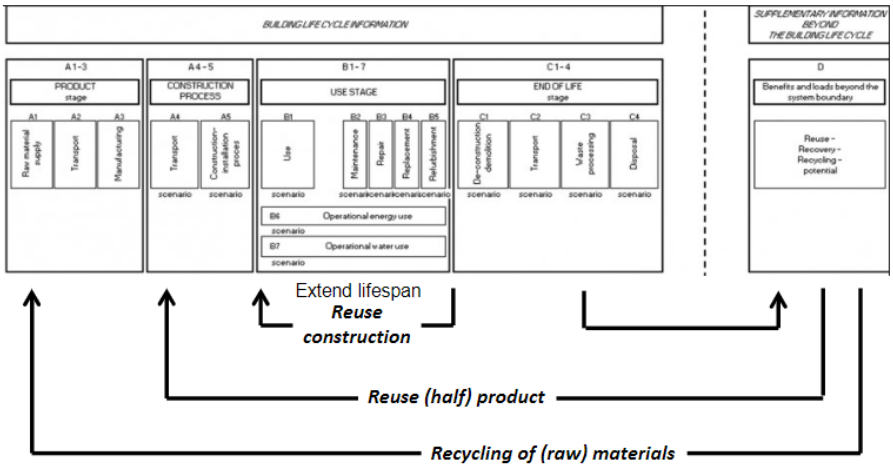

Figure 5.4: Life Cycle Stages and circularity stages [113]

For every product, the environmental impact per Life Cycle Stage is listed in an Environmental Product Declaration (EPD) for multiple environmental impact categories. For this research, the effect on the carbon footprint is investigated. Therefore, the total Global Warming Potential in kg CO_2-equivalents is used.

5.2. Sustainability Assessment

For both the existing and improved tram track structures at the case study location, the sustainability performance is assessed. The climate resilient factors are discussed qualitatively, whereas the carbon footprint is discussed quantitatively based on the EPDs.

5.2.1. Existing Track Structure

First, the sustainability performance of the existing track structure is assessed.

Risk of heat stress

As can be observed in figure 5.2b, there is sufficient vegetation around the case study location. The tram track is embedded in grass, which enhances the latent heat flux and reduces the sensible heat flux. Note that the Sky View Factor is high, which could still result in a high Physiological Equivalent Temperature (PET). However, trees close to the track structure are not preferred, since the roots might damage the slab track. The hedgerows are a suitable alternative. So overall, regarding the possible options nearby the tram track structure, this is the most optimal solution. In contradiction to the tram track nearby Keizerswaard, the tram track nearby tram stop Akkeroord is embedded in ballast, which is unfavourable for the risk of heat stress. However, the surrounding vegetation around the tram track structure already provides cooling.

The Dutch government has published maps which display the temperature increase due to the Urban Heat Island effect and the cooling provided by vegetation and nearby waterbodies. These are displayed in figure 5.5a and 5.5b respectively. Especially figure 5.5a clearly displays that the vegetation around the tram track structure and the roads has a cooling effect on the area compared to the surrounding building blocks and shopping centre.

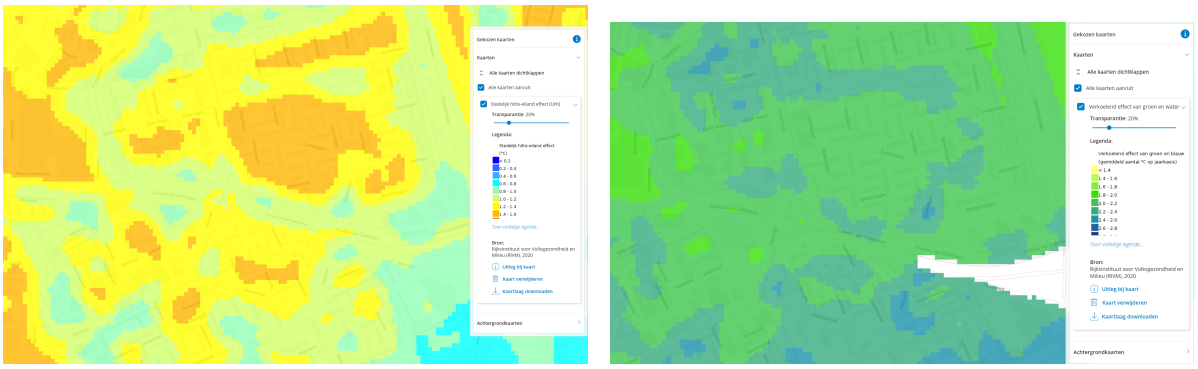

(a) Urban Heat Island temperature increase

(b) Cooling effect of vegetation and water bodies

Figure 5.5: Heat stress maps Groeninx van Zoelenlaan - Keizerswaard [114]

This is a huge contradiction compared to the tram track at the Coolsingel (figure 5.2a). The temperature increase due to the Urban Heat Island effect is significantly higher in the city center, which can be observed in figure 5.6. These high temperatures are caused by the high percentage of impervious surfaces and the low percentage of vegetation.

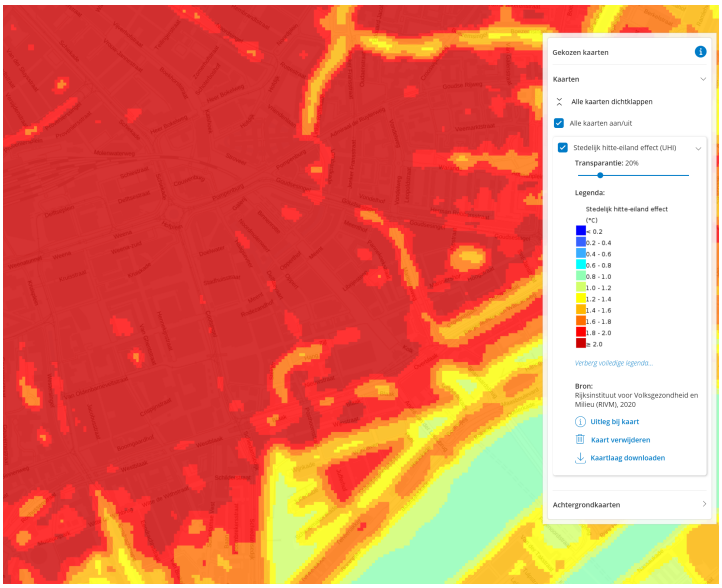

Figure 5.6: Urban Heat Island - City centre Rotterdam [114]

At the Weena, which is characterised as a Compact High Rise LCZ, the tram track is embedded in grass. However, no reduction of the Urban Heat Island effect was observed, as shown in figure 5.6.

Risk of flooding

In addition, the Dutch government has published a map which shows the risk of flooding after extreme precipitation. This map is displayed in figure 5.7.

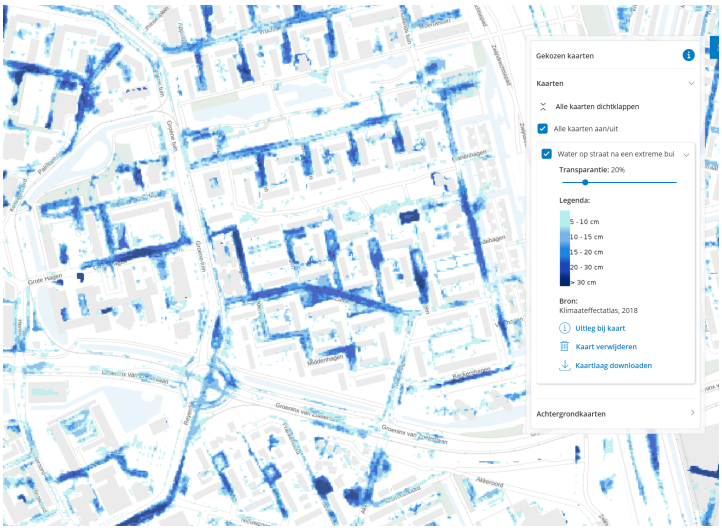

Figure 5.7: Flood risk map Groeninx van Zoelenlaan - Keizerswaard [114]

Around the project location, there is a relatively small flood risk compared to the street in the surrounding neighbourhood. However, there is a risk of 10 centimetres of flooding at certain parts of the roundabout. This hinders traffic on the roundabout and causes disruptions of the tram line operations. An adequate drainage and/or water buffer system could reduce the risk of flooding and the risk of overflow of the sewage system.

Carbon footprint

The total Global Warming Potential in kg CO_2-equivalents can be calculated for the tram track structure. This data can be found in the EPD for every single material used. However, the functional unit for the materials may differ. For the tram track structure, a functional unit of 1 meter length is selected. In addition to that, the life time of the structure should also be taken into consideration. The existing tram track structure at the case study location does not meet the design life time criterion of 30 years, but has been operational for only 18 years. All data should eventually be multiplied with a factor of $\frac{30}{18}$.

Rails

For the rails, the EPD of AcelorMittal is used. The rails have a weight of 60.59 kilogram per meter. For every cross-section there are two tracks, which means that there are four rails in total. The functional unit of this EPD is per tonne (or 1000 kg), which means that for the functional unit of 1 meter track structure the values in the EPD should be multiplied with 0.06059 for the weight and 4 for the total amount of rails used. The influence of transportation to the construction site on the equivalent CO_2-emissions is unknown. A plausible reason is that the transportation is related to the specific project location and the location of the blast furnace, which are not generic. A recyclability potential of 99% is assumed [115]. The equivalent CO_2-emissions for one meter of tram track structure is listed in table 5.1.

Table 5.1: Equivalent CO_2-emissions per meter track - Rails (based on [115])

Indicator	Unit		A1-3	C1	C2	C3	C4	D
GWP-total	kg eq.	CO_2-	6.20E+02	1.05E+01	5.16E+00	3.71E-01	3.51E-02	-4.14E+02

Concrete
The RET has multiple type of concrete mixtures that can be used for the tram track structure. The contractor is free to choose which mixture should be used, usually depending on the rate of strength development. In general, there are three types of mixtures used:

1. Strength class C30/37 CEM III/B 42.5 N
2. Strength class C25/30 CEM I 52.5 R
3. Strength class C25/30 CEM I 52.5 R (+ 25% CEM I)

For the used type of cement, N stands for normal strength development and R stands for rapid strength development. Furthermore, for the last mixture design, extra CEM I is added to further enhance the strength development rate. This mixture design and feature is probably desired when the track structure must be available very soon to continue line operations.

The equivalent CO_2-emissions for 1 meter track with a width of 6.1 [m] and a structural height of 0.17 [m] are listed for every life cycle stage in table 5.2, 5.3 and 5.4 for mixture 1, 2 and 3 respectively. The concrete mixtures are made by Betonmortelcentrale De Lek B.V. in Groot-Ammers. The company calculated the GWP values for stage A1-3 and D, so only the part of the production process they are accountable for. No clarification was given for the obtained values in module D.

The value for A4 is calculated based on the CO_2-emissions for a transportation distance between Groot-Ammers and Rotterdam, which is roughly 40 km. The GWP value for a EURO 6 cement truck which travels 25 km is reported by A/S Ikast Betonvarefabrik [116]. This value is directly converted to 40 km by using a multiplication factor of $\frac{40}{25}$.

Table 5.2: Equivalent CO_2-emissions per meter track - C30/37 CEM III (based on [116], [117])

Indicator	Unit	A1-3	A4	C1	C2	C3	C4	D
GWP-total	kg CO_2-eq.	1.28E+02	8.13E+00	0E+00	0E+00	0E+00	0E+00	0E+00

Table 5.3: Equivalent CO_2-emissions per meter track - C25/30 CEM I (based on [116], [118])

Indicator	Unit	A1-3	A4	C1	C2	C3	C4	D
GWP-total	kg CO_2-eq.	1.17E+02	8.13E+00	0E+00	0E+00	0E+00	0E+00	6.79E-04

Table 5.4: Equivalent CO_2-emissions per meter track - 25% C25/30 extra CEM I (based on [116], [119])

Indicator	Unit	A1-3	A4	C1	C2	C3	C4	D
GWP-total	kg CO_2-eq.	1.93E+02	8.13E+00	0E+00	0E+00	0E+00	0E+00	6.79E-04

Grass

The turfgrass big slabs are placed on top of the concrete slab. The top of the grass is on the same height as the head of the Ri60 grooved rail. These slabs grow externally before being transported and installed on site on a layer of sandy clay.

The GWP-total value for the turfgrass big slabs per meter tram track structure is listed in table 5.5. Deducting the width of the grooved rails from the total width of the slab track gives a width of 5.65 [m] per meter track. For transportation from the production site to the project location, a lorry is used. The distance between the production site and the product location is assumed to be 62 [km]. As a end-of-life scenario is assumed that the grass is part of the natural environment and therefore, no recycling or waste landfill scenario is assumed [120].

There is no data available regarding the use stage. However, maintenance is necessary during this stage. The carbon footprint during this stage is related to the mowing frequency and the type of lawn mower used. Taking into consideration the length of the entire network, the impact per meter track is considered to be extremely low and can therefore be neglected.

In the used EPD, no explanation is given for the emissions in stage C4. A plausible explanation is that all embodied carbon can be released when the material is combusted or when the grass dies after mowing.

Table 5.5: Equivalent CO_2-emissions per meter track - turfgrass big slab (based on [120])

Indicator	Unit	A1-3	A4	C1	C2	C3	C4	D
GWP-total	kg CO_2-eq.	-2.77E+01	6.44E-01	0E+00	0E+00	0E+00	2.86E+01	0E+00

Ballast

The Dutch infrastructure manager ProRail has performed the LCA for the ballast used in the national railway network in collaboration with RoyalHaskoningDHV [121]. The ballast quarries are spread over Europe. For example, contractor Strukton obtains new ballast from quarries in Norway, Germany and Belgium and recycled ballast from the recycling plant in the Dutch city of Roosendaal [122]. The study for Strukton and ProRail both show that the main contributor to the carbon footprint is the transportation of the material. Moreover, this is related to transportation distances and mode of transportation. Especially transport only with trucks has a bad influence on the CO_2-emissions [122].

The average results for the ballast in the Dutch railway sector from ProRail are used for this research. However, since the ballast for the tram track structure is only used to embed the rails, tamping ballast is not necessary. Therefore, the value in the A5- and B-module corresponding to this activity is set to 0. Furthermore, the values for 1 ton ballast are converted to the used weight for 1 meter track structure. The effective width is 5.65 [m] and the height of the ballast layer is 0.165 [m]. Multiplying with the density of ballast gives a weight of 1.04 [tons] of ballast per meter track structure. The equivalent CO_2-emissions for the used ballast per meter track is listed in table 5.6 below.

Table 5.6: Equivalent CO_2-emissions per meter track - ballast (based on [121])

Indicator	Unit	A1-3	A4	A5	C1	C2	C3	C4	D
GWP-total	kg CO_2-eq.	3.20E+01	1.20E+01	3.13E-01	2.09E-01	4.80E+00	6.26E-01	5.22E-01	-3.05E+01

Total emissions tram track structure
To conclude, the following six combinations are possible:

1. C30/37 CEM III/B 42.5 N - embedded in ballast
2. C30/37 CEM III/B 42.5 N - embedded in grass
3. C25/30 CEM I 52.5 R - embedded in ballast
4. C25/30 CEM I 52.5 R - embedded in grass
5. C25/30 CEM I 52.5 R (+ 25% CEM I) - embedded in ballast
6. C25/30 CEM I 52.5 R (+ 25% CEM I) - embedded in grass

The total equivalent CO_2-emissions are listed in table 5.7 for all six types of structures.

Table 5.7: Equivalent CO_2-emissions per meter track in [kg CO_2-eq.] - Existing track structure (lifespan 30 years)

	CEM III - Ballast	CEM III - Grass	CEM I - Ballast	CEM I - Grass	extra CEM I - Ballast	extra CEM I - Grass
Rails	2.22E+02	2.22E+02	2.22E+02	2.22E+02	2.22E+02	2.22E+02
Concrete	1.37E+02	1.37E+02	1.25E+02	1.25E+02	2.01E+02	2.01E+02
Ballast	1.99E+01	0E+00	1.99E+01	0E+00	1.99E+01	0E+00
Grass	0E+00	1.55E+00	0E+00	1.55E+00	0E+00	1.55E+00
Total	3.79E+02	3.60E+02	3.67E+02	3.49E+02	4.43E+02	4.24E+02

Since the track structure is completely renewed 18 years after construction instead of 30, all calculated values are corrected with a factor of $\frac{30}{18}$ to compensate for the short life span. These results are listed in table 5.8.

Table 5.8: Equivalent CO_2-emissions per meter track in [kg CO_2-eq.] - Existing track structure (lifespan 18 years)

	CEM III - Ballast	CEM III - Grass	CEM I - Ballast	CEM I - Grass	extra CEM I - Ballast	extra CEM I - Grass
Rails	3.70E+02	3.70E+02	3.70E+02	3.70E+02	3.70E+02	3.70E+02
Concrete	2.41E+02	2.41E+02	2.21E+02	2.21E+02	3.54E+02	3.54E+02
Ballast	3.32E+01	0E+00	3.32E+01	0E+00	3.32E+01	0E+00
Grass	0E+00	2.58E+00	0E+00	2.58E+00	0E+00	2.58E+00
Total	6.45E+02	6.14E+02	6.24E+02	5.93E+02	7.58E+02	7.27E+02

In addition, a bar chart which graphically displays the results is displayed in figure 5.8.

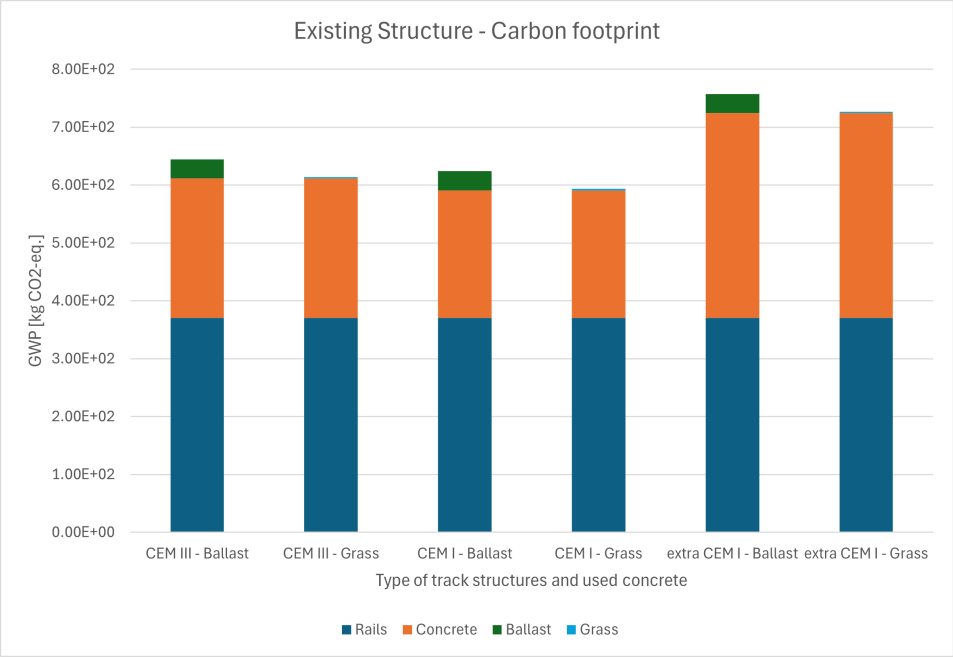

Figure 5.8: Carbon footprint of the existing track structure (lifetime 18 years)

Conclusion
Based on the results in table 5.7, 5.8 and figure 5.8, the following conclusions can be drawn:

- The main contributor to the carbon footprint of the tram track structure is the rails, which is 370 [kg CO_2-eq.]. For the most sustainable alternative, which is a CEM I tram track structure embedded in grass, this is 62.4% of the total carbon footprint.
- Whereas for the standard CEM I and CEM III concrete slab track almost similar results are reported, there is a significantly higher footprint for the structure when 25% extra CEM I is added to the mixture. This gives for the concrete a carbon footprint increase of 46.7% and 60.8% compared to CEM III and standard CEM I respectively.
- The big slabs grass have a very low carbon footprint per meter track of only 2.58 [kg CO_2-eq.]. This is 92.2% less compared to a layer of ballast. The carbon footprint for the ballast track is mainly related to the transportation of the material from the quarry to the project location. To reduce the carbon footprint, a nearby quarry should be selected (such as Porfier in Belgium) and sustainable transportation methods should be used, such as freight trains. Moreover, inland vessels are preferred over trucks [121].
- The most sustainable existing track structure is the CEM I track structure embedded in grass with a total amount of equivalent CO_2-emissions of 5.93E+02 [kg] per meter track structure. This is 21.7% lower than the least sustainable option, which is the ballast track structure with extra CEM I. That structure has a total carbon footprint of 7.58E+02 [kg CO_2-eq.] per meter track structure.

5.2.2. Improved Track Structure - Rockwool: Rockflow
Furthermore, the sustainability assessment is performed for the improved tram track structures. The first alternative are the Rockflow elements made from rockwool.

Risk of heat stress
The rockwool elements are installed underneath the tram track structure. For both the structure embedded in grass and ballast, the rockwool elements mitigate the vertical settlements sufficiently. For the current case study location, there is sufficient vegetation to provide cooling. Furthermore, the Urban Heat Island temperature increase is minimised. Overall, installing the rockwool elements underneath different types of track structures does not influence the risk of heat stress.

Risk of flooding

As displayed in figure 5.7, there is a small risk of flooding at the case study location. Installing Rockflow underneath the track structure provides an extra water buffer and reduces the risk of overflow of the sewer. Moreover, the polluted storm water from the tram tracks is filtered in the rockwool elements, hence improving the water quality before diverting to the sewage system or nearby canals.

Carbon footprint

Rockwool is made when basalt and recycled products, such as recycled stone wool, slags and alumina, are melted at 1500 °C. Subsequently, the melted product goes thorough a spinning machine, where the fibres are formed. During this process, a binder is added to the material. Then, the material is cured in an oven, where the binder is polymerised. At last, the product is removed from the oven and cooled down before being convected to the desired shape [91], [123].

The slags and alumina used are considered as by-product from the metallurgic industry. For all these products, the environmental impact has already been accounted for. Furthermore, pig-iron is a co-product created during the production process, which is subsequently sold to the market. Therefore, economic allocation is applied.

The producer, Lapinus, offers a recycling service in the Benelux at the end-of-life stage. 50% of the material is transported to the factory in Roermond, whereas the other 50% is brought to landfill. The recyclability potential of 50% of the material and the recyclability potential of the waste in phase A is considered in stage D [91].

The equivalent CO_2-emissions for the Rockwool WM2007 elements per 1 meter track are listed in table 5.9.

Table 5.9: Equivalent CO_2-emissions per meter track - Rockflow WM2007 (based on [91])

Indicator	Unit	A1-3	A4	A5	C1	C2	C3	C4	D
GWP-total	kg CO_2-eq.	3.85E+02	2.09E+01	1.54E+01	5.55E+00	6.96E+00	0.00E+00	1.29E+00	-4.80E+00

The melting process is one of the main contributors to the high carbon footprint during the production stage. For the current production process, cokes are used to heat up the oven. The Rockwool factory in Roermond has planned to electrify 2 production lines. When green electricity is used, the CO_2-emissions drop with 80% for these production lines and reduce with 50% for the entire factory [124], [125]. Although the exact changes compared to the data in table 5.9 are not known, a simple assumption can be made that the value for A1-3 decreases with 50%, resulting in a reduction of 1.93E+02 [kg CO_2-eq.].

For simplicity, the most sustainable track structures (with CEM I) embedded in grass and ballast are selected and compared to the structure with Rockwool, which has a life span of 30 years. The results are reported in table 5.10.

Table 5.10: Equivalent CO_2-emissions per meter track in [kg CO_2-eq.] - Existing track structure (lifespan 18 years) vs Rockwool (lifespan 30 years)

	Existing CEM I - Ballast	Existing CEM I - Grass	Rockwool - Ballast	Rockwool - Grass
Rails	3.70E+02	3.70E+02	2.22E+02	2.22E+02
Concrete	2.21E+02	2.21E+02	1.25E+02	1.25E+02
Ballast	3.32E+01	0E+00	1.99E+01	0E+00
Grass	0E+00	2.58E+00	0E+00	1.55E+00
Rockwool	0E+00	0E+00	4.27E+02	4.27E+02
Total	6.24E+02	5.93E+02	7.94E+02	7.76E+02

Furthermore, these results are shown in the bar chart in figure 5.9.

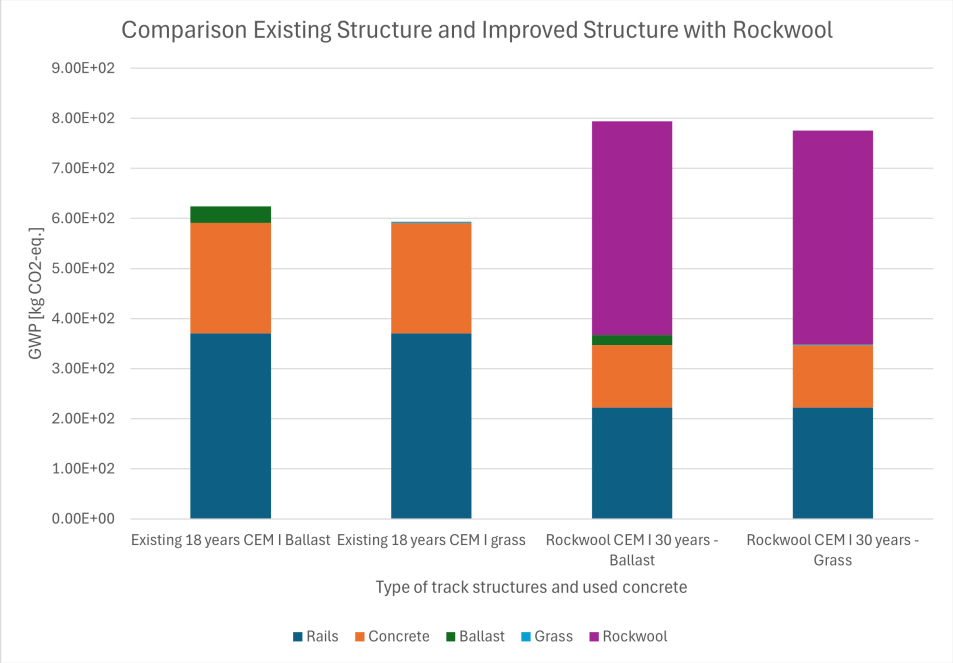

Figure 5.9: Carbon footprint of the existing and improved track structure with Rockwool

Based on the results reported in table 5.10 and shown in figure 5.9, the following trends are observed:

- For the track embedded in ballast, the carbon footprint has increased with 27.2% from 6.24E+02 to 7.94E+02 [kg CO_2-eq.] per meter track.
- For the track embedded in grass, the carbon footprint has increased with 30.9% from 5.93E+02 to 7.76E+02 [kg CO_2-eq.] per meter track.

Therefore, applying Rockwool underneath the track structure still leads to a higher carbon footprint, even when the lifespan of the structure increases. Note that this increase is largest for the most sustainable track structure. For less sustainable structure, such as the track embedded in ballast with extra CEM I, this increase will be lower.

5.2.3. Improved Track Structure - Foam Concrete

As discussed in chapter 4, the second alternative for an improved type of foundation is foam concrete.

Risk of heat stress

The foam concrete is casted into the trench of removed sandfill. The superstructure and therefore the risk of heat stress remains unchanged compared to the current situation.

Risk of flooding

In contrast to the Rockflow elements, the foam concrete foundation cannot buffer water. Therefore, the risk of flooding around the case study location remains unchanged.

Carbon footprint

Foam concrete mixtures consists of cement, water, filler, admixtures and foam. The carbon footprint is highly dependent on the desired density. The higher the density, the higher the required filler and cement. Not many EPDs are publicly available. The used EPD for this research is from the Company Fixit, which produces foam concrete (POR® Schaummörtel/-beton) which ranges in density from 200 to 1400 [kg/m^3] [126].

For this EPD, the reference life time of the foam concrete is assumed to be 40 years, which is higher than the intended life span of the structure, which is 30 years. At the End-of-life stage, 97% of the material can be recycled. The foam concrete can be crushed and the aggregates can be reused as backfill material. This recyclability-potential is included in Life-cycle-stage D.

The equivalent CO_2-emissions for the foam concrete layer with a density of 600 [kg/m^3] per 1 meter track are listed in table 5.11. The data in the original EPD are given for 300 [kg/m^3], but can be scaled linearly to a density of 600 [kg/m^3]. So, all values are multiplied with a factor 2.

Table 5.11: Equivalent CO_2-emissions per meter track - Foam concrete (based on [126])

Indicator	Unit	A1-3	A4	A5	C1	C2	C3	C4	D
GWP-total	kg CO_2-eq.	8.62E+02	2.64E+01	4.74E-01	1.47E-01	1.65E+00	7.10E+00	0E+00	-1.54E+01

Just as for Rockwool, the most sustainable existing track structures with CEM I embedded in grass and ballast are compared to a structure with foam concrete, which then has a life span of 30 years. The results are listed in table 5.12.

Table 5.12: Equivalent CO_2-emissions per meter track in [kg CO_2-eq.] - Existing track structure (lifespan 18 years) vs Foam concrete (lifespan 30 years)

	Existing CEM I - Ballast	Existing CEM I - Grass	Foam concrete - Ballast	Foam concrete - Grass
Rails	3.70E+02	3.70E+02	2.22E+02	2.22E+02
Concrete	2.21E+02	2.21E+02	1.25E+02	1.25E+02
Ballast	3.32E+01	0E+00	1.99E+01	0E+00
Grass	0E+00	2.58E+00	0E+00	1.55E+00
Foam concrete	0E+00	0E+00	8.59E+02	8.59E+02
Total	6.24E+02	5.93E+02	1.23E+03	1.21E+03

In addition, these results are displayed in a bar chart in figure 5.10 below.

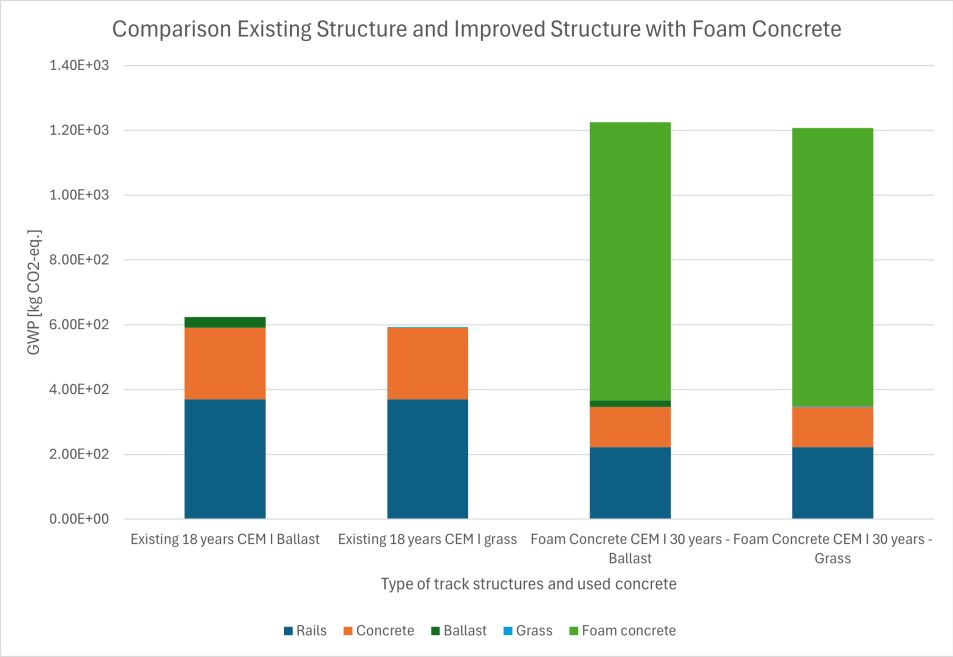

Figure 5.10: Carbon footprint of the existing and improved track structure with foam concrete

In figure 5.10 can clearly be observed that adding foam concrete significantly increases the carbon footprint per meter track structure. For the track structure in ballast, the total carbon footprint over 30 years increases with 97.1% when a foundation of foam concrete is used. This can be mainly related to the large volume of foam concrete that is required to minimize the settlements. Moreover, this mixture consists of 75 % Portland cement, which is characterised by a high carbon footprint.

5.2.4. Improved Track Structure - EPS

Another alternative foundation which ensures the longer lifetime of the tram track structure is EPS.

Risk of heat stress

The EPS elements are placed underneath the concrete slab of the tram track structure. Therefore, just as for the Rockwool elements, there is no influence on the risk of heat stress.

Risk of flooding

In contradiction to the Rockflow elements, the EPS elements underneath the structure do not provide an extra water buffer. Therefore, the risk of flooding is not reduced when installing EPS elements underneath the structure.

Carbon footprint

EPS production is based on a petrochemical process, as was discussed in section 4.2. Due to the low density of the material, relatively less of this material has to be applied compared to Rockwool and foam concrete.

For this analysis, an EPD for EPS with a density of 20 [kg/m^3] is used. However, this type of EPS is tailored to insulation boards for the Scandinavian market [127]. However, the material production and the density are similar to the EPS blocks used for the foundation of the tram track structure. Therefore, this EPD is assumed to give a good impression on the total GWP.

The total results of the GWP are stated in table 5.13. As end-of-Life scenario is assumed that the elements are fully incinerated. The resulting energy is stated in module D.

Table 5.13: Equivalent CO_2-emissions per meter track - EPS (based on [127])

Indicator	Unit	A1-3	A4	A5	C1	C2	C3	C4	D
GWP-total	kg CO_2-eq.	9.15E+01	1.08E+01	2.20E+00	0.00E+00	1.79E-01	1.26E+02	0E+00	-6.95E+00

In addition, the most sustainable existing track structures with CEM I embedded in grass and ballast are compared to a structure with foam concrete, which then has a life span of 30 years. The results are listed in table 5.14.

Table 5.14: Equivalent CO_2-emissions per meter track in [kg CO_2-eq.] - Existing track structure (lifespan 18 years) vs EPS (lifespan 30 years)

	Existing CEM I - Ballast	Existing CEM I - Grass	EPS - Ballast	EPS - Grass
Rails	3.70E+02	3.70E+02	2.22E+02	2.22E+02
Concrete	2.21E+02	2.21E+02	1.25E+02	1.25E+02
Ballast	3.32E+01	0E+00	1.99E+01	0E+00
Grass	0E+00	2.58E+00	0E+00	1.55E+00
Foam concrete	0E+00	0E+00	2.24E+02	2.24E+02
Total	6.24E+02	5.93E+02	5.91E+02	5.73E+02

Furthermore, these results are displayed in a bar chart in figure 5.11. When EPS is used as foundation, a reduction in carbon footprint of 5.2% and 3.4% is achieved for the structure embedded in ballast and grass respectively.

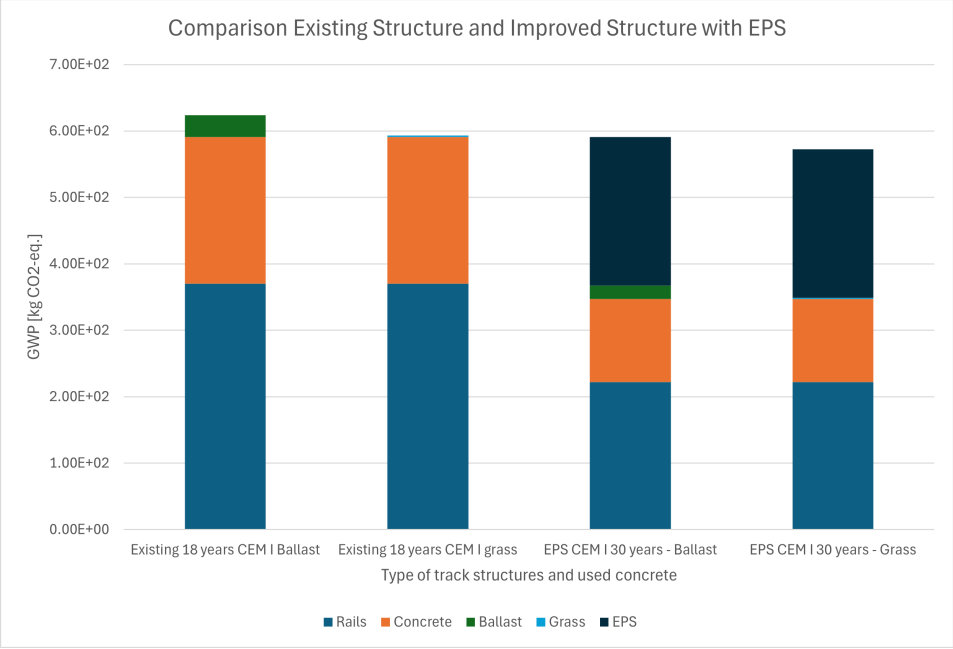

Figure 5.11: Carbon footprint of the existing and improved track structure with EPS

5.3. Overview carbon footprint per material

To conclude, an overview is given of the numerical results for a structure with a concrete mixture with cement type CEM I embedded in grass. These results are listed in table 5.15.

Table 5.15: Equivalent CO_2-emissions per meter track in [kg CO_2-eq.] - Existing track structure (lifespan 18 years) vs all materials (lifespan 30 years)

	Existing CEM I - Grass	Rockwool - Grass	Foam Concrete - Grass	EPS - Grass
Rails	3.70E+02	3.70E+02	2.22E+02	2.22E+02
Concrete	2.21E+02	2.21E+02	1.25E+02	1.25E+02
Grass	2.58E+00	2.58E+00	1.55E+00	1.55E+00
Rockwool	0E+00	4.27E+02	0E+00	0E+00
Foam concrete	0E+00	0E+00	8.59E+02	0E+00
EPS	0E+00	0E+00	0E+00	2.24E+02
Total	5.93E+02	7.76E+02	1.21E+03	5.73E+02

These results are graphically shown in figure 5.12.

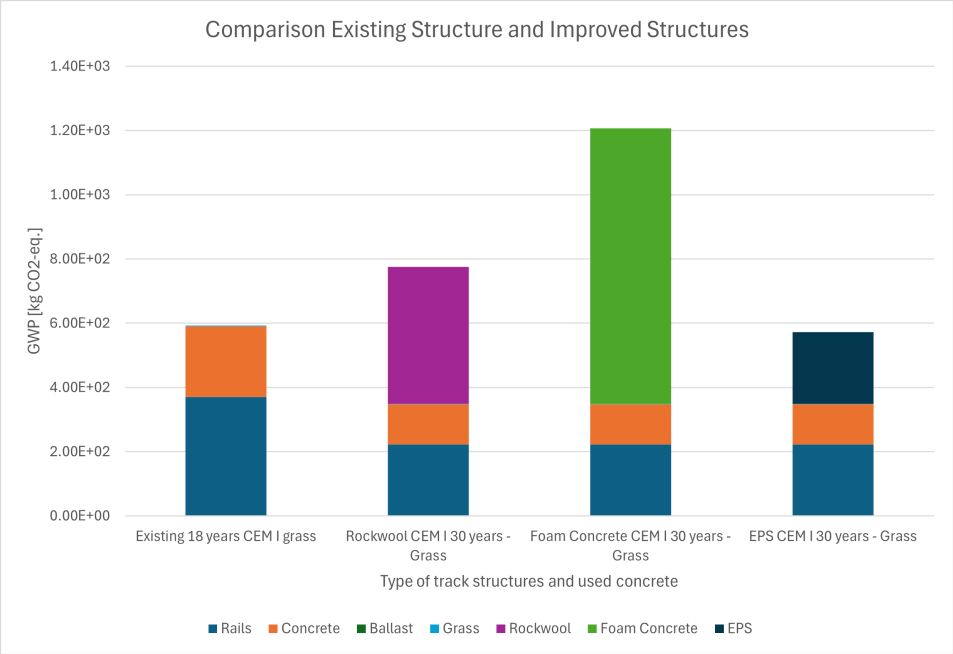

Figure 5.12: Overview - Carbon footprint of the existing and improved track structures

Based on the results from table 5.15 and figure 5.12, the following conclusions are drawn:

- EPS is the only light-weight filler material for which the carbon footprint of the structure over 30 years decreases when this material is implemented in the track structure design. This is mainly related to the low volume required for the design requirements, based on the low density of the material.
- Foam concrete has the worst impact on the total equivalent CO_2-emissions per meter track. The carbon footprint increases with 97.1 % over a life-span of 30 years.

- Installing Rockwool leads to an increase in carbon footprint of 30.9% compared to the existing structure with a life-span of 18 years. As was mentioned before, when the production process in the Rockwool factory is electrified, the CO_2-emissions of the entire factory drop with 50%. When assuming a reduction in equivalent CO_2-emissions of 1.93E+02 [kg], the total equivalent CO_2-emissions reduce to 5.84E+02 [kg], which is only 1.5% below the GWP for the existing structure.

In short, using EPS (and Rockwool after electrifying the factory) increases the durability of the structure without increasing the carbon footprint of the structure over the life span of 30 years.

5.4. Implementation Sustainability Improvements

Now that the sustainability performance for the existing and improved track structures has been evaluated, further improvements regarding the sustainability performance can be proposed.

The following steps are proposed based on the observations of the carbon footprint:

- The main contributor in equivalent CO_2-emissions is the steel rails, which is made from iron ores and cokes in blast furnaces. Using electric arc furnaces and recycled steel scrap in the production of the rails should reduce the carbon footprint significantly.
- The use of recycled concrete aggregates in the concrete mixture.
- The use of geopolymer concrete instead of conventional concrete.
- The use of olivine ballast to embed the track structure.

5.4.1. Circularity of the rails - Recycled rails

In the Dutch railway industry, only virgin steel is used, which is produced in blast furnaces across Europe. Steel is an alloy made of iron and carbon. In the conventional production process, iron ores, cokes and limestone are heated to temperatures up to almost 2000 °C in a blast furnace. The produced products are pig iron and slags. Subsequently, the pig irons are heated in a Basic Oxygen Furnace (BOF), where oxygen is blasted into the oven to remove carbon and impurities from the pig iron to get structural steel. This production process is highly energy intensive and therefore contributes to the high carbon footprint of the material. The European steel industry is responsible for 6% of the total CO_2-emissions in the European Union [128].

A sustainable alternative is using recycled steel and an electric arc furnace (EAF). High power electric arcs are created by carbon anodes to melt the steel scrap. Furthermore, coal or natural gas and iron ores are added to the steel scrap in the furnace. Due to the high temperature, the steel scrap melts and new steel is formed [128], [129]. In France, SNCF Réseau is currently using new rails made from 100% recycled steel in EAFs, resulting in 70% less CO_2-equivalent emissions compared to rails made of virgin steel in BOFs [130].

5.4.2. Circularity of the concrete track structure - Recycled Concrete Aggregates (RCA)

As mentioned during the introduction of this chapter, to minimise the carbon footprint of the tram track structure and minimise the demand for raw/virgin materials, the loop of construction materials should be closed. This means that the obtained materials at the end-of-life stage should be recycled. For the RET tram track structure, only virgin materials are used. Furthermore, at the end-of-life-stage, the concrete is transported to a company which recycles concrete. However, the recycled concrete is not directly used in a new tram track structure. To reduce the carbon footprint and the demand for virgin materials, enhancing circularity in the tram track design seems like a promising solution.

Recycled Concrete Aggregates (RCA) are aggregates which are obtained when concrete demolition waste is crushed and ground. The RCA are aggregates which do not only contain granular material, but also hardened cement paste. This hardened cement paste is highly porous, even 10 to 20 times more compared to natural aggregates. This water absorption influences the workability of the concrete mixture [131].

The use of RCA in the tram track structure is not new in The Netherlands. In Amsterdam, KWS and GVB use 50% of recycled concrete in the top layer of concrete (when the track is embedded in pavement) and 30% recycled concrete in the concrete foundation plate [132].

Replacing the virgin aggregates with recycled aggregates has influence on the mechanical performance of the concrete. Studies point out the following differences:

- Studies have shown a reduction in workability due to water absorption and the more angular shape of the aggregates [131], [133]. Moreover, not correcting the mixture design for this porosity and water absorption of the aggregates could result in insufficient compressive strength and reduced durability performance [131].
- A total substitution of the virgin aggregates with recycled aggregates shows a reduction of 30% in the 7 and 28 day compressive strength. However, this effect is minimal when up to 35% recycled aggregates are used [134].

The RET tram track structure differs from the GVB tram track structure. The concrete foundation base plate used in Amsterdam is continuous, whereas in Rotterdam, concrete is casted around the duo-block sleepers. Care should be paid to the bonding between the duo-block sleepers and the concrete base plate. Although no studies have been performed regarding this very specific question, research has been done regarding the bonding strength between reinforcement bars and concrete beams made of 100% RCA. For concrete made with natural aggregates with 30 MPa compressive strength, the bond strength is 10.4 to 19% higher compared to concrete with RCA [133]. Compared to the situation with the tram track structure and the duo-block sleepers, the bonding interface is more favourable due to the shape of the sleeper and the occurring stresses are significantly higher. Therefore, the use of RCA in the RET tram track structure should not have a negative influence on the bonding properties between the duo-block sleeper and the concrete plate.

Overall, using RCA seems a plausible and suitable method to reduce the raw material resource demand and the carbon footprint of the tram track structure. However, to meet the strength requirements, only a part of the natural aggregates can be substituted by RCA, as was documented by Abera [134]. Just as in line with this study and the experience from GVB in Amsterdam, a safe and realistic RCA rate of 30% can be used in the mixture design for the concrete slab.

Quantification of the potential reduction in carbon footprint is not possible yet. This depends on he transportation distance between the construction site, concrete recycling plant and the concrete batch plant. In 2018, GVB and KWS started with this circularity project, where only 30% RCA was used in the top layer concrete. No specific results in CO_2-reduction are reported, apart from the qualitative improvements regarding reduction in natural aggregate demand and carbon footprint. RET should collaborate with a contractor, concrete recycling company and concrete producer to make this transition possible and quantify the decrease in CO_2-emissions. However, based on the current mix design with the standard amount of CEM I, the effect on the GWP is assumed to be low for the following reasons [118]:

- The CEM I production in stage A1 already represents 69.95% of the GWP.
- The transportation of course and fine aggregates to the concrete plant represents 7.3 and 1.94 % of the carbon footprint, respectively. This will only be replaced by 30% RCA, which are transported by truck.
- The impact on the equivalent CO_2-emissions of the used sand and aggregates in stage A1 is only 5.25% and 1.57% respectively. These values are already low and will only be replaced by 30% of RCA.

5.4.3. Geopolymer concrete

Another promising solution to reduce the carbon footprint of the tram track structure is geopolymer concrete. Just as for conventional concrete, geopolymer concrete consists of coarse aggregates, fine aggregates, water and a binder. In conventional concrete, the binder is portland cement, which has a very high carbon footprint. However, geopolymer concrete consists of Alkali Activated Cementitious Materials, which functions as binder. Geopolymer has for instance the following beneficial properties [135]–[137]:

- High compressive strength (after hardening)
- Good resistance against freeze-thaw cycli when properly designed
- Rapid strength development
- Good resistance against chemical compounds, such as sulphates
- The bond strength of (self-compacted) geopolymer concrete is 24.5-31.7% higher compared to the conventional concrete with portland cement. Hence, for this case, there is sufficient bonding between the concrete base plate and the duo-block sleepers.
- Carbon-footprint reduction of 60-70% compared to CEM I cement

However, there are also some drawbacks. These are for instance:

- A majority of the current Eurocode design codes are emperical formulae based on the 28-day-strength of the concrete. For concrete with ordinary portland cement, the compressive strength tends to increase further over time, even after the 28-day-strength. However, the material properties of geopolymer concrete, such as bending stiffness, tensile splitting strength and elastic compressive modulus decrease over time [138].
- Lower Young's Modulus [135]
- The fatigue resistance can significantly be improved by adding steel fibres [139]
- Workability challenges, especially for in situ application [136]. However, certain contractors have tested the workability after keeping the mixture in the concrete mixture for the same duration as the transportation time. The contractor has optimised the mixture to obtain good workability results [140].
- Geopolymer concrete shows significant shrinkage behaviour, which is related to the relative humidity. Shrinkage causes cracking of the concrete. The shrinkage is most extreme at a relative humidity of 65% and decreases at higher and lower rates of relative humidity [141]. So, curing of the geopolymer concrete requires great attention.

Overall, regarding the current state-of-the-art geopolymer concrete practices, in situ casting of the tram track structure seems challenging. Especially shrinking problems due to inadequate curing pose a risk that the concrete plate does not have sufficient bonding with the sleepers. Especially on soft soils, this might result in excessive rail deflection and pavement distresses. Therefore, the only way to make this possible is by constructing smaller prefab elements of track structure and transport and install these structures on site.

5.4.4. Olivine ballast

The sensitivity analysis in section 3.6 has shown that the self-weight of the existing structure is one of the driving mechanisms of the settlements of the track structure. The tram track embedded in grass settles 10% more compared to the same track structure embedded in ballast. However, as can be observed in figure 5.8 and figure 5.9, the grass track structure has a significantly lower carbon footprint. For further comparison, a third alternative is proposed, which is olivine ballast. The RET has already successfully implemented olivine ballast in the inspection paths adjacent to the Hoekse Lijn between Schiedam and Hoek van Holland. This granular material captures CO_2 during the weathering process [142]. Furthermore, the Spanish railway infrastructure manager ADIF has implemented olivine ballast in two high speed track sections. This ballast has almost the same particle size distribution as prescribed by the regulations of the Dutch infrastructure manager ProRail.

However, the Dutch railway industry has been reluctant to implement olivine ballast in the railway tracks, since olivine is geologically characterised in the same categories as asbestos. However, lab tests have proven that asbestos are not present in olivine ballast [143].

Van Dijk Maasland has inventoried the carbon footprint of the entire olivine (ballast) supply chain [144]. The exact amount of CO_2-absorption is dependent on multiple factors, such as the particle size (distribution) and local environmental conditions, such as the pH-value and the average temperature. For olivine gravel with a 0/8 particle size distribution, 200 kg CO_2 is absorbed per ton olivine over 50 years and 267 kg CO_2 over 100 years. Taking a density of 1400 [kg/m^3], which is higher than conventional ballast, the total mass per meter track is 1.32 tons. This gives a total CO_2-absorption of 264 [kg] per meter track over 50 years.

5.4.5. Most sustainable track structure

Based on these sustainability innovations, the carbon footprint of the structure can be further reduced. As was mentioned before, the following two options have the biggest influence to further reduce the carbon footprint of the structure:

- Producing the rails from recycled steel in electric arc furnaces reduces the carbon footprint for this material with 70 %.
- Embedding the track in olivine ballast
- Electrifying the Rockwool factory

The results are reported in table 5.16.

Table 5.16: Equivalent CO_2-emissions per meter track in [kg CO_2-eq.] - Implementation sustainability innovations

	Existing CEM I - Grass	**EPS - Grass**	**EPS - Sustainable**	**Rockwool - Sustainable**
Rails	3.70E+02	2.22E+02	6.66E+01	6.66E+01
Concrete	2.21E+02	1.25E+02	1.25E+02	1.25E+02
Grass	2.58E+00	1.55E+00	0E+00	0E+00
Olivine ballast	0E+00	0E+00	-2.64E+02	-2.64E+02
Rockwool	0E+00	0E+00	0E+00	2.34E+02
EPS	0E+00	2.24E+02	2.24E+02	0E+00
Total	5.93E+02	5.73E+02	1.52E+02	1.62E+02

These results are displayed in a bar chart in figure 5.13 below.

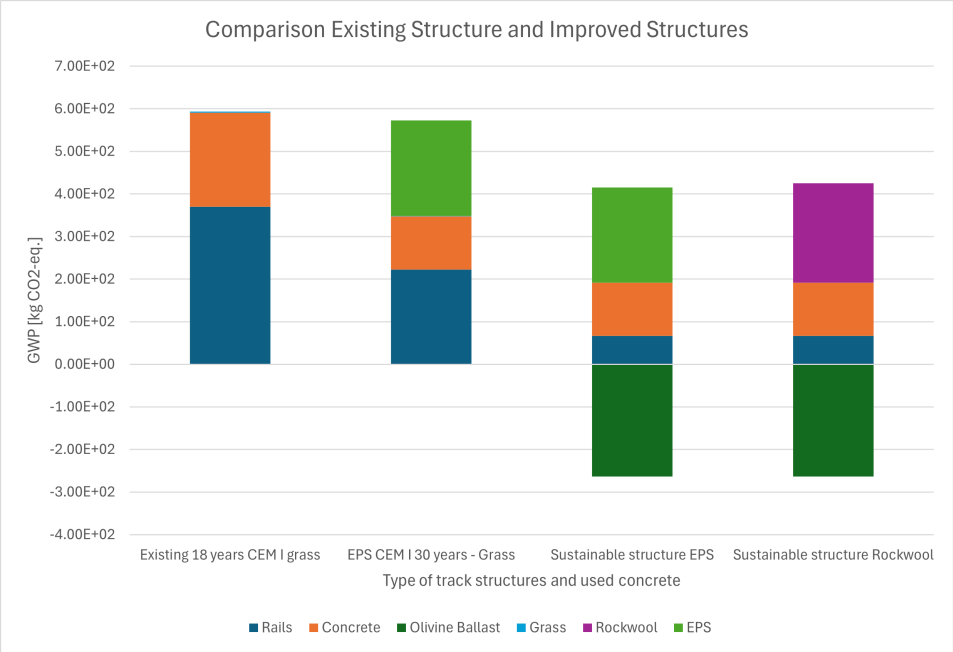

Figure 5.13: Overview - Comparison in carbon footprint of the existing structure and structures with implemented sustainability innovations

The following conclusions can be drawn based on these results:

- Implementing the sustainability innovations gives a significant reduction in carbon footprint. Compared to the existing structure with a life span of 18 years, the carbon footprint reduces with 74.4% and 72.3% for a structure with a foundation of EPS and Rockwool respectively.
- Compared to the structure with EPS and a life-span of 30 years, implementing the sustainability innovations still gives a significant reduction in equivalent CO_2-emissions. This yields a decrease of 73.5% and 71.7% for a structure with a foundation of EPS and Rockwool respectively.

Please note the small difference in carbon footprint between the structure with a foundation of EPS and a structure where Rockwool is used as foundation. Taking the reduced flood risk into consideration, a track structure with a foundation of Rockflow elements is overall the most sustainable option.

5.5. Conclusion

Based on the theoretical framework of urban sustainability and the sustainability assessments of the existing and improved structures, the following conclusions can be drawn:

- Providing green in the urban environment reduces the risk of heat stress. Embedding the track in grass seems a logical solution. However, only embedding the tram track structure in grass has little effect on the Urban Heat Island effect. This phenomenon works both ways:
  - At the case study location in IJsselmonde, there is sufficient green and water bodies in the surrounding area, which provides cooling. Embedding the track in ballast does not have a negative influence on the risk of heat stress.
  - In the city centre of Rotterdam, tram tracks are embedded in grass, such as at the Hofplein and at the Weena. However, no temperature reduction for the urban Heat Island effect was observed at that location.

  Therefore, the overall urban green layout is more contributing to a reduction in heat stress than if only the track structure is embedded in grass.

- At the roundabout at the Groeninx van Zoelenlaan, there is a risk of 10 centimeters of flooding during extreme precipitation. At the project location, there is a high ground water table and an inadequate drainage system. The Rockwool elements are the only suitable mitigation measure to reduce the flood risk during extreme precipitation.
- For the existing structure, the main contributor to the carbon footprint of the tram track structure is the rails. For the most sustainable tram track structure (CEM I tram track embedded in grass), the rails contribute 62.4% of the total carbon footprint. The French infrastructure manager SNCF Réseau reports a carbon footprint reduction of 70% when rails are made from recycled steel in EAFs.
- Adding 25% extra CEM I cement to the concrete mixture has a significant effect on the total equivalent CO_2-emissions. The GWP of the concrete increases with 46.7% and 60.8% compared to concrete mixtures with standard CEM III and standard CEM I respectively.
- Although not contributing significantly to a reduction of heat stress in the urban environment, grass slabs have a significantly lower carbon footprint than a layer of conventional ballast. However, olivine ballast can actually capture CO_2. Per meter track, 264 [kg] of CO_2 can be captured over 50 years.
- Although the life-span of the structure increases, installing Rockwool elements underneath the track structure increases the total GWP with 27.2% or 30.9% for a track embedded in ballast and grass respectively.
- Constructing a foam concrete foundation underneath the slab track has a very negative impact on the carbon footprint of the structure over the entire life-cycle. Even though the life-span of the structure increases to 30 years, the carbon footprint rises dramatically by 97.1%.
- EPS is the only type of foundation which does not result in an increase in CO_2-emissions over the design life time of 30 years. The carbon footprint decreases with 3.4% for a track embedded in grass.
- Even though the carbon footprint of a concrete tram track structure with 30% RCA has not exactly been quantified yet, the influence on the total equivalent CO_2-emissions is low. The impact of fine and coarse aggregates in LCA stage A1 and A2 are already relatively low (16.06%) compared to the contribution of CEM I in stage A1 (69.95%). Only 30 percent of these aggregates are replaced with RCA. Hence, the influence on the total GWP is considered to be low.
- In situ construction of a tram track structure made of geopolymer concrete faces challenges regarding workability and curing. This raises questions about the durability performance of the structure and is therefore not preferred. However, a geopolymer track structure might be possible if smaller elements are prefabricated and installed on site.
- When implementing olivine ballast and recycled rails for a structure built on EPS, the carbon footprint reduces with 74.4% to the current situation.
- When implementing olivine ballast, recycled rails for a structure built on Rockwool after electrification of the factory has been completed, the carbon footprint reduces with 72.3% compared to the current situation. This is almost the same result as for a structure built on EPS. Taking the reduced flood risk into consideration, a track structure with a foundation of Rockflow elements is overall the most sustainable.

So, in short, the answers for sub-question 3 ("*How sustainable are the proposed tram track structures and which engineering solutions can be applied to improve the sustainability performance of these structure?*") and sub-question 4 ("*To what extent are the state-of-the-art engineering solutions affecting the sustainability performance of the tram track structure and how does this relate to the lifetime equivalent CO_2 emissions?*") are as follows:

- Increasing the life-span of the structure with the state-of-the-art engineering solutions results only in a reduction in equivalent CO_2-emissions when EPS is used as foundation. Rockwool hits this target as well when the factory is electrified.
- The following sustainability innovations can be implemented to further reduce the carbon footprint of the structure:
  - Producing rails from recycled steel in electric arc furnaces
  - Embedding the track in olivine ballast
  - Electrifying the Rockwool factory

  When these innovations are implemented, the equivalent CO_2-emissions per meter track for a structure built on EPS or Rockwool reduce to 152 [kg] and 162 [kg] respectively. Compared to the existing structure with a life-span of 18 years, this is a reduction of 74.4% and 72.3% respectively.
- Rockwool is the only material which reduces the risk of flooding.
- The risk of heat stress is mostly related to the urban design. The type of embedment of the track structure has little influence.

Overall, when considering both climate resilience and climate mitigation, a track structure built on Rockwool foundation is the most sustainable option.

5.6. Discussion and recommendations

The following points from this study should be taken into consideration when interpreting the results:

- The selected track components for the total GWP calculations are the components with the biggest volume and thus have the highest influence on the total equivalent CO_2-emissions per meter track. However, there are several smaller components used as well, such as collar screws, plates and tension clambs (see Appendix A). To get a more detailed result, the EPDs of all these components should be taken into consideration as well.
- During periods of drought, the grass on the tram tracks becomes barren. Thus, during summers with extreme heat and drought, the effect of the grass on the Urban Heat Island effect is minimal.
- The exact CO_2-reduction when using recycled steel from EAFs in the track structure design is dependent on the location of the EAF for the following two reasons:
  - The transportation distance and mode of transportation from the EAF to the construction site
  - The local energy mix used.

  France's energy mix has a low carbon footprint due to the high percentage of generated nuclear energy, which is 64.2% of the electricity mix in 2023. Moreover, in the same year, 25.7% was generated by renewable sources. These are wind, solar energy and hydropower [145]. The 70% CO_2-reduction for green rails reported by SNCF Réseau is thus strongly related to this low carbon footprint energy mix and might be higher for rails produced in EAFs in different countries.
- The captured CO_2 by olivine is strongly related to the particle size distribution and not linear over time. Therefore, the exact amount of captured CO_2 over 30 years is not reported. Moreover, the particle size distribution used to determine the carbon capture was 0/8. Since the ballast is only used for embedding the structure, this gradation can be used. However, when a conventional ballast gradation is used, the carbon capture might differ from the reported values.

6

Conclusion

Based on the drawn conclusions for the 4 sub-questions, the main research question, "***To what extent can the durability and sustainability performance of a tram track structure on soft soil conditions be improved while preserving the vertical track geometry?***", can be answered. In this chapter, the main conclusions for the sub-questions are listed and the overall conclusions are drawn, which answer the main research question.

Sub-question 1: "What are the main driving mechanisms for the vertical deformation of the tram tracks?"
Based on the literature study and PLAXIS calculations, the following main driving mechanisms are identified:

- The subsoil consists of thick layers of Holocene deposits, such as peat and clay, which are highly susceptible to consolidation and creep under loading
- The high ground water table
- The self-weight of the structure

However, this does not clarify the extreme settlement rate and observed damages and distresses at the pit towards shopping center Keizerswaard (figure 1.3). This section was constructed between a preloaded track in 2014, which has a very limited settlement rate, and the roundabout, which was already constructed in 2008. Hence, this connection has a higher settlement rate and a different different vertical stiffness of track support and can therefore be characterised as a **transition zone**. As a result, water flows to the pit and the sand fill layer underneath the structure gets saturated. The dynamic loading of the trams causes this saturated sand fill to flow out from underneath the structure, hence resulting in severe deflections of the tram track structure.

Sub-question 2: "Which state-of-the-art engineering solutions could mitigate the vertical settlement of the tram track on the soft soil?"
Based on the findings from the previous sub-question, a light-weight filler material which has sufficient bearing resistance and does not flow out under saturated conditions should be selected to increase the durability of the tram track structure. This is the case for the following three materials:

- Rockwool: Rockflow (Type WM2007)
- Foam concrete
- EPS

However, foam concrete leads to significant less deflection of the rail (-36.1%) and thus has a larger track stiffness k compared to the existing tracks. Implementing this design might result in transition zone problems further down the line where the existing structure is still in place.

Moreover, the study shows that conventional elevation of sand fill to restore this alignment is not an appropriate solution for the following two reasons:

- The extra load of the sand fill increases the effective stresses in the subsoil and leads to further primary and secondary settlements.
- The saturated sand fill foundation can still flow out from underneath the structure, which keeps resulting in extreme pavement distresses and application of the emergency brakes of the trams.

Sub-question 3: "How sustainable are the proposed tram track structures and which engineering solutions can be applied to improve the sustainability performance of these structure?"
For infrastructure manager RET, the sustainability parameters of interest for the tram track structure are as follows:

- Climate-resilience against heat stress and flooding
- Carbon-footprint of the materials
- Circularity of building materials

The risk of heat stress is reduced when sufficient vegetation and waterbodies are present in the urban landscape. However, only embedding a tram track structure in grass does not lead to a reduction in air temperature, but is mainly related to the overall urban design at a location.

The risk of flooding is present at the roundabout of the Groeninx van Zoelenlaan. When the most extreme rainfall in 100 years occurs, there is a risk of 10 centimetres of flooding. To provide an extra water buffer and avoid flooding of the sewer system, the Rockflow-elements can be installed underneath the track structure at the case study location.

Regarding the carbon footprint of the structure, the following conclusions can be drawn:

- The current tram track structure embedded in grass with CEM I cement has a carbon footprint of 593 [kg CO_2-eq.] per meter track for a life span of 30 years. Note that due to the problems with the vertical alignment, the actual life span of the structure itself is only 18 years. The correction for the shorter lifespan is already included in the computed CO_2-emissions.
- The rails is the main contributor to the total carbon footprint of the structure, which is 370 [kg CO_2-eq.]
- Adding 25% extra CEM I to the concrete mixture to enhance the strength development rate gives for the concrete a carbon footprint increase of 133 [kg CO_2-eq.] compared to the standard concrete mixture with CEM I.

To further reduce the carbon footprint of the structure, the following innovations should be used:

- Producing rails from recycled steel in Electric Arc Furnaces. The French infrastructure manager SNCF Réseau reports a carbon footprint reduction of 70%.
- Embedding the track in olivine ballast, which absorbs 264 [kg] CO_2 per meter track over 50 years.

Sub-question 4: "To what extent are the state-of-the-art engineering solutions affecting the sustainability performance of the tram track structure and how does this relate to the lifetime equivalent CO_2 emissions?"
Although the life-span of the structure increases, does this not lead to a decrease of the carbon footprint for all the state-of-the-art engineering solutions. The following conclusions are drawn:

- Using EPS as foundation reduces the carbon footprint with 3.4% over 30 years compared to the existing structure with a life span of 18 years.
- Rockwool elements only have a lower carbon footprint over 30 years when the factory is electrified. For the current production process, the total GWP increases with 30.9% for a track embedded in grass. When the electrification process has been completed, the carbon footprint is 584 [kg CO_2-eq.], which is only 1.5% lower than the carbon footprint of the existing structure.
- Implementing foam concrete as foundation almost doubles the carbon footprint of the structure over 30 years. The GWP increase is computed to be 97.1%.

When taking into consideration the reduced flood risk at the case study location, Rockwool is considered to be the most sustainable alternative.

Main research question: "To what extent can the durability and sustainability performance of a tram track structure on soft soil conditions be improved while preserving the vertical track geometry?"
Based on the conclusions for the sub-questions, the main research question can be answered.

The durability performance of the structure can be improved by using Rockwool, foam concrete or EPS as foundation of the tram track structure on the soft soils at the case study location. The life span of the structure increases from 18 years to 30 years. However, when these materials are used, the overall carbon footprint of the structure does not necessarily decrease. This research has shown that for current practises, only EPS leads to a total reduction in carbon footprint over a life-span of 30 years. In the near future, when the Rockwool factory is electrified, Rockwool has nearly a similar GWP as EPS. Using foam concrete, however, leads to a GWP which is almost twice the reported value for the existing structure with a life span of 18 years.

The carbon footprint of the structure can be significantly reduced when the rails are produced from recycled rails in electric arc furnaces and the track is embedded in olivine ballast. Compared to the existing structure with a life-span of 18 years, this leads to a carbon footprint reduction of 74.4% and 72.3% for when respectively EPS or Rockwool is used.

When the climate-resilience sustainability factor is taken into consideration is Rockwool the only material which improves the sustainability performance of the structure. The Rockwool elements provide an extra water buffer underneath the structure, which reduces the risk of overflow of the combined sewage system. So, overall, when climate-mitigation and climate-resilience are both taken into consideration, Rockwool is the best alternative.

To conclude, this research has shown that when the right material is selected, the increased durability performance on soft soils does not lead to a worse sustainability performance or vice versa. Both performances can be improved while preserving the vertical track geometry.

7

Discussion and Recommendations

In this chapter, the results of this research are discussed and recommendations for further research on this topic are given.

7.1. Discussion

The following points should be taken into consideration when interpreting the results and conclusions:

- The results for the existing settlement and settlement rate have extensively been validated with the InSAR satellite data between 2017 and 2022, measurement data on site and the ZETDYK model. However, to improve the accuracy of the validation method, a longer reference period for InSAR satellite measurements was preferred.
- The obtained results in this case study are tailored to this specific location, track structure and local soil conditions. Extrapolating the numerically obtained results for the geotechnical calculations is therefore not possible. Furthermore, the selected light-weight filler materials, the conclusions on the balance between sustainability and durability and the sustainability optimisation are specifically based on these soil conditions and type of track structure.
  However, the used methodology still holds and can be used for different track structures and soil conditions.
- Note that the selected light-weight filler materials are directly related to the type of track structure used. For example, glass foam can be used in railway engineering practises underneath a sand fill layer of 60 [cm], mainly to avoid crushing of the glass foam aggregates under dynamic loading conditions. So, for different type of track structures, such as structures built on embankments, the most sustainable track structure might be constructed with a different type of light-weight filler material.
- For the PLAXIS 3D model and the validation of this model, the wheel load was assumed based on the maximum tram load and a Dynamic Amplification Factor of 1.3. This might be a too conservative approach. To get more certainty of the actual wheel load, dynamic Weighing in Motion sensors should be installed. Using this measurement data for the PLAXIS 3D simulation should eventually lead to a more accurate prediction and validation of the occurring rail deflection and bending moments in the slab.
- The CO_2-absorption of olivine ballast is together with producing rails from recycled steel in Electric Arc Furnaces one of the main measures to further reduce the carbon footprint in the sustainability optimisation step. Note that in practise, this is not always possible, for example when the track is embedded in pavement.

7.2. Recommendations for further research

The recommended topics for further research are as follows:

- The nuisance of noise and vibrations was regarding complexity and time limitations not covered in the scope of this research. However, avoiding nuisance of noise and vibrations is directly related to the well-being of the residents and hence the sustainability of the living-quarter. For the vibration analysis, the PLAXIS 3D model can be extended in x-direction towards the pile foundation of the surrounding buildings. The effect of changing the type of foundation underneath the tram track structure on the propagation of these waves and the perceived amplitudes and frequencies at the nearby foundations could be predicted. Multiple soil accelerometers can be installed between the the track and the foundation to validate the damping of the wave in the soil.
- Monitor the long-term settlement behaviour of the tram track structure after having installed the new type of foundation and compare these settlements with the predicted settlement (rate) from the PLAXIS 2D model for scenario 2.
- In the PLAXIS 3D model, the slab track is modelled as a plate element, which resembles a shell. In practise, a continuous concrete slab is casted around the duo-bloc sleepers. The PLAXIS 3D model does not give insight on the exact force distribution and internal stress-paths within the slab. To accurately obtain this data, other finite element software programs should be used to model the tram track structure, such as DIANA or ANSYS.
- To further investigate the possibilities of using geopolymer concrete in the track design, smaller prefabricated elements should be used and assembled on site. This track structure has to be designed in detail regarding optimal shape and connections. Moreover, once being designed, the long-term performance under repetitive loading must be investigated.

References

[1] R. C. P. van der Poel, *Groeninx van Zoelenlaan - richting Beverwaard 1*.

[2] L. P. van der Tang, *Settlements of the tram track in Beverwaard*.

[3] DINOloket. "Ondergrondgegevens." (), [Online]. Available: https://www.dinoloket.nl/ondergrondgegevens (visited on 11/13/2024).

[4] Bodemdalingskaart 2.0, 2022. [Online]. Available: https://bodemdalingskaart.portal.skygeo.com/portal/bodemdalingskaart/u2/viewers/basic/.

[5] A. Verruijt and W. Broere, *Grondmechanica*, 9th ed. VSSD, 2012.

[6] V. L. Markine and Z. Li, *Transportation Infrastructures - Unit 1 - Railways - Week 2: Basic principles, Forces*, 2024. [Online]. Available: https://brightspace.tudelft.nl/d2l/le/content/594955/viewContent/3446399/View.

[7] H. M. Jonkers and M. Ottelé, *Lecture 1.1 Sustainable Cities - Module Introduction*, Nov. 11, 2024. [Online]. Available: https://brightspace.tudelft.nl/d2l/le/content/680258/viewContent/3824213/View.

[8] RET. "Kijkje achter de schermen bij de remise Beverwaard." (), [Online]. Available: https://www.ret.nl/home/sociale-media/blog/kijkje-achter-de-schermen-bij-de-remise-beverwaard.html (visited on 11/27/2024).

[9] RET, *Tram regio Rotterdam*, 2024. [Online]. Available: https://bestanden.ret.nl/RET_Tramnet_210x148_v5.png.

[10] RET. "Materieel - RET." (), [Online]. Available: https://corporate.ret.nl/over-ret/materieel#:~:text=Dagelijks%20vervoeren%20we%20zo'n,112%20trams%20en%20165%20metro's. (visited on 11/28/2024).

[11] RET. "Tram - RET." (), [Online]. Available: https://corporate.ret.nl/over-ret/materieel/tram (visited on 11/28/2024).

[12] J. Ihme, *Rail Vehicle Technology*, 1st ed. Springer Wiesbaden, Jan. 1, 2022. DOI: 10.1007/978-3-658-36969-9. [Online]. Available: https://doi.org/10.1007/978-3-658-36969-9.

[13] *Draaistel Alstom Citadis RET - In beeld: Open dagen RET werkplaats Kleiweg in Rotterdam*, Jul. 11, 2022. [Online]. Available: https://www.mp-produktie.nl/Images%20Speciaal-3/2022-07-02%20Open%20dag%20RET%20werkplaat%20Kleiweg%20Rotterdam%20-%20RET%2095%20Jaar%20(33).JPG.

[14] Y. Zeng, *Hunting Phenomenon in Dynamic Train-track Interaction*, 2024. [Online]. Available: https://brightspace.tudelft.nl/d2l/le/content/594955/viewContent/3657155/View.

[15] Google. "Sattelite photograph around shopping center Keizerswaard." (2024), [Online]. Available: https://www.google.nl/maps/@51.8876135,4.5497728,677m/data=!3m1!1e3?entry=ttu&g_ep=EgoyMDI0MTExMy4xIKXMDSoASAFQAw%3D%3D (visited on 11/16/2024).

[16] R. Keus, *Remise Beverwaard met tram*. [Online]. Available: https://corporate.ret.nl/media/1225/rkeus_20120501_3965_01.jpg.

[17] Like je wijk - Beverwaard, *Buslijn 175 ingekort door indienstelling tram(s) over de Roseknoop – LikeJeWijk IJsselmonde*, Oct. 2, 2023. [Online]. Available: https://likejewijk.nl/ijsselmonde/ijsselmonde/buslijn-175-ingekort-door-indienstelling-trams-over-de-roseknoop/.

[18] R. Keus, *Infra spoorwerkzaamheden (2)*. [Online]. Available: https://corporate.ret.nl/media/3474/2021_jul_aug_infra_spoorwerkzaamheden_rkeus-60.jpg.

[19] Gemeente Rotterdam. "Grondwater." (), [Online]. Available: https://www.gis.rotterdam.nl/Gisweb2/Default.aspx?context=MIJNPROJECT.1091# (visited on 12/06/2024).

[20] Metropoolregio Rotterdam Den Haag (MRDH). “Concessies openbaar vervoer.” (), [Online]. Available: https://mrdh.nl/project/concessies-openbaar-vervoer (visited on 12/07/2024).

[21] Waterschap Hollandse Delta. “Zorgen voor voldoende water.” (Sep. 20, 2024), [Online]. Available: https://www.wshd.nl/zorgen-voor-voldoende-water (visited on 12/07/2024).

[22] Gemeente Rotterdam. “Rotterdams weerwoord.” (), [Online]. Available: https://www.rotterdam.nl/rotterdams-weerwoord (visited on 12/03/2024).

[23] Gemeente Rotterdam. “Bodemdaling.” (), [Online]. Available: https://www.rotterdam.nl/bodemdaling (visited on 12/02/2024).

[24] Houben, *CTB3320 Weg- en Railbouwkunde, Deel 2: Onderbouw*. Feb. 2020.

[25] R. Keus, *Tram Hofplein*. [Online]. Available: https://corporate.ret.nl/media/1031/rkeus2011072760556_01.jpg.

[26] De Lijn. “Trambaan op palen is Antwerps unicum.” (Oct. 28, 2021), [Online]. Available: https://delijn.prezly.com/trambaan-op-palen-is-antwerps-unicum (visited on 12/02/2024).

[27] N. Rouvrois. “Spoorwerken Blancefloerlaan op schema voor indiensttreding in november.” (Sep. 22, 2021), [Online]. Available: https://www.gww-bouw.be/algemeen/spoorwerken-blancefloerlaan-op-schema-voor-indiensttreding-in-november/ (visited on 12/02/2024).

[28] M. S. S. Almeida, M. Ehrlich, A. P. Spotti, and M. E. S. Marques, “Embankment supported on piles with biaxial geogrids,” *Proceedings of the Institution of Civil Engineers - Geotechnical Engineering*, vol. 160, no. 4, pp. 185–192, Sep. 5, 2007. DOI: 10.1680/geng.2007.160.4.185. [Online]. Available: https://doi.org/10.1680/geng.2007.160.4.185.

[29] CUR Bouw & Infra, “CUR Bouw & Infra publicatie 226,” 2009. [Online]. Available: https://publicwiki.deltares.nl/download/attachments/112166128/Paalmatrassen%20-%20lijst%20voorbeeldprojecten%20met%20specs.pdf?version=1&modificationDate=1432189306000&api=v2.

[30] Y. Shan, A. Huang, X. Qin, S. Zhou, and X. Zhou, “Long-term in-situ monitoring on foundation settlement and service performance of a novel pile-plank-supported ballastless tram track in soft soil regions,” *Transportation Geotechnics*, vol. 36, p. 100 821, Jul. 25, 2022. DOI: 10.1016/j.trgeo.2022.100821. [Online]. Available: https://doi.org/10.1016/j.trgeo.2022.100821.

[31] F. Xiao, Y. Shan, G. Zhou, W. Lin, and J. Li, “Critical transverse differential settlement between modern tram pile-plank-supported subgrade and surrounding pavement subgrade,” *Transportation Geotechnics*, vol. 38, p. 100 896, Nov. 5, 2022. DOI: 10.1016/j.trgeo.2022.100896. [Online]. Available: https://doi.org/10.1016/j.trgeo.2022.100896.

[32] ProRail, *Onderzoek naar baanstabiliteit | ProRail*, Jan. 23, 2024. [Online]. Available: https://www.youtube.com/watch?v=YjXHB-hyhu8 (visited on 01/01/2025).

[33] Y. Li, *Lecture 4.7: Design and Construction of Embankment – Part 1*, Jun. 2024. [Online]. Available: https://brightspace.tudelft.nl/d2l/le/content/594955/viewContent/3725621/View.

[34] Network Rail, “Earthworks Technical Strategy,” Jun. 2018. [Online]. Available: https://www.networkrail.co.uk/wp-content/uploads/2018/07/Earthworks-Technical-Strategy.pdf (visited on 01/01/2025).

[35] R. Sañudo, L. dell’Olio, J. Casado, I. Carrascal, and S. Diego, “Track transitions in railways: A review,” *Construction and Building Materials*, vol. 112, pp. 140–157, Mar. 1, 2016. DOI: 10.1016/j.conbuildmat.2016.02.084. [Online]. Available: https://doi.org/10.1016/j.conbuildmat.2016.02.084.

[36] H. Wang and V. L. Markine, “Methodology for the comprehensive analysis of railway transition zones,” *Computers and Geotechnics*, vol. 99, pp. 64–79, Mar. 9, 2018. DOI: 10.1016/j.compgeo.2018.03.001. [Online]. Available: https://doi.org/10.1016/j.compgeo.2018.03.001.

[37] van Wessem, “Horizontal deformation of the High Speed Rail track, A study into the horizontal deformation of a sand embankment on asymmetrical soft soil for a high speed rail track - Case study HSL Rijpwetering,” 2020. (visited on 12/03/2024).

[38] RET - Ingenieursbureau, “Technisch Programma van Eisen Trambaan, Rail en Baan Deel C1,” 1835468057-273, Nov. 2, 2022. (visited on 02/17/2025).

[39] Railpro. “Steenslag,31,5/50-1,6 ton in big bag.” (), [Online]. Available: https://www.railpro.online/nl_NL/p/steenslag-31-5-50-1-6-ton-in-big-bag/3303/ (visited on 02/10/2025).

[40] A. Nottbeck, “Untersuchungen zu Auswirkungen von Geschwindigkeitserhöhungen auf Bahnstrecken im Bestand,” Mar. 15, 2016. [Online]. Available: https://mediatum.ub.tum.de/doc/1295100/document.pdf (visited on 02/07/2025).

[41] A. Rodríguez, R. Sañudo, M. Miranda, A. Gómez, and J. Benavente, “Smartphones and tablets applications in railways, ride comfort and track quality. transition zones analysis,” *Measurement*, vol. 182, p. 109 644, Jun. 6, 2021. DOI: 10.1016/j.measurement.2021.109644. [Online]. Available: https://doi.org/10.1016/j.measurement.2021.109644.

[42] Seequent. “How the Past 30 Years of PLAXIS History Pave the Way for a Promising Future.” (Sep. 28, 2023), [Online]. Available: https://www.seequent.com/how-the-past-30-years-of-plaxis-history-pave-the-way-for-a-promising-future/ (visited on 12/03/2024).

[43] Bentley, *General three-dimensional coordinate system and sign convention for stresses*, May 7, 2024. [Online]. Available: https://bentleysystems.service-now.com/sys_attachment.do?sys_id=39ecf0b287a0dad8abaf2fc6cebb3530.

[44] Bentley. “Material Models Manual 2D - PLAXIS 2D 2024.2.” (May 7, 2024), [Online]. Available: https://bentleysystems.service-now.com/sys_attachment.do?sys_id=39ecf0b287a0dad8abaf2fc6cebb3530 (visited on 12/03/2024).

[45] I. Stikvoort, “Old quay walls,” 2014. [Online]. Available: http://resolver.tudelft.nl/uuid:3c0bf0bc-8e52-49a6-81ea-bdc2efb8247d (visited on 02/17/2025).

[46] S. van Baars, “SOFT SOIL CREEP MODELLING OF LARGE SETTLEMENTS,” 2003. [Online]. Available: https://www.researchgate.net/publication/237657988_SOFT_SOIL_CREEP_MODELLING_OF_LARGE_SETTLEMENTS (visited on 02/12/2025).

[47] I. Marzouk, R. Brinkgreve, A. Lengkeek, and F. Tschuchnigg, “APD: An automated parameter determination system based on in-situ tests,” *Computers and Geotechnics*, vol. 176, p. 106 799, Oct. 7, 2024. DOI: 10.1016/j.compgeo.2024.106799. [Online]. Available: https://doi.org/10.1016/j.compgeo.2024.106799.

[48] Bentley. “Reference Manual 2D - PLAXIS 2D 2024.2.” (May 7, 2024), [Online]. Available: https://bentleysystems.service-now.com/sys_attachment.do?sys_id=d5ec70b287a0dad8abaf2fc6cebb35f4 (visited on 12/03/2024).

[49] H. Ahmad, “Two-dimensional study of the inclusions of skirt sand and deep cement piles to improve the load□displacement behavior of circular foundations on soft clay soil,” *Heliyon*, vol. 9, no. 2, e13627, Feb. 1, 2023. DOI: 10.1016/j.heliyon.2023.e13627. [Online]. Available: https://doi.org/10.1016/j.heliyon.2023.e13627.

[50] Tromp and Korff, “Bouwen op slappe bodems,” Delft, 429980-400-0007 v01, Feb. 2008. [Online]. Available: https://www.cob.nl/document/bouwen-op-slappe-bodems/ (visited on 02/02/2025).

[51] D. van Zanten, P. Leezenberg, J. van Dalen, M. de Vries, R. Spruit, and H. Maljaars, “Insar voor geotechnische beoordeling van hoogbouwprojecten,” *GEOTECHNIEK*, Sep. 2024. [Online]. Available: https://www.vakbladgeotechniek.nl/files/GEO2024-03-P30-Maljaars.pdf.

[52] Deltares, TNO, and Wageningen Environmental Research (WENR). “Bodemdalingsvoorspellingskaarten.” (), [Online]. Available: https://www.klimaateffectatlas.nl/nl/bodemdalingsvoorspellings-kaarten (visited on 03/10/2025).

[53] K. Han, J. Wang, T. Xiao, S. Li, D. Zhang, and H. Dong, “Effects of train vibration load on the structure and hydraulic properties of soils,” *Scientific Reports*, vol. 14, no. 1, Mar. 28, 2024. DOI: 10.1038/s41598-024-57956-5. [Online]. Available: https://www.nature.com/articles/s41598-024-57956-5.

[54] T. R. Oke, G. Mills, A. Christen, and J. A. Voogt, *Urban climates*, 1st ed. Cambridge University Press, Aug. 31, 2017. DOI: 10.1017/9781139016476. [Online]. Available: https://doi.org/10.1017/9781139016476.

[55] ROCKWOOL Rainwater Systems. “Rockflow onder de trambaan op de Amsterdamse Nieuwezijds Voorburgwal.” (Jun. 24, 2021), [Online]. Available: https://rain.rockwool.com/nl/cases/amsterdam-nieuwe-zijde/ (visited on 12/03/2024).

[56] ROCKWOOL Rainwater Systems, *Rockflow onder de trambaan op de Amsterdamse Nieuwezijds Voorburgwal*, Jun. 24, 2021. [Online]. Available: https://rain.rockwool.com/nl/cases/amsterdam-nieuwe-zijde/ (visited on 02/20/2025).

[57] ROCKWOOL Rainwater Systems. “Oplossingen met Rockflow.” (Nov. 12, 2024), [Online]. Available: https://rain.rockwool.com/nl/oplossingen/ (visited on 03/03/2025).

[58] Rotterdams Weerwoord. “Neerslag - Rotterdams weerwoord.” (Dec. 11, 2023), [Online]. Available: https://rotterdamsweerwoord.nl/opgave/neerslag/ (visited on 02/21/2025).

[59] Lapinus, “Resilient railway systems with stone wool, How stone wool effectively controls vibration and extends structural life for rail tracks,” 2021, p. 2. [Online]. Available: https://www.lapinus.com/syssiteassets/technical-resources/downloads/rockdelta/whitepaper/rockdelta_whitepaper_lapinus_en.pdf (visited on 03/03/2025).

[60] K. B. Gatzwiller, *Large-Scale fatigue test of stone wool based anti-vibration Mats*. Berlin, Heidelberg: Springer, Apr. 9, 2008, vol. 99, pp. 454–460. DOI: 10.1007/978-3-540-74893-9_64. [Online]. Available: https://doi.org/10.1007/978-3-540-74893-9_64.

[61] N. Trads and N. Katić, “Strength and stiffness properties of stonewool used as cloudburst reservoir under roads,” *IOP Conference Series Earth and Environmental Science*, vol. 710, no. 1, p. 012 029, Apr. 1, 2021. DOI: 10.1088/1755-1315/710/1/012029. [Online]. Available: https://doi.org/10.1088/1755-1315/710/1/012029.

[62] Lapinus, “RAIL DEFLECTION PREDICTION FOR SLAB TRACK,” Jun. 25, 2021. (visited on 03/12/2025).

[63] Rockwool, “PRODUCT DATA SHEET Rockflow® WM Elements,” Sep. 2021. (visited on 03/12/2025).

[64] E. Tutumluer, M. Kang, and I. I. Qamhia, “Geosynthetic stabilization of road pavements, railroads, and airfields,” *Transportation Geotechnics*, p. 101 321, Jul. 1, 2024. DOI: 10.1016/j.trgeo.2024.101321. [Online]. Available: https://doi.org/10.1016/j.trgeo.2024.101321.

[65] Tensar, *Rehabilitation of Curtici - Simeria Frontier Railway*. [Online]. Available: https://www.tensarinternational.com/getmedia/7a43a78d-307f-4736-a388-92c3d60c064b/case-study-curtici-railway-580-580.png?width=580&height=580&ext=.png.

[66] Presto Geosystems, *GEOWEB® Geocells for Railways*, Feb. 16, 2022. [Online]. Available: https://www.google.com/url?sa=i&url=https%3A%2F%2Frailway-news.com%2Fgeoweb-geocells-for-railways-intermodal-port-stabilisation%2F&psig=AOvVaw2DEP6U3mwL3fDd50ci3Xqp&ust=1742368918358000&source=images&cd=vfe&opi=89978449&ved=0CBQQjRxqGAoTCKCZ8paMk4wDFQAAAAAdAAAAABCaAg.

[67] Tensar, *How TriAx Geogrids Work: Mechanical Interlock*. [Online]. Available: https://www.tensarcorp.com/getmedia/8487e1da-902f-484f-ba74-3f3a2023741a/TriAx%20Grid%20Aggregate%202011_1.png.

[68] Tensar, *Tensar TriAx Geogrids are used to stabilize the trackbed structure in two ways: Subballast Railway Stabilization*. [Online]. Available: https://www.tensarcorp.com/getmedia/857f62f1-5a7c-40c4-9205-fbf219019ccd/RailwayIllustrations-ImprovedBearingCapacity_1.png.

[69] Network Rail, “The Use of Geocells in the UK Railway Track Bed, Technical Guide,” 2021. [Online]. Available: https://www.researchgate.net/profile/Mohamed-Wehbi/publication/349213343_The_Use_of_Geocells_in_the_UK_Railway_Track_Bed_Technical_Guide/links/6025219492851c4ed563afb7/The-Use-of-Geocells-in-the-UK-Railway-Track-Bed-Technical-Guide.pdf (visited on 03/18/2025).

[70] O. Yaba, “Improvement of Railway Trackbeds using Geogrids - Analysis of Mechanical Behavior, Settlement Reduction and Increase in Effective Bearing Capacity,” Jan. 2, 2024. [Online]. Available: https://theses.hal.science/tel-04368949v1/file/YABA_2022_archivage.pdf (visited on 03/18/2025).

[71] OSKA Werkgroep verkenning standaarden bodemdaling, “Klimaatbestendige realisatie van infrastructuur op slappe bodem,” Jun. 9, 2021. [Online]. Available: https://klimaatadaptatienederland.nl/publish/pages/191818/verkenning-klimaatbestendige-realisatie-van-infrastructuur-op-slappe-bodem.pdf (visited on 03/18/2025).

[72] Glasopor AS. “Glasopor | Lightweight Sustainable Building Material.” (Dec. 3, 2024), [Online]. Available: https://glasopor.no/english/ (visited on 03/18/2025).

[73] C. Chen, B. Indraratna, G. McDowell, and C. Rujikiatkamjorn, “Discrete element modelling of lateral displacement of a granular assembly under cyclic loading,” *Computers and Geotechnics*, vol. 69, pp. 474–484, Jun. 29, 2015. DOI: 10.1016/j.compgeo.2015.06.006. [Online]. Available: https://doi.org/10.1016/j.compgeo.2015.06.006.

[74] Foamit Group, “Environmental Product Declaration for FOAM GLASS AGGREGATE 0-60 mm from FOAMIT,” Nov. 4, 2022. [Online]. Available: https://glasopor.no/wp-content/uploads/2023/12/EPD-Foamit_FV_certified_04_11_22.pdf (visited on 03/25/2025).

[75] W. S. Mustafa and J. Szendefy, “Uniaxial dynamic behavior of foam glass aggregate under oedometric (fully side restrained) condition at different compaction ratios,” *Construction and Building Materials*, vol. 396, p. 132 327, Jul. 5, 2023. DOI: 10.1016/j.conbuildmat.2023.132327. [Online]. Available: https://doi.org/10.1016/j.conbuildmat.2023.132327.

[76] Brouwer and Van Laerhoven, “The use of foam glass for a lightweight fill and highway foundation on soft soil conditions,” 2024. [Online]. Available: https://geobest.nl/wp-content/uploads/2024/09/Civiele-Techniek-2024-7-The-use-of-foam-glass-for-a-lightweight-fill-and-highway-foundation-of-soft-soil-conditions.pdf.

[77] R. van Gils. “Yalibims: Feather light but stable foundation material.” (Dec. 29, 2021), [Online]. Available: https://gww-bouw.nl/en/specials/yearbook/yalibims-feather-light-but-stable-foundation-material/ (visited on 03/19/2025).

[78] Steinag B.V. “Spoorwegen.” (), [Online]. Available: https://steinag.nl/producten/spoorwegen (visited on 03/19/2025).

[79] Z. Shen, F. Shu, Y. Zhao, S. Xia, Z. Wang, and H. Gao, “Structure feature and compressive crushing behavior of lightweight clay aggregate particle: Experiments and numerical simulations,” *Acta Geotechnica*, vol. 19, no. 5, pp. 2579–2605, Jan. 23, 2024. DOI: 10.1007/s11440-023-02200-z. [Online]. Available: https://doi.org/10.1007/s11440-023-02200-z.

[80] M. Duškov, “Eps as a light-weight sub-base material in pavement structures,” Jun. 18, 1997. [Online]. Available: https://repository.tudelft.nl/file/File_1193397f-993c-4bcc-aaab-5ce0655f1187?preview=1.

[81] A. J. Puppala, S. Saride, R. V. Yenigalla, B. C. S. Chittoori, and E. Archeewa, “Long-Term Performance of a Highway Embankment Built with Lightweight Aggregates,” *Journal of Performance of Constructed Facilities*, vol. 31, no. 5, Mar. 16, 2017. DOI: 10.1061/(asce)cf.1943-5509.0001043. [Online]. Available: https://doi.org/10.1061/(asce)cf.1943-5509.0001043.

[82] Argex NV, “Technical sheet 2024.” [Online]. Available: https://argex.eu/wp-content/uploads/Technical/ENG/AR_4_10_430_DOP_1_TS_ENG.pdf (visited on 03/19/2025).

[83] van Dijk, “Schuimbeton,” 2001. [Online]. Available: https://schuimbetoninfo.nl/wp-content/uploads/2019/07/technisch-rapport-over-het-construeren-met-schuimbeton.pdf (visited on 03/19/2025).

[84] Betonhuis, *Betonpocket*, 8e ongewijzigde herdruk 2021. Betonhuis, May 2021. [Online]. Available: https://betonhuis.nl/system/files/2022-01/Betonpocket_2020%20Herdruk%202021%20lr.pdf.

[85] T. Frydenlund and R. Aabøe, “LONG TERM PERFORMANCE AND DURABILITY OF EPS AS a LIGHTWEIGHT FILLING MATERIAL,” *EPS Geofoam 2001, 3rd International Conference*, pp. 1–, 2001. [Online]. Available: https://universalconstructionfoam.com/downloads/durability-of-eps.pdf.

[86] Epsole. “How is EPS made? How to manufacture expanded polystyrene.” (Mar. 24, 2025), [Online]. Available: https://epsole.com/what-is-eps-made/ (visited on 03/28/2025).

[87] C. Esveld, V. Markine, and M. Duškov, “FEASIBILITY OF EPS AS A LIGHTWEIGHT SUB-BASE MATERIAL IN RAILWAY TRACK STRUCTURES,” 2001. [Online]. Available: http://geofoam.syr.edu/EPS_2001/Session_2%20_Design_and_Construction/Feasibility%20of%20EPS%20as%20a%20Lightweight%20Sub-Base%20Material%20in%20Rail.pdf (visited on 03/20/2025).

[88] Van Dijk Maasland. “Schuimbeton.” (), [Online]. Available: https://vandijkmaasland.nl/expertises/schuimbeton/ (visited on 03/25/2025).

[89] ROCKWOOL Rainwater Systems, “Factsheet - Lange levensduur en gemakkelijk in onderhoud.” [Online]. Available: https://rain.rockwool.com/globalassets/rockwool-rainwater-systems/downloads/fact-sheets/factsheet_lange-levensduur_RW-LF-MV.pdf (visited on 05/14/2025).

[90] URETEK Benelux. “Verzakte vloer? URETEK lift de verzakte vloer snel en doeltreffend naar het juiste niveau.” (), [Online]. Available: https://www.uretek.nl/techniek/methoden/uretek-floorlift/ (visited on 05/14/2025).

[91] ROCKWOOL B.V. - Lapinus, “Rockflow environmental product declaration,” 2021. (visited on 03/25/2025).

[92] Leca International, “Environmental product declaration,” Jan. 25, 2024. [Online]. Available: https://www.epd-norge.no/getfile.php/13193477-1741696322/EPDer/Byggevarer/Isolasjon/NEPD-5894-5164_Leca--sora-4-32-mm--Leca-Finland.pdf (visited on 03/25/2025).

[93] ARGEX, “ENVIRONMENTAL PRODUCT DECLARATION Lightweight Expanded Clay Aggregate ARGEX Lightweight filling applications,” Sep. 6, 2021. [Online]. Available: https://argex.eu/wp-content/uploads/EPD/NL_EPD_cradle-to-grave_AR8-16_AR4-10_AG4-8_AG0-4_Geo%20applications.pdf (visited on 03/25/2025).

[94] BEWI ASA, “ENVIRONMENTAL PRODUCT DECLARATION,” Apr. 27, 2021, pp. 2–7. [Online]. Available: https://epd-global.com/getfile.php/13194217-1741697835/EPDer/Byggevarer/Isolasjon/NEPD-2796-1492_BEWi-EPS-80---EPS-Insulation-Boards.pdf.

[95] Stybenex (Vereniging van EPS fabrikanten), “Recycling EPS: 100 procent recyclebaar, 100 procent duurzaam,” 2013. [Online]. Available: https://www.isobouw.nl/media/9974/84315_eps_recycle_folder_stybenex.pdf (visited on 03/25/2025).

[96] E. Kunicka, “Concrete slab beneath ballast bed - an abatement measure for railway induced vibration,” 2019. [Online]. Available: https://repository.tudelft.nl/file/File_2c88c403-2bcd-4f31-964f-eda87cbef80c?preview=1 (visited on 05/21/2025).

[97] Bentley. “Scientific Manual 2D - PLAXIS 3D 2024.3.” (May 7, 2024), [Online]. Available: https://bentleysystems.service-now.com/sys_attachment.do?sys_id=601d3ad79751a61081d373b0f053af86 (visited on 06/12/2025).

[98] ArcelorMittal, *Grooved rails / rillenschienen / rail à gorge*. [Online]. Available: https://projects.arcelormittal.com/cca/repo/FS/60R1_(Ri60).pdf.

[99] Dow Building Solutions, *Floormate™ 200-a - technische eigenschappen*.

[100] J. Real, P. Martínez, L. Montalbán, and A. Villanueva, “Modelling vibrations caused by tram movement on slab track line,” *Mathematical and Computer Modelling*, vol. 54, no. 1-2, pp. 280–291, Feb. 16, 2011. DOI: 10.1016/j.mcm.2011.02.010. [Online]. Available: https://doi.org/10.1016/j.mcm.2011.02.010.

[101] G. Lombaert and G. Degrande, “Ground-borne vibration due to static and dynamic axle loads of InterCity and high-speed trains,” *Journal of Sound and Vibration*, vol. 319, no. 3-5, pp. 1036–1066, Aug. 20, 2008. DOI: 10.1016/j.jsv.2008.07.003. [Online]. Available: https://doi.org/10.1016/j.jsv.2008.07.003.

[102] G. Degrande and L. Schillemans, “FREE FIELD VIBRATIONS DURING THE PASSAGE OF A THALYS HIGH-SPEED TRAIN AT VARIABLE SPEED,” *Journal of Sound and Vibration*, vol. 247, no. 1, pp. 131–144, Oct. 1, 2001. DOI: 10.1006/jsvi.2001.3718. [Online]. Available: https://doi.org/10.1006/jsvi.2001.3718.

[103] J. C. Verduijn and J. M. M. Vossen, “Geluid- en trillingonderzoek RET 2025, Nulmetingen rotonde Groeninx van Zoelenlaan P.25.008 Rotterdam,” R002_01_L240468, Oct. 15, 2024. (visited on 06/22/2025).

[104] S. Koziak, R. Melnik, and B. Firlik, "Tram track stiffness measurement based on the vision method," *WUT Journal of Transportation Engineering*, no. 125, pp. 45–52, Jun. 1, 2019. DOI: 10.5604/01.3001.0013.6494.

[105] R. van der Poel and O. Misca, "Evaluatie hoogte correctie Rotonde Groeninx van Zoelenlaan en problematiek hoge grondwaterstanden deelgemeente IJsselmonde.," Rotterdam, Jan. 31, 2024. (visited on 06/10/2025).

[106] C. Esveld, *Modern Railway Track*. Duisburg: MRT-Productions, 1989, ISBN: 90-800324-1-7.

[107] Althen Sensors & Controls. "Weighing in Motion (AWIM)." (Jun. 11, 2025), [Online]. Available: https://www.althensensors.com/measurement-systems/railway-measurement-systems/train-tram-weighing-systems/weighing-in-motion-awim/ (visited on 06/29/2025).

[108] KNMI, "KNMI'23 klimaatscenario's voor Nederland," Oct. 9, 2023. (visited on 02/21/2025).

[109] I. D. Stewart and T. R. Oke, "Local Climate Zones for Urban Temperature Studies," *Bulletin of the American Meteorological Society*, vol. 93, no. 12, pp. 1879–1900, 2012. DOI: 10.1175/bams-d-11-00019.1. [Online]. Available: https://doi.org/10.1175/bams-d-11-00019.1.

[110] T. R. Oke, G. Mills, A. Christen, and J. A. Voogt, *Schematic of the fluxes in the SEB of an urban building-soil-air volume*, Aug. 31, 2017. DOI: 10.1017/9781139016476. [Online]. Available: https://doi.org/10.1017/9781139016476.

[111] Gemeente Rotterdam. "Riolering." (), [Online]. Available: https://www.rotterdam.nl/riolering (visited on 02/21/2025).

[112] United Nations Environment Programme. "Building Materials and the climate: Constructing a new future." (Sep. 1, 2023), [Online]. Available: https://wedocs.unep.org/20.500.11822/43293 (visited on 02/21/2025).

[113] H. Jonkers, *Lect. 2 - Introduction to LCA: method for quantification of the environmental footprint of materials and products*, Sep. 2024. [Online]. Available: https://brightspace.tudelft.nl/d2l/le/content/680498/viewContent/4004630/View.

[114] Atlas Leefomgeving. "Kaarten." (2020), [Online]. Available: https://www.atlasleefomgeving.nl/kaarten (visited on 03/06/2025).

[115] ArcelorMittal. "EPD: Rails for transport, tramways, rail track devices and cranes BOF-based." (Mar. 29, 2024), [Online]. Available: https://api.environdec.com/api/v1/EPDLibrary/Files/febc8f5c-1c9d-4687-fa09-08dc4f0a3212/Data (visited on 03/06/2025).

[116] A/S Ikast Betonvarefabrik. "Readymix concrete C30/37 Moderate SCC. CEM I 52,5 N MS/LA - IBF Give." (Mar. 8, 2024), [Online]. Available: https://www.epd-norge.no/getfile.php/1355965-1709891938/EPDer/Byggevarer/Ferdig%20betong/NEPD-6231-5505_Readymix-concrete-C30-37-Moderate-SCC-CEM-I-52-5-N-MS-LA---IBF-Give.pdf (visited on 03/06/2025).

[117] Betonmortelcentrale De Lek bv, *MKI en GWP berekening 4050 HoA C30/37 S3 0.475*, 2025.

[118] Betonmortelcentrale De Lek bv, *MKI en GWP berekening 3340 EC C25/30 S3 0.50*, 2025.

[119] Betonmortelcentrale De Lek bv, *MKI en GWP berekening 3340 EC C25/30 S3 0.50 + cor 1046 25% CEMI*, 2025.

[120] Utomhus Østfold Gress AS, "Environmental Product Declaration - Turfgrass," NEPD-5883-5157-EN, Feb. 5, 2024. [Online]. Available: https://www.epd-norge.no/getfile.php/13190573-1741689329/EPDer/Byggevarer/NEPD-5883-5157_Turfgrass.pdf (visited on 04/11/2025).

[121] M. Berg, M. Wolbers, and N. Zaadnoordijk, "Rapport 0-in-de-ketenanalyse ballast," Dec. 23, 2019. [Online]. Available: https://www.prorail.nl/siteassets/homepage/toekomst/documenten/ketenanalyse-ballast.pdf.

[122] A. Kok, Strukton Rail, and J. Vroonhof, "Ketenanalyse ballastmateriaal," 2024. [Online]. Available: https://strukton.nl/wp-content/uploads/2024/05/Ketenanalyse-ballastmateriaal.pdf (visited on 04/23/2025).

[123] ROCKWOOL B.V. "Hoe wordt steenwol gemaakt?" (), [Online]. Available: https://www.rockwool.com/nl/advies-en-inspiratie/kennisverdieping/duurzaamheid-en-circulariteit/hoe-wordt-steenwol-gemaakt/ (visited on 05/07/2025).

[124] Nationaal Programma Verduurzaming Industrie. “Rockwool elektrificeert smeltproces.” (Mar. 12, 2024), [Online]. Available: https://www.verduurzamingindustrie.nl/industrieroutes/elektrificatie/nieuws-elektrificatie/2676731.aspx (visited on 05/07/2025).

[125] ROCKWOOL B.V. “Rockwool roermond versnelt co2-reductie met elektrificatie van het smeltproces.” (Feb. 28, 2024), [Online]. Available: https://www.rockwool.com/nl/over-ons/nieuws/rockwool-elektrificeert-smeltproces/ (visited on 05/07/2025).

[126] FIXIT TM Holding GmbH, “Umwelt-produktdeklaration nach iso 14025 und en 15804+a2, Por® schaummörtel/-beton (200 - 1.400 kg/m³) fixit, hasit, röfix, kreisel, greutol,” Berlin, de, EPD-FIX-20230428-CBF1-DE, Sep. 20, 2024. [Online]. Available: https://cdn.dam.fixit-holding.com/assets/api/d49c50e5-9ac6-4d24-b935-4fa24a1e9ec6/original/EPD---Fixit-POR-9060-Schaumbeton-ca-600-kg-m%C2%B3-(trocken)-Ausgleichsmasse.pdf (visited on 06/04/2025).

[127] EUMEPS – European Association of EPS, “Environmental product declaration eumeps (skandinavien) – eps,” 2021. [Online]. Available: https://www.bewi.com/wp-content/uploads/2021/02/EPD.pdf (visited on 06/04/2025).

[128] D. Frans, C. Veenman, and E. ten Hove, “Circularity for rails,” Mar. 14, 2023. [Online]. Available: https://www.prorail.nl/siteassets/homepage/toekomst/duurzaamheid/documenten/230414_final-draft-prorail-study-on-circular-rail---update-definitieve-versie.pdf (visited on 04/25/2025).

[129] T. Tankova, *CIEM5000: Sustainable Construction Members and Systems - Lecture 2.1.2 – Introduction to steel structures, basic material properties, products and design*, 2024. [Online]. Available: https://brightspace.tudelft.nl/d2l/le/content/680476/viewContent/3826590/View.

[130] Groupe SNCF. “« Rails décarbonés » : l’économie circulaire chez SNCF Réseau.” (Feb. 5, 2025), [Online]. Available: https://www.groupe-sncf.com/fr/engagements/developpement-durable/rail-vert (visited on 04/25/2025).

[131] F. Thériné, E. Keita, J. Naël-Redolfi, P. Boustingorry, L. Bonafous, and N. Roussel, “Water absorption of recycled aggregates: Measurements, influence of temperature and practical consequences,” *Cement and Concrete Research*, vol. 137, p. 106 196, Sep. 6, 2020. DOI: 10.1016/j.cemconres.2020.106196. [Online]. Available: https://doi.org/10.1016/j.cemconres.2020.106196.

[132] KWS, *SAMEN OP WEG | Aflevering 1: 40 jaar KWS en GVB*, Feb. 8, 2024. [Online]. Available: https://www.youtube.com/watch?v=hpqd2Li-htg (visited on 04/15/2025).

[133] L. Butler, J. West, and S. Tighe, “The effect of recycled concrete aggregate properties on the bond strength between rca concrete and steel reinforcement,” *Cement and Concrete Research*, vol. 41, no. 10, pp. 1037–1049, Jul. 1, 2011. DOI: 10.1016/j.cemconres.2011.06.004. [Online]. Available: https://doi.org/10.1016/j.cemconres.2011.06.004.

[134] Y. A. Abera, “Performance of concrete materials containing recycled aggregate from construction and demolition waste,” *Results in Materials*, vol. 14, p. 100 278, Apr. 23, 2022. DOI: 10.1016/j.rinma.2022.100278. [Online]. Available: https://doi.org/10.1016/j.rinma.2022.100278.

[135] F. Leenders. “Pijlers galgenveldbrug in geopolymeerbeton, Aantonen gelijkwaardigheid van geopolymeerbeton en de toepasbaarheid van eurocode 2.” (Jul. 11, 2023), [Online]. Available: https://www-cementonline-nl.tudelft.idm.oclc.org/artikelen/pijlers-galgenveldbrug-in-geopolymeerbeton (visited on 04/16/2025).

[136] P. de Vries. “Kan cement zonder klinker?” (Nov. 1, 2013), [Online]. Available: https://www-cementonline-nl.tudelft.idm.oclc.org/artikelen/kan-cement-zonder-klinker?file=10210.pdf (visited on 04/16/2025).

[137] F. Xu, G. Chen, K. Li, *et al.*, “Interfacial bond behavior between normal opc concrete and self-compacting geopolymer concrete enhanced by nano-sio2,” *Construction and Building Materials*, vol. 411, p. 134 617, Dec. 18, 2023. DOI: 10.1016/j.conbuildmat.2023.134617. [Online]. Available: https://doi.org/10.1016/j.conbuildmat.2023.134617.

[138] H. Bezemer, N. Awasthy, and M. Luković, “Multiscale analysis of long-term mechanical and durability behaviour of two alkali-activated slag-based types of concrete,” *Construction and Building Materials*, vol. 407, p. 133 507, Sep. 28, 2023. DOI: 10.1016/j.conbuildmat.2023.133507. [Online]. Available: https://doi.org/10.1016/j.conbuildmat.2023.133507.

[139] M. Maaz, R. A. Khan, and R. Sharma, “Fatigue and fracture behaviour of geopolymer concrete,” *Materials Today Proceedings*, vol. 93, pp. 163–169, Jan. 1, 2023. DOI: 10.1016/j.matpr.2023.07.113. [Online]. Available: https://doi.org/10.1016/j.matpr.2023.07.113.

[140] M. Verweij and H. Heijsters, “Milieuaspecten en technische eigenschappen geopolymeerbeton,” 2022, pp. 10–12. [Online]. Available: https://pointer.kro-ncrv.nl/system/files/2022-12/Betoniek%20okt%202022%20GPB.pdf (visited on 04/16/2025).

[141] Y. Seyrek, O. Rudić, J. Juhart, *et al.*, “On drying shrinkage of geopolymer and how to mitigate it with vegetable oil,” *Construction and Building Materials*, vol. 436, p. 137 013, Jun. 12, 2024. DOI: 10.1016/j.conbuildmat.2024.137013. [Online]. Available: https://doi.org/10.1016/j.conbuildmat.2024.137013.

[142] greenSand. “Cleaning up CO2 along the Hoekse line.” (), [Online]. Available: https://greensand.com/en/blogs/projecten/de-hoekse-lijn?srsltid=AfmBOooLI7h74NFVmO3s2fkUL86EhaWSjDUArFqabJmKQswbiNgBtl2t (visited on 04/28/2025).

[143] J. P. M. Vink, “Geschiktheid van olivijn als ballastmateriaal,” Dec. 13, 2021, pp. 1–45. [Online]. Available: https://publications.deltares.nl/11207232_002.pdf.

[144] Van Dijk Maasland, “Ketenanalyse olivijn, Incl. plan van aanpak co2-reductie scope 3,” Dec. 2023. [Online]. Available: https://vandijkmaasland.nl/wp-content/uploads/2024/08/4A1_4B1_Ketenanalyse-en-Plan-van-Aanpak-scope-3-Van-Dijk-Maasland_totaal-2023.pdf (visited on 04/28/2025).

[145] International Energy Agency. “Energy system of france.” (2023), [Online]. Available: https://www.iea.org/countries/france (visited on 04/30/2025).

[146] Peter K. J. Robertson, “Soil behaviour type from the CPT: an update,” 2010. [Online]. Available: https://api.semanticscholar.org/CorpusID:15373054.

[147] Robertson and Cabal, “Estimating soil unit weight from CPT,” 2010. [Online]. Available: https://www.cpt-robertson.com/PublicationsPDF/Unit%20Weight%20Rob%20%26%20Cabal%20CPT10.pdf (visited on 02/11/2025).

[148] Tromp and Korff, *Tijd-zettingsverloop in de tijd van verschillende grondsoorten*, Delft, Feb. 2008. [Online]. Available: https://www.cob.nl/document/bouwen-op-slappe-bodems/ (visited on 02/02/2025).

[149] “NEN 9997-1+C2 Geotechnical Design of Structures, Part 1: General rules,” Nov. 2017. [Online]. Available: https://connect.nen.nl/Standard/PopUpHtml?RNR=3535337&search=&Native=1&token=03c21091-680c-45ac-bd51-f54f1ab29b16 (visited on 02/03/2025).

[150] D. Sipkema, “a,b,c-Isotachenmodel, Van a,b,c, tot zetting,” Jun. 2006. [Online]. Available: https://repository.tudelft.nl/file/File_8dd028db-9034-4d0a-b839-4277047d3891?preview=1 (visited on 03/05/2025).

[151] D. Sipkema, *NEN / Bjerrum parameterbepaling*, Jun. 2006. [Online]. Available: https://repository.tudelft.nl/file/File_8dd028db-9034-4d0a-b839-4277047d3891?preview=1 (visited on 03/05/2025).

[152] H. Kooi, “Toetsing isotachenmodel met gegevens van bodemdalingsmonitoringssites,” Jun. 21, 2024, pp. 4–25. [Online]. Available: https://publications.deltares.nl/11206019_004_0006.pdf.

[153] H. Kooi, *Toestandsdiagram voor het isotachenmodel op basis van natuurlijke rek*. Jun. 21, 2024. [Online]. Available: https://publications.deltares.nl/11206019_004_0006.pdf.

[154] H. Kooi, *Toestandsdiagram voor het isotachenmodel op basis van lineaire rek*. Jun. 21, 2024. [Online]. Available: https://publications.deltares.nl/11206019_004_0006.pdf.

[155] L. Laloui and A. F. R. Loria, *Thermohydromechanical behaviour of soils and soil–structure interfaces*. Nov. 22, 2019, pp. 209–269. DOI: 10.1016/b978-0-12-816223-1.00005-9. [Online]. Available: https://doi.org/10.1016/b978-0-12-816223-1.00005-9.

[156] DINOLoket. "Ondergrondmodellen." (), [Online]. Available: https://www.dinoloket.nl/ondergrondmodellen/kaart (visited on 02/03/2025).

[157] M. Hijma, "Geology of the Dutch Coast, The effect of lithological variation on coastal morphodynamics," 1220040-007-ZKS-0003, Feb. 24, 2017. [Online]. Available: https://publications.deltares.nl/1220040_007_0003.pdf (visited on 02/03/2025).

A

Cross-sections RET

The RET has a variety of standard tram track structures used throughout the tram network. In this section, the technical drawings of this structure is displayed of the following types of cross-sections

- Tram slab track embedded in grass (Code 826, section A.1)
- Tram slab track embedded in asphalt pavement (Code 828, section A.2)
- Tram slab track embedded in ballast (Code 825, section A.3)

A.1. Tram slab track embedded in grass

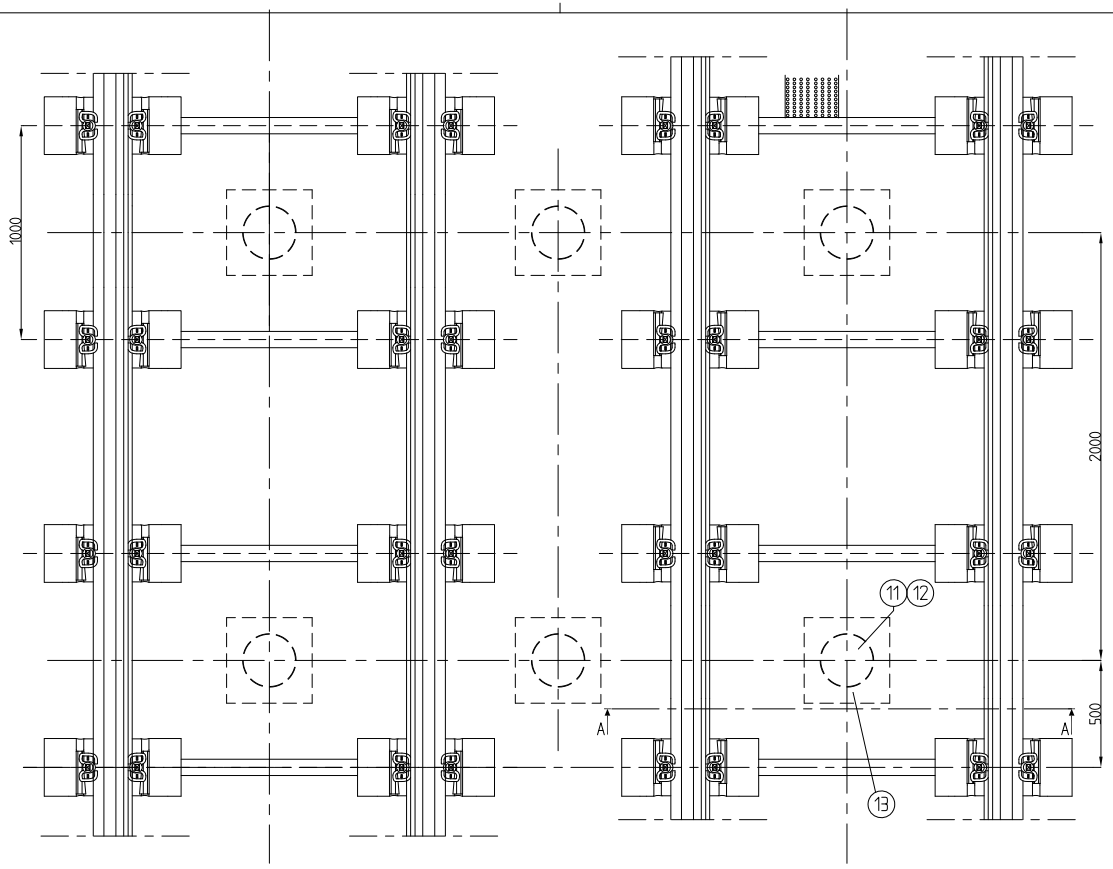

BOVENAANZICHT Schaal 1:25

STUK NR.	AANTAL	BENAMING	OPMERKING / TEK.NR.	AFMETING OF NORMAAL AANDUIDING	MATERIAAL MAGAZIJN NR	MATERIAAL SOORT	MAGAZIJN NR ONDERDEEL
1		RAILPROFIEL Ri 60	W2-27794	ONGEBOORD			901.722.00
2	1	BETONDWARSLIGGER	W2-57333-IV				906.220.00
3	2	VULPLAAT	W2-58148	DEEL 1, TYPE RECHTS		K-Wpf 14	904.951.50
4	2	VULPLAAT	W2-58148	DEEL 2, TYPE RECHTS		K-Wpf 14	
5	2	VULPLAAT	W2-58148	DEEL 1, TYPE LINKS		K-Wpf 14	904.951.60
6	2	VULPLAAT	W2-58148	DEEL 2, TYPE LINKS		K-Wpf 14	
7	4	SPANKLEM	W2-56393	DIN 17.221 - SKL 14V		38 Si 7	904.218.00
8	4	KRAAGSCHROEF	W2-56397	GEGALVANISEERD		4.6	904.246.00
9	2	TUSSENPLAAT	W2-58839	175 x 200 x 6		KURKR. Fc846	905.802.70
9	2	TUSSENPLAAT	W2-58839	175 x 200 x 6		KURKR. Fc846	905.802.70
10	4	ISOLATIEPLAATJE	W2-60736	104 x 25 x 6		P.A.6.0.40% GG	907.200.00
11		Drainage koker		ϕ 250		PVC	
12		Grind		22/40		PORFIER	
13		Vliesmembraan		400 x 400		Bidim B7	
14		HDPE KOKER	W2-60786	ϕ125 - 6m		HDPE	348.124.60
		TECTYL					
		NOXYDE					

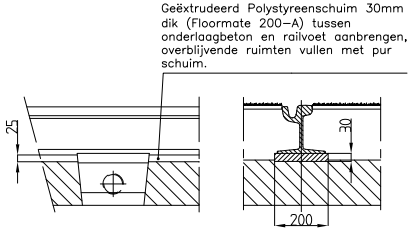

ZIJAANZICHT Schaal 1:20 VOORAANZICHT

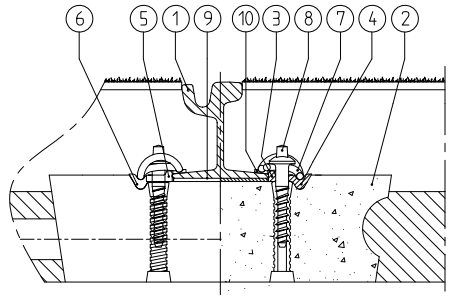

DETAIL A Schaal 1:10

Na ontroesten de rail insmeren of spuiten met Noxyde.
De dikte van de droge laag moet minimaal 0,500 mm zijn.
Verbruik is ca. 500 g/m1 spoorstaaf.

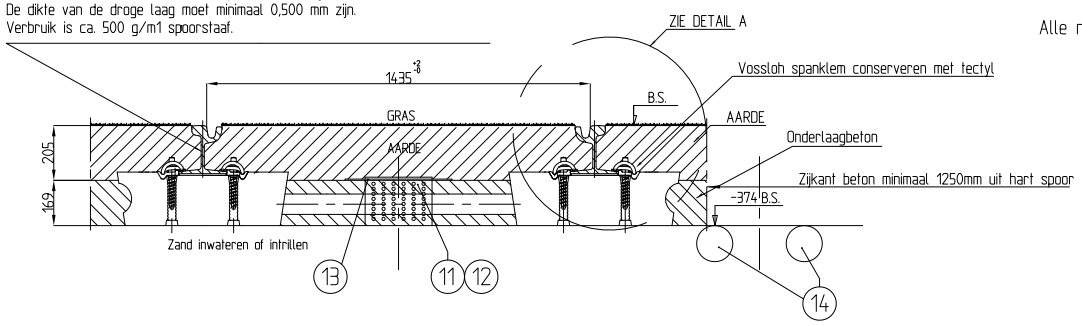

DOORSNEDE A-A Schaal 1:20

Alle niet getolereerde maten zijn theoretische maten

Maateenheid : mm

VERSIE	DATUM	GET.	OMSCHRIJVING
F	29-0-'07	PV	Postnummer 11 toegevoegd
G	07-08-'07	PV	Drainage gewijzigd
H	03-01-'08	PV	Koker gewijzigd
D	31-01-'06	PV	Aanzicht en tekst toegevoegd, materiaal gewijzigd
E	30-11-'06	PV	Isolatieplaatje toegevoegd

PROJECTIE	PROJECT	PROJECTNR.	VAN	ORDERNR.	ROUTE	FASE	TYPE TEK.	BEHOORT BIJ
	LOKATIE	PROJECTCODE	TOT	OBJECT	RAYON	MAGNR.CPL.	TECHNIEK	WIJZIGING

RET

SPOORCONSTRUCTIE Ri 60
Op betondwarsligger op/ in (code 826)
beton, bovenlaag gras

GET.: L.A.
GEC.:
ACC.:
STATUS.: D.O.
DATUM.: 05-08-'02

BEHEER & ONTWIKKELING	BLAD	FASE	SCHAAL 1 :	FORMAAT	TEKENINGNUMMER	WIJZ.:
			div.	A3	W2-60159	H

A3

A.2. Tram slab track embedded in asphalt pavement

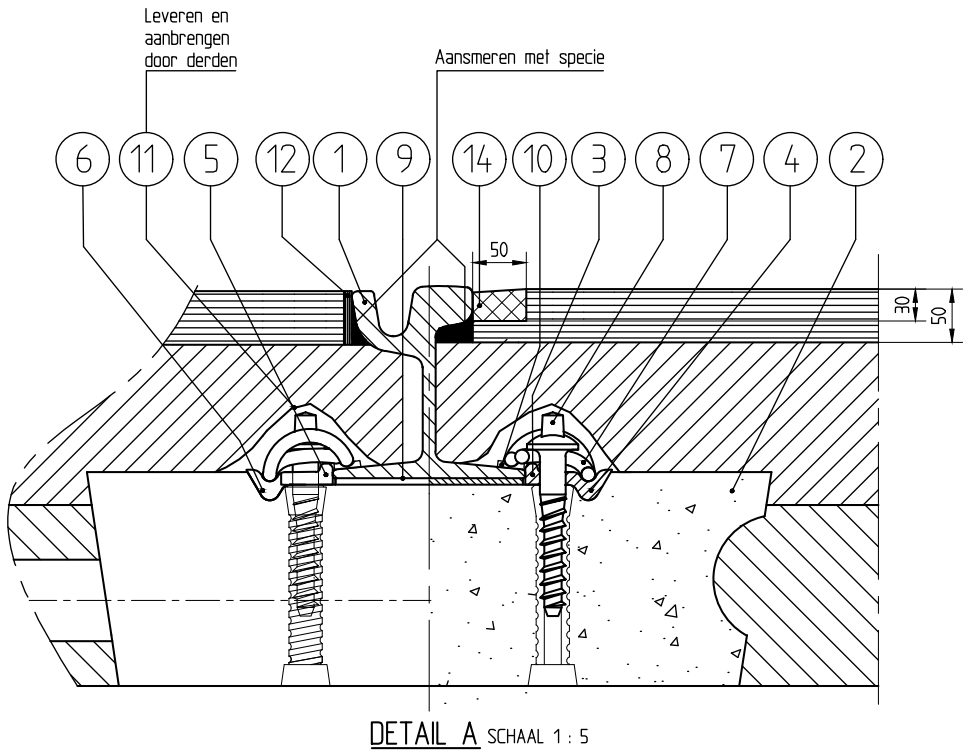

DETAIL A SCHAAL 1 : 5

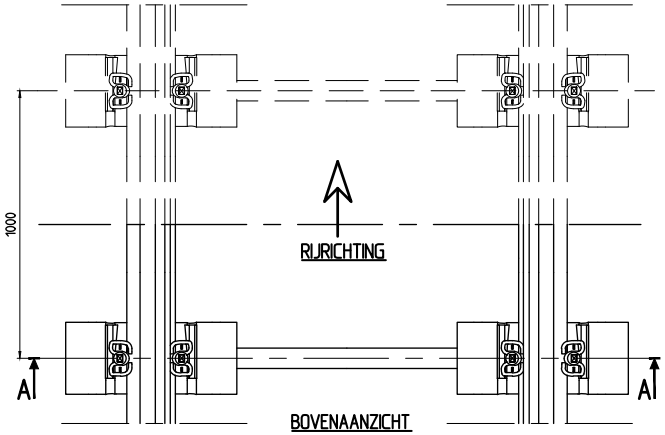

BOVENAANZICHT SCHAAL 1 : 20

Na ontroesten de rail insmeren of spuiten met Noxyde.
De dikte van de droge laag moet minimaal 0,350 mm zijn.
verbruik is ca. 350 g/m1 spoorstaaf.

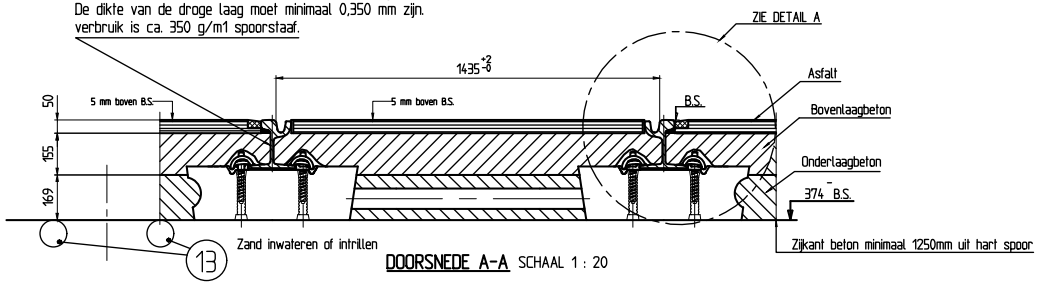

DOORSNEDE A-A SCHAAL 1 : 20

STUK NR.	AANTAL	BENAMING	OPMERKING / TEK.NR.	AFMETING OF NORMAAL AANDUIDING	MATERIAAL MAGAZIJN NR	MATERIAAL SOORT	MAGAZIJN NR ONDERDEEL
1		RAILPROFIEL 60R1	W2-27794	ONGEBOORD			901.722.00
2	1	BETONDWARSLIGGER	W2-57333-IV				906.220.00
3	2	VULPLAAT	W2-58148	DEEL 1, TYPE RECHTS		K-Wpf 14	904.951.50
4	2	VULPLAAT	W2-58148	DEEL 2, TYPE RECHTS		K-Wpf 14	
5	2	VULPLAAT	W2-58148	DEEL 1, TYPE LINKS		K-Wpf 14	904.951.60
6	2	VULPLAAT	W2-58148	DEEL 2, TYPE LINKS		K-Wpf 14	
7	4	SPANKLEM	W2-56393	DIN 17.221 - SKL 14V		38 Si 7	904.218.00
8	4	KRAAGSCHROEF	W2-56397	GEGALVANISEERD		4.6	904.246.00
9	2	TUSSENPLAAT	W2-58839	175 x 200 x 7	Rubber	EPDM 700	905.802.70
10	4	ISOLATIEPLAATJE	W2-60736	104 x 25 x 6			907.200.00
11		AFDEKFOLIE		TER BESCHERMING RAILBEV.			
12		BITUMENSTRIP		10 x 50			
13		HDPE koker	W2-60786	Φ125 - 6m		HDPE	348.124.60
14		Voegvulling	Hd 20-25 Shore	50 x 30	Bitumineuse	Gietmassa	

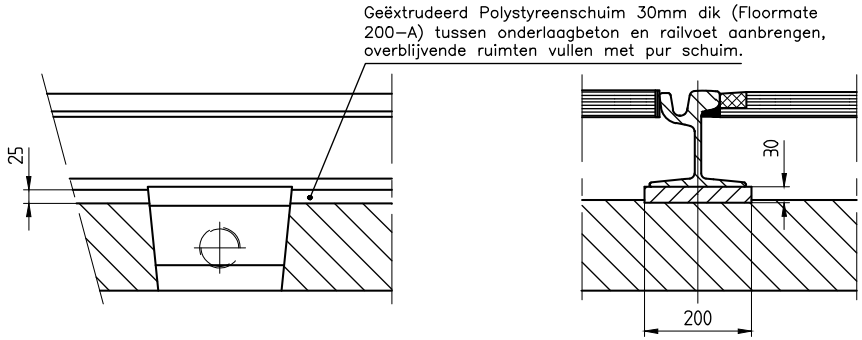

ZIJAANZICHT SCHAAL 1 : 10

DOORSNEDE SCHAAL 1 : 10

Alle niet getolereerde maten zijn theoretische maten

Maateenheid : mm

WIJZIGING	DATUM	GET.	OMSCHRIJVING
V	11-06-2013	WT	Pos 9 + pos 14 toegev.
Y	07-06-'14	WT	Hoogte asfalt
W	15-10-'13	WT	Pos 9 mag. nr. toegev.

PROJECTIE	PROJECT	PROJECTNR.	VAN	ORDERNR.	ROUTE	FASE	TYPE TEK.	BEHOORT BIJ
	LOKATIE	PROJECTCODE	TDT	OBJECT	RAYON	MAGNR.CPL.	TECHNIEK	WIJZIGING

RET

INGENIEURSBUREAU

SPOORCONSTRUCTIE 60R1 (code 828)
Op betondwarsligger in beton, bovenlaag asfalt

BLAD	FASE	SCHAAL 1 :	FORMAAT	TEKENINGNUMMER	WIJZ.:
		div.	A3	W2-58380	Y

GET.: HvdM
GEC.:
ACC.:
STATUS.: D.O.
DATUM.: 05-08-'02

A3

A.3. Tram slab track embedded in ballast

STUK NR.	AANTAL	BENAMING	OPMERKING / TEK.NR.	AFMETING OF NORMAAL AANDUIDING	MATERIAAL MAGAZIJN NR	MATERIAAL SOORT	MAGAZIJN NR ONDERDEEL
1		RAILPROFIEL 60R1	W2-27794	ONGEBOORD			901.722.00
2	1	BETONDWARSLIGGER	W2-57333-IV				906.220.00
3	2	VULPLAAT	W2-58148	DEEL 1, TYPE RECHTS		K-Wpf 3b	904.951.50
4	2	VULPLAAT	W2-58148	DEEL 2, TYPE RECHTS		K-Wpf 3b	
5	2	VULPLAAT	W2-58148	DEEL 1, TYPE LINKS		K-Wpf 3b	904.951.60
6	2	VULPLAAT	W2-58148	DEEL 2, TYPE LINKS		K-Wpf 3b	
7	4	SPANKLEM	W2-56393	DIN 17.221		38 Si 7	904.218.00
8	4	KRAAGSCHROEF	W2-56397	GEGALVANISEERD		4.6	904.246.00
9	2	TUSSENPLAAT	W2-58839	175 x 200 x 7	Rubber	EPDM 700	905.802.70
10	4	ISOLATIEPLAATJE	W2-60736	104 X 25 X 6			907.200.00
11		GRIND		GRADATIE 22/40		PORFIER	
12		HDPE Koker	W2-60786	Φ125 - 6m		HDPE	348.124.60
13		Drainage koker		Φ250		PVC	
14		Grind		22/40		PORFIER	
15		Vliesmembraan		400 x 400		Bidim B7	
		Noxyde					

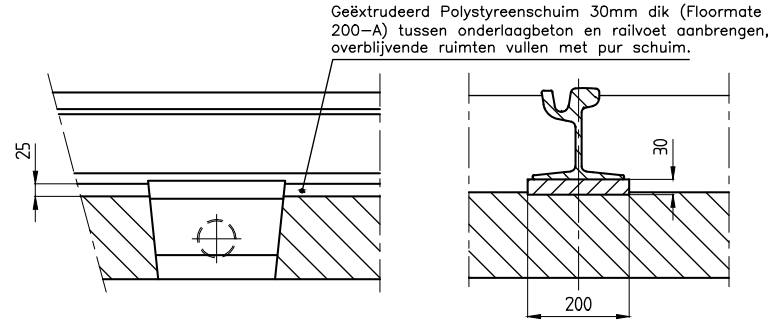

ZIJAANZICHT SCHAAL 1 : 10

DOORSNEDE SCHAAL 1 : 10

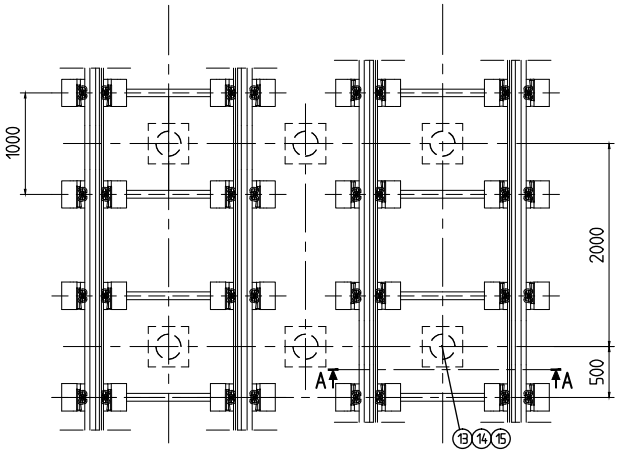

BOVENAANZICHT SCHAAL 1 : 50

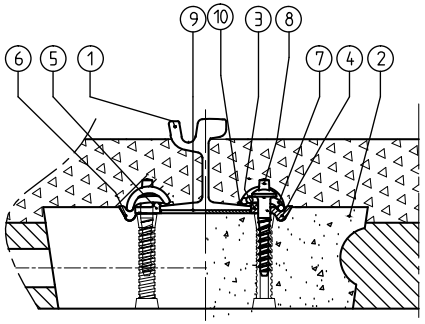

DETAIL A SCHAAL 1 : 10

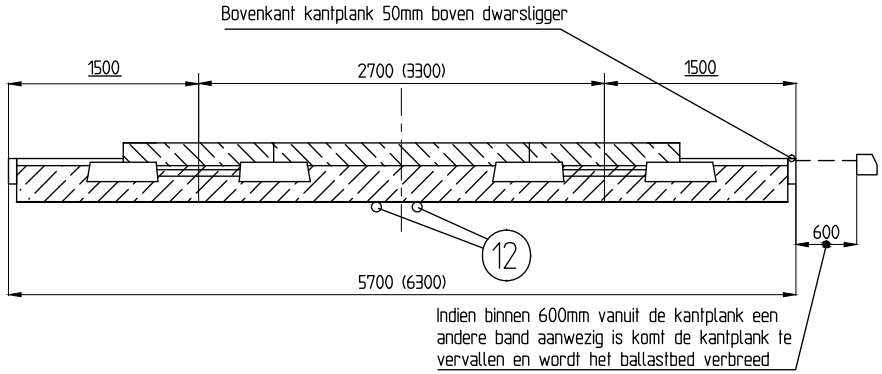

DWARSPROFIEL MET VLIESMEMBRAAN SCHAAL 1 : 50

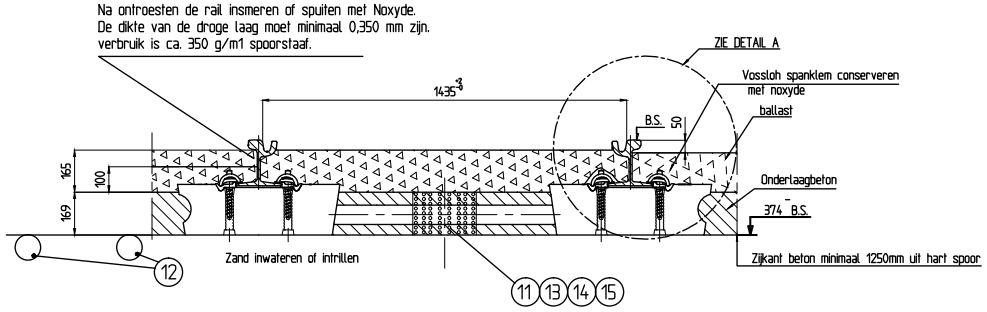

DOORSNEDE A-A SCHAAL 1 : 20

Alle niet getolereerde maten zijn theoretische maten

Maateenheid : mm

WIJZIGING	DATUM	GET.	OMSCHRIJVING
F	11-06-2013	WT	Pos 9
H	15-10-'13	WT	Pos 9 mag.nr. toegev.
G	07-08-'13	WT	Dikte NOXYDE

PROJECTIE	PROJECT	PROJECTNR.	VAN	ORDERNR.	ROUTE	FASE	TYPE TEK.	BEHOORT BIJ
	LOKATIE	PROJECTCODE	TOT	OBJECT	RAYON	MAGNR.CPL.	TECHNIEK	WIJZIGING

RET

SPOORWEGTECHNIEK

SPOORCONSTRUCTIE 60R1 (code 825)
Op betondwarsligger op/in beton, bovenlaag ballast

BLAD	FASE	SCHAAL 1 :	FORMAAT	TEKENINGNUMMER	WIJZ.:
		div.	A3	W2-60220	H

GET.: A.S.
GEC.:
AGC.:
STATUS: D.O.
DATUM: 19-05-'03

A3

B

Cone Penetration Tests

This appendix contains the CPTs from the database of the City of Rotterdam around the project location. The CPTs H4 LL0287, H4 LL0288, H4 LL0555, H4 LL0366, H4 LL0351 and H4 LL0487 are used for this research. The exact locations of these CPTs are displayed in figure B.1. Furthermore, the used methods to derive the corresponding soil types and unit weights are discussed in section B.7.

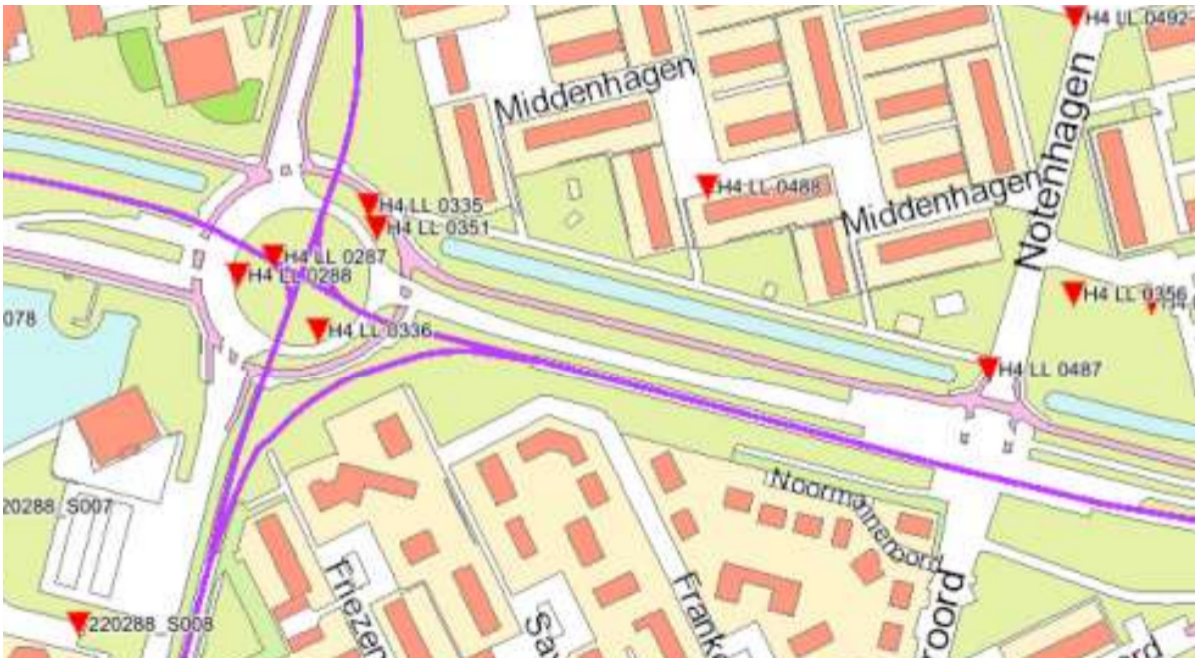

Figure B.1: Locations used CPT data

B.1. CPT H4 LL 0287

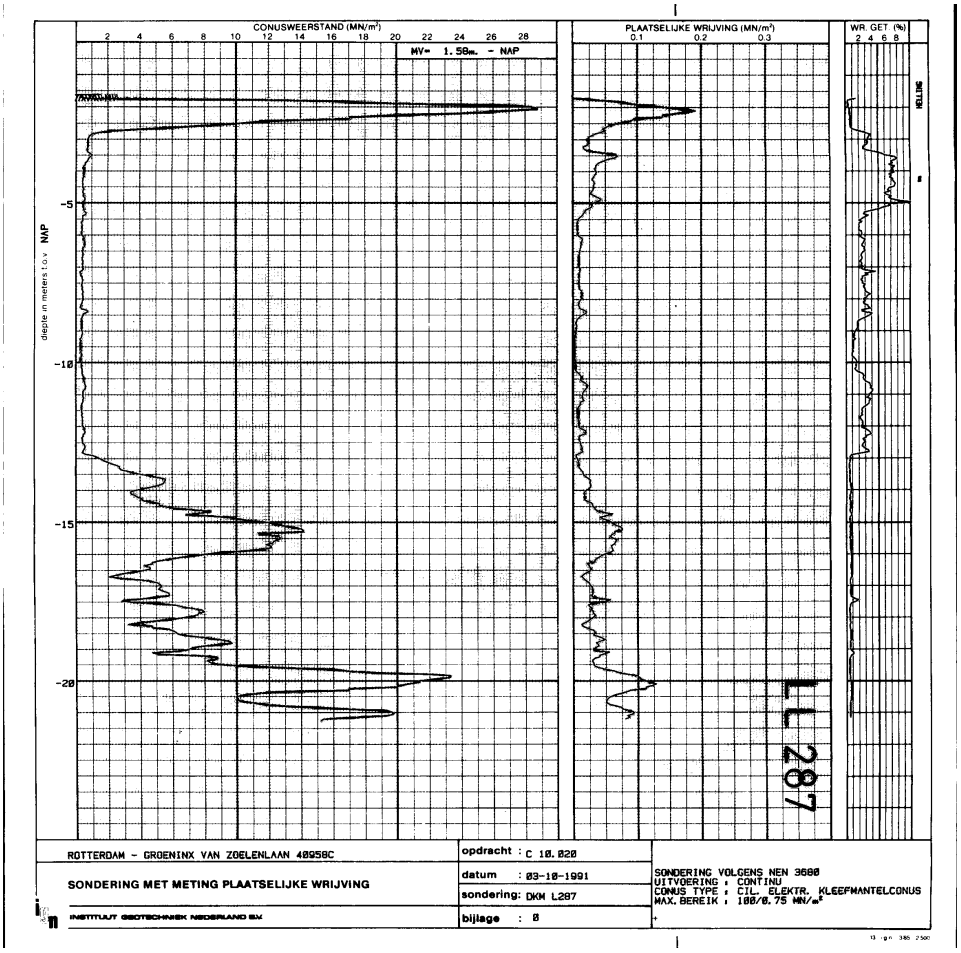

B.2. CPT H4 LL 0288

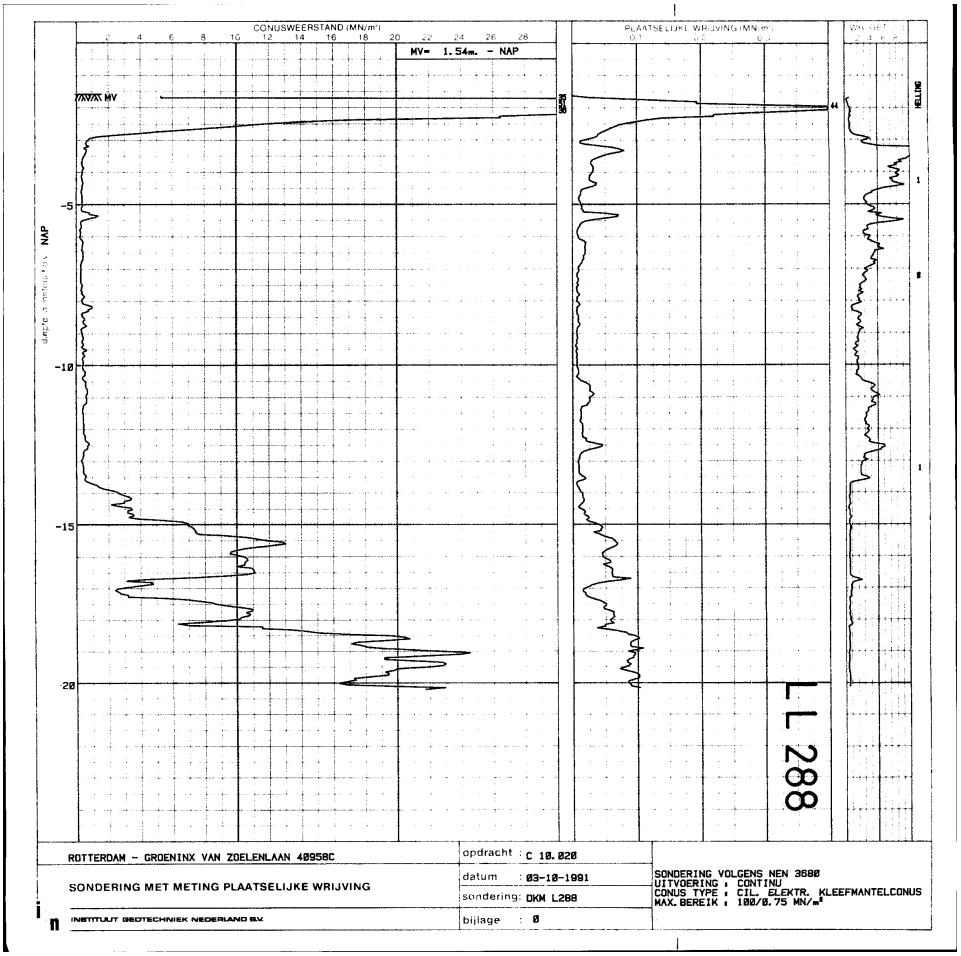

B.3. CPT H4 LL 0335

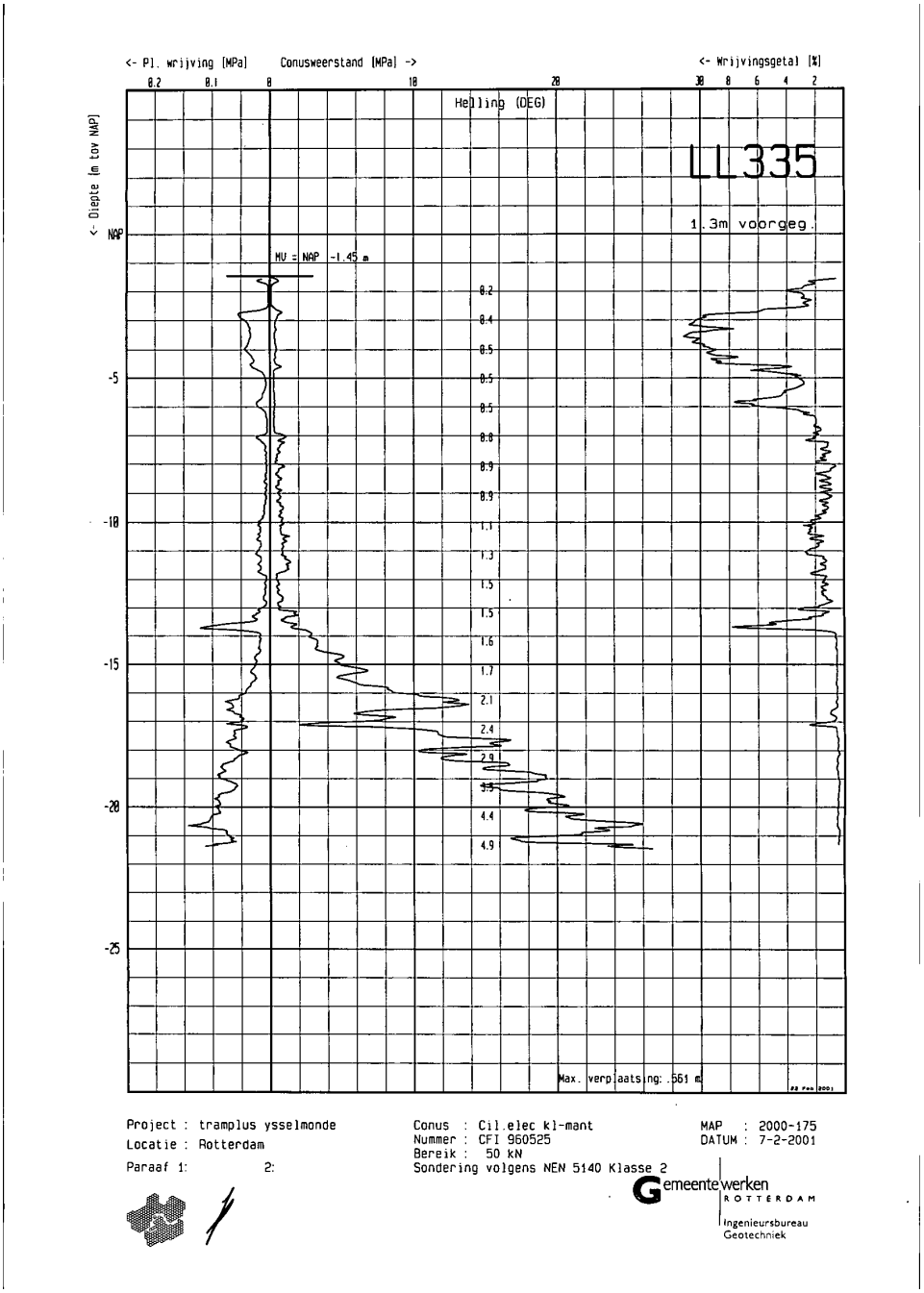

B.4. CPT H4 LL 0336

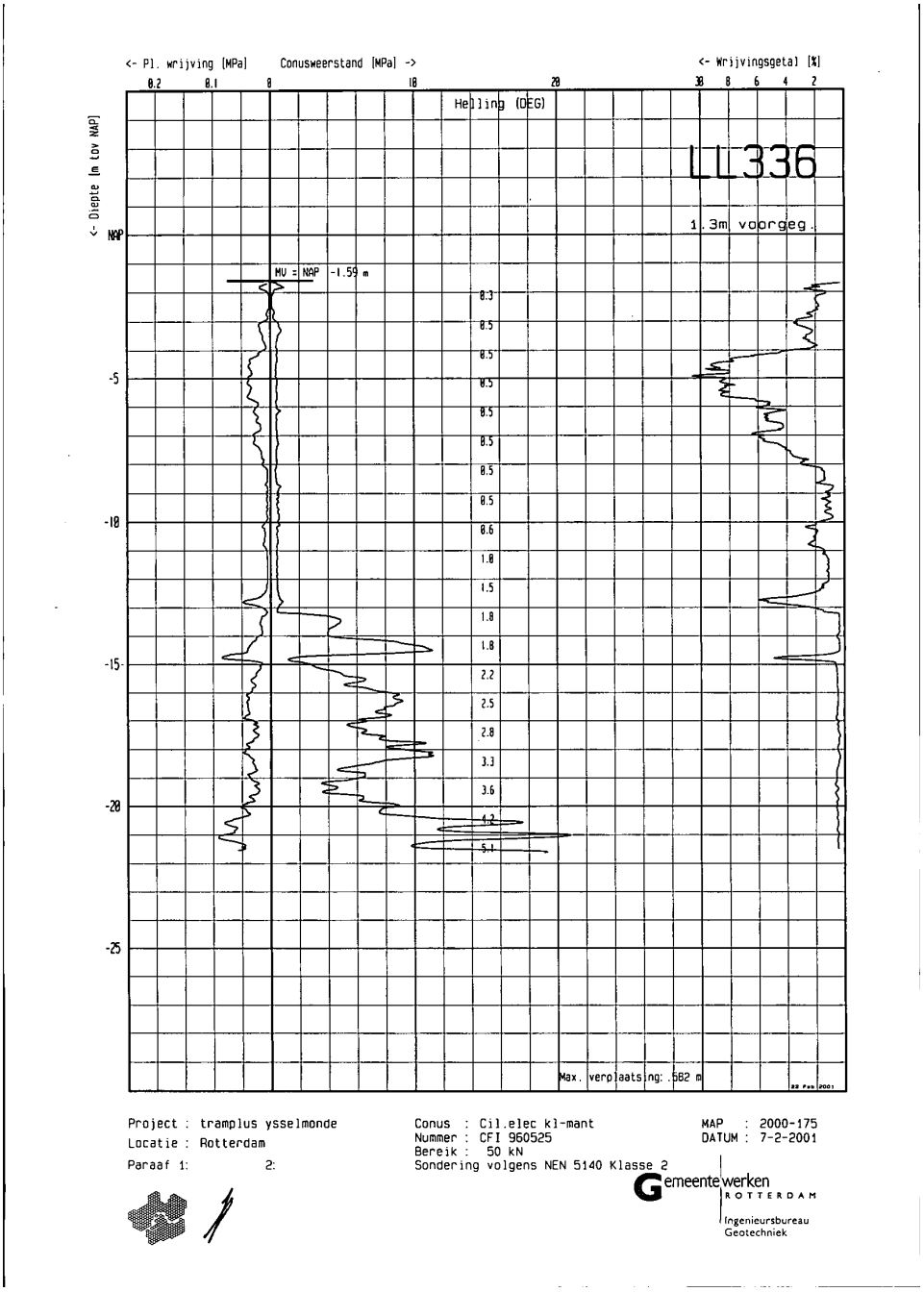

B.5. CPT H4 LL 0351

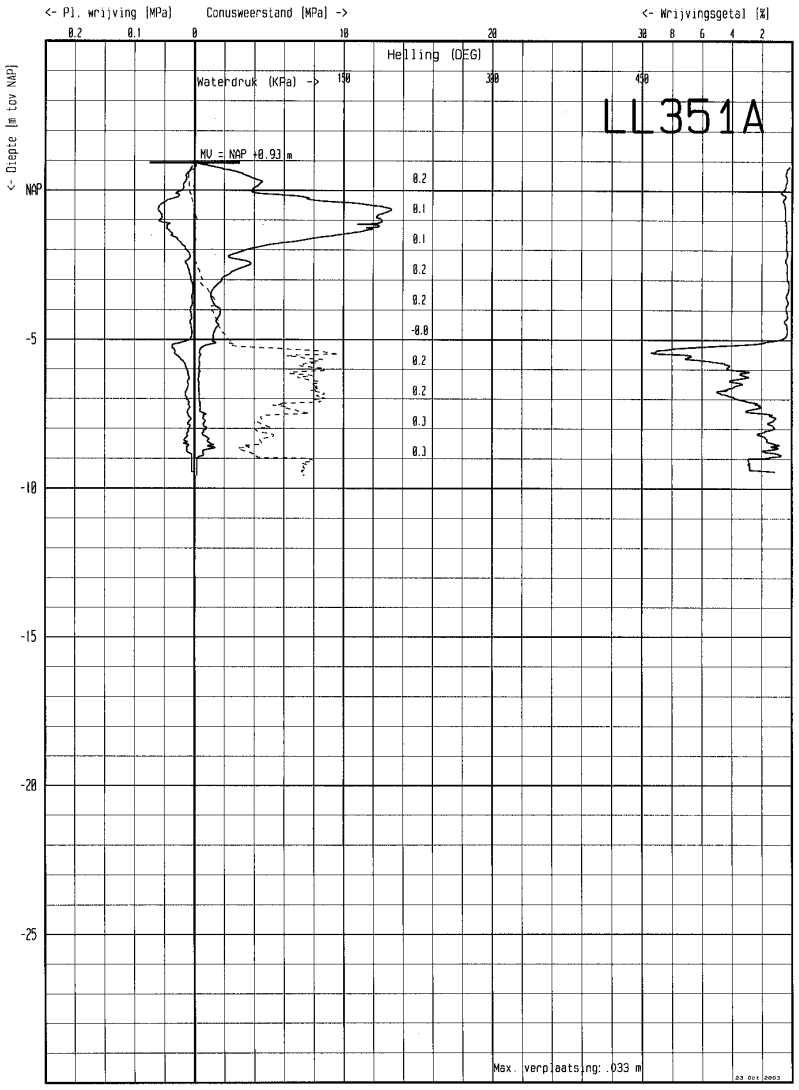

B.6. CPT H4 LL 0487

Gemeente Rotterdam
Ingenieursbureau
Afdeling Geotechniek

Marconistraat 1a
NL-3029AE, Rotterdam
Tel. 010 489 9700

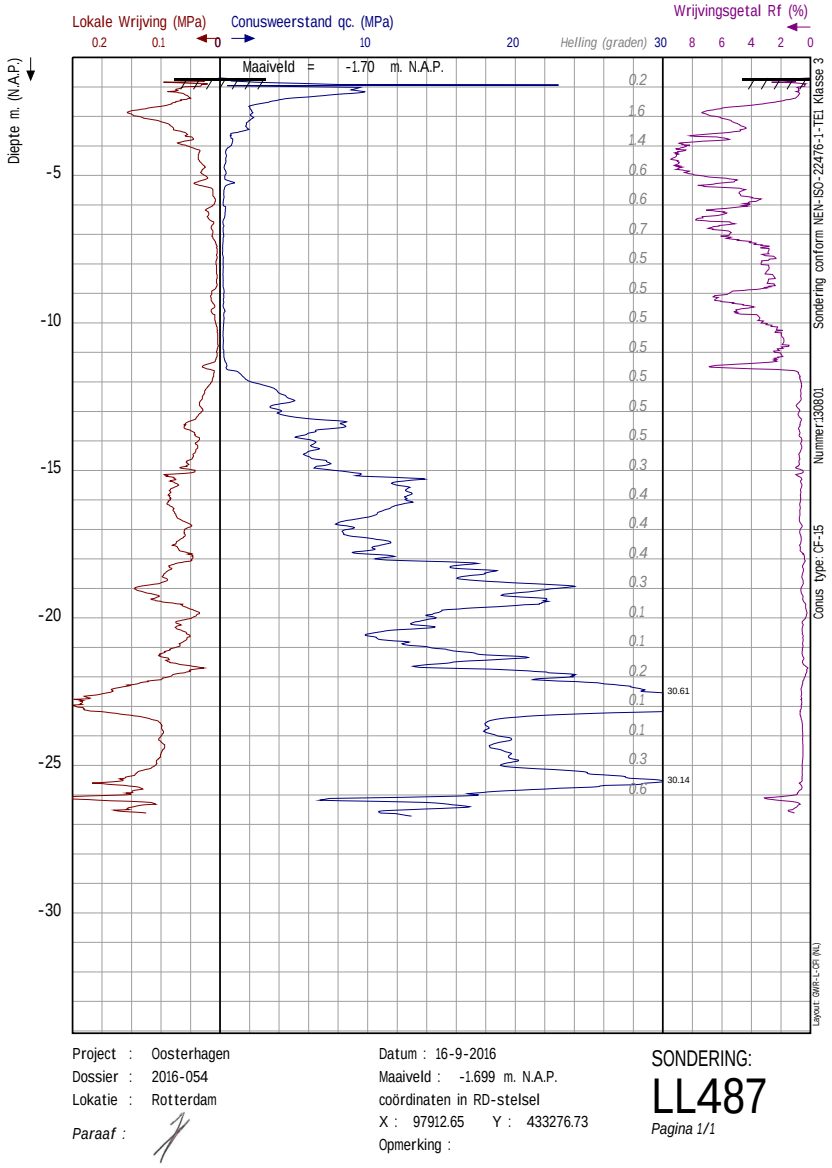

Project : Oosterhagen
Dossier : 2016-054
Lokatie : Rotterdam
Paraaf :

Datum : 16-9-2016
Maaiveld : -1.699 m. N.A.P.
coördinaten in RD-stelsel
X : 97912.65 Y : 433276.73
Opmerking :

SONDERING:
LL487
Pagina 1/1

B.7. Soil classification

During a CPT test, a cone is driven into the ground at a constant rate. The following measurements are performed:

- Resistance at the tip of the conus q_t
- Friction around the sleeve of the conus f_s
- Pore water pressure

Based on these characteristics, the soil types on the location can be determined based on the Robertson Chart. The Robertson Chart is displayed in figure B.2.

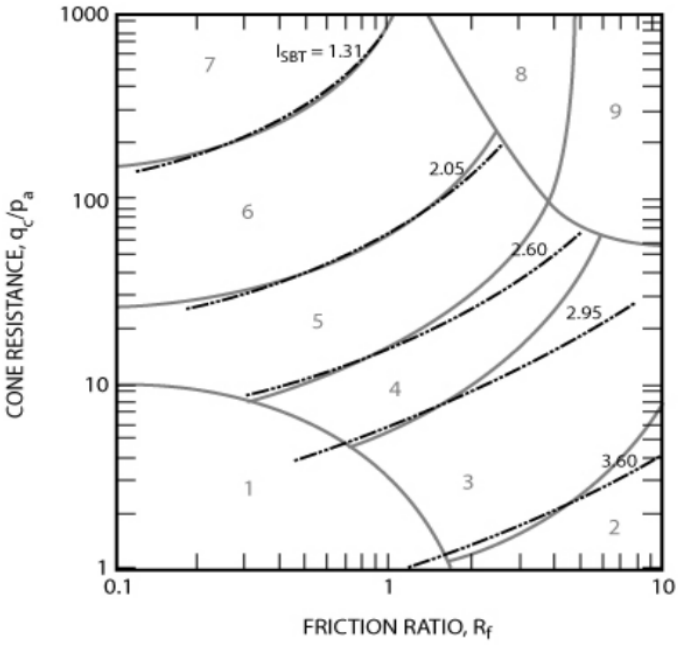

Zone	Soil Behaviour Type (SBT)
1	*Sensitive fine-grained*
2	*Clay - organic soil*
3	*Clays: clay to silty clay*
4	*Silt mixtures: clayey silt & silty clay*
5	*Sand mixtures: silty sand to sandy silt*
6	*Sands: clean sands to silty sands*
7	*Dense sand to gravelly sand*
8	*Stiff sand to clayey sand**
9	*Stiff fine-grained**

** Overconsolidated or cemented*

Figure B.2: Robertson Chart [146]

For the Robertson Chart, the friction ratio R_f is used, which is the ratio between the friction around the sleeve and the resistance at the tip of the conus. This relation is described in equation B.1.

$$R_f = \frac{f_s}{q_t} \cdot 100\% \tag{B.1}$$

B.8. Unit weight

To derive the soil unit weight γ from the CPT test, Robertson and Cabal developed the following equation [147]:

$$\frac{\gamma}{\gamma_w} = 0.27 \log R_f + 0.36 \log \left(\frac{q_t}{p_a} \right) + 1.236 \tag{B.2}$$

Where:

- R_f = friction ratio = $\left(\frac{f_s}{q_t} \right) \cdot 100\%$ [-]
- γ_w = unit weight of water in the same units as γ
- p_a = atmospheric pressure in the same units as q_t

Based on the unit weight, many soil parameters can be derived, as studied by Stikvoort [45] and further discussed in Appendix section C.5.

B.9. Permeability

The permeability of the soil layer can also be determined based on the CPT tests. As a first step, the Normalised Cone Resistance Q_t should be calculated with equation B.3

$$Q_t = \frac{q_t - \sigma_{v0}}{\sigma'_{v0}} \tag{B.3}$$

Where:

- q_t = cone resistance [kPa]
- σ_{v0} = total stress at depth z [kPa]
- σ'_{v0} = effective stress at depth z [kPa]

The Normalised Cone Resistance is an input for the Soil Behaviour Type Index I_c, which can be eventually be used to calculate the permeability. I_c expresses the radius of concentric circles in the Robertson Chart. The equation is defined as follows:

$$I_c = \sqrt{((3.47 - log(Q_t))^2 + (log(R_f) + 1.22)^2)} \tag{B.4}$$

Where:

- Q_t = Normalised Cone Resistance
- R_f = Friction Ratio

Once having obtained the Soil Behaviour Type Index from equation B.4, the permeability of the soil can be calculated with equation B.5

$$k = \begin{cases} 10^{0.952 - 3.04 I_c}, & \text{for } I_c \leq 3.27 \\ 10^{-4.52 - 1.37 I_c}, & \text{otherwise} \end{cases} \tag{B.5}$$

C

Soil Characteristics

Soils are usually inhomogeneous materials, which consist of grains and voids. These voids can (partially) be filled with water [5], [50]. Soils can be divided into various types, which have different mechanical properties. The most common distinction between these soil types is based on the grain size of the soils. These soil types and the corresponding ranges in size are stated in table C.1 below.

Table C.1: Soil type based on grain sizes [5], [50]

Soil type	Minimum	Maximum
Clay	0	0.02 [mm]
Silt	0.02 [mm]	0.063 [mm]
Sand	0.063 [mm]	2 [mm]
Gravel	2 [mm]	63 [mm]

In the Netherlands, the soil mainly consists of the following three types of soil [50]:

- Peat
- Clay
- Sand

C.1. Peat

Peat consists of organic materials, such as decayed plants. Although peat particles are small, it is difficult to characterise the material based on the limits from table C.1, because of the presence of bigger organic particles such as wood in the soil [5]. Peat is softer than clay and sand. Moreover, peat has a low permeability compared to sand. This implies that primary settlements (consolidation) take a long time to develop, since the water is slowly expulsed out of the soil. Peat also shows secondary settlements (creep). In addition, oxidation of the organic materials in peat also lead to settlements of the soil. This process is only possible when the peat is exposed to open air and therefore, these settlements are directly related to the ground water table [23], [50]. Literature studies have reported settlements of 5 to 15 [mm/year] when the ground water table is 1 [m] below ground level [50].

C.2. Clay

Clay mainly consists of minerals, which have been created by chemical erosion [5]. Clay sediments have been deposited by rivers or the sea and are therefore more present in the western parts of the Netherlands. Clay has a low permeability, just as peat. Therefore, clays also have a strongly time dependent settlement behaviour. The consolidation and creep settlements take a long time to develop. However, the final settlements are less than for peat, as can be observed in figure C.1 [50].

C.3. Sand

Sand sediments usually consist of rock decomposition material. Sand is much stiffer than peat and clay. In addition, there is no cohesion between the sand particles. Since the sand particles are loose and highly permeable, the initial settlements under loading are much higher, whereas the primary settlements take much less time to develop. Secondary settlements (creep) do not occur [50].

C.4. Deformations and settlements

Settlements occur when an increment of effective stresses leads to a volume change of the soil. Settlements of the soil can be defined in three different stages [50]:

1. **Initial settlements**
   Initial settlements immediately occur when loads are applied on the soil.
2. **Primary settlements** (Consolidation)
   Loading of the soil results in a volume reduction of the soil. Therefore, the water has to be expulsed out of the voids. This process is related to the permeability of the soil layer and therefore time-dependent. So, these deformations can take a long time to develop for soft soils with a low permeability, such as clay. However, for sand soils, the water can quickly flow out and therefore, deformations occur immediately.
3. **Secondary settlements** (Creep)
   Secondary settlements (creep) occur for soft soils, such as peat and clay. Even when the consolidation process has finished and the effective stresses on the soil are constant, there still is deformation of the soil. This deformation rate decays over time and therefore, the settlement process is assumed to be zero after 10^4 days (or 30 years).

A graphical illustration related to the time-dependent settlements for different soil types is shown in figure C.1.

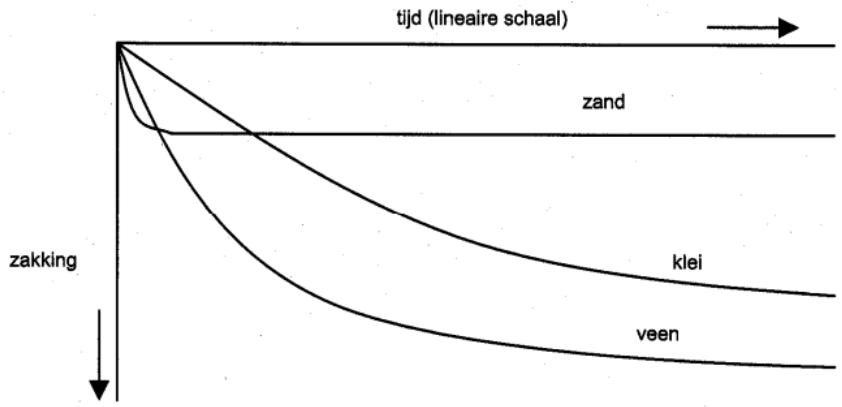

Figure C.1: Time-dependent settlements for sand (zand), peat (veen) and clay (klei) [148]

In the Netherlands, there are multiple models and equations used to describe and calculate the settlements. These are:

- Koppejan-model
- NEN/Bjerrum
- abc-model

C.4.1. Koppejan-model

Koppejan has developed an equation to determine the strain in the of the soil, related to the time, initial stress and stress increment due to loading. This equation is as follows [5]:

$$\varepsilon = -\left[\frac{1}{C_p} + \frac{1}{C_s}\log\left(\frac{t}{t_0}\right)\right]\log\left(\frac{\sigma}{\sigma_1}\right) \tag{C.1}$$

With:

- ε = strain [-]
- C_p = primary consolidation coefficient
- C_s = secondary consolidation coefficient
- t = time [days]
- t_0 = unit of time (in this case 1 day)
- σ = stress under loading [kPa]
- σ_1 = the stress of the soil layer before loading [kPa]

The consolidation coefficients are determined by performing soil compression tests.

The settlement formulae in Eurocode 7 (NEN 9997-1+C2) [149] are based on equation C.1. The equations for the primary settlement S1 and the secondary settlement S2 are stated in equation C.2 and C.3 respectively.

$$S_1 = \sum_{j=0}^{n} \frac{1}{C'_{p,j}} \times d_j \times \ln\left(\frac{\sigma'_{v;z,0;d} + \Delta\sigma'_{v;z,d}}{\sigma'_{v;z,0;d}}\right) \tag{C.2}$$

With:

- S_1 = primary settlements [m]
- $C'_{p,j}$ = primary consolidation coefficient for layer j
- d_j = thickness of soil layer j [m]
- t = time [days]
- $\sigma'_{v;z,0;d}$ = effective vertical stress before loading in the middle of a layer at depth z [kPa]
- $\Delta\sigma'_{v;z,0;d}$ = effective vertical stress increment due to loading in the middle of a layer at depth z [kPa]

$$S_2 = \sum_{j=0}^{n} \frac{1}{C'_{s,j}} \times d_j \times \log\left(\frac{t}{t_0}\right) \times \ln\left(\frac{\sigma'_{v;z,0;d} + \Delta\sigma'_{v;z,d}}{\sigma'_{v;z,0;d}}\right) \tag{C.3}$$

With:

- S_2 = secondary settlements [m]
- $C'_{s,j}$ = primary consolidation coefficient for layer j
- d_j = thickness of soil layer j [m]
- t = time [days] (assume 10^4)
- t_0 = unit of time (in this case 1 day)
- $\sigma'_{v;z,0;d}$ = effective vertical stress before loading in the middle of a layer at depth z [kPa]
- $\Delta\sigma'_{v;z,0;d}$ = effective vertical stress increment due to loading in the middle of a layer at depth z [kPa]

C.4.2. NEN Bjerrum

The NEN Bjerrum model shows similarities with the internationally used method to calculate consolidation parameters and settlements. The internationally used parameters for consolidation are the compression index C_c, the swelling index C_{sw} and the recompression index C_r. The corresponding Bjerrum parameters are SR, RR and CR. In figure C.2, the determination of these parameters for both models based on compression tests is displayed. The difference between the graphs is that the internationally used parameters are related to the the change in void ratio Δe, whereas the NEN Bjerrum parameters are related to the vertical strain ε_v of the specimen. The latter can actually be measured during the compression test [150].

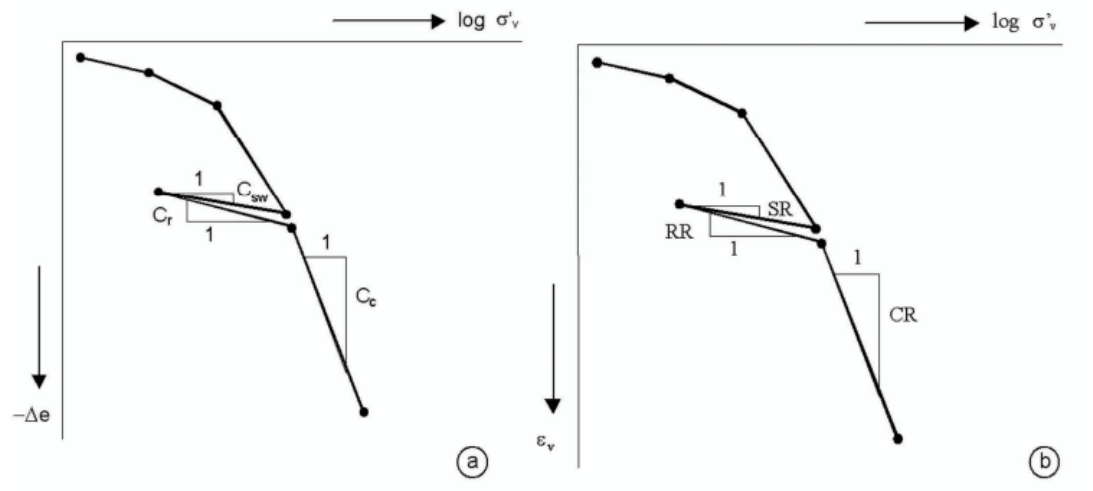

Figure C.2: Determination of internationally used (a) and the Bjerrum (b) compression parameters [151]

The parameters C_{SW} and C_r are based on the unloading and reloading of the specimen and are therefore lower than preconsolidation stress σ'_p, whereas the compression index C_c is related to the compression above the preconsolidation stress σ'_p.

Moreover, the creep parameter C_α is also based on a compression test. For a specimen with a height of 2 centimetre and a double-sided outflow of water, it is assumed that consolidation has finished after 1 day of loading. The tangent of the logarithmic time-settlement diagram at $t_i = 1$ [day] gives the value for C_α [150].

The Eurocode 7 (NEN 9997-1+C2) provides also settlement formulae based on these internationally used compression parameters C_c and C_α. The primary settlement is calculated in equation C.4 and the secondary settlement is computed in equation C.5 [149].

$$S_1 = \sum_{j=0}^{n} \frac{C_{c;j}}{1+e_j} \times d_j \times \log\left(\frac{\sigma'_{v;z,0;d} + \Delta\sigma'_{v;z,d}}{\sigma'_{v;z,0;d}}\right) \tag{C.4}$$

With:

- S_1 = primary settlements [m]
- C_c = compression index for layer j [-]
- e_j = void ratio for layer j [-]
- d_j = thickness of soil layer j [m]
- $\sigma'_{v;z,0;d}$ = effective vertical stress before loading in the middle of a layer at depth z [kPa]
- $\Delta\sigma'_{v;z,0;d}$ = effective vertical stress increment due to loading in the middle of a layer at depth z [kPa]

$$S_2 = \sum_{j=0}^{n} C_{\alpha;j} \times d_j \times \log\left(\frac{t_\infty}{t_1}\right) \tag{C.5}$$

With:

- S_2 = secondary settlements [m]
- C_α = creep parameter [-]
- d_j = thickness of soil layer j [m]
- t_∞ = time [days] (assume 10^4)
- t_1 = start time of loading in days, $t_1 = 1$ [day]

C.4.3. abc-model

Instead of using linear strain, the abc-model model is based on natural strain, which gives more accurate results for the compression of soft soil layers. Moreover, the strain rate is related to the effective stresses and the total strain. The parameters are determined by using a $K_0 - CRS$-test. The representation of the used a, b, c-parameters is displayed in the graph in figure C.3a. The representation of the NEN Bjerrum parameters are displayed in the graph in figure C.3b. The main differences between the two plots in figure C.3 are the type of strain on the y-axis (natural strain for a,b,c-model and linear strain for NEN Bjerrum) and the type of logarithmic scale on the x-axis ($\ln$ for the a,b,c-model and $\log$ for NEN Bjerrum) [152].

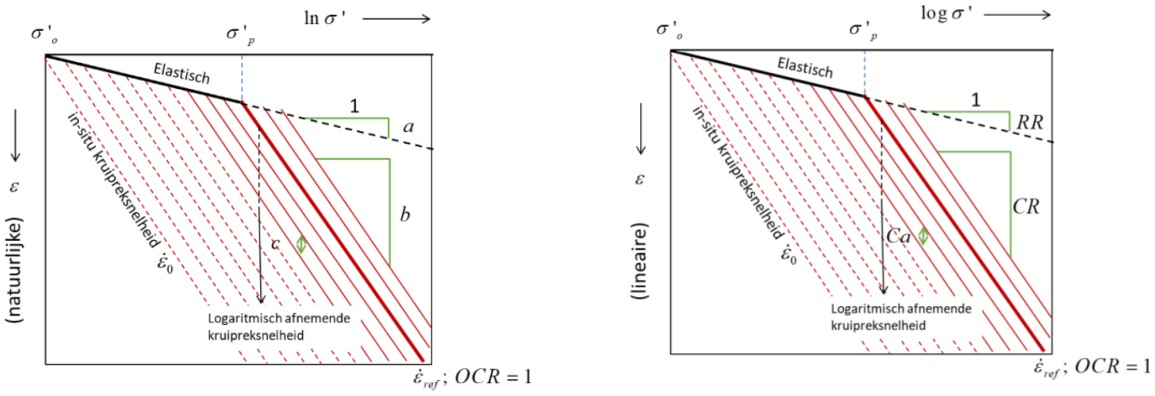

(a) Determination of the a,b,c-parameters [153]

(b) Determination of the NEN Bjerrum parameters [154]

Figure C.3: Comparison of the a,b,c-model parameters and NEN Bjerrum parameters

The red diagonal lines represent lines of equal strain rate ($\dot{\varepsilon}_0$). Moreover, these lines are related to the overconsolidation ratio (OCR). The over-consolidation ratio (OCR) is related to the highest stress ever applied on the soil (preconsolidation stress σ'_p) compared to the effective vertical stress in the soil σ'_z. The OCR can thus be calculated according to equation C.6 [155].

$$OCR = \frac{\sigma'_p}{\sigma'_z} \tag{C.6}$$

C.5. Characteristic values per soil type

The characteristic values and parameters are stated in Eurocode 7 (NEN 9997-1+C2). The table is shown in figure C.4 below.

Grondsoort			Karakteristieke waarde [a] van grondeigenschap											
Hoofd-naam	Bijmengsel	Consistentie [b]	γ [c] kN/m³	γ_{sat} kN/m³	q_c [d g] MPa	C'_p [g]	C'_s	$C_c/(1+e_0)$ [g] [-]	C_α [f] [-]	$C_{sw}/(1+e_0)$ [g] [-]	E_{100} [g h] MPa	φ' [g] Graden	c' kPa	c_u kPa
Grind	Zwak siltig	Los	17	19	15	500	∞	0,004 6	0	0,001 5	45	32,5	0	
		Matig	18	20	25	1 000	∞	0,002 3	0	0,000 8	75	35,0	0	N.v.t.
		Vast	19 20	21 22	30	1 200 1 400	∞	0,001 9 0,001 6	0	0,000 6 0,000 5	90 105	37,5 40,0	0	
	Sterk siltig	Los	18	20	10	400	∞	0,005 8	0	0,001 9	30	30,0	0	
		Matig	19	21	15	600	∞	0,003 8	0	0,001 3	45	32,5	0	N.v.t.
		Vast	20 21	22 22,5	25	1 000 1 500	∞	0,002 3 0,001 5	0	0,000 8 0,000 5	75 110	35,0 40,0	0	
Zand	Schoon	Los	17	19	5	200	∞	0,011 5	0	0,003 8	15	30,0	0	
		Matig	18	20	15	600	∞	0,003 8	0	0,001 3	45	32,5	0	N.v.t.
		Vast	19 20	21 22	25	1 000 1 500	∞	0,002 3 0,001 5	0	0,000 8 0,000 5	75 110	35,0 40,0	0	
	Zwak siltig, kleiig		18 19	20 21	12	450 650	∞	0,005 1 0,003 5	0	0,001 7 0,001 2	35 50	27,0 32,5	0	N.v.t.
	Sterk siltig, kleiig		18 19	20 21	8	200 400	∞	0,011 5 0,005 8	0	0,003 8 0,001 9	15 30	25,0 30,0	0	N.v.t.
Leem [e]	Zwak zandig	Slap	19	19	1	25	650	0,092 0	0,003 7	0,030 7	2	27,5 30,0	0	50
		Matig	20	20	2	45	1 300	0,051 1	0,002 0	0,017 0	3	27,5 32,5	1	100
		Vast	21 22	21 22	3	70 100	1 900 2 500	0,032 9 0,023 0	0,001 3 0,000 9	0,011 0 0,007 7	5 7	27,5 35,0	2,5 3,8	200 300
	Sterk zandig		19 20	19 20	2	45 70	1 300 2 000	0,051 1 0,032 9	0,002 0 0,001 3	0,017 0 0,011 0	3 5	27,5 35,0	0 1	50 100
Klei	Schoon	Slap	14	14	0,5	7	80	0,328 6	0,013 1	0,109 5	1	17,5	0	25
		Matig	17	17	1,0	15	160	0,153 3	0,006 1	0,051 1	2	17,5	5	50
		Vast	19 20	19 20	2,0	25 30	320 500	0,092 0 0,076 7	0,003 7 0,003 1	0,030 7 0,025 6	4 10	17,5 25,0	13 15	100 200
	Zwak zandig	Slap	15	15	0,7	10	110	0,230 0	0,009 2	0,076 7	1,5	22,5	0	40
		Matig	18	18	1,5	20	240	0,115 0	0,004 6	0,038 3	3	22,5	5	80
		Vast	20 21	20 21	2,5	30 50	400 600	0,076 7 0,046 0	0,003 1 0,001 8	0,025 6 0,015 3	5 10	22,5 27,5	13 15	120 170
	Sterk zandig	-	18 20	18 20	1,0	25 140	320 1 680	0,092 0 0,016 4	0,003 7 0,000 7	0,030 7 0,005 5	2 5	27,5 32,5	0 1	0 10
	Organisch	Slap	13	13	0,2	7,5	30	0,306 7	0,015 3	0,102 2	0,5	15,0	0 1	10
		Matig	15 16	15 16	0,5	10 15	40 60	0,230 0 0,153 3	0,011 5 0,007 7	0,076 7 0,051 1	1,0 2,0	15,0	0 1	25 30
Veen	Niet voorbelast	Slap	10 12	10 12	0,1	5 7,5	20 30	0,460 0 0,306 7	0,023 0 0,015 3	0,153 3 0,102 2	0,2 0,5	15,0	1 2,5	10 20
	Matig voorbelast	Matig	12 13	12 13	0,2	7,5 10	30 40	0,306 7 0,230 0	0,015 3 0,011 5	0,102 2 0,076 7	0,5 1,0	15,0	2,5 5	20 30
Variatiecoëfficiënt v			0,05		–	0,25					0,10		0,20	

[a] De tabel geeft van de desbetreffende grondsoort de lage, respectievelijk de hoge karakteristieke waarde van gemiddelden. Binnen een gebied, vastgesteld door de rij van het bijmengsel en de kolom van de parameter (een cel), geldt:

— als een verhoging van de waarde van een van de grondeigenschappen tot een ongunstiger situatie leidt dan de toepassing van de in de tabel gepresenteerde lagere karakteristieke waarde, moet de rechterwaarde op dezelfde regel zijn gebruikt. Is er rechts geen waarde vermeld, dan moet de waarde er recht onder zijn toegepast;
OPMERKING Dit is bijvoorbeeld het geval bij negatieve kleef op een paal waar een hogere waarde van φ', c' en c_u ook een hogere waarde van de negatieve kleef oplevert.

— voor $C_c/(1+e_0)$, C_α en $C_{sw}/(1+e_0)$ zijn in de tabel de hoge karakteristieke gemiddelde waarden vermeld.

Figure C.4: Characteristic values per soil type [149]

However, these values can largely differ from local triaxial test results, as was studied by Stikvoort [45]. PLAXIS calculations based on values from table C.4 and local triaxial tests have shown different displacements for an old quay wall. Due to higher values for the angle of internal friction, cohesions and Young's moduli, the total displacements are 4 times lower when using the local triaxial test results.

The same study focussed on a correlation between cohesion c, angle of internal friction φ, secant stiffness E_{50}^{ref} and the wet volumetric weight γ_w of cohesive and non-cohesive soils. Per volumetric weight, the friction angles φ are normally distributed. The cohesion c and E_{50}^{ref} are log-normally distributed. The characteristic values are calculated for the low 5% left tail of the distribution [45]. In short, using these values based on the volumetric weight should give a more accurate representation compared to the values stated in table C.4 from Eurocode 7.

C.6. Soil conditions Rotterdam

Based on the equations and the theory of the settlements can be concluded that large settlements of the soil especially occur on thick layers of soft soils. The soil in the city of Rotterdam consists of relatively young Holocene sediments. In the South and the East of the Netherlands, the soil consists of older deposits [156]. Moreover, in certain parts of the northern provinces of Groningen and Friesland, the soil deposits date back from the periods where ice sheets reached the Netherlands. The deposits were compressed and are therefore considered as over consolidated [157].

In figure C.5, a geological map of the Netherlands is displayed. This map shows in green the young holocene sediments in the western part of the Netherlands, whereas in the South and East, the sand layers from the older formations are displayed in yellow. The glacial deposited clays in the North are depicted in red. The city of Rotterdam is fully located in the green area in the South-West of the country.

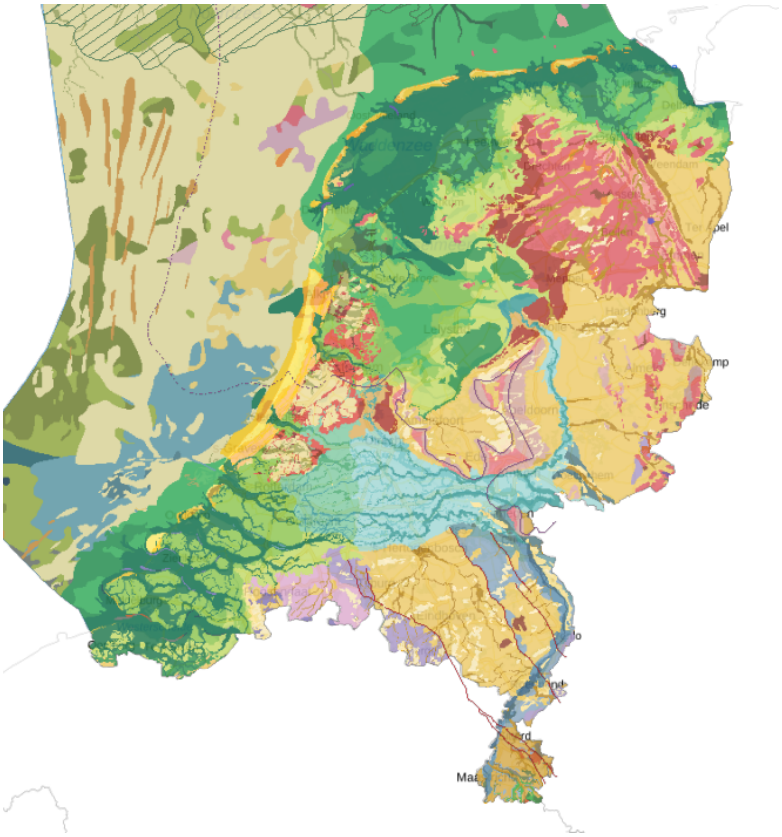

Figure C.5: Geological Map of The Netherlands [156]

In addition, the strength of any type of soil is related to the loading history. Since the soft soils in Rotterdam have not always been loaded before, these are considered normally consolidated or near normally-consolidated soils.

D

PLAXIS Simulation - Results Engineering Solutions Cross-section 1

In this appendix, the graphs of the PLAXIS simulation results for the state-of-the-art engineering solutions for cross-section 1 (Roundabout Groeninx van Zoelenlaan) are displayed. The numerical results are stated and discussed in section 4.7.5. In general, the results for cross-section 1 for all materials and scenarios is slightly higher due to the higher self-weight of the tram track structure and thicker peat layer in the subsoil.

D.1. Conventional method - Sand fill elevation

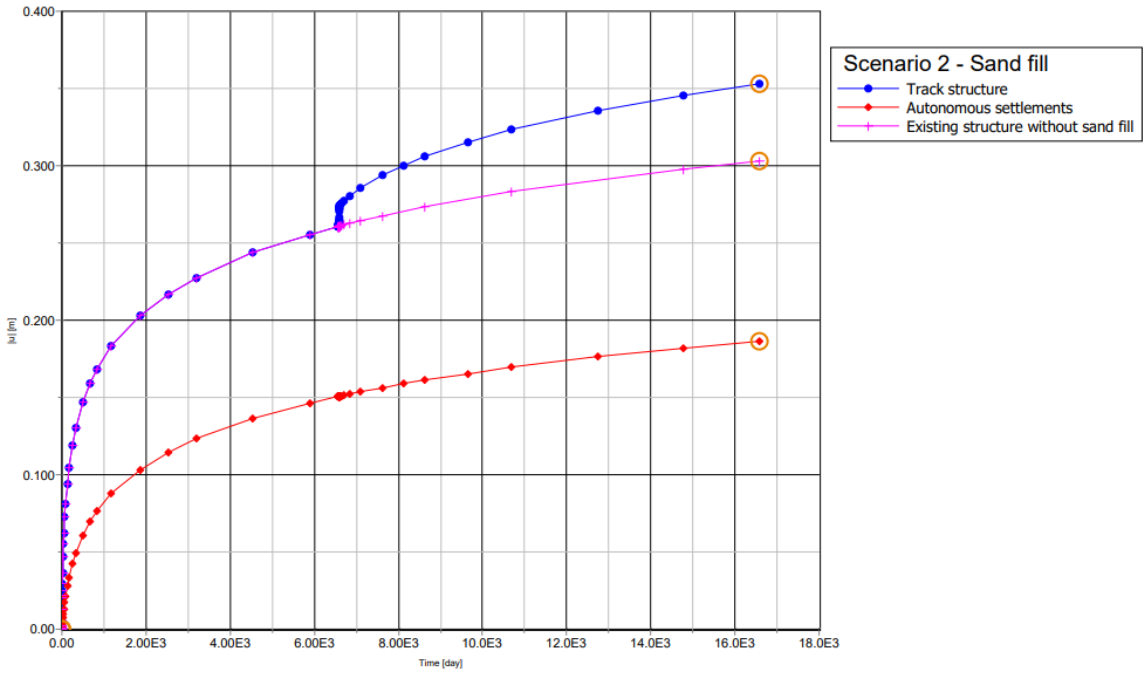

Figure D.1: Settlements of the tram track structure - 20 cm sand fill elevation (Cross-section 1)

D.2. Rockwool: Rockflow

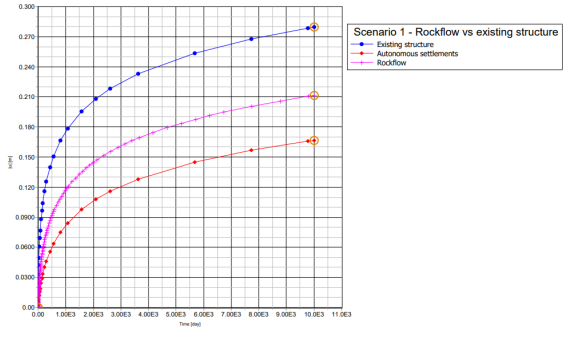

(a) Rockflow - Scenario 1

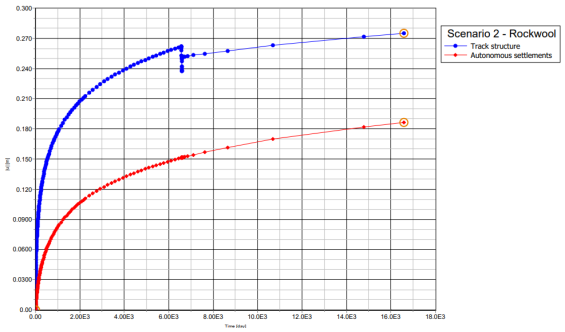

(b) Rockflow - Scenario 2

Figure D.2: Rockflow - Settlement graphs of the tram track structure (Cross-section 1)

D.3. Foam concrete

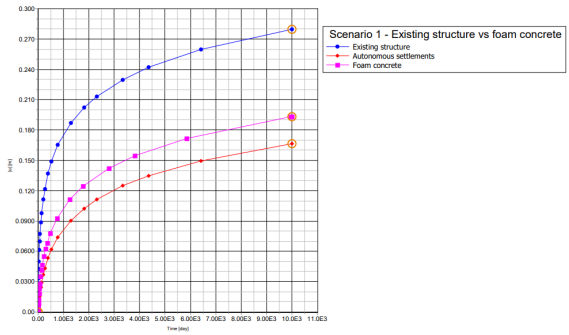

(a) Foam concrete - Scenario 1

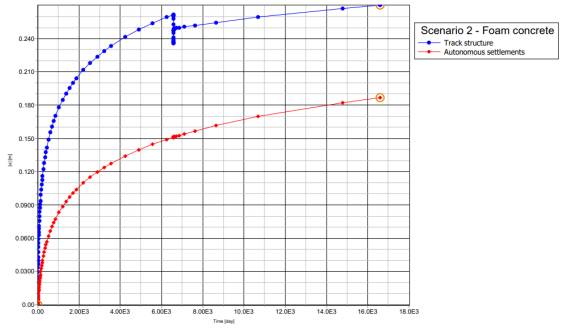

(b) Rockflow - Scenario 2

Figure D.3: Foam concrete - Settlement graphs of the tram track structure (Cross-section 1)

D.4. EPS

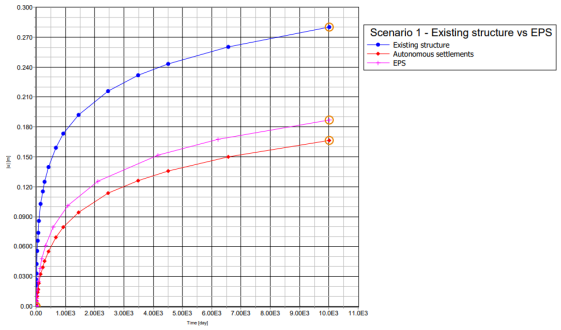

(a) EPS - Scenario 1

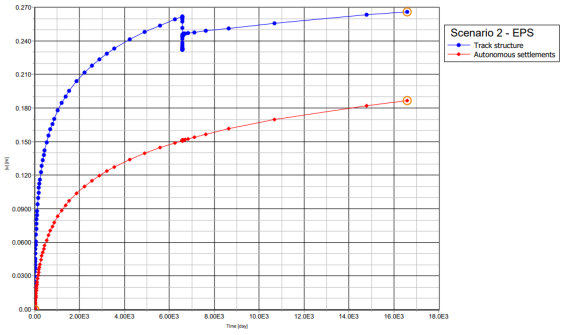

(b) Rockflow - Scenario 2

Figure D.4: EPS - Settlement graphs of the tram track structure (Cross-section 1)

E

Python script - Rail deflection

```
# Import modules
import numpy as np
import matplotlib.pyplot as plt

# Vehicle properties
vehicle_load = 372  # weight empty vehicle [kN]
Q = vehicle_load / 6  # load [N] (4 bogies, two axles)
axles = 2  # number of axles
d = 1.87  # distance between axles [m]

# Track properties
EI = 14002800  # bending stiffness 2 grooved rails Ri60 [Nm^2]
k = 6200000    # foundation coefficient [N/m2]

# Determine characteristic length L
L = ((4 * (EI) / k) ** 0.25)  # characteristic length [m]


# Calculate and plot rail displacements u(x)
x = np.linspace(-10, 10, 1000)

w1 = (((Q*10**(3))/(2*k*L)) * np.exp(-abs(x-0.5*d)/L) * (np.cos((x-0.5*d)/L) +
↪  np.sin(abs(x-0.5*d)/L))) # displacement in [m]
w2 = (((Q*10**(3))/(2*k*L)) * np.exp(-abs(x+0.5*d)/L) * (np.cos((x+0.5*d)/L) +
↪  np.sin(abs(x+0.5*d)/L))) # displacement in [m]
w = -1*(w1 + w2)*(10**3) # add the two single axle loads and conversion to show negative
↪  displacement in [mm]

# plot displacement
plt.figure(figsize=(18, 6))
plt.plot(x, w)
plt.xlabel('x-axis [m]')
plt.ylabel('W(x) [mm]')
plt.title(f'Displacement infinite beam for d = {d} [m]')
```